frontiers | Research Topics

Realization of ecological product value, land use change and environment

Edited by
Hualin Xie, Hua Lu and Yujia Zhang

Published in
Frontiers in Environmental Science
Frontiers in Sustainable Food Systems

ISSN 1664-8714
ISBN 978-2-8325-4778-6
DOI 10.3389/978-2-8325-4778-6

About Frontiers

Frontiers is more than just an open access publisher of scholarly articles: it is a pioneering approach to the world of academia, radically improving the way scholarly research is managed. The grand vision of Frontiers is a world where all people have an equal opportunity to seek, share and generate knowledge. Frontiers provides immediate and permanent online open access to all its publications, but this alone is not enough to realize our grand goals.

Frontiers journal series

The Frontiers journal series is a multi-tier and interdisciplinary set of open-access, online journals, promising a paradigm shift from the current review, selection and dissemination processes in academic publishing. All Frontiers journals are driven by researchers for researchers; therefore, they constitute a service to the scholarly community. At the same time, the *Frontiers journal series* operates on a revolutionary invention, the tiered publishing system, initially addressing specific communities of scholars, and gradually climbing up to broader public understanding, thus serving the interests of the lay society, too.

Dedication to quality

Each Frontiers article is a landmark of the highest quality, thanks to genuinely collaborative interactions between authors and review editors, who include some of the world's best academicians. Research must be certified by peers before entering a stream of knowledge that may eventually reach the public - and shape society; therefore, Frontiers only applies the most rigorous and unbiased reviews. Frontiers revolutionizes research publishing by freely delivering the most outstanding research, evaluated with no bias from both the academic and social point of view. By applying the most advanced information technologies, Frontiers is catapulting scholarly publishing into a new generation.

What are Frontiers Research Topics?

Frontiers Research Topics are very popular trademarks of the *Frontiers journals series*: they are collections of at least ten articles, all centered on a particular subject. With their unique mix of varied contributions from Original Research to Review Articles, Frontiers Research Topics unify the most influential researchers, the latest key findings and historical advances in a hot research area.

Find out more on how to host your own Frontiers Research Topic or contribute to one as an author by contacting the Frontiers editorial office: frontiersin.org/about/contact

Realization of ecological product value, land use change and environment

Topic editors

Hualin Xie — Jiangxi University of Finance and Economics, China

Hua Lu — Jiangxi University of Finance and Economics, China

Yujia Zhang — University of California, Riverside, United States

Citation

Xie, H., Lu, H., Zhang, Y., eds. (2024). *Realization of ecological product value, land use change and environment*. Lausanne: Frontiers Media SA.

doi: 10.3389/978-2-8325-4778-6

Table of contents

04 Influence of risk perception and policy support on the deviation of rural households' demands and adoption behavior of the forestry socialized service
Wenmei Liao, Ruolan Yuan, Xu Zhang, Chang Zhang and Na Li

18 Effect of ecological civilization pilot demonstration area construction on urban land green use efficiency
Shaojie Li, Duoduo Wang and Qin Wu

36 Dilemmas and theoretical exploration of China's rural land property rights system reform
Zhou Laiyou and Luo Jiawei

44 Impact of high standard farmland construction policy on chemical fertilizer reduction: a case study of China
Yang Liu, Wenmei Liao, Xu Zhang and Hailan Qiu

57 Quantifying vegetation change and driving mechanism analysis in Sichuan from 2000 to 2020
Lina Ning, Wenfu Peng, Yanan Yu, JiaYao Xiang and Yong Wang

72 Spatio-temporal relationship between carbon emission and ecosystem service value under land use change: a case study of the Guanzhong Plain Urban Agglomeration, China
Shuo Yang and Xiaozheng Zheng

86 Analysis of temporal and spatial evolution characteristics and influencing factors of land use transformation in Hebei Province from the perspective of supply and demand
Lijun Ma, Fengyu Guo, Hao Hu, Yu Guo, Lei Xu and Shi Yin

102 Reduced grazing and changes in the area of agroforestry in Europe
Judit Rubio-Delgado, Susanne Schnabel, Paul J. Burgess and Sara Burbi

121 Simulation and prediction of land use in urban agglomerations based on the PLUS model: a case study of the Pearl River Delta, China
Jing Gong, Hongyan Du, Yong Sun and Yun Zhan

133 Impact of land use changes on the land surface thermal environment in Nanchang, Jiangxi province, China
Yujia Zhang, Haisheng Cai, Taifeng Zhu, Xigen Guo, Jiaxi Zeng and Liang Huang

146 Study on multi-scenarios regulating strategy of land use conflict in urban agglomerations under the perspective of "three-zone space": a case study of Harbin-Changchun urban agglomerations, China
Wei Zheng, Bin Guo, Hao Su and Zijun Liu

frontiers | Frontiers in Environmental Science

TYPE Original Research
PUBLISHED 05 June 2023
DOI 10.3389/fenvs.2023.1211310

OPEN ACCESS

EDITED BY
Hua Lu,
Jiangxi University of Finance and Economics, China

REVIEWED BY
Minzhe Du,
South China Normal University, China
Liping Liao,
Guangdong University of Finance and Economics, China

*CORRESPONDENCE
Chang Zhang,
2016012957@stu.zuel.edu.cn
Na Li,
lina1724@foxmail.com

RECEIVED 24 April 2023
ACCEPTED 24 May 2023
PUBLISHED 05 June 2023

CITATION
Liao W, Yuan R, Zhang X, Zhang C and Li N (2023), Influence of risk perception and policy support on the deviation of rural households' demands and adoption behavior of the forestry socialized service.
Front. Environ. Sci. 11:1211310.
doi: 10.3389/fenvs.2023.1211310

Influence of risk perception and policy support on the deviation of rural households' demands and adoption behavior of the forestry socialized service

Wenmei Liao[1,2], Ruolan Yuan[1], Xu Zhang[1], Chang Zhang[3]* and Na Li[1]*

[1]School of Economics and Management, Jiangxi Agricultural University, Nanchang, China, [2]Jiangxi Rural Revitalization Strategy Research Institute, Nanchang, China, [3]School of Finances, Zhongnan University of Economics and Law, Wuhan, China

This study explores the impact mechanism of risk perception and policy support on the deviation of rural households' demands and adoption behavior (RHDAB) of the forestry socialized service (FSS). It provides a decision-making basis for promoting the construction of a collective FSS system and realizing the value of ecological products. Survey data from 787 rural households in Zhejiang, Fujian, and Jiangxi provinces were used to quantify the influence of risk perception and policy support on the deviation of RHDAB of the FSS using the Mv-probit model and Poisson model. The results revealed that: 1) there were deviations between RHDAB for different types of FSS, with 57.71% and 66.20% for good seeds and cultivation technology services and product collection and marketing services, respectively. 2) Risk perception accelerated the deviation and degree of deviation between RHDAB of the FSS, particularly the technology risk perception. Meanwhile, policy support was shown to mitigate the effect of risk perception on rural households' deviation and deviation degree. 3) Business risk perceptions had a more significant impact on the deviation of RHDAB in middle and high-economic development areas compared to technology risk perception and financial risk perceptions in low-economic development areas. Additionally, business risk perception was found to have a significant positive effect on the deviation of small and large operation-scale rural households, while technology risk perception significantly impacted the deviation of small operation-scale rural households. Consequently, this study suggests the need for a sound forestry risk management system to address the variability of the deviation of RHDAB across different regions and operation scales, as well as to improve the service quality of forestry insurance, accelerate the speed and benefit of inclusive rural finance, and cultivate new supply bodies of socialized services, thereby promoting the construction of collective FSS system and realizing the value of ecological products.

KEYWORDS

adoption behavior, risk perception, ecological product realization mechanism, China, forestry socialized service

1 Introduction

The Reform of the Collective Forest Property Rights System (RCFPRS) in China began in 2003 as a pilot project and was implemented nationally in 2008. It attempted to establish a set of management and development mechanisms designed to promote forestry and enrich the populace by "clarifying property rights, liberalizing management rights, implementing disposal rights, and guaranteeing revenue rights" (Liu et al., 2017; Hyde and Yin, 2018). The RCFPRS aimed to provide better security of ownership of forestland, and a more clear and harmonized property rights system, to increase farmers' motivation to manage forests, and enhance the productivity of forest ecosystems. It sought to incentivize farmers to cultivate forest land, thus increasing their household income in the context of a rural land property rights system that promotes income growth. However, as the RCFPRS process advances, irregular transfers of forest rights and an imperfect supporting policy system have emerged, hindering the development of forestry modernization. Therefore, accelerating and perfecting the FSS system is an important content of deepening the RCFPRS and an inevitable requirement for comprehensively improving the level of collective forestry management modernization. In response, the Chinese central government has implemented a series of supportive policies, such as stressing in the No. 1 Central Document the need to improve the socialized agricultural service system, enhance the supply capacity and level of agricultural socialized services, and accelerate the development of socialized agricultural services. Additionally, the Fourth Plenary Session of the 19th Central Committee of the Communist Party of China put forward the significant task of further deepening the RCFPRS in rural areas. In this context, the FSS system plays an irreplaceable and essential role in consolidating the achievements of the RCFPRS. Moreover, in 2021, the Opinions on Establishing and Improving the Mechanism for Realizing the Value of Ecological Products highlighted the necessity of establishing and improving the mechanism for realizing the value of ecological products in forestry.

FSS has been identified as an important mode to enhance the value realization of ecological forestry products, thereby accelerating the cultivation of ecological product market operators, also conducive to ecological and environmental protection (Du et al., 2022). However, despite the implementation of the RCFPRS, Chinese forestry production continues to face the fundamental contradiction between small-scale family operations and large markets. Numerous problems persist, such as high labor costs, low efficiency of forest product production and management, forestland fragmentation, restricted logging, lack of information regarding market supply and demand, and weak ability to resist market risks and natural disasters. These issues have hindered the effective improvement of forest farmers' enthusiasm (Yin et al., 2013a; Yin et al., 2013b; Xie et al., 2014; Liu et al., 2016). There is an urgent need for FSS to resolve various risks and resource constraints in the process of realizing forestry ecological products. A study of 1,400 surveyed households found that 75.26% had an urgent demand for the FSS, yet 87.6% had not adopted the service (Liao et al., 2016). This discrepancy between demand and adoption, or the obstacles in the process of transforming demand into adoption behavior, has significantly impeded the progress of improving the FSS system, limited the advancement of collective forestry operation development levels, and slowed the construction of forestry modernization (Kong et al., 2017). As such, it is necessary to further explore the inner mechanism of the deviation of RHDAB of the FSS, which has important practical implications for deepening the RCFPRS.

Deviations between RHDAB are due to various complex factors influencing rural households' demands during the transformation into adoption behavior, resulting in a discrepancy between their final behavior and initial demands. This may convey incomplete information to policymakers, harming the implementation effect of relevant policies and leading to policy failure and inefficiency. On the surface, the deviation may be attributed to factors on the supply side of the service, such as the ability of the service to solve rural households' practical problems in household management. However, it is mainly caused by factors on the demand side of the service, such as risk perception in the forestry management process. Different types of risk perception can modify the RHDAB of socialized services. However, the academic community has not yet been able to give a definite answer to how risk perception factors affect RHDAB of the FSS and what is the specific impact mechanism. Therefore, this paper utilizes a standard econometric analysis method to investigate the influence of risk perception on the RHDAB of the FSS and explore the moderating role of policy support to provide suggestions to further improve the FSS system.

The marginal contribution of this study lies in the in-depth analysis of the impact of risk perception on the deviation of RHDAB for FSS, and the policy support is placed under the same research framework to further investigate the role of government support, which makes the research content more perfect. In addition, the Mv-Probit model and Possion model were selected for empirical analysis, which not only took into account the interaction between different types of FSS but also analyzed the influence on the degree of deviation, which is conducive to improving the accuracy of research results.

2 Literature review

Land scale operation refers to the mode in which the optimal combination of various production factors (land, labor, capital, technology, etc.) operates effectively under certain environmental and socio-economic conditions and achieves the best economic benefits. There are two ways to realize land scale management, and two views on scale management have been gradually formed in academic circles: one is land scale management by new agricultural operators through land transfer to change the management pattern of dispersed small-scale farmers in China, to improve the efficiency of resource allocation (Yao, 2017). However, the national land transfer situation is not optimistic, and there is a gap between academic theory and reality, but this does not negate the significance of "land scale management." The other is that economies of scale are derived from the economy of the division of labor. The production efficiency of factors can be improved by the specialization of production links (Youno, 1928). The subdivision of farmers' management rights and the division of labor in society can help promote service scale operation in agriculture, which can significantly improve the external division of labor and economies of scale in agriculture, and thus promote the

transformation of agricultural scale operation from "land scale" to "service scale." (Luo, 2017), and this is especially true for forestry scale management.

As one of the essential ways to innovate large-scale management, the FSS has received much attention from scholars and government departments. After the RCFPRS, rural households' demand for the FSS has diversified. The demand for production and marketing services is robust (Martell et al., 2016). Demand intensity is positively correlated with the proportion of the total household income related to technical service and whether the rural households have encountered technical problems in production. Household resource endowment significantly affects the RHDAB of technical services, such as the increase in labor cost due to household labor transfer (Schmook and Radel, 2008; Xie et al., 2014), which promotes the capitalization of rural households' forestry input structure (Haas, 2006; Hull, 2007). However, this promotion effect is regulated by the supply level of the FSS, the plots' location, and the forest resources' endowment (Zhang et al., 2001). The difference in household factor allocation, production mode, and production purpose will also lead to the heterogeneity of social service demand (Skoufias and Olivieri, 2013). Land size is one of the most important factors in determining the productive investment patterns of rural households. Still, existing studies have not reached a consistent conclusion. Some studies suggest a negative relationship between the two (Xie et al., 2014), with the fragmentation of forest land increasing the cost of implementing technology services and thus discouraging the adoption of new forestry technologies by rural households. Some studies suggest a positive relationship between the two, with small-scale rural households investing in machinery production and processing not being a rational choice, leading to a higher demand for outsourced machinery services (Olmstead, 1975). There is an inverted "U" shaped relationship between the two and an inflection point between the scale of forest land management and rural households' productive outsourcing behavior (Luo et al., 2016). Therefore, the factors related to the scale of operation are important factors affecting the adoption of services. This study will then analyze the operation scale and regional economic development level heterogeneity.

The above studies examined the influence of different factors on rural households' social service adoption behavior. The large investment and long cycle of forestry production, the coexistence of natural risk, social risk, and business risk perception, and the high probability of occurrence during the business cycle have an important impact on rural households' social service adoption behavior (Duan et al., 2021). Still, the existing studies have not paid enough attention to rural households' risk perception. Prospect theory suggests that individual decision-making behavior is determined by a combination of risk preferences and subjective judgments of objective probabilities. Socialized service adoption behavior has the effect of resisting natural, social, and business risk perceptions (Kahneman and Tversky, 2013). Therefore, rural households' risk perceptions are closely related to social service adoption behavior. Domestic and foreign scholars have widely studied the influence of risk perception and rural households' decision-making behavior. Roumasset (1977) and Scott (1977) were the first to suggest that farmers are risk averters. Then, Just and Pope, (1979) introduced the risk aversion effect into the agricultural input-output model for the first time. Howard et al. (1991) further pointed out that producers need to analyze farmers' decision-making behaviors under different risk perceptions. In the study on risk perception and farmers' decision-making behavior, it is found that reducing the risk perception of termination of property rights contract will increase farmers' marginal willingness to pay for contract (Qin et al., 2011), which also indicates that their decision-making behavior is constrained by risk perception (Liu and Huang, 2013). The stronger the risk perception, the more willing to take measures to avoid risks (Botzenetal et al., 2009). In recent years, China has taken some supportive policy measures to encourage agricultural production, mainly in the form of various agricultural subsidies, which have been found to promote agricultural production behavior and increase rural households' motivation to produce food (Kurkalova et al., 2006; Ji et al., 2017). However, some studies believe subsidy policies have little effect on promoting farmers' behaviors. For example, agricultural input subsidies can reduce agricultural production costs and improve agricultural productivity in early. Still, they cannot guarantee farmers' economic benefits with increased agricultural input factor prices (Dorward and Chirwa., 2011). The above research literature indicates that academics consider risk perception and policy support to be important factors in studying demands or behavior. Risk perception can be an important reason for the deviation of RHDAB.

In summary, the existing researches have conducted fruitful explorations of the demand and adoption behavior of FSS and their influencing factors, but there is still room for further research. Firstly, there are few existing studies on the deviation of RHDAB of FSS. Meanwhile, in terms of research methods, more binary Logit and Probit models are used; there is no in-depth consideration of the interaction between different types of services. Secondly, more studies only study the FSS from the perspective of demand but do not deeply explore the inconsistency between demand and adoption behavior, which may lead to policy failure. Because of this, this paper uses the survey data of farmers in Zhejiang Province, Fujian Province, and Jiangxi Province, and based on the heterogeneous perspective of regional economic development level and operation scale, uses the Mv-Probit model and Possion model to analyze the influence of risk perception on the deviation of RHDAB of FSS. It also examines whether the government support policy can alleviate the regulatory effect of risk perception and puts forward countermeasures and suggestions to improve the FSS system.

3 Theoretical basis and variable selection

3.1 Theoretical analysis

According to the theory of rural household behavior, rural households' decision-making behaviors, including production behavior, operation behavior, and purchasing behavior, all have economic attributes. As a boundedly rational economic man, rural households will aim at maximizing personal or family income, evaluate the results of decisions or choices based on their values and preferences, and finally choose the conclusion that they think

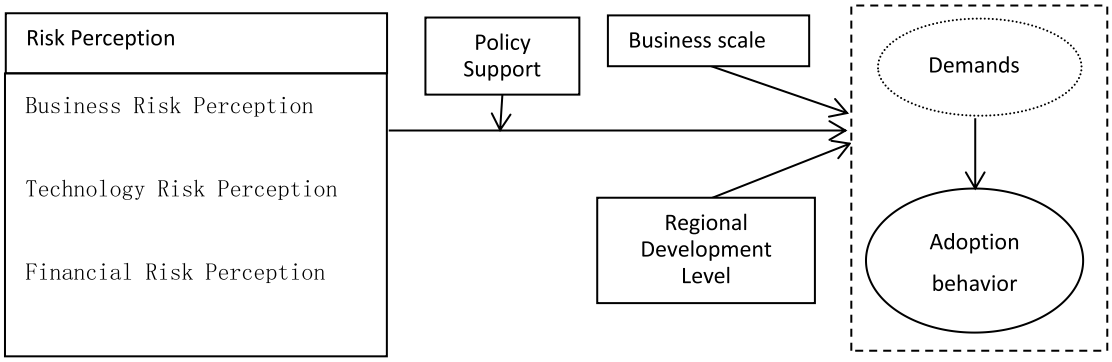

FIGURE 1
Demand-behavior model of forestry socialization services.

can maximize the utility of their desired goals. According to the theory of the small peasant economy, rural household production in modern China is in a stage of rural economic transition, with agricultural products and labor gradually entering the market, showing the characteristics of commercialization of agricultural products and part-time work. Therefore, the behavior of rural households is subject to the constraints of product market, technology, and capital factors, and uncertainty risks arise with fluctuations in product market price and production cost. Under the combined effect of constraints on relevant factors and risk perception, rural households constantly modify their business objectives and production behavior to maximize their business returns. Risk perception refers to farmers' judgment and assessment of the risks of strange things according to their own experience (Slovic, 1987). It is expressed as the perception of the uncertainty of future benefits or costs. Risk perception largely influences decision-making when decision-makers change, postpone, or cancel behavioral decisions (Kotler and Armstrong, 1994). Numerous studies have concluded that risk perception is a more robust explanation for decision behavior than expected benefits (Mitchell, 1999). This means that the study of risk perception is more important than the expected benefits in accurately grasping and understanding decision-maker's behavior. The stronger the rural households' risk perception is, the more likely they will adopt risk-resistant behavior to avoid risks (Lusk and Coble, 2005).

In the deviation of RHDAB of the FSS, risk perception refers to the fact that forestry operations may also encounter technology use risk, operation risk, and fund-raising risk in adopting FSS. Unlike agricultural production, the cycle of forestry production and operation is longer. Once a socialized service is adopted in the operation process, a long cycle is needed, such as good seed service, which starts from the selection of suitable seeds to cultivation and fertilization, branch pruning, pest control, and so on, until maturity, all of which cannot be separated from the good seed service provider. The longer the adoption cycle, the higher the degree of risk perception and the higher the risk cost that must be borne, directly affecting the transformation from demands to adoption behavior. The state subsidy policy effectively alleviates the hesitant attitude of adoption behavior or reduces the risk cost and compensates for the risk loss in the operation process, which plays an essential moderating role in the deviation of RHDAB of the FSS. Based on this, this paper investigates the direction, extent, and mechanism of the influence of risk perception on the deviation of RHDAB of FSS and clarifies whether this influence is moderated by policy support. It is shown in Figure 1.

3.2 Variable selection and hypothesis

3.2.1 Explained variables

This paper mainly investigates the influencing factors and mechanisms of RHDAB of FSS. The explained variables focus on the most urgent socialized services in rural households' forest land management: forestry seed and cultivation technology services (FSCTS), pest control services (PCS), and forest products collection and marketing services (FPCMS). In this paper, we study the deviation of RHDAB of FSS, which is divided into two parts: 1) the deviation of RHDAB of FSS. There are two patterns of deviation between demands and behavior, one is they have demands of FSS but no adoption behavior, i.e., "demands without behavior"; the other is they have no demand of FSS but adoption behavior, i.e., "no demand but behavior," but in the actual research, there is no such situation. Therefore, the deviation of RHDAB of FSS in this paper refers to "demand without behavior," which is assigned a value of 1; the opposite is 0. The same is done for FSCTS, FPCMS, and PCS. 2) To further quantify the deviation level of RHDAB of FSS in the whole process of forestry production activities, this paper takes the number of behavior deviations as the measurement index and sums the deviation number of the FSCTS, the PCS, and the FPCMS.

3.2.2 Core explanatory variables

The field research revealed three categories of rural households' risk perceptions that are most evident. Firstly, business risk perception in forestry. Business risk refers to the loss caused by poor management of forestry, the loss caused by the lack of necessary management experience or unscientific management,

TABLE 1 Definition of variables and descriptive statistics.

	Variable name	Variable definition	Mean	SD
1) Explained variables				
Types of behavior deviations	The FSCTS	0 = no deviation, 1 = deviation	0.571	0.495
	The PCS	0 = no deviation, 1 = deviation	0.277	0.448
	The FPCMS	0 = no deviation, 1 = deviation	0.662	0.473
The degree of behavior deviation	The degree of deviation of the three types of services	0 = no deviation, 1 = 1 deviation, 2 = 2 deviations, 3 = 3 deviations	0.848	0.766
2) Explanatory variables				
Risk Perception	Business risk perception	1 = low risk, 2 = average risk, 3 = high risk	1.967	0.511
	Technology risk perception	1 = low risk, 2 = average risk, 3 = high risk	2.241	0.767
	Financial risk perception	0 = own funds risk, 1 = borrowed funds risk	0.783	0.413
Policy support	Forestry subsidies	0 = no forestry subsidy, 1 = forestry subsidy	0.102	0.302
3) Control variables				
Householder characteristics	Age	1 = 0–30 years old, 2 = 31–40 years old, 3 = 41–50 years old, 4 = 51–60 years old, 5 = ≧ 60 years old	3.628	0.975
	Education level	1 = Elementary school and below, 2 = Elementary school, 3 = Junior high school, 4 = High school, 5 = College and above	1.571	0.698
	Whether he/she is a village cadre	0 = No, 1 = Yes	0.156	0.363
	Forestry motivation	1 = declining, 2 = no change, 3 = raising	2.704	0.510
Woodland elements	Forest land management area	Actual operating area (mu)	48.704	89.715
	Forest land fine fragmentation	Woodland area/number of woodland blocks	9.441	20.710
Workforce Factors	Number of laborers	Number of household laborers	2.962	1.210
Funding Elements	Forestry revenue share	Share of forestry income in total household income (%)	19.229	26.191
	Share of non-farm income	Share of non-farm income in total household income (%)	27.472	32.091
Location factors	Regional economic development level	1 = low, 2 = medium, 3 = high	2.503	0.761
	Terrain conditions	1 = Plain, 2 = Hill, 3 = Mountain	2.868	0.339

10.3389/fenvs.2023.1211310

TABLE 2 Results of the model of farm households' demands of the FSS.

	Variable name	Mv-probit model			Poisson model
		Model (1): FSCTS	Model (2): PCS	Model (3): FPCMS	Model (4): Degree of deviation
Risk perception	Business risk perception	0.418***	0.041	0.553***	0.184***
		(0.105)	(0.102)	(0.107)	(0.063)
	Technology risk perception	0.118*	0.166**	0.222***	0.106***
		(0.064)	(0.066)	(0.064)	(0.041)
	Financial risk perception	0.100	0.029	0.252**	0.066
		(0.124)	(0.127)	(0.123)	(0.082)
Policy support	Forestry subsidies	−1.375***	−1.072***	−1.078***	−1.443***
		(0.176)	(0.228)	(0.157)	(0.223)
Householder characteristics	Age of householder	0.031	0.013	−0.058	0.018
		(0.057)	(0.059)	(0.057)	(0.036)
	Education level of the householder	0.158*	0.095	0.079	0.094**
		(0.081)	(0.079)	(0.080)	(0.047)
	Whether he/she is a village cadre	−0.628***	−0.137	−0.347**	−0.312***
		(0.142)	(0.146)	(0.137)	(0.108)
	Forestry motivation	−0.240**	−0.121	−0.196*	−0.126***
		(0.098)	(0.097)	(0.100)	(0.041)
Woodland elements	Forest land fine fragmentation	0.006*	0.007**	0.005	0.004***
		(0.004)	(0.003)	(0.004)	(0.001)
	Forest land management area	−0.000	−0.002**	−0.000	−0.001
		(0.001)	(0.001)	(0.001)	(0.000)
Funding Elements	Forestry revenue share	0.226	0.647***	0.047	0.329***
		(0.202)	(0.196)	(0.204)	(0.116)
	Non-farm income share	−0.270	0.112	−0.182	−0.090
		(0.171)	(0.172)	(0.171)	(0.113)
Workforce Factors	Number of laborers	−0.055	0.039	−0.029	−0.011
		(0.042)	(0.043)	(0.042)	(0.026)

(Continued on following page)

10.3389/fenvs.2023.1211310

TABLE 2 (*Continued*) Results of the model of farm households' demands of the FSS.

Variable name		Mv-probit model			Poisson model
		Model (1): FSCTS	Model (2): PCS	Model (3): FPCMS	Model (4): Degree of deviation
Regional development level		−0.153**	−0.097	0.080	−0.095**
		(0.071)	(0.072)	(0.070)	(0.043)
Terrain conditions		−0.381**	0.111	−0.065	−0.131
		(0.149)	(0.152)	(0.150)	(0.087)
Constant		1.230*	−1.167	−0.430	0.094
		(0.703)	(0.718)	(0.701)	(0.439)
atrho21		0.524*** (0.069)			
atrho31		0.812*** (0.073)			
atrho32		0.359*** (0.066)			
Wald value		203.19			112.63
Log-likelihood		−1,247.817			−855.4326

Note: ***, **, and * indicate significance at the 1%, 5%, and 10% statistical significance levels, respectively, and the standard errors are in parentheses corresponding to the regression coefficients.

such as the destruction of young trees, theft of trees, low afforestation survival rate, artificial fires, rising labor costs, etc. Secondly, technology risk perception in forestry. Certain risks accompany the adoption of each technology. Technology risk refers to the forestry risk brought by the limitation of technical conditions in cultivating forests, including the adaptability of technology, such as mechanical damage to above-ground and below-ground parts caused by tilling the soil, death of seedlings due to excessive use of pesticides, etc. Adopting new technologies can reduce the risk but may also increase the risk of forestry, but generally, mature new forestry technologies will reduce the risk. Thirdly, financial risk perception of forest management. Suppose the rural households' forestry operation funds come from borrowing. In that case, they need to bear a greater financial risk perception. As rational economic men, they will be more cautious about using forestry funds, which will easily produce a deviation between the demands and adoption behavior of the FSS. Rural households' judgment of forestry business risk, technical risk, and financial risk will directly affect the deviation of their demands and adoption behavior of the FSS, so the risk perception in this paper is measured from three aspects: business risk, technical risk, and financial risk.

3.2.3 Moderator variables

Policy support refers to the government's formulation of financial subsidies, subsidized loans, technical training, and other related policy measures to stimulate rural households' enthusiasm for forestry production and operation and to promote rural households' choice of the FSS to a certain extent. Forestry subsidies are the main and important form of policy support, which is to give certain subsidies to the main body of artificial afforestation, renewal, and transformation, including afforestation subsidies, forest nurturing subsidies, forest tree seed subsidies, etc. Subsidies can reduce the comparative cost of afforestation, improve the comparative income, and reduce all risks. Therefore, the policy support referred to in this paper is mainly measured by "whether the rural households receive forestry subsidies." 1 is assigned if the household has received forestry subsidies and 0 if not.

3.2.4 Control variables

According to the existing relevant studies, other factors that affect the deviation of RHDAB of the FSS are selected as control variables: 1) Production and operation characteristics. As a category of economics, production factors include all social resources needed for production and operation activities, mainly labor, land, and capital. 1) Labor factor: the more labor force a household has, the more labor resources it can allocate and the slighter the possibility of deviation. The labor factor is set as the number of household laborers. 2) Forest land factor: the area of forest land is an important production factor that determines the forestry operation of rural households and the choice of social services. Within a specific area of forest land, the larger the area of forest land operation, the higher the production factor allocation capacity requirement, and the slighter the possibility of deviation. Land fragmentation will increase the cost of the FSS, thus inhibiting the selection behavior of rural households' socialized services and

TABLE 3 Analysis of the moderating effect of policy support.

Variable name	Mv-probit model			Poisson model
	Model (4): FSCTS	Model (5): PCS	Model (6): FPCMS	Degree of deviation
Business Risk Perception	0.476***	0.050	0.583***	0.193***
	(0.110)	(0.105)	(0.114)	(0.064)
Technology Risk Perception	0.121*	0.176**	0.226***	0.111***
	(0.067)	(0.069)	(0.069)	(0.041)
Financial Risk Perception	0.127	0.092	0.367***	0.084
	(0.134)	(0.133)	(0.134)	(0.084)
Policy Support	0.737	0.705	1.044	0.497
	(1.020)	(1.247)	(0.895)	(1.432)
Business risk perception x policy support	−0.713*	−0.076	−0.355	−0.396
	(0.385)	(0.494)	(0.336)	(0.511)
Technology risk perception x policy support	−0.151	−0.443	−0.286	−0.297
	(0.225)	(0.298)	(0.200)	(0.277)
Financial risk perception x policy support	−0.287	−1.014*	−0.932***	−0.565
	(0.391)	(0.534)	(0.358)	(0.446)
Control variables	Controlled			
Constant	1.088	−1.189*	−0.526	0.063
	(0.708)	(0.722)	(0.709)	(0.440)
atrho21	0.522*** (0.069)			
atrho31	0.806*** (0.074)			
atrho32	0.353*** (0.066)			
Wald value	212.36			117.02
Log-likelihood	−1,239.932			−854.097

increasing the possibility of deviation (Xie et al., 2014). 3) Financial factor: the higher the proportion of forestry income, the greater the dependence of rural households on forestry, the greater the forestry input, and the slighter the possibility of deviation. The proportion of non-agricultural income reflects the degree of rural households' departure from agriculture. The greater the value of non-farm income, the greater the possibility of deviation. 2) Rural households' characteristics. As forestry operators, rural households' characteristics influence their demands and adoption behavior of socialized services, including age, education level, whether they are village cadres, and enthusiasm for the forestry business. 3) Location factors: the location factor is an important indicator of economic quality (economic, geographical condition). The production environment and living standards differ in locations and geographical conditions, resulting in differences in RHDAB in the FSS (Liao et al., 2016). This has been the consensus of academic and governmental sectors. This paper measures the location conditions by two indicators: regional economic development and topographic conditions.

4 Model specification, data, and variable descriptions

4.1 Model specification

4.1.1 Mv-probit model

The deviation of RHDAB on the FSS is a binary choice problem, and the binary Probit model is usually adopted, but the assumption is that the alternative options are independent. Rural households may have several service options in the production process, and these services are not exclusive to each other, so the simple binary Probit model cannot solve the correlation between service choice behaviors. In contrast, the Mv-Probit model (Multivariate Probit) can not only estimate the regression results of rural households' single service choice behavior but also give the likelihood ratio test of the regression results of each service. Then the likelihood ratio can determine the interrelationship among the services, which improves the estimation accuracy and efficiency.

Therefore, the Mv-Probit model is adopted in this paper to analyze the factors influencing rural households' adoption behavior

TABLE 4 Heterogeneity analysis of different levels of economic development.

Variable name	Low level of economic development			Economic development level in			High level of economic development		
	Model (7): FSCTS	Model (8): PCS	Model (9): FPCMS	Model (10): FSCTS	Model (11): PCS	Model (12): FPCMS	Model (13): FSCTS	Model (14): PCS	Model (15): FPCMS
Business Risk Perception	0.393	−0.199	1.070***	0.450*	0.397*	0.714**	0.356***	−0.023	0.4072***
	(0.276)	(0.247)	(0.296)	(0.267)	(0.237)	(0.290)	(0.132)	(0.137)	(0.1349)
Technology Risk Perception	0.330**	0.426***	0.338**	0.036	0.071	0.044	0.062	0.071	0.1582*
	(0.161)	(0.165)	(0.149)	(0.184)	(0.171)	(0.178)	(0.081)	(0.086)	(0.0820)
Financial Risk Perception	0.855**	0.261	0.778**	−0.396	−0.446	0.026	0.134	0.118	0.2875*
	(0.340)	(0.311)	(0.308)	(0.311)	(0.280)	(0.312)	(0.163)	(0.177)	(0.1621)
Policy Support	−1.708***	−5.591	−1.408***	−1.789***	−1.220***	−1.497***	−1.060***	−0.913***	−0.8087***
	(0.473)	(119.873)	(0.415)	0.450*	0.397*	0.714**	(0.236)	(0.333)	(0.2128)
Control variables	Controlled			Controlled			Controlled		
Constant	1.485	−2.117	−1.033	−0.191	−2.007*	−0.148	1.113	−0.796	0.5057
	(1.749)	(1.508)	(1.605)	(1.305)	(1.152)	(1.295)	(0.693)	(0.722)	(0.6958)
atrho21	0.954*** (0.265)			0.753*** (0.205)			0.323*** (0.078)		
atrho31	1.434*** (0.377)			0.895*** (0.193)			0.685*** (0.082)		
atrho32	0.853*** (0.298)			0.947*** (0.281)			0.310*** (0.078)		
Wald value	74.11			67.87			95.85		
Log-likelihood	−150.582			−168.220			−868.825		

in the FSS under the differences in production factor endowments. The specific form of the model is as follows.

$$y^{\star} = \partial_0 + \sum_i \partial_i x_i + \varepsilon \tag{1}$$

$$y = \begin{cases} 1, y^{\star} > 0 \\ 0, \text{else} \end{cases} \tag{2}$$

In both equations, $y^{\star}$ is the latent variable, y is the observed variable of the dependent variable, x_i is the explanatory variable, and i is the number of explanatory variables. It can be seen from Equation 2 that if $y^{\star} > 0$, then $y = 1$, indicates that there is a deviation between rural households' demands and adoption behavior of services; ∂_i , β_i are estimated parameters and ε is a random disturbance term that follows the mean of 0, a multivariate normal distribution of covariance which is ψ , i.e., $\varepsilon \sim MVN(0, \psi)$. The simulated maximum likelihood estimation of Equation 3 can be used to obtain the estimated value of the model parameters.

4.1.2 Poisson model

The degree of deviation of RHDAB on FSS is to count the number of deviations between rural households' demands and adoption behavior in a production cycle by the Poisson Model. The dependent variable Y denotes the number of behavior deviations of the FSS following a Poisson distribution with expectation u. The expression is.

$$P = \{Y = n|\mu\} = \frac{e^{-\mu}\mu^n}{n!} \tag{3}$$

Where $E(Y) = Var(Y) = \mu$. n denotes the number of outsourcing links ($0 \le n \le 3$), while assuming that X_{hl} denotes the matrix of observations obtained from h independent variables after l observations, the Poisson regression model can be obtained by introducing the linkage function $\ln(\mu)$.

$$\ln(E(Y|X)) = \ln(\mu) = X\alpha = \sum_h \alpha_h x_h \tag{4}$$

The estimated value of α_h the equation indicates that the expected value becomes a multiple $\exp(\alpha_h)$ when the independent variable x_h is changed by one unit.

4.2 Data

The data in this paper come from the subject group's research of 787 farm households in 6 counties (cities) in Zhejiang, Jiangxi, and Fujian provinces. The reason why we choose to investigate the farmers of forestry production and operation in Zhejiang, Jiangxi, and Fujian is that these three provinces are all important forestry provinces in south China, with forest coverage rates above 60%. They are also important timber and bamboo forest production areas

TABLE 5 Heterogeneity analysis of different forestry operation scales.

Variable name	Smallholder rural household			Scale households		
	Model (16): FSCTS	Model (17): PCS	Model (18): FPCMS	Model (19): FSCTS	Model (20): PCS	Model (21): FPCMS
Business Risk Perception	0.404***	0.055	0.579***	0.418**	0.010	0.511**
	(0.127)	(0.125)	(0.128)	(0.198)	(0.188)	(0.203)
Technology Risk Perception	0.131*	0.153**	0.190**	0.074	0.207	0.284**
	(0.075)	(0.078)	(0.075)	(0.128)	(0.134)	(0.127)
Financial Risk Perception	0.216	0.179	0.222	−0.206	−0.292	0.297
	(0.153)	(0.159)	(0.153)	(0.238)	(0.228)	(0.221)
Policy Support	−1.332***	−1.052***	−1.129***	−1.523***	−1.269***	−1.089***
	(0.220)	(0.284)	(0.192)	(0.306)	(0.406)	(0.271)
Control variables	Controlled			Controlled		
Constant	0.618	−1.150	−0.383	1.889*	−0.693	−1.034
	(0.787)	(0.799)	(0.784)	(1.113)	(1.080)	(1.063)
atrho21	0.461*** (0.081)			0.523*** (0.136)		
atrho31	0.794*** (0.083)			0.836*** (0.157)		
atrho32	0.320*** (0.077)			0.567*** (0.147)		
Wald value	137.01			98.44		
Log likelihood	−901.509			−327.558		

in China. Therefore, it is more representative to investigate the influence of the deviation of RHDAB there, which can also be used as a reference for other provinces. The research team selected the samples strictly following the stratification principle of random sampling. According to the forestry production in each region, two counties (6 in total) were selected in each sample province, three townships were randomly selected in each county according to the level of economic development, three villages were randomly selected in the selected townships, a total of 54 villages were obtained, and then 10–16 farm households were randomly selected in each village according to the size of the villages. A total of 850 questionnaires were distributed to the rural households, 820 of which were returned, and 787 valid samples were obtained by excluding those with missing key variables and major logical errors, with an effective rate of 92.59%.

4.3 Statistical description of variables

The definitions, descriptions, and descriptive statistics of all relevant variables are shown in Table 1. The mean value of the deviation of RHDAB of the FSCTS and FPCMS in the sample area was high, 0.571 and 0.662, respectively. The mean value of business risk perception was 1.967, indicating that most rural households considered the business risk perception average. Still, the technology risk perception was relatively large, and the source of funds was mainly borrowing. The average age of the sample household heads is around 50 years old, the education level is low, the percentage of village cadres is relatively small, the average number of household laborers is 2.962, the degree of forest land fragmentation is 9.441, the plots are relatively scattered, and the average household operation scale is 48.704 mu.

5 Empirical results

5.1 The influence of risk perception on the deviation of RHDAB of the FSS

This paper empirically analyzed the effects of risk perception and policy support on the deviation of RHDAB of the FSS using Stata 16.0 software. The regression results are shown in Table 2. The Wald and atrho values of the Mv-probit model passed the significance test at the 1% level, indicating that the deviation of RHDAB of each link is not independent, indicating that the model's overall estimation results are good. Model 1), model 2), and model 3) are the regression results of the Mv-probit model on the deviations of RHDAB of the FSCTS, the PCS, and the FPCMS, respectively, and model 4) is the regression results of the degree of deviations of the three services above.

From the empirical results of the model in Table 2, rural households' business risk perception has a significant positive effect on the RHDAB of the FSCTS and the FPCMS. The reason may be that rural households usually consider both profit maximization and risk minimization in the production decision

TABLE 6 Robustness tests of the replacement model.

Variable name	Binary probit model			Probit model
	Model (16): FSCTS	Model (17): PCS	Model (18): FPCMS	Degree of deviation
Business risk perception	0.437***	0.042	0.567***	0.252***
	(0.101)	(0.101)	(0.100)	(0.088)
Technology risk perception	0.115*	0.157**	0.206***	0.140***
	(0.063)	(0.067)	(0.063)	(0.053)
Financial risk perception	0.111	0.036	0.220*	0.072
	(0.125)	(0.133)	(0.123)	(0.108)
Policy support	−1.436***	−1.077***	−1.068***	−1.359***
	(0.189)	(0.238)	(0.167)	(0.164)
Control variables	Controlled			
Constant	1.294*	−1.018	−0.362	
	(0.686)	(0.716)	(0.701)	
Wald value	119.17	42.97	96.84	121.11
Log likelihood	−467.695	−437.604	−450.736	−779.018

TABLE 7 Results of Heckman's two-stage endogeneity treatment.

Variable name	Model (19) whether to deviate		Model (20) degree of deviation	
Business risk perception	0.524***	(0.118)	0.122*	(0.067)
Technology risk perception	0.275***	(0.068)	0.060	(0.041)
Financial risk perception	0.093	(0.135)	−0.048	(0.075)
Policy support	−1.138***	(0.159)	−0.969***	(0.146)
Control variables	Controlled		Controlled	
Constant	−0.250	(0.721)	0.562**	(0.284)
Inverse mills ratio (λ)			0.516***	(0.142)

process, the forest products market is a buyer's market because of the long production cycle, and the market risk is uncontrollable. Therefore, they are more inclined to adopt conservative production and management behaviors before and after production to avoid risks, making the consistency of demands and adoption behavior of the FSS lower and prone to deviation. The perception of technical risk has a significant positive effect on the RHDAB of the FSCTS, the PCS, and the FPCMS, which indicates that the higher rural households' perception of technical risk of the FSS, the more likely they are to reduce the adoption of the FSS and avoid the production risks brought by the adoption of the FSS. Thus the deviation occurs. The perception of financing risk only has a significant positive effect on the deviation of RHDAB of FPCMS, probably because FPCMS directly affects rural households' operating income. When rural households' forestry operating funds come from borrowing, they need to bear greater financing risk compared with their own funds, so to reduce financing risk, rural households are more willing to choose sale by themselves rather than choosing FPCMS, which leads to the deviation. On the other hand, in terms of the degree of deviation between the demands and adoption behavior of the FSS, it is found that the perception of operational risk and technical risk significantly contribute to the degree of deviation between the demands and adoption behavior of the FSS, probably because when rural households are not optimistic about their operational expectations and the quality of socialized services, they are willing to adopt socialized services, but they still choose to produce on their own to reduce operating costs out of the consideration of cost-benefit.

Policy support has a significant negative effect on the deviation of RHDAB of the FSCTS, the PCS, and the FPCMS, i.e., government subsidies for rural households' forestry operations can help promote their adoption behavior of the FSS and promote rural households to

convert their demands of the FSS into adoption behavior. At the same time, it can significantly reduce the degree of deviation of RHDAB of the FSS. Government subsidies help rural households alleviate the financial constraints of forestry operation, reduce production costs, and stimulate their enthusiasm for forestry production and operation, increasing the probability of choosing the FSS and reducing the possibility of deviation. Among the control variables, whether he/she is a village cadre significantly reduces the deviation of RHDAB of the FSCTS and FPCMS and also has a suppressive effect on the degree of deviation, possibly because village cadres have a better understanding of the FSS and choose to adopt the FSS in order to reduce labor constraints, making the demands and adoption behavior consistent. The large share of forestry revenue has a positive effect on the deviation of the PCS, while forestry enthusiasm, forest land area, regional development level, and topography all have a suppressive effect on the deviation of RHDAB of the FSS to some extent.

5.2 Analysis of the moderating mechanism of policy support

The results of the above study show that risk perception has a positive and significant effect on the deviation of RHDAB of the FSS, while policy support significantly reduces the deviation. Therefore, we will further analyze the moderating effect of policy support on the impact of risk perception on RHDAB of the FSS. After adding the interaction term of risk perception and policy support to the baseline regression, the model results are shown in Table 3. After controlling other factors, the interaction term of business risk perception and policy support have a positive and significant effect on the deviation of demands and adoption behavior of the FSCTS at the 10% statistical level with a negative coefficient. This indicates that policy support can alleviate the inhibitory effect of business risk perception on RHDAB of the FSCTS. Government subsidies for rural households' forestry operations increase the marginal expectation of rural households' adoption of the FSCTS and mitigate the negative effect of business risk perception. The interaction term of technology risk perception and policy support did not have a significant effect, i.e., government subsidies did not improve the effect of rural households' technology risk perception on behavior deviation. The effect of the interaction term of financial risk perception and policy support on behavior deviation of the PCS and FPCMS was significant at the 10% and 1% levels, respectively. While the interaction term of financial risk perception and policy support also had a significant inhibitory effect on the degree of deviation. The cause maybe is that government financial subsidies, to a certain extent, alleviate the constraints of rural households' operating funds and make them more willing to optimize resource allocation through the FSS, thus reducing the deviation.

5.3 Heterogeneity analysis

5.3.1 Heterogeneity analysis of economic development levels

China has a vast territory, and different regions have differences in capital endowment, such as physical capital, human capital, and social capital, and differences in factors, such as economic development level, resulting in obvious regional imbalance. The demands and adoption behavior of FSS is not only influenced by risk perception and policy support but also rooted in the local economic environment. Therefore, there may be regional differences in RHDAB of FSS. To further explore the differences among different levels of economic development, this paper conducted group regressions according to low, medium, and high levels of economic growth, and the results are shown in Table 4. Compared with the low economic development level area, the effect of business risk perception on the deviation of RHDAB of the FSS is more prominent in the medium and high economic development level area. The reason is that rural households in low economic development level areas are more involved in the forestry business and have more in-depth knowledge of forestry business risk perception. Still, more rural households are part-time and mainly non-farm work in high economic development areas. This quickly reduces the adoption behavior of the FSS due to business risk perception and hinders the conversion of demands into adoption behavior. In contrast, the technology risk perception and the financial risk perception have a more significant positive effect on the deviation of RHDAB of the FSS in areas with low economic development. i.e., it prevents rural households in areas with low economic development from converting their demands into adoption behavior on the FSS. This may be because rural households in low economic development areas do not have timely access to information, do not know enough about forestry technology, are also influenced by financial constraints, and tend to rely on family businesses rather than adopting the FSS in order to avoid risks.

5.3.2 Heterogeneity analysis of forestry operation scale

The continuous promotion of collective forest rights reform, forest land transfer, and moderate scale operation make the main forestry production body present the *status quo* of scale operation main body, and small rural households co-exist. Farmers of different operation scales have differences in resource endowment and production conditions, which may lead to different response levels to risk perception and policy support, and ultimately affect the deviation degree of RHDAB of FSS. In view of this, this paper regressed the forestry operation area in groups according to the mean value, and the forestry operation area of small-scale households was less than the mean value of 48 mu. In comparison, the large-scale households were greater than 48 mu. The regression results in Table 5 show that the business risk perception significantly promotes the deviation of RHDAB of the FSCTS and FPCMS for both small and large scale households. This indicates that both small-scale and large-scale households, when their business risk perception is large, will reduce the probability of outsourcing, which easily affects the output and operating income level. The technology risk perception only has a significant positive effect on the deviation of demands and adoption behavior of the FPCMS for large-scale households. However, it has a significant promoting effect on the deviation of all three segments of the FSS for small-scale households, indicating that the technology risk perception has a more significant effect on the deviation for small-scale households than for large-scale households. It may be that small-scale households have a low level of knowledge about forestry production technology and have a path dependence on traditional forestry management. So they will choose to operate their business by themselves to ensure that forestry output will not be affected when unsure about the technology risk perception, which will be more likely to have the deviation of demands and adoption behavior.

5.4 Robustness test

5.4.1 Replacement model

The previous analysis concluded that risk perception significantly promotes the deviation of RHDAB of the FSS. This paper further replaces the estimation method for validation to test the robustness of the findings. Specifically, a binary probit model was used to explore the effect of risk perception on the deviation of RHDAB of the FSS in different segments. From the results in Table 6, we can see that business risk perception has a significant positive effect on the deviation of RHDAB of the FSCTS and the FPCMS. In contrast, technology risk perception has a significant positive effect on the deviation of RHDAB of the FSS in the three segments. Financial risk perception only has a significant positive effect on the deviation of RHDAB of the FPCMS. Regarding the effect on the degree of deviation, both the business risk perception and the technology risk perception significantly promote the degree of deviation. On the other hand, policy support has a significant inhibitory effect on both the deviation of RHDAB of the FSS in each segment and the degree of deviation, contributing to the consistency of demands and adoption behavior. This is consistent with the previous study's findings, which verifies the validity of the analysis.

5.4.2 Heckman's two-stage approach to test and deal with endogeneity

Rural households follow two steps in making decisions about the deviation of demands and adoption behavior of the FSS: the first step is whether to deviate, and the second step is the degree of deviation. Therefore, direct estimation of the deviation of RHDAB of the FSS may have the sample bias of "focusing on the outcome but neglecting the choice." In order to accurately analyze the effect of risk perception and government support on the deviation of RHDAB of FSS, this paper uses the Heckman two-step method to eliminate the endogeneity problem caused by sample selection and enhance the robustness of its findings. As shown in Table 7, the inverse Mills coefficient passes the significance test, indicating that there is a certain selection bias in the sample. Still, the results of the Heckman two-step method show that the business risk perception and the technology risk perception have a significant positive effect on the deviation of RHDAB of FSS and the deviation degree. In contrast, government support significantly negatively affects the deviation and the deviation degree. The results are generally consistent with the above analysis, indicating that although there is some endogeneity, the baseline regression results are still reliable.

6 Conclusions and policy recommendations

Based on the rural households' behavior theory and a survey of 787 rural households, this paper constructs a theoretical framework for the deviation of RHDAB of the FSS and the individual response mechanism of the deviation degree. The Mv-probit and Poisson models empirically analyze the risk perception and policy support on the deviation. Findings indicate that: 1) There is a large deviation of RHDAB of different types of FSS, with 57.71% and 66.20% for forestry seed and cultivation technology services and forestry product collection and marketing services, respectively. 2) Risk perception accelerates the deviation of RHDAB of FSS and the deviation degree. Technology risk perception is found to have a significant effect on the deviation of all three services, while financial risk perception only has a significant positive effect on the deviation of the forestry product collection and marketing services. Policy support is effective in significantly reducing the deviation of RHDAB of FSS and the deviation degree. 3) Policy support attenuates the influence of operational risk perception on the deviation of RHDAB of FSCTS, while policy support also moderates the deviation of financial risk perception on the deviation of the PCS and the FSCTS, with a significant negative moderating effect. 4) Heterogeneity analysis reveals that business risk perception has a more significant effect on the deviation of RHDAB in areas with medium to high economic development levels, while technology risk perception and financial risk perception have a positive effect on the deviation of RHDAB mainly in areas with low economic development levels. For rural households of different forestry business scales, business risk perception has a significant positive effect on the deviation of RHDAB for both small and large scale rural households. However, technology risk perception has a more significant effect on the deviation for small rural households.

In light of the research findings, this paper provides several policy recommendations: First, a sound forestry risk management system is needed to reduce farmer management risk reasonably. To expand the coverage of forestry insurance, adjust and improve the forest insurance system, encourage all localities to carry out insurance of forest products with advantages and characteristics according to local conditions, and accelerate the extension of forestry insurance to the whole forestry industry chain. We should give full play to the guiding role of reinsurance, establish a risk-sharing mechanism, prevent and resolve systemic risks in the forestry operation process, and strengthen the strategic layout and forward-looking plan of forestry risk management. Second, accelerate the development of inclusive finance in rural areas and increase policy support for forestry. Solve the problem of farmers' loans through multiple channels, and dissolve the financial constraints of farmers' purchase of services, such as establishing a special fund, reducing the loan interest rate, or implementing financial policy discounts. Promoting the allocation of financial resources to farmers in remote forest areas, and ensuring that total credit to farmers in forest areas continues to increase and the proportion of loans to farmers is not reduced. Third, establish a regional forestry socialized service platform to strengthen the function of the FSS system. More attention should be paid to the socialized service supply in forestry production and marketing links. Exchanges between service subjects, between service subjects and rural households, and between rural households on the supply of good seed, forestry cultivation techniques, and forest product sales experience should be carried out from time to time to improve rural households' rational decision-making ability in the demand for FSS and guide and stimulate the conversions of rural households' demand to adopt behavior with high-quality and efficient services.

Data availability statement

The datasets used during the current study are available from the corresponding author on reasonable request.

Author contributions

WL: writing, methodology, software; RY: data curation, writing—original draft preparation; XZ: validation, investigation. NL: software, validation. CZ: writing—reviewing and editing. All authors contributed to the article and approved the submitted version.

Funding

This study was financially supported by the National Natural Science Foundation of China (71873060, 71934003, 72263017), the Social Science Foundation Project of Jiangxi Province (22YJ40), the University's Humanities and Social Sciences Youth Project of the Jiangxi Province (JJ21205), Jiangxi Post-doctoral Science Foundation (2021RC05) and Jiangxi Post-graduate Innovation Fundation (YC2022-B105).

Acknowledgments

The authors thank referees for their helpful comments.

Conflict of interest

The authors declare that the research was conducted in the absence of any commercial or financial relationships that could be construed as a potential conflict of interest.

Publisher's note

References

Botzen, W., Aerts, J., and van den Bergh, J. C. J. M. (2009). Willingness of homeowners to mitigate climate risk through insurance. *Ecol. Econ.* 68 (8-9), 2265–2277. doi:10.1016/j.ecolecon.2009.02.019

Dorward, A., and Chirwa, E. (2011). The Malawi agricultural input subsidy programme: 2005/06 to 2008/09. *Int. J. Agric. Sustain.* 9 (1), 232–247. doi:10.3763/ijas.2010.0567

Du, M., Feng, R., and Chen, Z. (2022). Blue sky defense in low-carbon pilot cities: A spatial spillover perspective of carbon emission efficiency. *Sci. Total Environ.* 2022, 157509. doi:10.1016/j.scitotenv.2022.157509

Duan, W., ShenHogarth, J. N. J., and Chen, Q. (2021). Risk preferences significantly affect household investment in timber forestry: Empirical evidence from fujian, China. *For. Policy Econ.* 125 (5), 102421. doi:10.1016/j.forpol.2021.102421

Haas, H. D. (2006). Migration, remittances and regional development in southern Morocco. *Geoforum* 37 (4), 565–580. doi:10.1016/j.geoforum.2005.11.007

Howard, D., Leathers, J., and Quiggin, C. (1991). Interactions between agricultural and resource policy: The importance of attitudes toward risk. *Am. J. Agr. Econ.* 73 (3), 757–764. doi:10.2307/1242828

Hull, J. R. (2007). Migration, remittances and monetization of farm labor in subsistence sending areas. *Asian Pac. Migr. J.* 16 (4), 451–484. doi:10.1177/011719680701600402

Hyde, W. F., and Yin, R. (2018). 40 years of China's forest reforms: Summary and outlook. *For. Policy Econ.* 98, 90–95. doi:10.1016/j.forpol.2018.09.008

Ji, C., Guo, H., Jin, S., Jin, Y., and Ma, W. (2017). Outsourcing agricultural production: Evidence from rice farmers in Zhejiang province. *PLoS One* 12 (1), e0170861. doi:10.1371/journal.pone.0170861

Just, R. E., and Pope, R. D. (1979). Production function estimation and related risk considerations. *Am. J. Agric. Econ.* 61 (2), 276–284. doi:10.2307/1239732

Kahneman, D., and Tversky, A. (2013). "Prospect theory: An analysis of decision under risk," in *Handbook of the fundamentals of financial decision making* (Columbia, Canada: University of British), 99–127.

Kong, F. B., Ruan, H., and Liao, W. M. (2017). Construction of a new socialized forestry service system: Literature review and research prospects. *Issues For. Econ.* (06), 90–96. (in chinese).

Kotler, P., and Armstrong, G.(1994).*Marketing management, analysis, planning, implementation, and control, Philip Kotler*. London: Prentice-Hall International.

Kurkalova, L. A., Kling, C. L., and Zhao, J. (2006). Green subsidies in agriculture: Estimating the adoption costs of conservation tillage from observed behavior. *Can. J. Agric. Economics/Revue Can. d'agroeconomie* 54 (2), 247–267. doi:10.1111/j.1744-7976.2006.00048.x

Liao, W. M., Zhang, G. L., and Kong, F. B. (2016). Analysis on characteristics and influencing factors of farmers' demand for the FSS: Based on a survey of 1413 farmers in 8 provinces (autonomous regions. *Sci. Silvae Sin.* 52 (11), 148–156. (in chinese).

Liu, C., Liu, H., and Wang, S. (2017). Has China's new round of collective forest reforms caused an increase in the use of productive forest inputs? *Land Use Policy* 64, 492–510. doi:10.1016/j.landusepol.2017.03.011

Liu, E. M., and Huang, J. K. (2013). Risk preferences and pesticide use by cotton farmers in China. *J. Dev. Econ.* 103, 202–215. doi:10.1016/j.jdeveco.2012.12.005

Liu, P., Yin, R. S., and Li, H. (2016). China's forest tenure reform and institutional change at a crossroads. *For. Policy Econ.* 72, 92–98. doi:10.1016/j.forpol.2016.06.019

Luo, B. L. (2017). On Service scale Management - from vertical division of labor to horizontal division of labor and serial specialization. *China Rural. Econ.* 11, 2–16. (in chinese).

Luo, X. F., Xiang, X. X., and Li, R. R. (2016). What are the most urgent agricultural socialization services for large growers. *J. Agrotechnical Econ.* (05), 4–12. (in chinese).

Lusk, J. L., and Coble, K. H. (2005). Risk perceptions, risk preference, and acceptance of risky food. *Am. J. Agric. Econ.* 87 (2), 393–405. doi:10.1111/j.1467-8276.2005.00730.x

Martell, D, L., Stocks, B., and Wang, J. (2016). Forest fire management expenditures in Canada: 1970-2013. *For. Chron.* 92, 298–306. doi:10.5558/tfc2016-056

Mitchell, V. W. (1999). Consumer perceived risk: Conceptualisations and models. *Eur. J. Mark.* 33 (1/2), 163–195. doi:10.1108/03090569910249229

Olmstead, A. L. (1975). The mechanization of reaping and mowing in American agriculture, 1833-1870. *J. Econ. Hist.* 35 (02), 327–352. doi:10.1017/s0022050700075082

Qin, P., Carlsson, F., and Xu, J. (2011). Forest tenure reform in China:a choice experiment on farmers' property rights preferences. *Land Econ.* 87 (3), 473–487. doi:10.3368/le.87.3.473

Roumasset, J. A. (1977). Rice and risk: Decision-making among low-income farmers. *Econ. J.* 87 (348), 825. doi:10.2307/2231398

Schmook, B., and Radel, C. (2008). International labor migration from a tropical development frontier: Globalizing households and an incipient forest transition. *Hum. Ecol.* 36 (6), 891–908. doi:10.1007/s10745-008-9207-0

Scott, J. C. (1977). *The moral economy of the peasant: Rebellion and subsistence in southeast asia*. Connecticut, U.S: Yale University Press.

Skoufias, E., and Olivieri, S. (2013). Sources of spatial welfare disparities in Indonesia: Household endowments or returns? *J. Asian Econ.* 29, 62–79. doi:10.1016/j.asieco.2013.08.004

Slovic, P. (1987). Perception of risk. *Science* 236 (4799), 280–285. doi:10.1126/science.3563507

Xie, Y., Gong, P., Han, X., and Wen, Y. (2014). The effect of collective forestland tenure reform in China: Does land parcelization reduce forest management intensity? *J. For. Econ.* 20 (2), 126–140. doi:10.1016/j.jfe.2014.03.001

Yao, Y. (2017). Smallholder economy is not out of date, so it should not take the "bad name. *Finance Econ.* (07), 84–85. (in chinese).

Yin, R. S., Yao, S. B., and Hu, X. X. (2013b). Deliberating how to resolve the major challenges facing China's forest tenure reform and institutional change. *Int. For. Rev.* 15, 534–543. doi:10.1505/146554813809025739

Yin, R., Yao, S., and Huo, X. (2013a). China's forest tenure reform and institutional change in the new century: What has been implemented and what remains to be pursued? *Land Use Policy* 30 (1), 825–833. doi:10.1016/j.landusepol.2012.06.010

Youno, A. A.(1928).Increasing returns and economic progress.*Econ. J.*38: 527–542.

Zhang, D. W., Flick, S., and Liao, W. A. (2001). Sticks, carrots, and reforestation investment. *Land Econ.* 77 (3), 443–456. doi:10.2307/3147135

frontiers | Frontiers in Environmental Science

TYPE Policy and Practice Reviews
PUBLISHED 08 June 2023
DOI 10.3389/fenvs.2023.1200171

OPEN ACCESS

EDITED BY
Hua Lu,
Jiangxi University of Finance and Economics, China

REVIEWED BY
Tiangui Lv,
Jiangxi University of Finance and Economics, China
Bo Wen,
Nanjing Forestry University, China

*CORRESPONDENCE
Qin Wu,
1939247214@qq.com

RECEIVED 04 April 2023
ACCEPTED 30 May 2023
PUBLISHED 08 June 2023

CITATION
Li S, Wang D and Wu Q (2023), Effect of ecological civilization pilot demonstration area construction on urban land green use efficiency. *Front. Environ. Sci.* 11:1200171. doi: 10.3389/fenvs.2023.1200171

Effect of ecological civilization pilot demonstration area construction on urban land green use efficiency

Shaojie Li[1], Duoduo Wang[2] and Qin Wu[3]*

[1]Hubei Institute of Economic and Social Development, Central China Normal University, Wuhan, China, [2]College of Agricultural Economics and Technology, Jiujiang Vocational University, Jiujiang, China, [3]School of Public Administration, Central China Normal University, Wuhan, China

Improvement of urban land green use efficiency (ULGUE) in the context of sustained economic growth is a major challenge for the regional sustainable development and ecological civilization construction in China. This study measures the ULGUE of 263 cities in China at the prefecture or above level, clarifies its spatio-temporal changes, investigates the effect of ecological civilization pilot demonstration area construction on ULGUE with the multi-period PSM-DID model and spatial Durbin difference model, and evaluates the spatial spillover effect of the policy. The results show that: 1) In terms of spatio-temporal changes, ULGUE shows a steady upward trend with time. From 2006 to 2019, the national mean value of ULGUE increases from 0.5284 to 0.6439, with an increase rate of 21.86%; in the spatial dimension, ULGUE is characterized by a pattern of eastern > national > central > western. 2) Ecological civilization pilot demonstration area construction has significantly improved the ULGUE of pilot cities by about 0.12% relative to that of non-pilot cities, which was validated by the robustness test. 3) Ecological civilization pilot demonstration area construction has significant positive spillover effects on the ULGUE of neighboring cities, which are related to the urban characteristics such as geographical location, resource endowment, and environmental protection intensity. 4) Ecological civilization pilot demonstration area construction has certain heterogeneity in its effect on ULGUE in different regions and cities, with a more significant promoting effect for non-eastern regions, non-resource-based cities, and non-key cities of environmental protection. Therefore, it is necessary to summarize the successful experience of ecological civilization pilot demonstration area construction and fully consider differential policies, so as to maximize the policy dividends while strengthening regional linkage, and further contribute to national popularization of this policy.

KEYWORDS

ecological civilization pilot demonstration area, urban land green use efficiency, multi-period PSM-DID model, policy spillover, spatial heterogeneity

1 Introduction

Urban land use efficiency is an important factor affecting urban sustainable development and high-quality economic development. In the early stage, countries in the world tend to promote national economic growth while overlooking environmental pollution. Due to its unique land-based development model, China has become the fastest growing economy in

the world over the past 30 years; however, as China's economic development stage changes, the unsustainability of the traditional land use model has become increasingly apparent (Liu S Y et al., 2020). With the continuous acceleration of urbanization in most countries around the world, a series of problems such as environmental degradation and human-land conflicts have emerged gradually, with corresponding countermeasures successively introduced by each country (Pata., 2018). China's built-up area grows to 62,400 km^2 by 2021, with an increase of 36.99% compared with that 10 years ago[1]. China's idle land in development zones alone reached 67,000 ha in 2020, with a continuous increase for two consecutive years[2]. The uncontrolled expansion of urban boundaries has resulted in inefficient urban land use and increasingly serious environmental pollution, leading to serious contradictions and conflicts between sustainable urban development and China's ecological security (Tan et al., 2005; Wei et al., 2016). It is urgent to transform the traditional extensive urban land use to green and intensive urban land use. Therefore, China has put forward the important concept of "Lucid waters and lush mountains are invaluable assets"[3], which is mainly aimed at transforming land use patterns, improving the living environment of both urban and rural residents, and strengthening the protection of resources and environment, and has expounded the great importance of green development. Accordingly, the focus of urban development in China has gradually shifted from blind pursuit of high-speed economic growth to seeking of a balance between economy and ecology, and environmental governance and ecological restoration have made certain progress. In this context, urban land green use efficiency (ULGUE), a new concept combining the two core elements of "green" and "efficiency", emerges as the focus of regional sustainable development, whose importance has been widely recognized by the political and academic communities (Zhang Q et al., 2022). As an important standard to evaluate the green use of urban land, ULGUE is different from traditional land utilization efficiency. The core of ULGUE is to minimize urban land input factors and environmental costs as much as possible under certain production technology conditions to achieve the maximum economic output. Tan et al. (2021) combine the environmental pollution characteristics of urban land use activities and consider urban pollution index as "undesirable" output, achieving an efficient and green land use evaluation system. Therefore, this study mainly considers the coordination and unity of economic and environmental factors in the process of urban land use.

In 2013, China's ecological civilization construction largely lagged behind the economic and social development as a whole. The laws, regulations, and their implementation could not meet the requirements of ecological civilization construction. Hence, China proposed to establish ecological civilization pilot demonstration area and plans by selecting regions with different developmental stages, resource endowments, and main functional requirements (provinces, cities, counties, towns, and villages), aiming to explore a typical and replicable mode of ecological civilization to be popularized nationwide, aiming to promote the economic indicators such as the total output value per unit area to the top in the country. Resource utilization indicators such as resource input-output ratio and resource consumption per unit output value have achieved significant breakthrough. Land resources such as forests and lakes have become low-carbon, green, and efficient in utilization, and the ecological environment has been restored. Fujian Province was appointed as the first ecological civilization pilot demonstration area in March 2014. In the following years, Fujian Province has achieved fruitful results in ecological construction: in 2020, its energy consumption per unit of GDP dropped by about 1.83% year on year[4], and its energy conservation and consumption reduction were always one of the highest in the country; in 2021, its forest coverage rate reached 66.80% and had ranked the first in the China for many consecutive years[5]. Then, based on voluntary application, the National Development and Reform Commission announced the list of two batches of ecological civilization pilot demonstration areas in 2014 and 2015, and successively approved a total of 100 regions such as Miyun County, Beijing, Chengde City, Hebei Province, Qingpu District, Shanghai, and Jialing River Basin in Sichuan Province as ecological civilization pilot demonstration areas, which cover 47 prefecture-level cities[6] (distribution of cities in the ecological civilization pilot demonstration area is shown in Figure 1).

Construction of ecological civilization pilot demonstration area is guided by ecological civilization and green development, aiming to significantly improve the level of urban greening by establishing a full-coverage indicator system. The system mainly includes the strictest protection and management for resources and environmental aspects such as land and resource allocation, green energy conservation and emission reduction, and ecological environment implemented to promote the construction of ecological civilization, so as to build a green development pattern with an appropriate balance between social or economic development and ecological civilization construction. According to the environmental Kuznets curve, the relationship between economic development level and environmental pollution degree displays an inverted "U" shape. In recent years, China has attached increasing importance to its own environmental problems, and the

1 The data is from the Ministry of Housing and Urban-Rural Development of China. https://www.ceicdata.com/zh-hans/china/urban-area/area-of-built-district

2 The data is from the "Notice on the Monitoring and Statistics of Land Intensive Use in National Development Zones in 2020" issued by the People's Government of the People's Republic of China. http://www.gov.cn/xinwen/2021-01/13/content_5579414.htm

3 Quoted in 《Readings from General Secretary Xi Jinping's Series of Important Speeches》, Study Press and People's Publishing House, 2016, p. 230

4 The data is from Fujian Provincial Statistical Yearbook

5 The data is from China Statistical Yearbook

6 The list is based on the relevant policy information published on the official website of the National Development and Reform Commission. The 47 prefecture level cities are Chengde, Zhangjiakou, Ordos, Bayannur, Siping, Yichun, Zhenjiang, Hangzhou, Lishui, Mount Huangshan, Linyi, Zibo, Zhengzhou, Nanyang, Shiyan, Yichang, Meizhou, Shaoguan, Yulin, Chengdu, Ya'an, Yan'an, Dingxi Qinhuangdao, Baotou, Wuhai, Dalian, Jilin, Baicheng, Mudanjiang, Qiqihar, Nanjing, Nantong, Ningbo, Xuancheng, Bengbu, Jinan, Xuchang, Puyang, Huangshi, Jingzhou, Hengyang, Dongguan, Guilin, Lanzhou, Jiuquan and Shizuishan

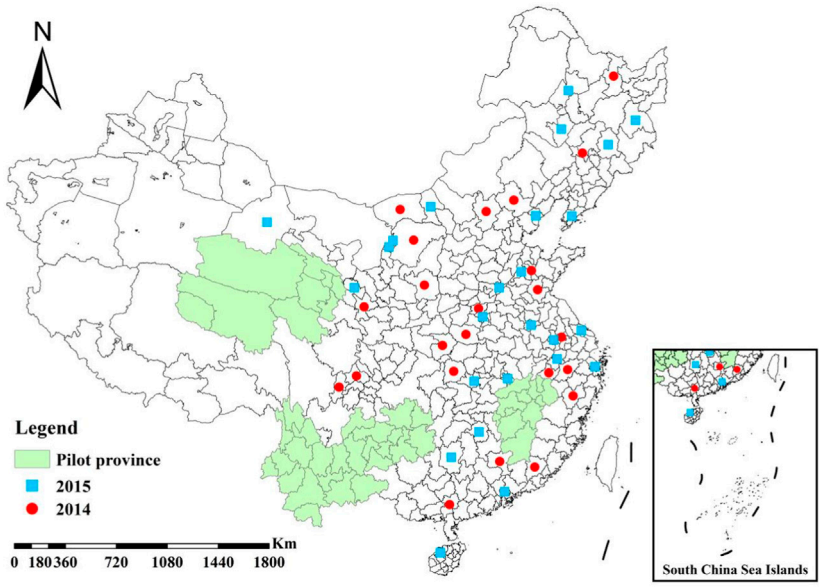

Note: This map is based on the standard map downloaded from the standard map service website of the Ministry of Natural Resources. The base map is unchanged, the same below.

FIGURE 1
Distribution of cities in the ecological civilization pilot demonstration area.

administrative units at different levels have been changing from mutual competition to cooperation, which has greatly advanced the arrival of "inflection point" of the inverted "U" curve. This not only helps China build strong confidence in dealing with environmental and development issues, but also plays an exemplary role in global environmental protection and green transformation and development, which is also of great significance to other developing countries. Obviously, whether from the perspective of practice or research value, the problems derived from interregional development in China are no longer limited to itself, but are becoming a major concern to the world. The starting point of this study is highly consistent with the above background, as it examines the policy effects presented by the ecological civilization pilot demonstration area construction, providing strong support for understanding the importance of public policies in green development. Therefore, exploring the impact of the construction of ecological civilization demonstration zones on the green utilization efficiency of urban land is a practical need to promote sustainable urban development and high-quality economic development. To this end, it is important to explore the effect of ecological civilization pilot demonstration policy on ULGUE in the pilot area and neighboring areas, and whether the effect has certain heterogeneity under different urban characteristics. This study seeks to answer these questions.

The possible marginal contributions of this study are as follows: 1) Theoretically, the connection channel between ecological civilization pilot demonstration policy and ULGUE is built at the municipal level. At the same time, by taking ULGUE as a breakthrough point, this study analyzes the policy effect of ecological civilization demonstration area construction, which is conducive to further enrichment of research on the theme of ULGUE and ecological civilization demonstration area construction. 2) Practically, the multi-period PSM-DID model and SDM-DID model are established in this study to solve the endogeneity problem in previous research, while the spatial Durbin difference model is adopted to deeply investigate the implementation effect of ecological civilization demonstration area construction with full consideration of spatial factors on policy effect, which not only helps to solve problems in the policy implementation process, but also provides a reference for the nationwide promotion of pilot policy.

2 Literature review

The literature related to this study can be mainly classified into two categories. The first category is related to ULGUE, and the research can be roughly divided into two stages. The first stage (2009–2019) is a concept formation stage, at which the concept of ULGUE is at its infant stage, but the prototype is already formed. Many researchers have noticed the relation between urban land use and green development, in view of the problem of pollution in the process of urban land use, and relevant studies have started to incorporate the pollutants of "three wastes" as an undesirable output into the measurement system of urban land use efficiency (Fukuyama and Weber, 2009; Verburg et al., 2010; Li et al., 2017; Zhao et al., 2018). The second stage (2019 to now) belongs to the concept development stage, at which ULGUE is explicitly introduced and conceptualized. The concept of ULGUE can be broadly divided into two schools of thoughts: one is defined based on the eco-socio-economic benefits of land use, and the other is defined through factor inputs and outputs (Wang and Pang, 2019; Liang

et al., 2019). In terms of the influencing factors of ULGUE, previous research is usually focused on four aspects: economic factors (Hu and Qian, 2017), social factors (Nesru et al., 2021; Zhao et al., 2021; Zhao and Jiang, 2022), traffic location (Desalvo and Su, 2017), and policy factors (Macedo., 2008; Wang and Chi-Man, 2017). Besides, there have also been some studies concerning the internal relationship of industrialization (Ghosh and Chifos, 2017; Bird and Venables, 2020), urbanization (Hsing-Fu and Ko-Wan, 2015; Marco et al., 2015), regional integration (Cancello et al., 2020) with ULGUE. In the above studies, the econometric model was the mostly used tool to analyze issues related to ULGUE, mainly including the parametric method represented by stochastic Frontier production function model (Dong et al., 2020; Liu S C et al., 2020; Lu X et al., 2022), the non-parametric method represented by Data Envelopment Analysis (DEA) model (Fang et al., 2013; Lu et al., 2020; Chen et al., 2021; Liu et al., 2021; Ruan et al., 2022), SBM model and its improved model (Lin and Ling, 2021; Tang et al., 2021; Li et al., 2022). Compared with non-parametric methods such as DEA, which measure the land use efficiency through the linear programming model, the stochastic Frontier production function model can eliminate the impact of random factors through parameter estimation, and is more advantageous in evaluating land use efficiency (Gong and Sickles, 1989). Construction of an input-output indicator system is the framework for using the SFA model to analyze the efficiency of urban land use. In the existing research, most scholars select labor, capital, and land in the classic production function as the main input factor indicators, and economic output value as the output indicator. Moreover, the specific indicators need to fully reflect the characteristics of non-agricultural production activities (Wang et al., 2015; Jin et al., 2018; Liu S Y et al., 2020; Zhang et al., 2020). This provides important technical support for this study to measure the ULGUE.

Furthermore, ULGUE is a dynamic evolution process. Considering the significant differences in geographical location, resource endowment, and environmental protection importance among different cities in China, ULGUE will exhibit unstable characteristics under the influence of various factors, with heterogeneity in different cities and development stages (Wang et al., 2018; Guo et al., 2021; Lu X H et al., 2022). Some studies have revealed the spatial correlation and evolution characteristics of ULGUE in Chinese cities from various dimensions such as national, provincial, and urban agglomeration (Yang et al., 2015). The data in different studies are selected from different periods. Non-parametric kernel density estimation and statistical charts are mainly used to reflect the evolution characteristics and trend changes of ULGUE in a specific time period (Hu et al., 2018).

The second category of literature is focused on ecological civilization construction. Western scholars prefer to study the relationship between urban economic development and ecological environment protection (Dixon, 1997; Ms et al., 2022). Although they rarely mention the term “ecological civilization”, their study focus is highly similar to the concept of “ecological civilization” in essence. Research on ecological civilization in China began in 1982. In terms of indicator construction, with the issuance of the Measures for Evaluation and Assessment of the Objectives of Ecological Civilization Construction, the evaluation system of ecological civilization construction has been gradually developed to integrate economy, society, and environment, to explore and analyze the balance between ecological civilization construction and various social systems (Chen et al., 2020). In the research on ecological civilization construction, evaluation of the effect of pilot policies has always been hotspot of research. Among them, research on “ecological civilization pilot demonstration area” is mainly carried out on the provincial (Lv et al., 2022) or national scale (Zhang and Fu, 2023), and the synthetic control method (Chai et al., 2022; Wang K L et al., 2022) and difference-in-difference model (Hou et al., 2022; Zhang et al., 2023) are the mostly used methods. It has been found that the construction of ecological civilization pilot demonstration area can improve agricultural green efficiency (Lu and Xiong, 2020) and ecological total factor productivity (Pan et al., 2022), as well as inhibit carbon emissions (Zhang and Fu, 2023). Some studies are also focused on ecological civilization construction and new urbanization (Wang W X et al., 2022), resource recycling (Wang A et al., 2021), and industrial green transformation (Zhang W X et al., 2022). Some scholars have also explored the relationship between ecological civilization construction and urban land use. Some of them believe that in the context of ecological civilization construction, attention should be paid not only to the efficiency of urban land use, but also to the “undesired output” in the process of urban land use, and to the low-carbon, green and circular development of urban land use to prevent the ecological environment of land resources from being threatened (Liu J et al., 2022; Xiao et al., 2022; Zhang and Zhang, 2022). Sheng and Tan (2014) explored urban land carrying capacity evaluation method under the requirement of ecological civilization. The case analysis shows that it is practical to carry out the ecological civilization-related method. In summary, studies have been conducted to initially assess the policy of “ecological civilization pilot demonstration area”. However, the content of the studies is relatively homogeneous, and there is little literature that directly integrates both urban land use efficiency and ecological civilization pilot demonstration area construction into a unified framework. Moreover, it remains unclear whether the ecological civilization pilot demonstration area can improve urban land green use efficiency, which is exactly the concern of this study.

3 Mechanism analysis

In order to clarify the effect of establishing ecological civilization demonstration areas on ULGUE, this study tries to explore the inherent logic of ecological civilization demonstration area construction influencing ULGUE. The specific aspects are as follows:

Direct effect. In 2013, the Chinese government issued “National Ecological Civilization Pilot Demonstration Area Construction Plan (Trial)", clearly stating that the ecological civilization pilot demonstration area in China aims to spur up high-quality economic development, promote the saving and utilization of resource and energy, enhance ecological construction and environmental protection, and cultivate ecological culture and corresponding system and mechanism, which are the five major construction targets. All these targets are likely to influence ULGUE to some extent. Some scholars have pointed out the bidirectional coupling relationship between high-quality economic development and ULGUE. Social and economic development depends on utilization activities on urban construction land, and urban land

use can help promote high-quality economic development (Yu et al., 2020; Zhou et al., 2020; Wu et al., 2021; Zhang and Dong, 2022). The saving and utilization of resource and energy as well as ecological construction and environmental protection include land development intensity, unit construction land production value, and industrial waste utilization rate into the indicator system. The system and mechanism construction further incorporates resource depletion, environmental damage, and ecological benefits into the indicator system. Therefore, based on the ecological civilization demonstration area policy itself, its construction goals exert a possible direct effect on ULGUE.

Indirect effect. The ecological civilization pilot demonstration area policy is essentially a pilot policy with comprehensive application of environmental regulation means, such as mandatory policies and targeted regulations, which are used by the government to reduce the negative externality of environmental pollution in production and life. According to the Porter hypothesis, on the one hand, environmental regulation advances technological innovation of enterprises through the "reversed transmission of pressure effect" caused by cost reduction. In the long term, the technical innovation will compensate for the costs brought by environmental regulation and thereby the comprehensive land output per unit area shows a significant upward trend (Linde, 1995). On the other hand, under limitations from the certain environmental protection policy framework, the "survival of the fittest" competition law brought about by environmental regulations facilitates the elimination of outdated production capacity. The long-term "competition effect" will promote the optimization and adjustment of industrial structure, thereby improving the output quality of urban use and reduce unexpected output, which contributes to elevation of ULGUE.

4 Research design

4.1 Stochastic frontier production function model

Traditional microeconomics assumes that production entities are all economically rational with the ability to achieve production optimization, and uncontrollable random factors are the only factors that may cause deviation from the state of optimum production. However, in reality, production entities will deviate from the optimum production state due to various factors, resulting in very low efficiencies. In stochastic Frontier theory, the goal of production entities to pursue optimum production is still valid, but in reality some other factors besides the uncontrollable random factors can also cause deviation from the optimum production state. Therefore, a concept of "production Frontier" emerges, which refers to the boundary of minimum input and maximum output for production entities under certain technical conditions. In the process of urban development, it is difficult for land use to achieve the optimal output with minimum input. Therefore, the stochastic Frontier theory can be used to analyze land use efficiency. It is believed that under certain technical conditions, the urban land use efficiency will be higher when the actual output of urban land use gets closer to the production Frontier, and *vice versa*. This study establishes the stochastic Frontier production function model in the Cobb-Douglas function form. The specific model is as follows:

$$Y_{it} = f\left(X_{it}, t; \beta\right) \exp\left(V_{it} - U_{it}\right) \tag{1}$$

In the formula, Y_{it} represents the output per unit area; f is the random Frontier production function; X_{it} is the input factor vector; β refers to the coefficient vector to be estimated; V_{it} is the random error term; i and t represent the city and time variable, respectively; U_{it} is the inefficiency item used to measure the technical inefficiency degree, which reveals the distance from the actual output of urban land use to production Frontier, and a higher value of U_{it} means that the actual output deviates farther from the production Frontier and the urban land use efficiency is lower.

This study adopts the non-agricultural GDP per unit area and industrial wastes (waste water, waste gas, and solid waste) to represent the desirable output and undesirable output of urban land use, respectively. In addition, by referring to, the model is treated by logarithmic transformation:

$$\ln\left(y_{it}\right) = \beta_0 + \beta_{1t}\ln\left(A_{it}\right) + \beta_{2t}\ln\left(B_{it}\right) + \beta_{3t}\ln\left(C_{it}\right) + v_{it} - u_{it} \tag{2}$$

In Formula 2, y_{it} refers to the non-agricultural GDP per unit area; A_{it}, B_{it} and C_{it} represent fixed asset investment per unit area (100 million yuan/km2), employees at the end of year per unit area (10000 people/km2), and scientific expenditure per unit area (100 million yuan/km2), respectively; β_0 is the intercept term, and β_{1t}, β_{2t} and β_{3t} are elastic coefficients, respectively; v_{it} is the random error term; u_{it} is the inefficiency item, which refers to the distance between the actual output of urban land use and the production Frontier. Only when the technology is fully effective ($u_{it} = 0$), the output can be located on the production Frontier.

ULGUE can be expressed as the ratio of mean actual output to the mean under fully effective technical conditions. The specific formula is as follows:

$$ULGUE_{it} = \frac{E\left(Y_{it}|U_{it}, X_{it}\right)}{E\left(Y_{it}^{*}|U_{it} = 0, X_{it}\right)} \tag{3}$$

where Y_{it} is the actual output of urban land use, and Y_{it}^{*} is the possible maximum output under the given input conditions. The value range of ULGUE is between 0 and 1, which rejects the assumption of least squares method. Therefore, the generalized likelihood ratio is adopted to test the applicability of SFA model:

$$LR = -2\left[L\left(\omega_0\right) - L\left(\omega_1\right)\right] \tag{4}$$

Based on the connotation of ULGUE and existing research results (Lu et al., 2020; Liu J L et al., 2022), this study constructs the following indicator system to measure ULGUE (more details in Table 1). In order to meet the single output for SFA model, this study uses the entropy weight method to construct a comprehensive index of desirable output and non-desirable output to calculate the pure output value.

4.2 Multi-period PSM-DID model

By taking the ecological civilization pilot demonstration area construction as a quasi-natural experiment, this study divides the sample cities into two groups according to whether they are ecological civilization pilot demonstration areas and then compares them to evaluate the effect of the pilot policy on

TABLE 1 Evaluation index system of urban land green use efficiency.

Indicator type	Primary indicator	Secondary indicator	Unit
Input	Capital	Fixed assets investment per unit area	100 million yuan/km2
	Labor	Employees at the end of year	10000 people/km2
	Science and technology	Scientific expenditure per unit area	100 million yuan/km2
Output	Expected output	Non-agricultural GDP per unit area	100 million yuan/km2
	Unexpected output	Industrial sulfur dioxide emission per unit area	ton/km2
		Industrial waste water per unit area	ton/km2
		Industrial smoke emission per unit area	ton/km2

ULGUE. The difference-in-difference model is usually applied to evaluate the policy effect. Since the ecological civilization pilot demonstration area construction is gradually carried out in different batches, we adopt the multi-period DID model at different time points. Moreover, in order to eliminate the selectivity bias on sample processing, the propensity score matching method is used. To sum up, this study uses multi-period PSM-DID for regression analysis, and the specific model is as follows:

$$ULGUE_{it} = \beta_0 + \beta_1 Treat_{it} \times Period_{it} + \delta X_{it} + v_i + u_t + \varepsilon_{it} \quad (5)$$

In the formula, i is the city and t is the time; $ULGUE_{it}$ is the dependent variable representing the ULGUE of city i in t period; $Treat_{it} \times Period_{it}$ is the core independent variable, which is the interactive item of policy impact variable and policy time dummy variable set in this study, as the dummy variable of pilot policy; $Treat_{it}$ is assigned to 1 when a city belongs to ecological civilization pilot demonstration area and 0 otherwise; $Period_{it}$ is assigned to 1 in the year of approval and subsequent years for cities in the pilot demonstration area and the rest is 0; β_1 is the core coefficient of this study, which measures the implementation effect of ecological civilization demonstration area policy. When β_1 is significantly positive, it reveals the area construction improves urban land green use efficiency. δX_{it} is a set of control variables; u_t represents time fixed effect; v_i means individual fixed effect; and ε_i is the random error term.

4.3 SDM-DID model

In the traditional difference model, it is necessary to satisfy the hypothesis of stable direction for individual treatment effects, which means that policy intervention will not produce spillover effect due to ignorance of the spatial spillover effect of the policy. In contrast, spatial factors are added in the SDID model, and the model effectively makes up the lack of observation on the control group in the implementation of the pilot policy by investigating the spatial spillover effect. By referring to existing results (Mi et al., 2017; Jia et al., 2021), this study further adds the spatial lag term of the dependent variable on the basis of SDID model, and obtains the spatial Durbin-difference model to investigate the spatial effect of ecological civilization pilot demonstration area policy on ULGUE. The specific construction model is as follows:

$$ULGUE_{it} = \alpha_0 + \rho\sum_j W_{ij} ULGUE_{it} + \alpha_1 sdid_{it} + \theta\sum_j W_{ij} sdid_{it} + \delta X_{it} + v_i + \mu_t + \varepsilon_{it} \quad (6)$$

In the formula, $ULGUE_{it}$ is the dependent variable, urban land green use efficiency; $sdid_{it}$ is the core independent variable, which represents the interactive item of cities in the ecological civilization pilot demonstration area; X_{it} is the control variable; W is the spatial weight matrix; $\rho\sum_j W_{ij} ULGUE_{it}$ is the spatial lag term of the dependent variable, which indicates the effect of ULGUE of neighboring cities on that of pilot cities; the regional fixed effect, time fixed effect, and residual term are respectively determined by v_i, μ_t and ε_{it}.

4.4 Variable selection and data description

4.4.1 Variable selection

(1) Dependent variable: *ULGUE* from the stochastic Frontier production function.

(2) Independent variable: the dummy variable of pilot policy of the ecological civilization pilot demonstration area, which is $Treat \times Period = DID$.

(3) Control variable: By considering that other urban characteristic factors may affect the ULGUE, this study selects six variables as control variables (Table 2 for details) A) Real estate investment level (re). Inspired by the policy, the local government tends to introduce financial expenditure to real estate industry with high returns. Hence, the impact of real estate investment level on ULGUE cannot be ignored, which is represented by the completed amount of real estate development investment (Su and Yang, 2022) B) informatization level (il). Informatization is the basic condition for urban economic development. Urban information level is expressed by the ratio of the number of employees in information transmission, computer service, and software industry to that at the end of year (Song et al., 2020) C) Industrial structure (is). The industrial structure determines urban land use structure, since different industries are of different land use modes. For example, the tertiary industry is usually characterized by a high plot ratio and great land use efficiency. This study selects the added value of the tertiary industry to represent industrial structure (Peng et al., 2017) D)

TABLE 2 Variable definition.

Variable type	Variable name	Variable symbol	Variable connotation
Dependent variable	Urban land green use efficiency	ULGUE	Urban land green use efficiency of 263 cities at prefecture level and above in China from 2006 to 2019
Independent variable	Policy effect	did	The pilot city is set as 1 in the establishment year and following years, otherwise 0
Control variable	Real estate investment level	re	the completed amount of real estate development investment
	Informatization level	il	the ratio of the number of employees in information transmission, computer service and software industry to that at the end of year
	Industrial structure	is	The added value of the tertiary industry
	Infrastructure investment	ii	Per capita road area
	Ecological environment	ee	Per capita green area
	Financial develop level	fdl	The *per capita* loan balance of financial institutions at the end of year

Infrastructure investment (ii). Investment in urban infrastructure can attract the flow of factors. For most cities, more complete urban infrastructure represents higher ULGUE. Infrastructure investment is represented by *per capita* road area (Ge et al., 2021) E) Ecological environment (ee). After the material satisfaction, people tend to pursue more beautiful and livable residences. This study reflects the level of urban greening based on the *per capita* green space area, and the impact of ecological environment greening on the ULGUE (Li et al., 2022) F) Financial development level (fdl). Financial support has certain impacts on the mode, structure, and efficiency of urban land use. This study selects the *per capita* loan balance of financial institutions at the end of year to represent the financial development level (Wang X M et al., 2021).

4.4.2 Data description

In view of different effects of the policy at different administrative levels such as provinces, cities, districts and towns as well as data availability, this study excludes provinces, districts, and towns in the list of ecological civilization pilot demonstration area and cities that were withdrawn or with serious missing of data during the study period. Finally, 263 cities at prefecture level and above are retained as samples (excluding data of Tibet, Hong Kong, Macao and Taiwan), as the prefecture level and above cities accounts for 90.38% of the total number of cities in China, which has good representativeness. A total of 47cities at the prefecture level included in the list published by the National Development and Reform Commission in 2014 and 2015 are assigned to the experimental group and the remaining 216 cities are classified into the control group. The research period is 2006–2019.

The data in this study were all derived from China City Statistical Yearbook, China Urban Construction Statistical Yearbook, and statistical yearbooks of provinces and cities. A few missing data were supplemented by linear interpolation. Furthermore, in order to reduce heteroscedasticity and avoid the influence of outliers on research results, this study takes logarithms for all numerical variables. Table 3 shows the descriptive statistical results of each variable.

TABLE 3 Descriptive statistical results.

Variable type	Symbol	N	Mean	Sd	min	Max
Independent variable	Did	3682	0.0671	0.250	0	1
Dependent variable	ULGUE	3682	0.588	0.0859	0.388	0.973
Control variable	Re	3682	13.85	1.360	9.268	17.61
	Il	3682	0.0126	0.00925	0.000459	0.109
	Is	3682	15.37	1.107	12.64	19.50
	Ii	3682	2.655	0.445	0.438	4.096
	Ee	3682	17.25	32.90	0.381	491.0
	Fdl	3682	10.16	1.115	7.584	13.87

TABLE 4 Estimation results of stochastic Frontier equation.

	Coefficient	Standard-error	T-ratio
β 0	−1.058	0.037	−28.362
β 1	0.029	0.008	3.484
β 2	0.105	0.005	21.008
β 3	0.004	0.003	1.339
sigma-squared	0.039	0.003	14.492
gamma	0.772	0.014	57.109
Mu	0.347	0.038	9.252
Eta	0.029	0.002	18.590
Log likelihood function	2707.436		
LR test of the one-sided error	1954.983		

5 Empirical analysis

5.1 ULGUE measurement

Based on the input-output panel data for 263 cities in China from 2006 to 2019, the random Frontier analysis is conducted through Frontier4.1 software. The measured ULGUE results are shown in Table 4.

From the test results, LR test of the one-sided error has passed the test, with a gamma value is 0.772, indicating that the technical inefficiency accounts a lot of the error. The parameter coefficients have all passed the *t*-test, and the parameter estimation is accurate at 99% confidence level. Therefore, it is applicable and scientific to use the SFA model to calculate ULGUE in this paper. From the elasticity of input-output, $\beta 1 = 0.029$, $\beta 2 = 0.105$, and $\beta 3 = 0.004$, indicating that the comprehensive output will increase by 0.029%, 0.105% and 0.004% respectively when the fixed-asset investment per unit area, the unit employees at the end of year per area, and the scientific expenditure per unit area all increase by 1%.

Figure 2 is a line chart for the mean values of ULGUE in different regions from 2006 to 2019. Due to the imbalanced development in China, cities in different locations may have significant differences, which is likely to lead to differences in ULGUE. Therefore, by referring to "Seventh Five Year Plan", the 263 cities in China are divided into eastern, central and western regions[7]. The results show that the overall ULGUE level has been steadily increasing, while the mean value of national ULGUE is about 0.58, indicating that there is still 42% of improvement room for national ULGUE in theory.

From the perspective of time, ULGUE shows a steadily rising trend. In general, the mean value of ULGUE for 263 cities in China in 2006, 2014, 2015, and 2019 is 0.5284, 0.6018, 0.6105, and 0.6439, respectively, with an increasing rate of 21.86% during the study period. From the regional perspective, the ULGUE value shows significant differences in different regions, which follows a general pattern of eastern > national > central > western.

According to statistics, the ULGUE had been improved from 2006 to 2019 (Table 5 below), but the degree of improvement shows some differential results, with the main transformation occurs from Class II to Class I, from Class III and Class IV to Class II, and from Class V to Class III. Among them, 100% of Class II cities (38 cities) have been transformed into Class I cities; 76.32% of Class III (58 cities) and 100% of Class IV cities (85 cities) have been transformed into Class II cities; and 90.91% of Class V cities (40 cities) have been transformed into Class III cities. According to the mean value of ULGUE of each city in 2006, cities at middle and low levels (Class III and below) account for 77.95%, including 205 individual cities; in 2019, cities at the middle and low levels (Class III and below) account for 15.21%, including 40 individual cities. These results demonstrate that ULGUE in China has been significantly improved year by year during the study period.

5.2 Benchmark regression

The estimated results for the effects of ecological civilization pilot demonstration area policy on ULGUE are shown in Table 6. The dependent variable is ULGUE, and the independent variable is the policy dummy variable did of ecological civilization pilot demonstration area, which is regressed by using stata16. Model 1) and model 2) are basic regression results obtained by the DID model before and after adding control variables, based on unmatched data. Model 3) and model 4) are regression results obtained by using the PSM-DID model without and with control variables, respectively. The regression results reveal that the independent variable did is significant in the 95% confidence interval, indicating that the ecological civilization pilot demonstration area policy has a significant improving effect on ULGUE, and ULGUE in pilot cities is about 0.12% higher than that in non-pilot cities.

Among the control variables, the real estate investment level (re) has a significant negative impact on ULGUE, while the informatization level (il), industrial structure (is), infrastructure investment (ii), ecological environment (ee) and financial development level (fl) have significant positive impacts. The possible reasons are as follows. In terms of the real estate investment level, the land fiscal expenditure of local government tends to flow to infrastructure and public services to enhance urban competitive advantage, and alleviate the boundary expansion of population pressure in the downtown. This preferential behavior will increase investment in the real estate and construction industries, and then induce overcapacity caused by excessive competition in upstream raw material industries, which will have certain inhibitory effects on ULGUE (Yu and Su, 2022). Improvement of informatization level can result in Jacobs

7 The eastern region includes 109 cities: Anshan, Baise, Baoding, Beihai, Beijing, Benxi, Binzhou, Cangzhou, Changzhou, Chaozhou, Chengde, Chongzuo, Dalian, Dandong, Dezhou, Dongguan, Dongying, Fangchenggang, Foshan, Fuzhou, Fushun, Fuxin, Guangzhou, Guigang, Guilin, Haikou, Handan, Hangzhou, Hechi, Heyuan, Hengshui, Huludao, Huai'an, Jinan, Jining, Jiaxing, Jiangmen, Jieyang, Jinhua, Jinzhou, Guests Langfang, Lishui, Lianyungang, Liaoyang, Liaocheng, Linyi, Liuzhou, Longyan, Maoming, Meizhou, Nanjing, Nanning, Nanping, Nantong, Ningbo, Ningde, Panjin, Putian, Qinzhou, Qinhuangdao, Qingdao, Qingyuan, Quzhou, Quanzhou, Rizhao, Sanming, Sanya, Xiamen, Shantou, Shanwei, Shanghai, Shaoguan, Shaoxing, Shenzhen, Shenyang, Shijiazhuang, Suzhou, Suqian, Taizhou, Tai'an, Taizhou, Tangshan, Tianjin Tieling, Weihai, Weifang, Wenzhou, Wuxi, Wuzhou, Xingtai, Xuzhou, Yantai, Yancheng, Yangzhou, Yangjiang, Yingkou, Yulin, Yunfu, Zaozhuang, Zhanjiang, Zhangjiakou, Zhangzhou, Zhaoqing, Zhenjiang, Zhongshan, Zhoushan, Zhuhai, Zibo; The central region includes 105 cities: Anqing, Anyang, Bayannur, Baicheng, Baishan, Bengbu, Baotou, Chenzhou, Chizhou, Chifeng, Chuzhou, Daqing, Datong, Ordos, Ezhou, Fuzhou, Fuyang, Ganzhou, Harbin, Hefei, Hebi, Hegang, Heihe, Hengyang, Hohhot, Hulunbeier, Huaihua, Huaibei, Huainan, Huanggang, Mount Huangshan, Huangshi, Jixi, Ji'an, Jiamusi, Jiaozuo, Jincheng, Jinzhong Jingmen, Jingzhou, Jingdezhen, Jiujiang, Kaifeng, Liaoyuan, Lu'an, Loudi, Luoyang, Luohe, Lvliang, Ma'anshan, Mudanjiang, Nanchang, Nanyang, Pingdingshan, Pingxiang, Puyang, Qitaihe, Qiqihar, Sanmenxia, Shangqiu, Shangrao, Shaoyang, Shiyan, Shuangyashan, Shuozhou, Siping, Songyuan, Suzhou, Suihua, Suizhou, Taiyuan, Tonghua, Tongliao, Tongling, Wuhai, Ulanqab, Wuhu, Wuhan, Xianning Xiangtan, Xiangyang, Xiaogan, Xinzhou, Xinxiang, Xinyu, Xinyang, Xuchang, Xuancheng, Yangquan, Yichun, Yichang, Yichun, Yiyang, Yingtan, Yongzhou, Yueyang, Yuncheng, Zhangjiajie, Changchun, Changsha, Changzhi, Zhengzhou, Zhoukou, Zhuzhou, Zhumadian; The western region includes 49 cities: Ankang, Anshun, Bazhong, Baiyin, Baoji, Baoshan, Chengdu, Dazhou, Deyang, Guang'an, Guangyuan, Guiyang, Hanzhong, Jiuquan, Kunming, Lanzhou, Leshan, Liupanshui, Luzhou, Meishan, Mianyang, Nanchong, Neijiang, Panzhihua, Qingyang, Qujing, Shangluo, Shizuishan, Suining, Tianshui, Tongchuan, Weinan, Wuzhong, Wuwei, Xi'an, Xining, Xianyang, Ya'an, Yan'an, Yibin Yinchuan, Yulin, Yuxi, Zhangye, Zhaotong, Chongqing, Ziyang, Zigong, Zunyi

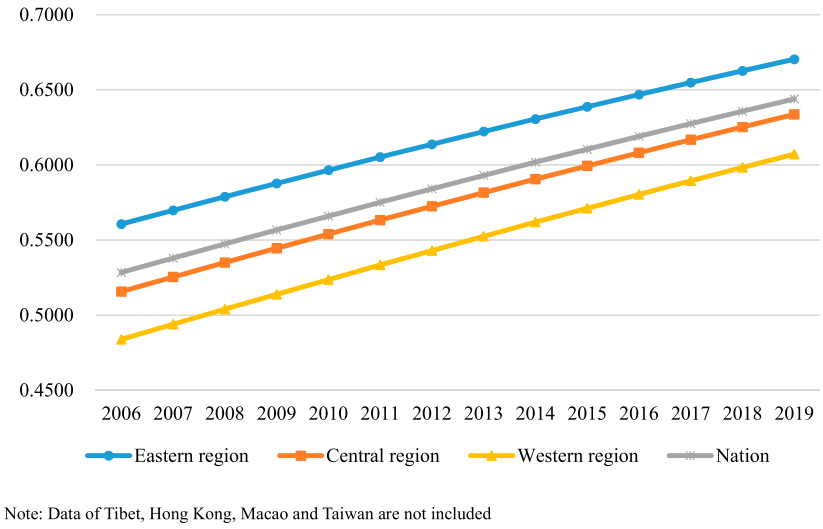

FIGURE 2
ULGUE values in different regions from 2006–2019.

technological externalities in the behavior of urban enterprises, and improve the ULGUE by enhancing economic output (Zhang and Dong, 2022). The added value of the tertiary industry, which is used to represent the industrial structure, shows a positive coefficient, possibly because the increasing added value of the tertiary industry can facilitate the steady growth of economic output per unit area and alleviate the pressure of environmental pollution caused by waste emissions, thereby improving the ULGUE. Urban infrastructure investment can attract and accelerate the flow of factors, which can stimulate the effective agglomeration of population and industries. The ecological environment can represent people's living environment and ecological benefits. Improvement of urban greenery level can improve the ULGUE by affecting the environmental output. A higher financial development level indicates that the capital is more likely to flow to high-benefit projects in a more competitive market, leading to a higher land development intensity, which can enhance the land use output and promote ULGUE.

5.3 Parallel trend test

Parallel trend test is the premise for using the difference-in-difference model to evaluate the policy effect. Based on previous research results (Beck et al., 2010), this study adopts the event study method to conduct the parallel trend test. Stata16 is used to draw the parallel trend test chart for more intuitive display of the results as shown in Figure 3, where the vertical axis represents estimated values of regression coefficients and the horizontal axis indicates the years before and after the implementation of ecological civilization pilot demonstration area policy.

As shown in Figure 3, regression coefficients are not significant before the implementation of ecological civilization pilot demonstration area policy, indicating that there is no significant difference in ULGUE before the implementation of the policy. After implementation of the policy, regression coefficients become significantly positive for three consecutive years, implying that implementation of ecological civilization pilot demonstration area policy has a significant impact on ULGUE. Therefore, it can be proved that the study passes the parallel trend test hypothesis.

5.4 Robustness test

Since an independent declaration of local government is necessary for the ecological civilization pilot demonstration area, there is a phenomenon of remarkable ecological civilization conditions in the declaration area, causing the endogeneity in this study. Therefore, a robustness test is conducted as follows. In this study, tail shrinkage treatment, lag treatment, placebo test and excluding the influence of other policies are used to test the robustness of research conclusions. For the tail shrinkage treatment, to avoid the interference of abnormal values or extreme values on the test results, core variables such as ULGUE are treated with regression after tail shrinkage of data, and the results are shown in Table 7. Model 1) is 1% tail shrinkage; model 2) is 5% tail shrinkage; and model 3) is 10% tail shrinkage. The results show that the regression coefficient is significant in the 99% confidence interval whether the samples are treated with 1%, 5% or 10% tail shrinkage, suggesting that the ecological civilization pilot demonstration area policy always has a significantly positive effect. For the lag treatment, in view of the hysteresis for the effect of ecological civilization pilot demonstration area policy, this study carries out lag treatment on the core independent variable "pilot cities", and the results are shown in columns 4) and 5) of Table 7. Among them, model 4) and model 5) display the regression results of one-period and two-period lag treatment, respectively, both of which show significantly positive coefficients. For the placebo test, experimental groups are randomly selected. To verify that the increase in ULGUE in the experimental group was indeed caused by the ecological civilization

TABLE 5 Transfer matrix of ULGUE in 2006–2019.

2006	2019					
	Class I	Class II	Class III	Class IV	Class V	Total
Class I	20	0	0	0	0	20
Class II	38	0	0	0	0	38
Class III	18	58	0	0	0	76
Class IV	0	85	0	0	0	85
Class V	0	4	40	0	0	44
Total	76	147	40	0	0	263

Note: The city numbers in Table 5 are the numbers of transformed cities. The natural breakpoint is used to classify urban land green use efficiency in 2006, and there are five types in total. Among them, Class I > 0.670, Class II (0.575~0.670); Class III (0.512~0.575); Class IV (0.456~0.512); Class V < 0.456.

TABLE 6 Benchmark regression results.

Variables	DID	DID	PSM-DID	PSM-DID
	(1)	(2)	(3)	(4)
Did	0.00131***	0.00120***	0.00132***	0.00116**
	(2.84)	(2.65)	(2.85)	(2.56)
Re		−0.00310***		−0.00320***
		(−12.57)		(−12.62)
Il		0.03267**		0.03294**
		(2.15)		(2.14)
Is		0.00518***		0.00531***
		(7.22)		(7.26)
Ii		0.00087**		0.00107**
		(1.97)		(2.32)
Ee		0.00004***		0.00005***
		(4.97)		(5.52)
Fdl		0.00232***		0.00245***
		(4.50)		(4.68)
Constant	0.52844***	0.46852***	0.52844***	0.46612***
	(1655.41)	(46.65)	(1629.83)	(45.61)
Year	Yes	Yes	Yes	Yes
City	Yes	Yes	Yes	Yes
Observations	3682	3682	3632	3632
Number of city	263	263	263	263

Note: Figures in brackets are all significant *p* values; ***, ** and * represent significance at the level of 1%, 5% and 10%, respectively, the same below.

pilot demonstration area construction, rather than being influenced by other non-observational factors, this study conducted a placebo test by randomly assigning ecological civilization demonstration zones and conducting 500 random sampling to obtain 500 estimation coefficients. Figure 4 shows the probability density distribution of the estimation coefficient, and the vertical solid line is the estimated value of the benchmark regression coefficient. It can be seen that the coefficient estimates obtained from the placebo test are concentrated around the 0 value, indicating that the random sampling sample combination has no effect on ULGUE. Therefore, it can be considered that the significant promoting effect of the ecological civilization demonstration area

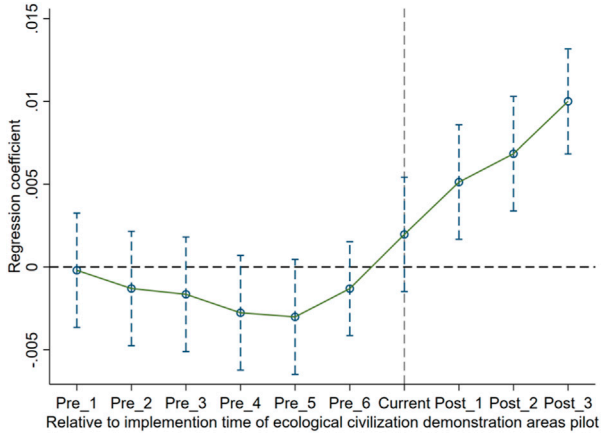

FIGURE 3
Parallel trend test.

on ULGUE is real, and the results in the benchmark regression are robust. For excluding the influence of other policies. During the long research period, ULGUE may be influenced by other similar policies. This study selects two types of policies, namely, "civilized city" and "low-carbon city", which are similar to the "ecological civilization pilot demonstration area" policy, to be included in the regression. The results are shown in Model 6) of Table 7. The results indicate that after adding other policies, the estimated coefficients remain significantly positive, with the coefficient sign unchanged and the value slightly increased, revealing that adding other policies will not affect research conclusions. These robustness test results further consolidate the reliability of basic regression results, indicating the reliability of the research conclusion that construction of ecological civilization pilot demonstration area can improve the ULGUE.

5.5 Spatial spillover effect

During the construction of an ecological civilization pilot demonstration area, neighboring cities may learn from, cooperate, and exchange with the pilot cities, which will boost the improvement of ULGUE in surrounding cities. Moreover, low-end industries unfavorable for regional development or with high pollution may be mitigated from pilot cities to neighboring cities, which will indirectly hinder the improvement of ULGUE in the neighboring areas. Hence, the next section will analyze the spatial spillover effect of ecological civilization pilot demonstration area policy.

First, a spatial autocorrelation test is performed on the dependent variable. This study conducts the global Moran test on ULGUE. A positive and negative value of Moran's I indicate the existence of positive and negative spatial correlations, respectively. Table 8 shows that in the adjacency matrix and inverse distance matrix, the Moran's I value of ULGUE is greater than 0 and increases year by year during the study period, which passes the significance test. These results indicate that the ULGUE in China has a positive correlation in space, and the clustering feature of positive correlation is increasing gradually.

Secondly, the ULGUE data in 2006 and 2019 are treated with local Moran test and a local Moran scatter diagram is plotted. The results are shown in Figure 5 (points represent cities). The first quadrant represents the "high-high" aggregation area; the second quadrant stands for the "low-high" aggregation area; the third quadrant represents the "low-low" aggregation area; and the fourth quadrant indicates the "high-low" aggregation area. As a result, most of ULGUE for Chinese cities is concentrated in the first and third quadrants, suggesting that cities in "high-high" and "low-low" aggregation areas are dominant. These results indicate that ULGUE of each city has an obvious spatial positive effect, which is consistent with the test results of global Moran's I.

Based on the above conclusions, the spatial Durbin model (SDM) is used to further estimate the effect of ecological civilization pilot demonstration area construction on ULGUE. According to the LR test and Hausman test, the results pass the significance test and reject the original hypothesis, indicating that the SDM will not degenerate into the spatial error model (SEM) and the spatial lag model (SLR) and support the fixed effect. Therefore, it is more appropriate to choose SDM with both time and individual fixed effects for analysis.

Table 9 summarizes the benchmark regression results of spatial Durbin and decomposition results of the spatial spillover effect. Among them, model 1) shows the benchmark regression results of SDM, and models (2–4) show the empirical results after decomposition of the spatial spillover effect generated by the ecological civilization pilot demonstration area policy determined with the partial differential method.

Based on the benchmark regression results of spatial Durbin, the core independent variable did is positive and significant at the level of 1%, suggesting that the implementation of ecological civilization pilot demonstration area policy contributes to the improvement of ULGUE. The spatial spillover effect is significantly positive, indicating that the implementation of this policy can improve the ULGUE of adjacent areas around pilot cities.

The direct effect in model 2) represents the local effect, which refers to the effect of ULGUE within pilot cities. The indirect effect in model 3) is the spillover effect of ecological civilization demonstration area construction in surrounding areas on the ULGUE of local areas (non-pilot cities). The total effect in model 4) represents the comprehensive impact. According to the decomposition results of spillover effect in further analysis, the direct effect, indirect effect, and total effect of ecological civilization pilot demonstration area construction are all positive and significant at the level of 1%, which is consistent with the above analysis.

These results indicate that the implementation of ecological civilization pilot policy can promote the ULGUE of the pilot cities and also have positive spillover effects on the neighboring cities. The possible reason is that the construction of pilot cities promotes the cross-regional flow of talents, capital, technologies and other factors through the scale effect and agglomeration effect, which has a spatial radiation effect on neighboring cities and then inspires surrounding cities to imitate the pilot cities, thereby indirectly achieving the upgradation of ULGUE of neighboring cities in the ecological civilization pilot demonstration area.

TABLE 7 Robustness test.

Variables	(1)	(2)	(3)	(4)	(5)	(6)
Did	0.00148***	0.00237***	0.00328***	0.00105**	0.00088*	0.00211*
	(2.65)	(2.80)	(2.88)	(2.30)	(1.68)	(1.77)
Re	−0.00364***	−0.00447***	−0.00435***	−0.00284***	−0.00249***	0.00901***
	(−11.30)	(−8.81)	(−6.15)	(−11.05)	(−8.41)	(18.97)
Il	0.05837***	0.26918***	0.43666***	0.02989*	0.03830**	0.17010***
	(2.72)	(5.30)	(5.19)	(1.94)	(2.17)	(4.39)
Is	0.00495***	0.00445***	0.00691***	0.00610***	0.00659***	0.01582***
	(5.65)	(3.82)	(5.03)	(7.47)	(6.86)	(13.83)
Ii	0.00156***	0.00241**	0.00322**	0.00081*	0.00058	0.00584***
	(2.67)	(2.49)	(2.28)	(1.76)	(1.07)	(6.08)
Ee	0.00009***	0.00015***	0.00021***	0.00005***	0.00005***	0.00020***
	(5.79)	(3.82)	(2.80)	(5.53)	(5.37)	(5.39)
Fdl	0.00288***	0.00333***	0.00165	0.00236***	0.00193***	0.02158***
	(4.45)	(3.64)	(1.51)	(4.39)	(3.17)	(25.95)
Constant	0.48472***	0.49785***	0.47769***	0.46118***	0.47842***	−0.04536***
	(39.99)	(32.33)	(27.32)	(39.82)	(34.70)	(-3.34)
Year	Yes	Yes	Yes	Yes	Yes	Yes
City	Yes	Yes	Yes	Yes	Yes	Yes
Observations	3632	3632	3632	3351	3083	3632
Number of city	263	263	263	263	263	263

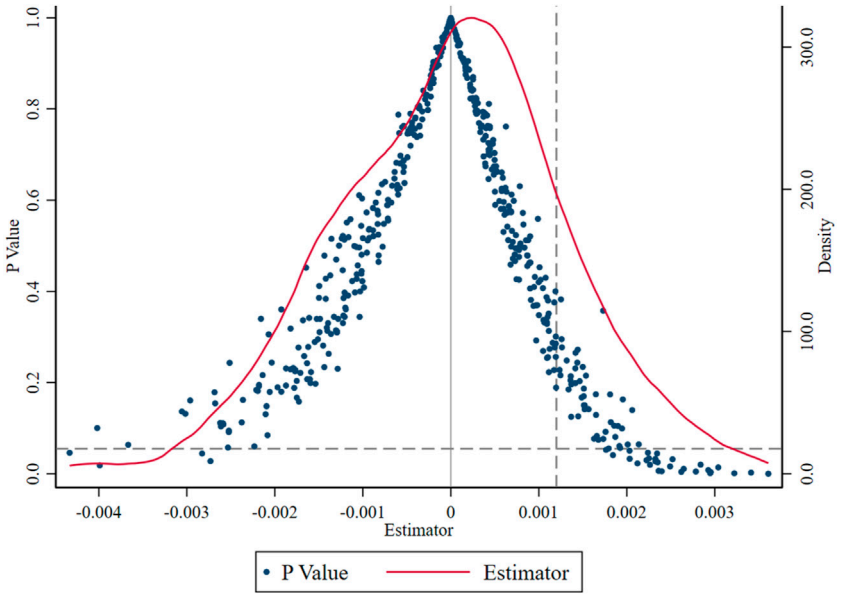

FIGURE 4
Placebo test.

TABLE 8 Global Moran's I of ULGUE in 2006–2019.

	Adjacency matrix			Inverse distance matrix		
	I	z	p	I	z	p
2006	0.361	8.635	0.000	0.064	8.982	0.000
2007	0.361	8.648	0.000	0.064	8.999	0.000
2008	0.362	8.661	0.000	0.065	9.016	0.000
2009	0.363	8.673	0.000	0.065	9.032	0.000
2010	0.363	8.684	0.000	0.065	9.048	0.000
2011	0.364	8.695	0.000	0.065	9.063	0.000
2012	0.364	8.706	0.000	0.065	9.077	0.000
2013	0.365	8.716	0.000	0.065	9.091	0.000
2014	0.365	8.725	0.000	0.065	9.104	0.000
2015	0.365	8.735	0.000	0.065	9.117	0.000
2016	0.366	8.744	0.000	0.065	9.129	0.000
2017	0.366	8.752	0.000	0.066	9.141	0.000
2018	0.367	8.760	0.000	0.066	9.152	0.000
2019	0.367	8.768	0.000	0.066	9.163	0.000

5.6 Further heterogeneity analysis

5.6.1 Urban geographical location

Up to now, the development differences between regions in China cannot be ignored, which may have great impacts on the implementation effect of pilot policy. To explore differences in the effect of ecological civilization pilot demonstration area policy on ULGUE of cities in different geographical locations, this study divides the sample cities into eastern and non-eastern cities according to their location for regression analysis, and the regression results are shown in Table 10.

Model 1) and model 3) show that the ecological civilization pilot demonstration area policy has a significant positive effect on ULGUE in non-eastern regions, but the effect is insignificant in eastern regions, indicating that ecological civilization construction can better promote the ULGUE in non-eastern regions. Model 2) and model 4) demonstrate that the ecological civilization pilot demonstration area policy has significant positive spatial spillover effects on ULGUE in both eastern and non-eastern regions, and the spatial spillover effect in non-eastern region is more significant than that in eastern region.

To sum up, the reason may be that ecological civilization construction in the non-eastern region is still at an early stage with a more significant marginal role. In contrast, developed economy and fierce competition among cities together with relatively fierce competition for professional talents and high-tech enterprises in the eastern region may have restrained the full release of policy dividend. This effect not only causes the insignificant policy effect on ULGUE for cities, but also results in a weaker spillover effect in the eastern region.

5.6.2 Urban resource endowment

Natural resource endowment is different between regions, which may lead to effect heterogeneity of ecological civilization pilot demonstration area policy on ULGUE. Hence, this study classifies sample cities into resource-based and non-resource-based cities for regression analysis according to the National Resource-based City Sustainable Development Plan issued by the State Council in 2013. The regression results are shown in Table 11.

As shown in model 1) and model 3), ecological civilization pilot demonstration area construction has a significant positive effect on ULGUE in non-resource-based cities, while has no significant effect on ULGUE in resource-based cities. This result indicates that for non-resource-based cities, ecological civilization construction can promote ULGUE, probably because the leading industry in resource-based cities is featured by resource exploitation and processing, where environmental pollution and resource waste are relatively serious, resulting in less effective policy dividend in resource-based cities.

Model 2) and model 4) show that in both resource-based and non-resource-based cities, implementation of ecological civilization pilot demonstration area policy has a significant positive spatial

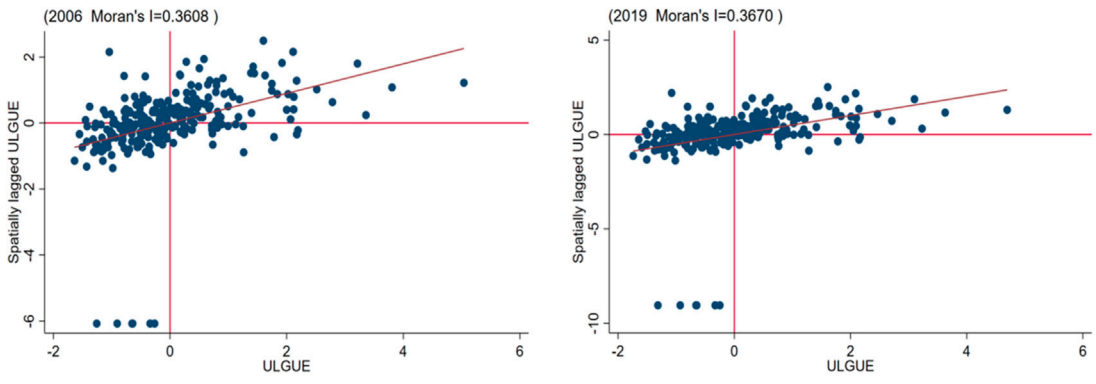

FIGURE 5
Scatter chart of local Moran's I in 2006 and 2019.

TABLE 9 Empirical results of ecological civilization demonstration area construction and ULGUE.

Variable	(1)	(2)	(3)	(4)
	Main	LR direct	LR indirect	LR total
Did	0.00217***	0.00314***	0.01212***	0.01525***
	(3.90)	(5.17)	(6.75)	(7.27)
Re	−0.00227***	−0.00244***	−0.00208***	−0.00452***
	(−7.80)	(−8.15)	(−7.84)	(−8.10)
Il	0.08729***	0.09548***	0.08116***	0.17664***
	(4.65)	(4.97)	(4.99)	(5.00)
Is	0.02245***	0.02404***	0.02045***	0.04449***
	(28.96)	(30.96)	(24.00)	(31.64)
Ii	0.00130**	0.00140**	0.00119**	0.00258**
	(2.36)	(2.45)	(2.47)	(2.46)
Ee	0.00011***	0.00012***	0.00010***	0.00021***
	(11.60)	(11.83)	(10.40)	(11.37)
Fdl	0.01010***	0.01083***	0.00920***	0.02003***
	(17.23)	(17.24)	(18.03)	(18.68)
Wx	0.00551***			
	(5.27)			
Constant	−0.12581***			
	(−17.42)			
Observations	3682	3682	3682	3682
Number of city	263	263	263	263

TABLE 10 Analysis of geographical location heterogeneity.

Variables	Western region		Non-eastern region	
	(1)	(2)	(3)	(4)
Did	0.00099	0.00195**	0.00090**	0.00222***
	(1.17)	(2.00)	(2.05)	(3.35)
Wx		0.00608***		0.00774***
		(3.43)		(6.03)
sigma2_e		0.00005***		0.00003***
		(26.36)		(31.21)
Constant	0.53573***	−0.11379***	0.47865***	−0.13092***
	(26.19)	(−8.40)	(50.11)	(−15.59)
Controlled variables	Yes	Yes	Yes	Yes
Observations	1526	1526	2156	2156
Number of cities	109	109	154	154

spillover effect on ULGUE in surrounding regions of pilot cities, particularly for non-resource-based cities. The reason may be that non-resource-based cities have lower environmental pollution, less pressure of economic transformation, and more focus on comprehensive benefits, which will be learnt and imitated by neighboring cities, thereby improving the spatial spillover effect.

TABLE 11 Analysis of resource endowment heterogeneity.

Variables	Resource-based city		Non-resource-based city	
	(1)	(2)	(3)	(4)
Did	0.00045	0.00448***	0.00151**	0.00636***
	(0.91)	(4.25)	(2.33)	(7.76)
Wx		0.00576***		0.00602***
		(4.22)		(3.99)
sigma2_e		0.00006***		0.00005***
		(25.27)		(32.31)
Constant	0.48063***	−0.18024***	0.48063***	−0.16953***
	(50.76)	(−14.85)	(50.76)	(−15.52)
Controlled variables	Yes	Yes	Yes	Yes
Observations	1428	1428	2254	2254
Number of city	102	102	161	161

5.6.3 Environmental protection policy intensity

Environmental protection policies may have certain synergistic effect with ecological civilization pilot demonstration area construction to improve ULGUE. Therefore, this study examines the heterogeneity of the effect of urban ecological civilization pilot demonstration area construction on cities with different environmental protection policy intensities. According to the 113"key cities for environmental protection[8]" designated in the "11th Five-Year Plan" for environmental protection issued by the State Council in 2007, the sample cities are divided into key and non-key cities of environmental protection for regression analysis. The regression results are shown in Table 12.

Model 1) and model 3) show that ecological civilization pilot demonstration area construction has a significant positive effect on ULGUE in non-key cities of environmental protection, but makes

8 List of key cities for environmental protection: Beijing, Tianjin, Shanghai, Chongqing, Shijiazhuang, Taiyuan, Hohhot, Shenyang, Changchun, Harbin, Nanjing, Hangzhou, Hefei, Fuzhou, Nanchang, Jinan, Zhengzhou, Wuhan, Changsha, Guangzhou, Nanning, Haikou, Chengdu, Guiyang, Kunming, Lhasa, Xi'an, Lanzhou, Xining, Yinchuan, Urumqi, Dalian, Qingdao, Ningbo, Xiamen, Shenzhen, Qinhuangdao, Tangshan Baoding, Handan, Changzhi, Linfen, Yangquan, Datong, Baotou, Chifeng, Anshan, Fushun, Benxi, Jinzhou, Jilin, Mudanjiang, Qiqihar, Daqing, Suzhou, Nantong, Lianyungang, Wuxi, Changzhou, Yangzhou, Xuzhou, Wenzhou, Jiaxing, Shaoxing, Taizhou, Huzhou, Maanshan, Wuhu, Quanzhou, Jiujiang, Yantai, Zibo, Tai'an, Weihai, Zaozhuang, Jining, Weifang, Rizhao, Luoyang, Anyang, Jiaozuo Kaifeng, Pingdingshan, Jingzhou, Yichang, Yueyang, Xiangtan, Zhangjiajie, Zhuzhou, Changde, Zhanjiang, Zhuhai, Shantou, Foshan, Zhongshan, Shaoguan, Guilin, Beihai, Sanya, Liuzhou, Mianyang, Panzhihua, Luzhou, Yibin, Zunyi, Qujing, Xianyang, Yan'an, Baoji, Tongchuan, Jinchang, Shizuishan, Karamay, 113 cities in total

TABLE 12 Heterogeneity analysis of environmental protection policy intensity.

Variables	Key cities for environmental protection		Non-key cities for environmental protection	
	(1)	(2)	(3)	(4)
did	0.00037	0.00445***	0.00172**	0.00508***
	(0.68)	(4.85)	(2.57)	(5.80)
Wx		0.00205		−0.00170
		(1.61)		(−1.18)
sigma2_e		0.00005***		0.00005***
		(25.98)		(31.62)
Constant	0.42816***	−0.23195***	0.48350***	−0.13670***
	(31.16)	(−19.53)	(35.33)	(−13.31)
Controlled variables	Yes	Yes	Yes	Yes
Observations	1470	1470	2212	2212
Number of cities	105	105	158	158

no significant difference in ULGUE in key cities. According to model 2) and model 4), implementation of ecological civilization pilot demonstration area policy has no significant spatial spillover effect in both key and non-key cities.

In summary, for key cities of environmental protection, the ecological civilization pilot demonstration area policy fails to promote the ULGUE of both local and neighboring cities. This result indicates that implementation of this policy has no remarkable contribution to ULGUE when the spatial spillover effect is considered, but may have potential growth effect in both local and adjacent areas. More effectively targeted policies will generate a positive influence on ULGUE in key cities of environmental protection. For those non-key cities of environmental protection, the pollution industry makes little contribution to urban economic growth, and there is relatively lower resistance for the improvement of ULGUE through policy regulation. Implementation of ecological civilization pilot demonstration area policy can better improve ULGUE, and its insignificant spatial spillover effect on neighboring cities may be related to the “siphon effect".

6 Conclusion and discussion

6.1 Conclusion

From the perspective of promoting regional sustainable development, breaking the bottleneck constraints of resources and environment and balancing the relationship between economic development and ecological civilization construction will be one of the important challenges faced by China’s sustainable development policies in the future. Evaluating the role of the “Ecological Civilization Pilot Demonstration Area” policy in improving the efficiency of urban land green utilization is of great significance for improving this policy and correctly handling the relationship between economic development and ecological civilization construction. Therefore, this study measures the ULGUE of 263 cities at the prefecture and above level in China from 2006 to 2019, and uses the multi-period PSM-DID model and SDM-DID spatial econometric model to empirically test the effect of ecological civilization pilot demonstration area policy on ULGUE. The main conclusions are as follows.

(1) The ecological civilization pilot demonstration area policy can significantly increase the ULGUE, as the ULGUE of pilot cities is about 0.12% higher than that of non-pilot cities. From the perspective of time, the ULGUE in China shows a steady upward trend. However, the overall ULGUE level is relatively low in China with obvious regional differences, and there is still 48% of space for improvement. From the perspective of space, the ULGUE presents a spatial pattern of eastern > national > central > western.
(2) The ecological civilization demonstration area policy has obvious spatial heterogeneity in its improving effect on ULGUE. From the perspective of geographical location, the policy has no significant promoting effect on ULGUE in the eastern region, but remarkably improves ULGUE in the non-eastern region. From the perspective of resource endowment, the policy has no significant effect on ULGUE in resource-based cities, but can significantly promote ULGUE in non-resource-based cities. From the perspective of environmental protection policy intensity, the policy can promote ULGUE in non-key cities of environmental protection, but shows no significant effect on ULGUE in key cities.
(3) Implementation of ecological civilization pilot demonstration area policy can not only promote the ULGUE of the pilot cities, but also help to improve the ULGUE in surrounding cities through the spatial spillover effect, which is related to urban characteristics such as urban geographical location, resource endowment, and environmental protection intensity. The non-eastern region and non-resource-based cities generally have stronger spatial spillover effects; key environmental protection cities have potential growth effect; while non-key environmental protection cities have no significant spatial spillover effect.

6.2 Policy recommendations

Based on the above findings, the policy recommendations of this study are as follows.

(1) More attention should be paid to the improving effect of ecological civilization demonstration area policy on ULGUE. Besides, the scope of pilot cities should be gradually expanded while summarizing and popularizing the pilot policy experiences. Cities that have not conducted ecological civilization pilot construction should fully mobilize their regional resources to learn from the successful cases in combination with their own urban characteristics. Moreover, the government should coordinate national strategic planning and deployment, so as to gradually expand the pilot scope of ecological civilization demonstration area and effectively achieve part-to-whole development.

(2) In the implementation of ecological civilization pilot demonstration area policy, full consideration should be given to the geographical location, resource endowment, environmental protection intensity, and other urban characteristics that may affect the policy implementation effect. In response to ecological civilization pilot policy, the local government should grasp the time node and refine the implementation plan of pilot policy in combination with actual urban situation. On the one hand, it is not rational to blindly copy the experience of surrounding cities or other pilot cities. On the other hand, the pilot policy has a more significant promoting effect on ULGUE in non-eastern regions, non-resource-based cities and non-key cities of environmental protection. Therefore, it is necessary to accelerate ecological civilization construction in such cities, so as to maximize the policy effectiveness and improve the ULGUE of these cities and even the whole region.

(3) In view of the spillover effect, the central and western regions and non-resource-based cities are supposed to strengthen infrastructure construction in relevant economic fields, so as to expand the scope of ecological civilization pilot cities and give full play to spillover dividends. The eastern region and resource-based cities should promote the integration and development of ecological civilization and social and economic industries. Moreover, it is necessary to strengthen industrial cooperation between regions and strictly prevent the transfer of pollution industries to neighboring regions. By establishing a cross-regional ecological compensation mechanism and industrial transfer guidelines, the industrial transfer should be carried out in a green way to promote the green and sustainable development of Chinese cities.

6.3 Limitations and future prospects

This study may have the following limitations.

1) Due to the lack of accurate and complete environmental data such as greenhouse gas emissions and soil erosion, this study only uses industrial wastes to measure the unexpected output for ULGUE, there is still space for improvement. In addition, the time limit for measuring the ULGUE in this study is 2019, which means that the follow-up study needs to select data with higher accuracies and updated years to measure national ULGUE. 2) By taking into account the difference in policy effect on administrative areas, this study only uses Chinese cities as the research object when empirically testing the ecological civilization pilot demonstration area policy. The effects of pilot policy at province, district, county and other levels also present in the ecological civilization pilot demonstration area are eliminated. Since we use municipal panel data, the regression coefficient between the two is relatively small when capturing the impact of ecological civilization pilot demonstration area construction on urban land green use efficiency, which is not only related to the setting of the explained variable ULGUE, but also limited by the availability of data. Therefore, when only considering prefecture level cities, the construction of ecological civilization demonstration zones is indeed limited in improving the overall ULGUE. Further research should pay more attention to this aspect, and further test the comprehensiveness of samples and the policy effect at different administrative levels. 3) This study is an exploratory study of the policy effect of ecological civilization pilot demonstration area construction on ULGUE. We have only qualitatively analyzed the impact mechanism of the construction of ecological civilization demonstration zones on the green utilization efficiency of urban land theoretically, and have not yet conducted quantitative analysis on it. Future research can be conducted to reveal the specific mechanism for ecological civilization pilot demonstration area policy to improve ULGUE.

Author contributions

Conceptualization, methodology, formal analysis, writing-original draft preparation and visualization, QW; Validation, DW; Writing-editing, SL. All authors contributed to the article and approved the submitted version.

Funding

This research was funded by the National Natural Science Foundation of China (42171286 and 71974071).

Conflict of interest

The authors declare that the research was conducted in the absence of any commercial or financial relationships that could be construed as a potential conflict of interest.

Publisher's note

References

Beck, T., Levine, R., and Levkov, A. (2010). Big bad banks? The winners and losers from bank deregulation in the United States. *J. finance* 65, 1637–1667. doi:10.1111/j.1540-6261.2010.01589.x

Bird, J., and Venables, A. J. (2020). Land tenure and land-use in a developing city: A quantitative spatial model applied to kampala, Uganda. *J. Urban Econ.* 119, 103268. doi:10.1016/j.jue.2020.103268

Cancello, R., Soranna, D., Zambra, G., Zambon, A., and Invitti, C. (2020). Determinants of the lifestyle changes during COVID-19 pandemic in the residents of northern Italy. *Int. J. Environ. Res. Public Health* 17, 6287. doi:10.3390/ijerph17176287

Chai, Z. Y., Guo, F., Cao, J. H., and Yang, X. D. (2022). The road to eco-efficiency: Can ecological civilization pilot zone be useful? New evidence from China. *J. Environ. Plan. Manag.*, 1–27. doi:10.1080/09640568.2022.2118571

Chen, H., Guo, W., Feng, X., Wei, W. D., Liu, H. B., Feng, Y., et al. (2021). The impact of low-carbon city pilot policy on the total factor productivity of listed enterprises in China. *Resour. Conservation Recycl.* 169, 105457. doi:10.1016/j.resconrec.2021.105457

Chen, Y., Zhu, M. K., Lu, J. L., Zhou, Q., and Ma, W. B. (2020). Evaluation of ecological city and analysis of obstacle factors under the background of high-quality development: Taking cities in the Yellow River Basin as examples. *Ecol. Indic.* 118, 106771. doi:10.1016/j.ecolind.2020.106771

Desalvo, J. S., and Su, Q. (2017). Determinants of urban sprawl: A panel data approach. *Univ. South Fla. Dep. Econ.* 4, 10574. doi:10.5296/IJRD.V4I2.10574

Dixon, D. S., and Dixon, C. (1997). Sustainable urbanization in vietnam. *Geoforum* 28, 21–38. doi:10.1016/S0016-7185(97)85525-X

Dong, Y., Jin, G., and Deng, X. Z. (2020). Dynamic interactive effects of urban land-use efficiency, industrial transformation, and carbon emissions. *J. Clean. Prod.* 270, 122547. doi:10.1016/j.jclepro.2020.122547

Fang, C. L., Guan, X. L., Lu, S. S., Zhou, M., and Deng, Y. (2013). Input-output efficiency of urban agglomerations in China: An application of data envelopment analysis (DEA). *Urban Stud.* 50, 2766–2790. doi:10.1177/0042098013477707

Fukuyama, H., and Weber, W. L. A. (2009). A directional slacks-based measure of technical inefficiency. *Socio-Economic Plan. Sci.* 43, 274–287. doi:10.1016/j.seps.2008.12.001

Ge, K., Zou, S., Ke, S., and Chen, D. (2021). Does urban agglomeration promote urban land green use efficiency? Take the yangtze river economic zone of China as an example. *Sustainability* 13, 10527–10619. doi:10.3390/su131910527

Ghosh, S., and Chifos, C. (2017). The 1985 siting of a Toyota manufacturing plant in rural Kentucky, USA: The ensuing land use change and implications for planning. *Landsc. Urban Plan.* 167, 288–301. doi:10.1016/j.landurbplan.2017.07.006

Gong, B. H., and Sickles, R. C. (1989). Finite sample evidence on the performance of stochastic frontier models using panel data. *J. Prod. Analysis* 1, 229–261. doi:10.1007/BF00158754

Guo, F. Y., Tong, L. J., Qiu, F. D., and Li, Y. M. (2021). Spatio-temporal differentiation characteristics and influencing factors of green development in the eco-economic corridor of the Yellow River Basin. *Acta Geogr. Sin.* 76 (3), 726–739. doi:10.11821/dlxb202103016

Hou, J., Zhou, R., Ding, F., and Guo, H. X. (2022). Does the construction of ecological civilization institution system promote the green innovation of enterprises? A quasi-natural experiment based on China's national ecological civilization pilot zones. *Environ. Sci. Pollut. Res.* 29, 67362–67379. doi:10.1007/s11356-022-20523-4

Hsing-Fu, K., and Ko-Wan, T. (2015). Application of environmental change efficiency to the sustainability of urban development at the neighborhood level. *Sustainability* 7, 10479–10498. doi:10.3390/su70810479

Hu, B. X., Li, J., and Kuang, B. (2018). Evolution characteristics and influencing factors of urban land use efficiency difference under the concept of green development. *Econ. Geogr.* 38 (12), 183–189. doi:10.15957/j.cnki.jjdl.2018.12.023

Hu, F., and Qian, J. (2017). Land-based finance, fiscal autonomy and land supply for affordable housing in urban China: A prefecture-level analysis. *Land Use Policy* 69, 454–460. doi:10.1016/j.landusepol.2017.09.050

Jia, R. N., Shao, S., and Yang, L. L. (2021). High-speed rail and CO2 emissions in urban China: A spatial difference-in-differences approach. *Energy Econ.* 99, 105271. doi:10.1016/j.eneco.2021.105271

Jin, G., Deng, X. Z., Zhao, X. D., Guo, B. S., and Yang, J. (2018). Spatio-temporal patterns of urban land use efficiency in the Yangtze River Economic Zone during 2005-2014. *Acta Geogr. Sin.* 73 (07), 1242–1252. doi:10.11821/dlxb201807005

Li, J. J., Zhu, J. B., Qiao, S. Y., Yu, Z. W., Wang, X. L., Liu, Y., et al. (2017). Processing of coal fly ash magnetic spheres for clay water flocculation. *Int. J. Mineral Process.* 169, 162–167. doi:10.1016/j.minpro.2017.11.006

Li, L., Pan, C., Ling, S., and Li, M. (2022). Ecological efficiency of urban industrial land in metropolitan areas: Evidence from China. *Land* 11, 10104. doi:10.3390/LAND11010104

Liang, L. T., Yong, Y. J., and Yuan, C. G. (2019). Measurement of urban land green use efficiency and lts spatial differentiation characteristics: An empirical study based on 284 cities. *China Land Sci.* 33, 80–87. doi:10.11994/zgtdkx.20190613.141215

Lin, Q., and Ling, H. (2021). Study on green utilization efficiency of urban land in yangtze river delta. *Sustainability* 13, 11907. doi:10.3390/su132111907

Linde, P., and Linde, C. v. d. (1995). Toward a new conception of the environment-competitiveness relationship. *J. Econ. Perspect.* 9 (4), 97–118. doi:10.1257/jep.9.4.97

Liu, J., Feng, H., and Wang, K. (2022). The low-carbon city pilot policy and urban land use efficiency: A policy assessment from China. *Land* 11, 604. doi:10.3390/land11050604

Liu, J. L., Peng, K. L., Zuo, C. C., and Li, Q. (2022). Spatiotemporal variation of land-use carbon emissions and its implications for low carbon and ecological civilization strategies: Evidence from Xiamen-Zhangzhou-Quanzhou metropolitan circle, China. *Sustain. Cities Soc.* 86, 104083. doi:10.1016/j.scs.2022.104083

Liu S C, S. C., Xiao, W., Li, L. L., Ye, Y. M., and Song, X. L. (2020). Urban land use efficiency and improvement potential in China: A stochastic frontier analysis. *Land Use Policy* 99, 105046. doi:10.1016/j.landusepol.2020.105046

Liu, S. C., Lin, Y. B., Ye, Y. M., and Xiao, W. (2021). Spatial-temporal characteristics of industrial land use efficiency in provincial China based on a stochastic frontier production function approach. *J. Clean. Prod.* 295, 126432. doi:10.1016/j.jclepro.2021.126432

Liu, S. Y., Wang, Z. F., Zhang, W. F., and Xiong, X. F. (2020). The exhaustion of China's "land-driven development" mode: An analysis based on threshold regression. *J. Manag. World* 36 (06), 80–92. doi:10.19744/j.cnki.11-1235/f.2020.0087

Lu, S., and Xiong, Q. (2020). Can the establishment of ecological civilization demonstration zones improve agricultural green efficiency? Based on the empirical data of hunan province. *J. Central South Univ. Sci.* 26, 90–101. doi:10.12062/cpre2022040

Lu X H, X. H., Li, J., Liu, C., Kuang, B., Cai, D. W., and Hou, J. (2022). Driving factors and spatial differentiation of urban land green use efficiency in China. *Sci. Geogr. Sin.* 42 (4), 611–621. doi:10.13249/j.cnki.sgs.2022.04.006

Lu, X. H., Chen, D. L., Kuang, B., Zhang, C. Z., and Cheng, C. (2020). Is high-tech zone a policy trap or a growth drive? Insights from the perspective of urban land use efficiency. *Land Use Policy* 95, 104583. doi:10.1016/j.landusepol.2020.104583

Lu, X., Shi, Z., Li, J., Dong, J., Song, M., and Hou, J. (2022). Research on the impact of factor flow on urban land use efficiency from the perspective of urbanization. *Land* 11, 389. doi:10.3390/land11030389

Lv, T. G., Hu, H., Zhang, X. M., Wang, L., and Fu, S. F. (2022). Impact of multidimensional urbanization on carbon emissions in an ecological civilization experimental area of China. *Phys. Chem. Earth, Parts A/B/C* 126, 103120. doi:10.1016/j.pce.2022.103120

Macedo, J. (2008). Urban land policy and new land tenure paradigms: Legitimacy vs. legality in Brazilian cities. *Land Use Policy* 25, 259–270. doi:10.1016/j.landusepol.2007.08.001

Marco, Z., Carlotta, F., Luigi, P., Margherita, C., and Luca, S. (2015). Long-term urban growth and land use efficiency in southern europe: Implications for sustainable land management. *Sustainability* 7, 3359–3385. doi:10.3390/su7033359

Mi, D., Delon, L., and Tien, F. S. (2017). Spatial-difference-in-differences models for impact of new mass rapid transit line on private housing values. *Regional Sci. Urban Econ.* 67, 64–77. doi:10.1016/j.regsciurbeco.2017.08.006

Ms, A., Wsb, C., and Bg, D. (2022). Could quality of governance influence pollution? Evidence from the revised environmental Kuznets curve in central and eastern European countries. *Energy Rep.* 8, 809–819. doi:10.1016/j.egyr.2021.12.031

Nesru, H. K., Monica, L., and Jaap, A. Z. (2021). Urbanization and urban land use efficiency: Evidence from regional and Addis Ababa satellite cities, Ethiopia. *Habitat Int.* 117, 102437. doi:10.1016/j.habitatint.2021.102437

Pan, X. Y., Song, M. L., Wang, Y. Q., Shen, Z. Y., Song, J. B., Xie, P. J., et al. (2022). Liability accounting of natural resource assets from the perspective of input Slack-An analysis based on the energy resource in 282 prefecture-level cities in China. *Resour. Policy* 78, 102867. doi:10.1016/j.resourpol.2022.102867

Pata, U. K. (2018). Renewable energy consumption, urbanization, financial development, income and CO2 emissions in Turkey: Testing EKC hypothesis with structural breaks. *J. Clean. Prod.* 187, 770–779. doi:10.1016/j.jclepro.2018.03.236

Peng, C., Xiao, H., Liu, Y., and Zhang, J. J. (2017). Economic structure and environmental quality and their impact on changing land use efficiency in China. *Front. Earth Sci.* 11, 372–384. doi:10.1007/s11707-016-0596-x

Ruan, L. L., He, T. T., Xiao, W., Chen, W. Q., Lu, D. B., and Liu, S. C. (2022). Measuring the coupling of built-up land intensity and use efficiency: An example of the Yangtze River Delta urban agglomeration. *Sustain. Cities Soc.* 87, 104224. doi:10.1016/j.scs.2022.104224

Sheng, Q., and Tan, Z. (2014). Exploring urban land carrying capacity under the requirement of ecological civilization in China. *Adv. Mater. Res.* 955-959, 4009–4012. doi:10.4028/www.scientific.net/amr.955-959.4009

Song, Y., Yeung, G., Zhu, D. L., Zhang, L. X., Xu, Y., and Zhang, L. Y. (2020). Efficiency of logistics land use: The case of yangtze river economic belt in China, 2000-2017. *J. Transp. Geogr.* 88, 102851. doi:10.1016/j.jtrangeo.2020.102851

Su, H., and Yang, S. (2022). Spatio-temporal urban land green use efficiency under carbon emission constraints in the yellow River Basin, China. *Int. J. Environ. Res. Public Health* 19, 12700. doi:10.3390/ijerph191912700

Tan, M., Li, X., Hui, X., and Lu, C. (2005). Urban land expansion and arable land loss in China—a case study of beijing–tianjin–hebei region. *Land Use Policy* 22, 187–196. doi:10.1016/j.landusepol.2004.03.003

Tan, S. K., Hu, B. X., and Zhou, M. (2021). Regional differences and dynamic evolution of urban land green use efficiency within the Yangtze River Delta, China. *Land Use Policy* 106, 105449. doi:10.1016/j.landusepol.2021.105449

Tang, Y., Wang, K., Ji, X., Xu, H., and Xiao, Y. (2021). Assessment and spatial-temporal evolution analysis of urban land use efficiency under green development orientation: Case of the yangtze river delta urban agglomerations. *Land* 10, 715. doi:10.3390/land10070715

Verburg, P. H., Berkel, D., Doorn, A., Eupen, M. V., and Harmvan den Heiligenberg, A. R. M. (2010). Trajectories of land use change in europe: A model-based exploration of rural futures. *Landsc. Ecol.* 25, 217–232. doi:10.1007/s10980-009-9347-7

Wang, A., Lin, W., Liu, B., Wang, H. Z., and Xu, H. (2021). Does smart city construction improve the green utilization efficiency of urban land? *Land* 10, 657. doi:10.3390/land10060657

Wang, H. J., Zhang, B., Liu, Y. L., Liu, Y. F., Xu, S., Deng, Y., et al. (2018). Multi-dimensional analysis of urban expansion patterns and their driving forces based on the center of gravity-GTWR model: A case study of the beijing-tianjin-hebei urban agglomeration. *Acta Geogr. Sin.* 73 (6), 1076–1092. doi:10.11821/dlxb201806007

Wang, K. L., Xu, R. Y., Zhang, F. Q., and Miao, Z. (2022). Impact of ecological civilization demonstration areas on carbon emission intensity. *China Population,Resources Environ.* 32, 57–70. doi:10.12062/cpre20220403

Wang, L. J., Li, H., and Shi, C. (2015). Urban land-use efficiency, spatial spillover, and determinants in China. *Acta Geogr. Sin.* 70 (11), 1788–1799. doi:10.11821/dlxb201511008

Wang, Q. D., and Pang, X. Q. (2019). Research on green land-use efficiency of Beijing-Tianjin-Hebei urban agglomeration. *China Popul. Resour. Environ.* 29, 68–76. doi:10.12062/cpre.20180522

Wang, W. X., Deng, X. Z., Wang, Y. F., Peng, L., and Yu, Z. Y. (2022). Impacts of infrastructure construction on ecosystem services in new-type urbanization area of North China Plain. *Resour. Conservation Recycl.* 185, 106376. doi:10.1016/j.resconrec.2022.106376

Wang, X. M., Ma, Y., Liu, W., Wang, Y. J., and Li, X. (2021). Coupling and coordination relationship between resource recycling and ecological civilization construction. *Resour. Sci.* 43, 577–587. doi:10.18402/resci.2021.03.14

Wang, Y., and Chi-Man, E. (2017). Are local governments maximizing land revenue? Evidence from China. *China Econ. Rev.* 43, 196–215. doi:10.1016/j.chieco.2017.02.005

Wei, Y., Huang, C., Li, J., and Xie, L. (2016). An evaluation model for urban carrying capacity: A case study of China's mega-cities. *Habitat Int.* 53, 87–96. doi:10.1016/j.habitatint.2015.10.025

Wu, S., Hu, S. G., and Frazier, Amy E. (2021). Spatio-temporal variation and driving factors of carbon emissions in three industrial land spaces in China from 1997 to 2016. *Technol. Forecast. Soc. Change* 169, 120837. doi:10.1016/j.techfore.2021.120837

Xiao, Y., Chen, J., Wang, X., and Lu, X. (2022). Regional green development level and its spatial spillover effects: Empirical evidence from Hubei Province, China. *Ecol. Indic.* 143, 109312. doi:10.1016/j.ecolind.2022.109312

Yang, H. Q., Hu, Y., and Wang, Q. X. (2015). Evaluation of land use efficiency in three major urban agglomerations of China in 2001-2012. *Sci. Geogr. Sin.* 35 (9), 1095–1100. doi:10.13249/j.cnki.sgs.2015.09.004

Yu, B. B., and Su, Y. M. (2022). How does land finance affect land use efficiency? Dynamic space Durbin model test based on the perspective of scale and technology. *Geogr. Res.* 41 (02), 527–545. doi:10.11821/dlyj020210006

Yu, J. Q., Zhou, K. L., and Yang, S. L. (2020). Land use efficiency and influencing factors of urban agglomerations in China. *Land Use Policy* 88, 104143. doi:10.1016/j.landusepol.2019.104143

Zhang, J. T., and Dong, Z. C. (2022). Assessment of coupling coordination degree and water resources carrying capacity of Hebei Province (China) based on WRESP2D2P framework and GTWR approach. *Sustain. Cities Soc.* 82, 103862. doi:10.1016/j.scs.2022.103862

Zhang, J., and Zhang, G. H. (2022). Spatio temporal evolution of urban land intensive utilization in Guangdong Province aiming at ecological civilization construction. *Bull. Soil Water Conserv.* 42, 233–238. doi:10.13961/j.cnki.stbctb.20220322.001

Zhang, L., Xiang, W., Shi, D., Liang, T., Xiong, X., Wu, S., et al. (2023). Impact of green development mechanism innovation on total-factor environmental efficiency: A quasi-natural experiment based on national pilot cities. *Sustainability* 15, 1543. doi:10.3390/su15021543

Zhang, M. S., Wang, H. Q., Dong, Y., Li, L., Sun, P. P., and Zhang, G. (2020). Evaluation of urban underground space resources using a negative list method: Taking Xi'an City as an example in China. *China Geol.* 1, 124–136. doi:10.31035/cg2020006

Zhang, Q., Xiang, T., Zhang, W., Wang, H. M., Jing, A., Li, X. P., et al. (2022). Co-benefits analysis of industrial symbiosis in China's key industries: Case of steel, cement, and power industries. *J. Industrial Ecol.* 26, 1714–1727. doi:10.1111/jiec.13320

Zhang, W. X., Wang, B., Wang, J., Wu, Q., and Wei, Y. H. D. (2022). How does industrial agglomeration affect urban land use efficiency? A spatial analysis of Chinese cities. *Land Use Policy* 119, 106178. doi:10.1016/j.landusepol.2022.106178

Zhang, Y. X., and Fu, B. W. (2023). Impact of China's establishment of ecological civilization pilot zones on carbon dioxide emissions. *J. Environ. Manag.* 325, 116652. doi:10.1016/j.jenvman.2022.116652

Zhao, J. M., Zhu, D. L., Cheng, J., Jiang, X., Lun, F., and Zhang, Q. (2021). Does regional economic integration promote urban land use efficiency? Evidence from the yangtze river delta, China. *Habitat Int.* 116, 102404. doi:10.1016/j.habitatint.2021.102404

Zhao, S. D., and Jiang, Y. M. (2022). Heterogeneous effects of rural–urban migration and migrant earnings on land efficiency: Empirical evidence from China. *Land Use Policy* 115, 106003. doi:10.1016/j.landusepol.2022.106003

Zhao, Z., Bai, Y. P., Wang, G. F., Chen, J. C., Yu, J. L., and Liu, W. (2018). Land eco-efficiency for new-type urbanization in the Beijing-Tianjin-Hebei Region. *Technol. Forecast. Soc. Change* 137, 19–26. doi:10.1016/j.techfore.2018.09.031

Zhou, D., Zhang, X., and Wang, X. (2020). Research on coupling degree and coupling path between China's carbon emission efficiency and industrial structure upgrading. *Environ. Sci. Pollut. Res.* 27, 25149–25162. doi:10.1007/s11356-020-08993-w

frontiers | Frontiers in Sustainable Food Systems

TYPE Original Research
PUBLISHED 27 July 2023
DOI 10.3389/fsufs.2023.1238241

OPEN ACCESS

EDITED BY
Hua Lu,
Jiangxi University of Finance and Economics, China

REVIEWED BY
Dengyan Ji,
East China University of Technology, China
Zhangsheng Liu,
Jiangxi Normal University, China
Lei Nie,
Shanxi University of Finance and Economics, China

*CORRESPONDENCE
Zhou Laiyou
✉ zhoulaiyou@xyc.edu.cn

RECEIVED 14 June 2023
ACCEPTED 14 July 2023
PUBLISHED 27 July 2023

CITATION
Laiyou Z and Jiawei L (2023) Dilemmas and theoretical exploration of China's rural land property rights system reform.
Front. Sustain. Food Syst. 7:1238241.
doi: 10.3389/fsufs.2023.1238241

Dilemmas and theoretical exploration of China's rural land property rights system reform

Zhou Laiyou[1,2]* and Luo Jiawei[3]

[1]School of Economics and Management, Xinyu University, Xinyu, China, [2]Institute of Ecological Civilization, Jiangxi University of Finance and Economics, Nanchang, China, [3]School of Applied Economics, Jiangxi University of Finance and Economics, Nanchang, China

Introduction: The property rights system, as the core component of the land system, is related to the long-term stability of the country, the well-being of farmers and the realization of the value of ecological products. The reform of China's rural land property rights system has long been controversial. This paper compares the main historical lines of the reform of the rural land property rights system since the founding of New China, notes its dilemmas, and theoretically explores its development.

Methods: This article adopted literature analysis method(LAT), Sorted out the historical mainline of rural land property rights system reform since the establishment of the People's Republic of China, proposed its reform path.

Results: The paper finds that the two main difficulties of the reform are the weakening of collective property rights, leading to the disintegration of rural public services, and the refinement of farmers' property rights, leading to an increase in agricultural operation costs. These issues lead to extremely high transaction costs in the process of agricultural production and operation, making agricultural production a worthless business activity.

Discussion: This paper argues that a complete market structure is a "unified" market structure that includes the government and the market, in which the government plays the role of defining property rights and reducing transaction costs.

KEYWORDS

rural land property rights system, reform, dilemma, theoretical exploration, China

1. Introduction

The value realization of ecological products is an issue of high interest in current academic research. It is believed that most ecological products are public goods, and their noncompetitive and nonexclusive nature can easily lead to "free-rider" behavior, resulting in the failure of market mechanisms (Gao et al., 2020) and the creation of very large hidden values that cannot be realized through transactions. The solution is to define the property rights of ecological products and then use the market system to trade and realize their values. Taking land resources as an example, after the reform and opening up, the household benefited from the implementation of the household joint production contract responsibility system and again became an independent property accounting unit, creating the second golden age in the history of China's agricultural development and leading grain production to rapidly increase (Zhao and Song, 2022). This world-renowned achievement is regarded and promoted as a classic case of the privatization of property rights in

TABLE 1 Changes in the rural land system (1949–1962).

Period	Ownership subjects	Subject of the right to use
The early years of New China	Privately owned by farmers	Privately owned by farmers
Primary cooperatives	Privately owned by farmers	Collective membership in primary cooperatives
Senior cooperatives	The working masses collectively share in the common resources	Collective membership in senior cooperatives
People's commune	Commune – brigade – production team three-level ownership	Commune – brigade – production team three-level collective

The history and logic of land system change in contemporary China (Cai and Li, 2021).

neoliberal economics. Subsequent reforms of rural land property rights have been carried out in the direction of weakening the collective and strengthening the individual, and there are even voices in academia that "deflate collective ownership" (Zhang and Cheng, 2012). However, the registration of rural land ownership, represented by "quasi privatization," which began in 2013, has not achieved the expected results, and the phenomenon of the abandonment of many arable land resources has led to widespread stagnation of the transfer of agricultural land and the sluggish growth of long-term investment in agricultural land (Liu and Luo, 2018; Luo and Hong, 2020). This result suggests that we have likely misunderstood the success of the household contract responsibility system and that overemphasizing private property rights at the expense of the role of public property rights has unintended consequences. As the main resource in rural areas, land resources carry most of the supply of ecological products. Is the privatization of land property rights the best way to optimize the allocation of land resources? Does the "property rights definition-economic incentives" framework of mainstream economics require preconditions? This paper will answer these questions. The research in this article helps deepen the academic community's understanding of the reform of the rural land property rights system in China and thereby provides a useful perspective supporting further research on the property rights system.

2. The real dilemma of rural land property rights system reform

2.1. The weakening of collective property rights leads to the disintegration of rural public services

After the founding of New China, many things were waiting to be done. Although farmers who had experienced land reform owned land, they still faced many limitations, such as fragmented production and operation, low technology level, and lack of production tools. To further demonstrate fairness and achieve common prosperity, the rural cooperative movement was promoted in 1953, and policy documents, such as the Resolution on Mutual Cooperation in Agricultural Production, the Model Charter for Agricultural Production Cooperatives, the Model Charter for Advanced Agricultural Production Cooperatives, and the Resolution on the Establishment of People's Communes in Rural Areas, were issued one after another (Yan et al., 2021). The development of agriculture and rural areas was gradually incorporated into the national economic development plan, eventually resulting in the land system of "one big, two publics" and "one fair, two transfers" (Bu, 2010; Yan et al., 2021). Then, in the 1960s, land became owned by the commune, brigade, and production team, basically forming a "three-tier ownership, team-based" rural land system (see Table 1). During this process, the public goods and services provided under the planned economic system met the basic needs of agricultural production and rural residents. Taking public infrastructure as an example, through a system using "government financial subsidies as a supplement, rural collective organizations as the main source of funding, and peasants' labor accumulation (work points) as an input of manpower" (Xu, 2002), many farmland irrigation and water conservancy facilities and rural roads were built, and agricultural production service institutions were established, greatly improving the backward state of rural infrastructure and strengthening the rural economy. During this period, rural collectives played a major role in solving the problem of inadequate public services faced by rural areas in general.

Nonetheless, policies in this period severely inhibited the incentive of individual production. Data show that in 1956, China's *per capita* grain production was 307 kg, basically reaching the caloric safety line. However, by 1974, the *per capita* grain production in China was still 317 kg, and it almost stagnated over 18 years,[1] showing the weak supply of land ecological products in this period. This led to widespread criticism in public opinion. The problem was blamed on the collective ownership system of the planned economy era, and the implementation of the household joint production contract responsibility system and the gradual disintegration and demise of the people's commune system were promoted. The public infrastructure built during the collective ownership period was revitalized, and agricultural production that had long been languishing saw a jump in growth, with grain production increasing from 300 million tons in 1978 to 400 million tons in 1984, an average annual growth of nearly 6% (Zhao and Song, 2022). Figure 1 shows the explosive growth in both total and *per capita* grain production in the initial period of reform and opening up.

The dramatic improvement in agricultural performance drew much attention from the public opinion community, and people began to reflect on why the ambitious collectivization transformation had failed (Liu, 2019). One explanation is that under the system of collective labor, the inadequate supervision and incomplete measurement of labor by production teams over their members led to insufficient incentives for laborers' efforts, resulting in lazy laborers and consequently low agricultural production performance (Lu, 1992). Later, academics further explored the reasons for the inadequate supervision of production teams over their members and the laziness of their members, arguing that the property rights characteristics of the collective system deprived production teams and the members of their residual claims and failed to provide effective incentives for these teams and their members (Chen, 1994; Zhou, 1995).

1 How the Chinese got enough to eat – A history of food production in New China – History – szhgh.com.

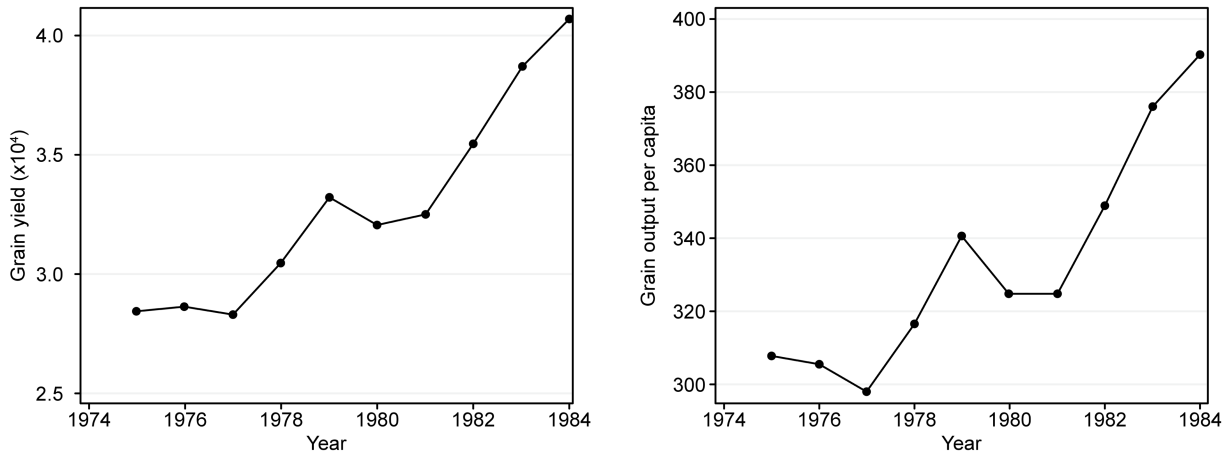

FIGURE 1
Graph of total grain production and *per capita* grain production, 1975–1984. The author developed these graphs based on the China statistical yearbook.

Logically, the reform of the household contract responsibility system has become a topic of high interest in academia. By constructing an econometric model, Lin Yifu calculated that the contribution of the reform of the household contract responsibility system to agricultural growth was 46.89% during 1978–1984 (Lin, 1992). Other scholars decomposed several institutional reforms and related policy adjustments carried out during the same period and concluded that the contribution of the household contract responsibility system to agricultural growth was 78%. However, some scholars have questioned this result, arguing that the contribution of the household contract responsibility system has been exaggerated. After deducting the contribution of technological advances in agricultural production and price reforms, the contribution of the household contract responsibility system to agricultural growth was found to be only approximately 30% (Huang and Rozelle, 1996). In any case, however, the great success of the household contract responsibility system is the consensus that has developed in public opinion. For example, Xu (2008) believes that the household contract responsibility system has the characteristics of "bottom-up" system construction, diversity in specific arrangements, flexibility, fuzziness and flexibility in the actual operation process, and fairness over efficiency.

For this reason, subsequent reforms of the land system have followed the direction of weakening the collective and strengthening the individual. National policies have also reflected this direction of reform, with the land contract period extending from 15 years in 1984 to 30 years after the expiration of the first round of contracts. The Third Plenary Session of the 17th Central Committee in 2008 proposed that the contract should remain unchanged for a long time, and then the 19th National Congress proposed that the second round of contracts should be extended for another 30 years after the expiration of the contract while maintaining the longevity of the contract (Chen, 2019). The land ownership registration system, which was promoted and implemented in 2013, further strengthens individual property rights and is considered by scholars to represent a process of land privatization (Luo and Hong, 2020). In the process, the collective economy was gradually dismantled. Before 2006, public services in rural areas were mainly maintained by collecting "three withdrawals and five integrations" from villagers; after the agricultural tax was abolished, the "three withdrawals and five integrations" were also abolished, and the contractual relationship between arable land owners and the state that had been implied for thousands of years disappeared (Zhao and Song, 2022). This means that an owner of arable land no longer has an obligation to the state to cultivate the land and can abandon it at will without punishment. The abolition of the "three mentions and five integrations" has resulted in the loss of funding sources for rural public infrastructure (public services) and the rapid disintegration of public services. After the depreciation of productive public goods, such as the original farm infrastructure, the cost of agricultural production increased rapidly and became an economic activity without any commercial value.

To strengthen grassroots construction and expand the collective economy, the state has started to adopt the policy of "industry feeding agriculture and cities supporting rural areas," and various places have explored ways to pay for public services in rural areas. For example, the "One Project One Discussion" financial award system has provided a source of funding for the provision of public goods in rural areas, but the inconsistency between the providers and beneficiaries of public goods has led to the failure of many places to break through the collective action dilemma in the provision of public goods at the village level (Li and Liu, 2016; Shi et al., 2021). This makes it unlikely that the organizational coordination of village collectives will be abandoned in favor of relying purely on villagers' autonomous consultation for decisions on the provision of public goods. Such a system would entail very large transaction costs, resulting in so-called "market failures." Many areas have been unable to provide public goods for agricultural production for many years due to failed negotiation and have been "resting on their laurels," with water conservancy facilities in disrepair and narrow field ridges impassable for agricultural machinery. The cost of agricultural production remains high. The evolutionary process, institutional performance, and causes of the rural land property rights system after the founding of New China are shown in Figure 2.

2.2. The refinement of farmers' property rights leads to an increase in agricultural operation costs

Mainstream economics argues that attributing property rights to households or individuals can effectively incentivize their

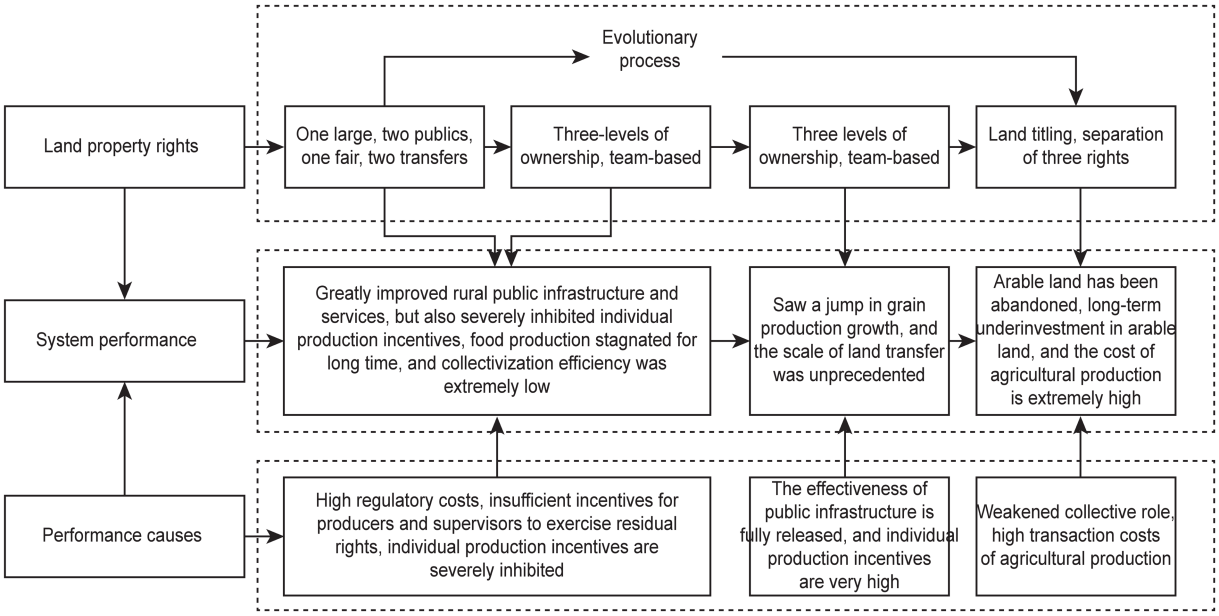

FIGURE 2
Evolutionary process, institutional performance, and factors of the rural land property rights system.

behavior and improve economic performance. The reform of China's rural land system follows this logic, and public opinion posits that rural problems can be solved only if the collective ownership system is thoroughly reformed and microentities are given sufficient incentives. As a result, the reform of China's "three rural policies" has been oriented toward the devolution of power and profit to farmers and the strengthening of the family contract responsibility system. Tax relief, the extension of the land contract period, land titling, and a greater role for the market are all included in the reform of the system.

In the early 1980s, when the land was divided among households, the village collective divided the land into several classes according to the abovementioned production conditions because of the large differences in the convenience of irrigation, fertility, distance, and convenience of transportation. As a result, the land is divided into several classes, and each class of land is divided equally among households, making the land occupied by farmers highly fragmented and dispersed (Wang, 2016). Especially in the southern hilly areas, due to the topography, the land is more fragmented, and households typically have less than ten mu scattered in eight or nine places. For example, a survey found that the average household land area in Shayang County, Hubei Province, is 7.7 mu, and the average number of land blocks per household is 8.7, with an average of 0.88 mu each; the same is true for Wucun, which is in the plain area of Inner Mongolia, where the average arable land *per capita* is 4.5 mu and the average household has seven arable plots (Lian et al., 2014; Wang, 2016).

The negative impact of land fragmentation in terms of agricultural production is self-evident (see Figure 3). Earlier studies found that land fragmentation caused numerous inconveniences to agricultural production, adversely affecting agricultural output, public infrastructure development, mechanized planting and harvesting, and the allocation of farm labor use (Wan and Cheng, 1996; Xu et al., 2008). The more severe the fragmentation of land is, the more severe the abandonment of arable land (Long et al., 2022). A study of Wucun in Inner Mongolia found that fragmented land property rights resulted in high costs of collective negotiation in the investment process of irrigation systems to the extent that land quality was difficult to improve; the additional protection and supervision costs incurred by farmers due to fragmented land property rights made farmers' use of land property rights less efficient; moreover, the fragmented land property rights increased farmers' information costs and caused difficulties in planting decisions for some farmers (Lian et al., 2014). A recent theoretical study shows that the uncertainty, immobility and other characteristics of fragmented land make farmers face transaction costs such as measurement costs and concerted action costs, thus increasing the cost of agricultural production and operation (Wang and Hu, 2018). The theoretical logic explaining the increase in agricultural operation costs due to land fragmentation is that land fragmentation increases the cost of collective negotiation, and the high transaction costs lead to the failure of collective action. However, these negative impacts of land fragmentation in China emerged during the period of rapid economic development after the reform and opening up and were not present at the beginning of the implementation of land distribution among households.

According to this logic, the reform of the "three rural policies" should focus on strengthening the role of the village collectives in coordinating and thus reducing transaction costs. However, the opposite is observed. First, the Circular of the CPC Central Committee on Rural Work in 1984, which was issued in 1984, clearly stated that farmers should have a contract period of at least 15 years for land, and the principle of "big stability and small adjustment" was established for land adjustment. In 1993, the Central Government issued a document entitled "Several Policy Measures for Current Agricultural and Rural Economic Development," stipulating that the original land contracting rights could be extended for another 30 years after the expiration of the contract and advocating the method of "increasing people without

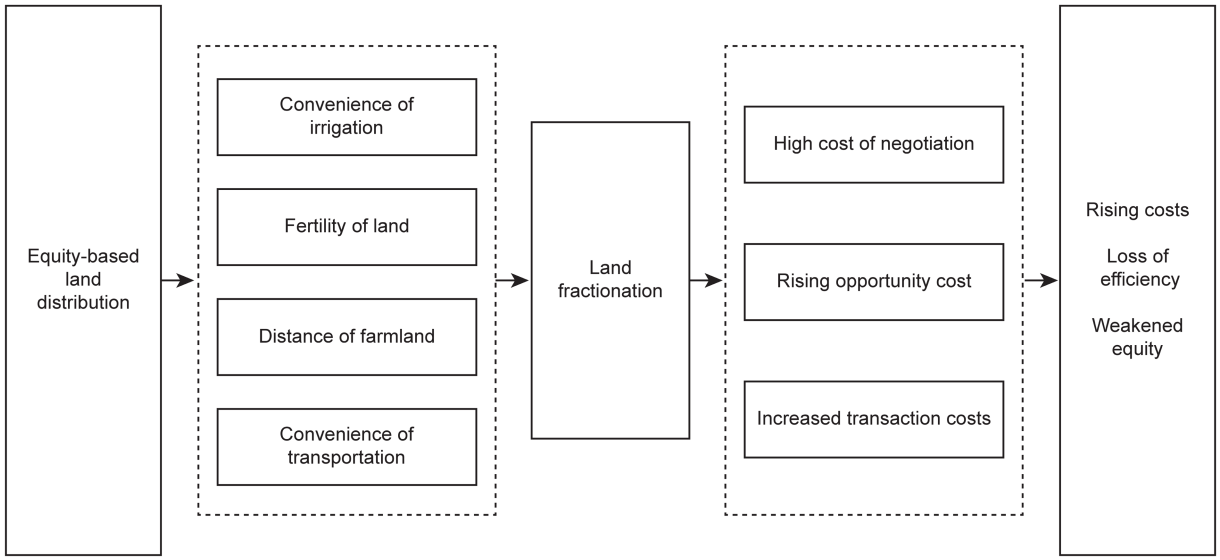

FIGURE 3
Logical chain of rising agricultural production costs due to land fragmentation.

increasing land and decreasing people without decreasing land" during the contract period, further solidifying the land contracting rights. Article 27 of the Rural Land Contract Law of 2002 stipulates that the contracting party shall not adjust the contracted land during the contracting period. Furthermore, the 2009 Central Government Document No. 1 stipulated that the existing land contracting relationship should be stabilized and remain unchanged for a long time. Until 2013, the nationwide comprehensive promotion of rural land contracting rights registration and issuance of certificates was carried out, and the specific location, area, and ownership of the land contracted by farmers were registered on the certificates by confirming the rights and issuing certificates. By now, the property rights of farmers' land have become clear. The evolution and changes of these policies are all in the direction of strengthening individual property rights. However, these clear and secure property rights have not effectively promoted the transfer of farmland but have rather led to increasing farmland abandonment (Luo et al., 2017); they have not encouraged long-term investment in farmland but have rather led farmers to increasingly use chemical fertilizers, etc. (Li et al., 2019); they have not effectively attracted migrant workers to return to their hometowns to start businesses but have rather experienced the loss of young and strong rural labor, resulting in the decay of rural areas. The policy of clear and secure property rights to individuals has not brought the expected effects, and the results have deviated from the original policy design.

3. Theoretical exploration of rural land property rights system reform

Fortunately, policymakers have taken note of the disappointing effects of the three rural policies in recent years, and from policymakers to academics, they have begun to pay attention to the role of village collective organizations. Recently, the central government has revisited the strengthening of the collective economy. In 2018, the Organization Department of the Central Committee of the CPC and three other departments jointly issued the Circular on Adhering to and Strengthening the Leadership of Rural Grassroots Party Organizations to Support and Grow the Village Collective Economy. In June 2019, the Ministry of Agriculture and Rural Affairs issued the Circular of the Ministry of Agriculture and Rural Affairs on Further Improving the Development of Villages with Weak Collective Economy in Poverty-stricken Areas. These circulars propose increasing policy support to develop and grow the collective economy. At the time of the centennial of the CPC founding, academics reflected on China's land system, especially the rural collective land system. In contrast to the previous overwhelming support for land privatization, there are currently more scholars supporting the strengthening of collective ownership. However, due to the lack of theoretical support, the discussion of strengthening collective ownership is still confined to traditional economics and cannot break away from the traditional paradigm of economic analysis. For example, some studies use concepts such as heavy assets and light assets[2] to distinguish between the behavioral categories of collectives and farmers. However, the concept of a heavy asset and a light asset is itself very vague.

The logical starting point of traditional economics is individual rationality, leading to a series of economic theories that start from individual behavior. Traditional economics assumes that clear and secure property rights can effectively create incentives for market players to improve economic performance. However, this paradigm incorrectly assumes that the fixed costs of numerous market players are zero and that the government, providing public goods and services, is an exogenous variable. This paradigm does not explain many economic realities and does not even answer the question "why does government exist," leading some economics schools to advocate "anarchism." In fact, a complete market structure should consist of a public sector that provides collective heavy assets and a private sector that produces

2 Similar to the concept of fixed cost and variable cost.

private goods, without either of which the market structure is incomplete. Such market structures are ubiquitous in real life, such as transportation markets consisting of roads (public) and cars (individual). Thus, it seems that the analytical paradigm that treats government and the market as an antagonistic relationship has long been outdated. However, the relationship between the government and the market is not the focus of this paper and will be left aside for now.

In a complete market structure, the role of the government is self-evident. On the one hand, to define property rights and ensure that they are clear and stable to meet the prerequisites of market transactions, it is necessary to make laws and regulations and establish a set of authorities to maintain the normal operation of the market economy. On the other hand, the government has the role of doing what the market wants to do but cannot do because of high transaction costs, as in the aforementioned transportation market—individuals do not build a road because they bought a car. Based on this, this paper introduces the concept of transaction costs and explores how the role of village collectives can reduce the transaction costs of rural land markets, promote the realization of the value of ecological products, and thus develop and grow the collective economy.

The concept of transaction costs was first introduced by Coase in 1937 in his article "The Nature of the Firm," in which he responded to the question "Why are there firms?" His answer was that there are costs associated with the use of markets to organize production, and these are transaction costs (Coase, 1937). This means that under certain constraints, the costs of using the market to organize production (transaction costs) are too high, and the firm is used as a form of organization for production. The enterprise organizes production internally, relying on the instructions of the general manager rather than on negotiations; eliminating the transaction costs of the market transaction process, such as negotiation, coordination, and contracting; and allowing production to be carried out at a low cost. At this point, the firm as an organization is analogous to the embryonic form of government, relying on administrative orders or plans (rather than market transactions) to direct the various departments involved in production.

Specifically, in the field of agricultural production, in addition to paying for individual agricultural production costs, farmers need to pay for costs attributed to public infrastructure, such as water or irrigation works, roads, water, and electricity. Obviously, the cost of such public infrastructure is extremely high, and thus, it is unaffordable for small farmers and is the greatest obstacle to the development of the rural economy. The construction, operation, and maintenance of such public infrastructure are obviously difficult to achieve through market transactions and are things that the market wants to do but cannot do, given the extremely high transaction costs. In this case, the role of the government or village collectives should be played, and these public infrastructures should be provided by the government or village collectives (see Figure 4).

The specific method of operation is as follows: by referencing the urban land transfer system, the rural collective land is assigned to national ownership, and the central government, as the representative of the people in the nation, holds ownership of the collective land for them. The central government can entrust local governments (county, township, and village governments, cooperatives, etc.) to hold the ownership of collective land for the people, and the farmers can no longer obtain farmland without compensation but can either rent it from the local government or rent (or sell) the farmland they now own to the local government or other members of the village collective. The income from the lease or sale of arable land by the local government is used to provide public infrastructure services (e.g., roads, water conservancy projects, water, and electricity facilities) for arable land. Farmers can contract farmland for a long or short period or even for one harvest period. Local governments are responsible for continuously improving and upgrading public infrastructure and services so that the value of cultivating the land in the region is increased and farmers inside or outside the region are continuously attracted to cultivate the land in the region.

One of the current problems that needs to be solved is how to give a proper name to the capital going to the countryside. The current system stipulates that the assets of village collective housing bases and farmland can be transferred only among the members of the village collective. This prevents the optimal allocation of village collective assets and the transfer of assets to the economic agents with optimal efficiency. The solution lies in building a unified market between urban and rural areas and promoting the free flow of production factors between urban and rural areas.

4. Discussion

Based on the perspective of ecological product value realization, this paper sorts out the real dilemma of ecological product value realization of land resources and concludes that the weakening of collective property rights leading to the disintegration of rural public services and the refinement of farmers' property rights leading to the rise of agricultural operation costs are the two main reasons for the dilemma of ecological product value realization of rural land resources. These two reasons show that agricultural production has become a worthless business activity due to the rising cost of land production and operation and high transaction costs. Then, the article constructs an analytical paradigm based on the concept of transaction costs and argues that the government and the market together form a "unified" market structure, in which the government plays an active role in defining property rights and reducing transaction costs. Finally, the paper proposes a method to realize the value of ecological products of land resources.

Before the reform and opening up, China's planned economic system brought the national economy to the brink of collapse, and after the reform and opening up, the contracting of production to households led to a spectacular increase in grain production. The theoretical and logical paradigm constructed by traditional economics has been empirically validated in rural China and thus has encouraged the academic community to criticize the rural collective ownership system and advocate the market economy system. However, the system of rural land rights registration and certification, represented by privatization, has not brought the expected results, and the widespread phenomenon of extensive abandonment of arable land in rural areas, long-term underinvestment in arable land, and slowing of agricultural land transfer shows that stable and clear property rights need antecedent conditions to produce effective incentives for market agents.

A very important precondition is the need for a complete market structure. Traditional economics, which takes rationality as a logical starting point, focuses on the behavior of microindividuals and regards the government, which provides public goods and services and plays a role in reducing transaction costs, as an exogenous variable, and the relationship between the two is antagonistic. In fact,

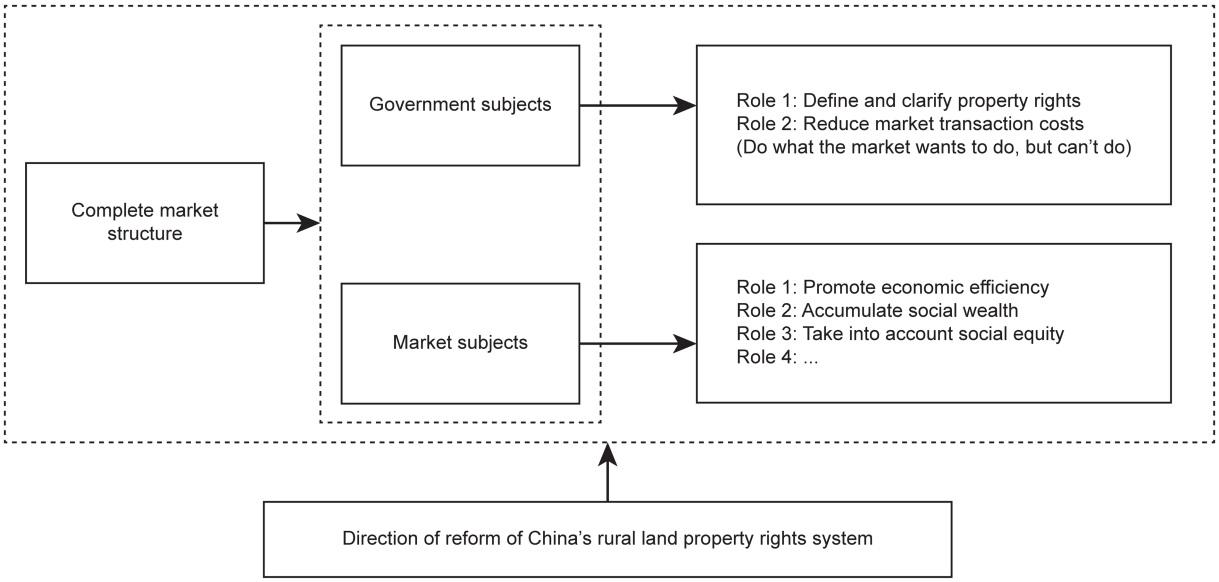

FIGURE 4
Direction of the reform of China's rural land property rights system.

this paper finds that a complete market structure should include not only independent individuals but also the government, which provides public goods and services to independent individuals and reduces the transaction costs incurred in transactions among them. This market structure is "unified" rather than a "dichotomy," similar to the relationship between the "stage" and "actors." "The "stage" is similar to the public goods or services provided by the government, while the "actors" are the independent individuals who conduct market transactions. Therefore, what the market cannot accomplish is left to the government; what the government cannot do well is left to the market. Only by combining the government and the market can we maximize the efficiency of resource allocation.

According to this logical paradigm, the direction of the future reform of the rural land system can be clearly noted. The future reform of the rural property rights system is neither a complete privatization, leaving small farmers to face the ever-changing market alone, nor a return to a planned economy, depriving small farmers of their economic autonomy. Rather, it is to reduce the transaction costs of rural economic development, to bring into play the role of local governments and village collectives, to provide the public infrastructure and services needed for agricultural production, to enable each farmer to carry out agricultural production at low cost and to make agricultural production an economically valuable business activity. The problems currently encountered cannot be solved by simple titling and licensing. If that were the case, would not the world be a very simple place? In fact, some developed economies in East Asia have smallholder economies, such as Japan, South Korea, and Taiwan, and their smallholder economies have survived and are doing well because they have collective organizations, such as the Farmers Association, that provide smallholder farmers with complete public goods and services and reduce the very large transaction costs faced by smallholder production. This success is not due to the private ownership of land.

China's basic state of a large population and a small land area, which is still in the primary stage of socialism, determines that China cannot simply apply the theoretical paradigm of traditional Western economics for economic development, as this is full of errors due to the lack of consideration of "transaction costs." Many economic theories derived from rationality have their own conditions of applicability. Ignoring the conditions of applicability of theories can mislead economic decisions, and the effect of policies is likely to be greatly reduced. For the future reform of rural land, the system should be carefully considered and acted upon in a way that is closely related to China's basic national conditions.

Data availability statement

The original contributions presented in the study are included in the article/supplementary material, further inquiries can be directed to the corresponding author.

Author contributions

ZL had the original idea and wrote the manuscript. All authors contributed to the article and approved the submitted version.

Funding

This work was supported by the Jiangxi Provincial Department of Education Science and Technology Project (No.: GJJ2202223).

Conflict of interest

The authors declare that the research was conducted in the absence of any commercial or financial relationships that could be construed as a potential conflict of interest.

Publisher's note

References

Bu, X. (2010). Institutional changes in the supply of public services in rural areas of New China. *J. Northwest. Univ. (Philos. Soc. Sci. Ed.)* 40, 98–101. doi: 10.16152/j.cnki.xdxbsk.2010.01.039

Cai, J., and Li, M. (2021). The history and logic of the changes in contemporary china's land system. *Econ. Dynamics* 12, 40–51.

Chen, J. (1994). The property system in people's commune—an institutional analysis on the exclusive system. *Econ. Res. J.* 7, 47–53.

Chen, X. (2019). Breakthroughs, achievements and revelations of forty years of rural reform. *China Agric. Dig-Agric. Eng.* 31, 5–9. doi: 10.19518/j.cnki.cn11-2531/s.2019.0018

Coase, R. H. (1937). The nature of the firm. *Economica* 4, 386–405. doi: 10.1111/j.1468-0335.1937.tb00002.x

Gao, X., Lin, Y., Xu, W., and Ouyang, Z. (2020). Research progress on the value realization of ecological products. *Acta Ecol. Sin.* 40, 24–33. doi: 10.5846/stxb201807211563

Huang, J., and Rozelle, S. (1996). Technological change: rediscovering the engine of productivity growth in China's rural economy. *J. Dev. Econ.* 49, 337–369. doi: 10.1016/0304-3878(95)00065-8

Li, X., and Liu, W. (2016). Village characteristics and village-level public goods supply in the new one-issue period-an empirical analysis based on Fujian. *Agric. Econ. Issues* 12, 51–62. doi: 10.13246/j.cnki.iae.2016.08.007

Li, Z. L., Luo, X. F., and Qiu, W. W. (2019). Business scale, land ownership stability and farmers' manure application behavior – a study based on the regulatory effect and Mesomeric effect model. *Resour. Environ. Yangtze River Basin* 8, 1918–1928. doi: 10.11870/cjlyzyyhj201908015

Lian, X., Mao, Y., and Wang, H. (2014). Fine-grained land property rights, transaction costs and agricultural production-an empirical investigation from wucun in the central plain of Inner Mongolia. *China Popul. Resour. Environ.* 24, 86–92.

Lin, J. Y. (1992). Rural reforms and agricultural growth in China. *Am. Econ. Rev.* 82, 34–51.

Liu, S. (2019). Collective land rights system changes and agricultural performance – a review of agricultural land system studies in China's 40 years of reform. *Agric. Technol. Econ.* 13, 4–16. doi: 10.13246/j.cnki.jae.2019.01.001

Liu, K., and Luo, M. (2018). Agricultural land titling, weakening of collective property rights and their impacts – a discussion based on a fine-grained scenario. *Econ. Jingwei* 35, 44–50. doi: 10.15931/j.cnki.1006-1096.20180925.002

Long, M. S., Zhao, Y. L., and Zhang, D. L. (2022). The impact of the fragmentation of arable land in mountainous areas on the abandonment of arable land by farmers. *J. Agric. Eng.* 21, 231–239. doi: 10.11975/j.issn.1002-6819.2022.21.027

Lu, X. (1992). *Rural areas and peasants in reform: an empirical study of 13 villages, including Dazhai, Liuzhuang, and Huaxi*. Party School of the Central Committee of the Communist Party of China Press.

Luo, B., and Hong, W. (2020). The logic of agricultural land titling and factor allocation of farm households. *Rural Econ.* 1, 1–7.

Luo, M. Z., Liu, K., and Zhu, W. J. (2017). Has the confirmation of rights reduced agricultural land abandonment? – a PSM empirical analysis based on a questionnaire survey of farmers in Sichuan, Henan, and Shanxi Provinces. *Agric. Technol. Econ.* 2, 15–27. doi: 10.13246/j.cnki.jae.2017.02.02

Shi, X., Hu, W., and Sun, Y. (2021). Sustainable rural construction and village public goods supply - dilemmas, causes, and institutional optimization. *Urban Plan.* 10, 45–58. doi: 10.11819/cpr20211003a

Wan, G., and Cheng, E. (1996). Economies of scale, land fragmentation and crop production in China. *China Rural Surv.* 3, 1–36.

Wang, H. (2016). *Making the Best of the Land: Research on the Use of Fragmented Agricultural Land* (doctoral dissertation, Huazhong University of Science and Technology). Available at: https://kns-cnki-net-443.webvpn.jsnu.edu.cn/KCMS/detail/detail.aspx?dbname=CDFDLAST2019&filename=1018801129.nh

Wang, H., and Hu, S. (2018). An analytical framework of land fragmentation and agricultural land system. *Soc. Sci.* 11, 62–74. doi: 10.13644/j.cnki.cn31-1112.2018.11.007

Xu, X. (2002). *Public services in rural China*. China Development Press.

Xu, Q. (2008). "Changes, characteristics and reform direction of the household responsibility system," World Economic Journal No. 182.01: 93–100.

Xu, Q., Tian, S., Xu, Z., and Shao, T. (2008). Agricultural land system, land fragmentation and farmers' income inequality. *Econ. Res.* 2, 83–92.

Yan, J., Guo, D., and Xia, F. (2021). The "historical logic, theoretical logic and practical logic" of the century-long land system change of the Chinese Communist Party. *Manag. World* 37, 19–31+12. doi: 10.19744/j.cnki.11-1235/f.2021.0089

Zhang, S., and Cheng, L. (2012). Complex property rights theory and effective property rights theory-an analytical framework for land rights changes in China. *Econ. (Q.).* 11, 1219–1238. doi: 10.13821/j.cnki.ceq.2012.04.005

Zhao, Y., and Song, T. (2022). Land rights subdivision, capital to the countryside and rural revitalization – based on the perspective of public services. *Soc. Sci. Front.* 1, 41–50+281–41–50+282.

Zhou, Q. (1995). China's rural reform: the changing relationship between state and ownership(above)-a review of the history of economic system change. *Manag. World* 3, 178–189+219–178–189+220. doi: 10.19744/j.cnki.11-1235/f.1995.03.029

frontiers | Frontiers in Environmental Science

TYPE Original Research
PUBLISHED 28 August 2023
DOI 10.3389/fenvs.2023.1256028

OPEN ACCESS

EDITED BY
Hua Lu,
Jiangxi University of Finance and Economics, China

REVIEWED BY
Yayun R. En,
Guizhou University of Finance and Economics, China
Dan Pan,
Jiangxi University of Finance and Economics, China
Yi Xie,
Museum of Beijing Forestry University, China

*CORRESPONDENCE
Wenmei Liao,
liaowenmei@126.com
Hailan Qiu,
qiuhailan@jxau.edu.cn

RECEIVED 11 July 2023
ACCEPTED 14 August 2023
PUBLISHED 28 August 2023

CITATION
Liu Y, Liao WM, Zhang X and Qiu HL (2023), Impact of high standard farmland construction policy on chemical fertilizer reduction: a case study of China. *Front. Environ. Sci.* 11:1256028. doi: 10.3389/fenvs.2023.1256028

Impact of high standard farmland construction policy on chemical fertilizer reduction: a case study of China

Yang Liu[1], Wenmei Liao[1,2]*, Xu Zhang[1] and Hailan Qiu[1,2]*

[1]School of Economics and Management, Jiangxi Agricultural University, Nanchang, China, [2]Jiangxi Rural Revitalization Strategy Research Institute, Nanchang, China

Promoting chemical fertilizer (CF) reduction is an inevitable requirement for achieving high-quality agricultural development, and high standard farmland construction (HSFC) provides a new path for promoting CF reduction. Takes the implementation of HSFC policy as the starting point, this paper uses the provincial panel data of China from 2005 to 2017 to analyze the impact of HSFC policy on CF reduction and its mechanism of action by using the continuous difference-in-difference (DID) model and mediating model. The baseline regression results show that implementing the HSFC policy has reduced the amount of CF per unit area by 8.9 % on average, which has a significant policy effect. The mechanism analysis shows that the HSFC policy can promote CF reduction by improving the agricultural mechanization level and expanding the scale of operations in agriculture. The results of heterogeneity analysis show that in the natural geographical location dimension, the effect of HSFC policy on CF reduction in the eastern and central regions is more obvious; In the dimension of functional areas of grain production, the impact of HSFC policy on CF reduction in major grain-producing regions is more obvious. Therefore, in the future, it is necessary to continue to vigorously promote the HSFC and give full play to the effective role of HSFC in CF reduction. China should vigorously promote the development level of agricultural mechanization and the large-scale operation of agriculture and further strengthen the HSFC in the western region and non-major grain-producing areas.

KEYWORDS

high standard farmland construction, chemical fertilizer reduction, continuous DID model, mediating model, agricultural mechanization, agricultural operation scale

1 Introduction

Since the reform and opening up, chemical fertilizer (CF) application has become increasingly common in agricultural production to improve soil fertility and has played an essential role in enhancing China's agricultural production efficiency and increasing crop yield (Lin J Y, 1992). For an extended period, to pursue high work and high efficiency, people have continuously improved the input of CF (Liu et al., 2020). According to the China Bureau of Statistics, the amount of CF applied in China increased from 58.892 kg/hm^2 to 307.730 kg/hm^2 from 1978 to 2021. However, we also clearly recognize that based on the law of diminishing returns to scale, excessive CF application is difficult to achieve sustained agricultural growth (Krugman, 1994). Applying large amounts of CF in agricultural production will lead to problems such as soil hardening and degradation, water

environment pollution, and higher production costs (Kumar R et al., 2019). For example, over-fertilization in China causes more than 10 million tons of nitrogen to be lost off farmland yearly, resulting in direct economic losses of about 30 billion yuan. Excessive CF will also infiltrate shallow groundwater within 20 m, increasing the nitrate content in groundwater, which is not conducive to ensuring China's food security and sustainable agricultural development. To improve soil fertility, increase grain production and stabilize grain production, in September 2011, the former Ministry of Land and Resources of China issued the "High Standard Basic Farmland Construction Specification (Trial)" for the first time, marking that China's high standard farmland construction (HSFC) policy has entered the pilot implementation stage. China's former Ministry of Agriculture promulgated the "high standard farmland construction standard" on 1 March 2012, to strictly protect cultivated land quality. In 2013, the State Council approved the "China Agricultural Comprehensive Development High Standard Farmland Construction Plan (2011–2020)" for the first time to cover HSFC measures in five aspects: water conservancy, agriculture, field road construction, forestry, and science and technology. The critical content involves farmland engineering, soil improvement, agricultural mechanization, stock breeding, and promotion of improved varieties. Since then, the importance of HSFC has been emphasized in China's Central No. 1 Document every year. By 2021, China's HSFC area has reached 910 million mu. The data showed that the mechanization level of high-standard farmland projects is 15–20 percentage points higher than that of non-project regions, and the water saving reaches 20%–30%. Can high-standard farmland projects reduce CF, agricultural production costs, and agricultural output efficiency? It is a topic worthy of further discussion.

Recently, China has implemented several CF reduction measures. Although the problem of excessive CF application has been alleviated, it has not been fundamentally solved (Huang J et al., 2017). Many scholars have tried to explore a fast and effective Chinese path to promote CF reduction from multiple perspectives, mainly including the following aspects. Firstly, from the standpoint of production technology, it focuses on the impact of CF or soil production factors, such as the scientific application of CF (Ju X et al., 2009), the use of biological fertilizers (Wang X Y et al., 2021), efficient rotation and intercropping (Han J et al., 2021), soil improvement (Abbruzzini T F et al., 2019), etc. Secondly, from the perspective of the main body of agricultural management, it focuses on the influence of farmers or rural households "factors, such as farmers" income level (Li D et al., 2012), cognitive characteristics (Li Y F et al., 2019), risk preference (Li X and Shang J., 2021), etc. Thirdly, from the perspective of agricultural management, focusing on the confirmation of land right (Holden and Yohannes, 2002), land tenure security (Li B and Zeng Q., 2022), scale management (Wu X. et al., 2021), agricultural specialization (Zhou S et al., 2023), agricultural mechanization level (Liu J et al., 2022); Fourthly, from the consumer side, focusing on guiding consumers to enhance their preferences for green or organic agricultural products, and forcing agricultural production to transition to CF reduction (Tian M et al., 2022). It can be seen that the research on the factors affecting the promotion of CF reduction is diversified, but the effect of HSFC policies is ignored. As the basis of farmland behavior, the cognition of HSFC policy is the critical step to promote the development of modern agriculture.

There are discussions on HSFC policies, mainly focusing on the planning and design of construction (Song W et al., 2019), suitability analysis of construction implementation (Wang Y et al., 2022), construction potential assessment (Pu L et al., 2019), status analysis of construction implementation (Ye F et al., 2023), and supervision of high standard farmland (Peng et al., 2022a). There are few studies on the performance evaluation of the policy, mainly focusing on evaluating the guarantee capacity of food security (Yan H et al., 2022). The environmental effects of the policy have not been fully discussed, such as the effect of CF reduction.

This paper uses the panel data of 31 provinces, municipalities, and autonomous regions in China from 2005 to 2017, uses the continuous difference-in-difference model to analyze the impact of HSFC on CF reduction empirically, and further analyzes and verifies its impact mechanism to provide scientific and reasonable policy reference for promoting CF reduction based on HSFC in the future. Compared with the existing literature, the main contributions of this paper are as follows: firstly, theoretical analysis of the influence logic of HSFC policy on CF application, deepen the understanding of the environmental effects of HSFC policy, and provide new ideas for promoting sustainable agriculture development in China; secondly, the continuous difference-in-differences method was used to explore the effect of HSFC policy on the amount of CF application and its heterogeneity, eliminate the confusing effects of unobservable factors that do not change with time, and improve the accuracy of the research conclusions; Thirdly, take the introduction of agricultural machinery and operation scale as mediating variables to reveal the internal mechanism and realization path of the reduction effect of HSFC policies on the total amount of CF application, so as to provide scientific and reasonable policy reference for promoting CF reduction based on HSFC in the future.

The rest of the paper proceeds as follows. The second section combs the theoretical logic of HSFC policy and CF reduction. The third section is the research design, including empirical models, variable selection, data sources, etc. The fourth section analyzes the impact of the policy on the amount of CF and its mechanism of action. The fifth section summarizes the research results and discusses policy recommendations.

2 Theoretical analysis and research hypothesis

2.1 Effect of HSFC policy on CF reduction

High-standard farmland refers to the bare farmland formed by rural land consolidation in a certain period, which is concentrated, equipped with facilities, high and stable yield, sound ecology, strong disaster resistance, and suitable for modern agricultural production and management. The implementation of HSFC policies has had an important impact on promoting CF reduction. Firstly, improving cultivated land quality is urgently needed to achieve CF reduction (Wu H. et al., 2021). The HSFC policy increases the organic matter content of the soil. It improves the quality and output capacity of cultivated land by establishing the monitoring point of cultivated land quality, tracking and monitoring the quality of cultivated land,

and taking measures such as applying organic fertilizer in time. Farmers' dependence on CF is reduced when cultivated land quality is improved. Secondly, through the transformation of field roads, the HSFC policy determines the width and density of roads according to the topographic conditions of various places, improves the degree of specialization of agricultural production and the organic composition of capital in the agricultural sector, and provides the possibility for the use of agricultural social services to promote CF reduction (Yang, C et al., 2022). Finally, HSFC helps reduce the cost of farmers' use of CF by realizing land leveling and centralized contiguous management and reducing cultivated land fragmentation (Hu et al., 2022). Therefore, on the whole, HSFC policies can promote CF reduction. Based on the above analysis, the research hypothesis is proposed:

Hypothesis 1: HSFC policies will promote CF reduction.

2.2 HSFC policy, agricultural mechanization, and CF reduction

The CF reduction depends not only on the progress of agricultural technology but also on the adoption of reduction technology by micro-business entities. The classical economic growth theory holds that farmers are an economic entity that passively adopts new technologies (Hu Y and Zhang Z H, 2018). For example, mechanical fertilization achieves CF reduction by uniforming operation quality and saving labor costs, but agricultural machinery's high investment cost limits farmers' investment motivation (Sarkar A, 2020). However, under an open factor market, many agricultural households choose to outsource production links, and CF reduction also has internal motivation. Whether farmers directly purchase machinery or purchase productive services such as machinery, they need to meet the requirements of agricultural machinery for road patency, ground leveling, and concentration of working areas. The HSFC policy optimizes the working environment of agricultural machinery. It promotes CF reduction through field road construction, land consolidation, and "change the land to fit the machine" (Wan L X and Yang G, 2023). Based on the above analysis, the research hypothesis is proposed:

Hypothesis 2: Improving the level of agricultural mechanization can promote CF reduction.

Hypothesis 3: HSFC policies can promote CF reduction by increasing agricultural mechanization levels.

2.3 HSFC, agricultural operation scale, and CF reduction

CF reduction is also closely related to the agricultural operation scale. On the one hand, CF reduction has specific requirements on the operation scale (Chen X and Liu T, 2023). Large-scale operations will reduce the cost of CF application per unit area, which is conducive to farmers' adoption of CF reduction (Guo J et al., 2022). For example, the promotion of soil testing and balanced fertilization technology has the disadvantages of difficulty, time-consuming and high cost, which makes the adoption of small-scale farmers relatively low (Wu H et al., 2022); On the other hand, the government has strict requirements on the use of CF by large-scale farmers. In addition, large-scale operations can facilitate government training and guidance on CF reduction (Wu Y et al., 2018). Therefore, within the appropriate scale, the expansion of the operation scale can promote CF reduction. HSFC policy will also have a certain impact on the operation scale. The HSFC can alleviate the fragmentation of farmland, promote the large-scale operation of farmland as a whole and improve the efficiency of agricultural technology (Bhatt and Bhat, 2014), release the scale economy effect, and further promote the development of moderate-scale operation. Based on the above analysis, the research hypothesis is proposed:

Hypothesis 4: Expanding the agricultural operation scale can promote CF reduction.

Hypothesis 5: HSFC policies can promote CF reduction by expanding the agricultural operation scale.

Based on the above theoretical analysis, the theoretical framework of this paper is shown in Figure 1.

3 Research design

3.1 Model design

The HSFC policy began to be standardized and implemented nationwide in 2011, which resulted in significant differences in the scale of land consolidation around 2011. At the same time, due to the spatial heterogeneity of policy implementation (Delgado and Florax, 2015), the HSFC policy can be used as a natural experiment to form a research space for policy effect evaluation. So this paper intends to use a continuous DID model to examine the effect of HSFC policies on CF reduction. The continuous DID can directly use continuous variables to distinguish the treatment group and the control group, which can capture more data variability and avoid the deviation caused by artificially setting the treatment group and the control group (Chen Y and Zhou L A, 2007). Specifically, this paper uses the continuous variable of "the proportion of land consolidation area" to distinguish the treatment group (samples with a large proportion of land consolidation area) and the control group (samples with a small proportion of land consolidation area).

3.1.1 Baseline regression model

To investigate the effect of HSFC policy on the amount of CF, referring to the practice of Fortson J G (2009), this paper constructs the following continuous DID model:

$$lnFertilizer_{it} = \alpha + \beta Lcap_i \times I_t^{post} + \delta X_{it} + \mu_i + \gamma_t + \varepsilon_{it} \quad (1)$$

In Eq. 1, $lnFertilizer_{it}$ is the explained variable, which represents the amount of CF per unit area of province i in period t and takes the natural logarithm; $Lcap_i$ represents the continuous variable of the proportion of land consolidation area; I_t^{post} represents the dummy variable of the time point of policy

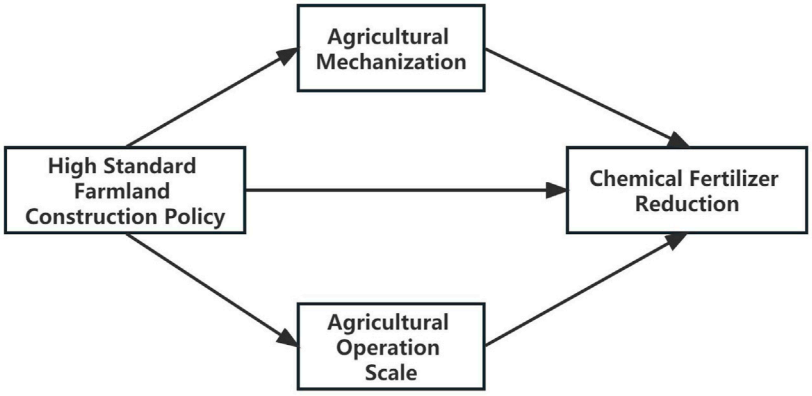

FIGURE 1
Chemical fertilizer reduction mechanism of high standard farmland construction policy.

implementation. When the time is taken during the policy implementation period, take 1; otherwise, 0; X_{it} represents a series of control variables; μ_i is the provincial fixed effect, γ_t is the time fixed effect, and ε_{it} is the random error term. α is a constant term, β and δ are the parameters to be estimated.

3.1.2 Parallel trend test model

Referring to the practice of Nunn and Qian (2011), the following model is constructed to test the parallel trend hypothesis:

$$lnFertilizer_{it} = \alpha + \sum_{t=2005}^{2017} \beta_t Lcap_i \times D_t + \delta X_{it} + \mu_i + \gamma_t + \varepsilon_{it} \quad (2)$$

D_t represents the year dummy variable. The remaining variables and symbols have the same meaning as Eq. 1.

3.1.3 Mechanism verification model

In order to identify whether HSFC policies affect CF reduction by expanding the agricultural operation scale and improving the agricultural mechanization level, the following models were constructed by referring to the mediating effect analysis method proposed by Wen Z L and Ye B J (2014):

$$M_{it} = \alpha + \theta Lcap_i \times I_t^{post} + \delta X_{it} + \mu_i + \gamma_t + \varepsilon_{it} \quad (3)$$

$$lnFertilizer_{it} = \alpha + \omega Lcap_i \times I_t^{post} + \tau M_{it} + \delta X_{it} + \mu_i + \gamma_t + \varepsilon_{it} \quad (4)$$

In Eqs 3, 4, M_{it} is the mechanism variable of concern: the agricultural mechanization level and the farm operation scale. θ, ω, and τ are the parameters to be estimated. The remaining variables are consistent with (1).

3.2 Variable selection

3.2.1 Explained variables

The amount of CF is characterized by the amount per unit area, calculated by dividing the total amount of CF application by the total sown area of crops.

3.2.2 Core explanatory variables

High standard farmland construction (HSFC) policy. The interaction term ($Lcap_i \times I_t^{post}$) between the proportion of land consolidation area and the dummy variable of the HSFC policy implementation time point was used to characterize. The proportion of land consolidation area is the percentage of low-yield and high-standard farmland in the total cultivated land area. At the same time, the interaction term ($Ainve_i \times I_t^{post}$) of agricultural comprehensive development investment and policy variables is used as a substitute variable for the core explanatory variable for the robustness test (Liang et al., 2021).

3.2.3 Control variables

In addition to the impact of HSFC policies on the amount of CF per unit area, it is also necessary to control the exogenous interference of other factors on the amount of fertilizer per unit area. Based on the practice of Xu et al. (2022) and Xiang et al. (2022), the following control variables are selected: Urbanization rate (*Urban*), the percentage of urban population in the total population; The number of agricultural labor force (*Labor*), expressed as the number of people employed in the primary industry; The average years of education (*Edu*) of rural labor force is calculated according to the weighted years of schooling at different learning stages; Planting structure (*Struc*) is expressed by the ratio of the sown area of grain crops to the total planted area of crops; The multiple cropping index (*Mcrop*) is described as the ratio of crop planting area to cultivated land area; The price of chemical fertilizer (*Fprice*) is characterized by the price index of chemical fertilizer production materials, with 2005 as the base period; The disaster rate (*Disas*) is the percentage of the affected area to the cultivated land area.

3.2.4 Mediating variable

According to the above theoretical analysis, the agricultural mechanization level (*Mech*) and the agricultural operation scale (*Scale*) are selected as the mechanism variables, and the ratio of agricultural machinery's total power to the cultivated land area is used to measure the farm mechanization level. Referring to Peng

TABLE 1 Descriptive statistics.

Variable abbreviation	Variable name	Mean	Standard deviation
Fertilizer	Chemical fertilizer amount (kg/hm$^{2)}$	363.374	132.313
Lcap	The proportion of land consolidation area (%)	37.072	21.627
Urban	Urbanization rate (%)	52.259	14.718
Labor	Amount of agricultural labor (million people)	900.835	661.016
Edu	The average years of education of the rural labor force (year)	7.502	0.816
Struc	Planting structure (%)	66.657	13.095
Mcrop	Multiple-crop index (%)	1.232	0.363
Fprice	Chemical Fertilizer Prices	103.696	10.242
Disaster	Disaster rate (%)	25.753	17.476
Mech	Agricultural mechanization level (Kw/hm$^{2)}$	7.584	3.715
Scale	Agriculture operation scale (hm^2/person)	0.614	0.319

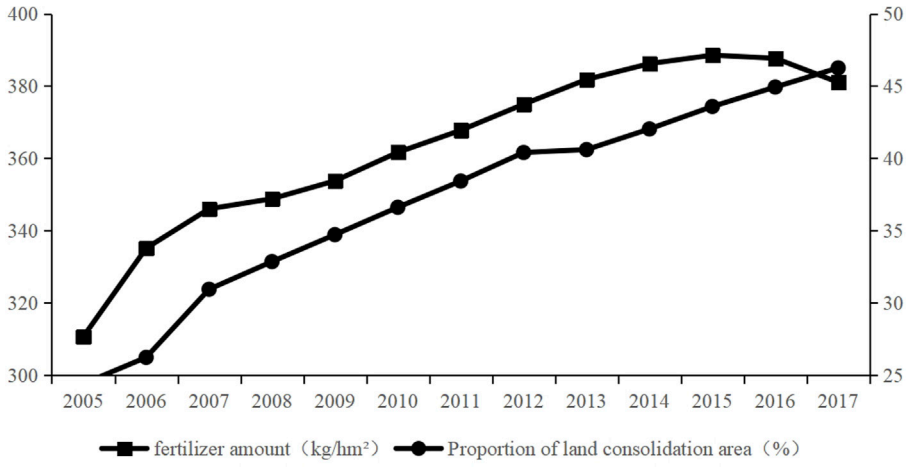

FIGURE 2
Proportion of land consolidation area and amount of chemical fertilizer.

et al. (2022b) research, this paper measures the scale of agricultural operation from the perspective of per labor crop planting area.

3.3 Data sources and descriptive evidence

This paper takes 31 provinces, municipalities, and autonomous regions from 2005 to 2017 (due to the serious lack of data in Hong Kong, Macao and Taiwan, it is eliminated) as the research object and analyzes the impact of HSFC policies on CF use. Among them, the amount of CF, the number of the agricultural labor force, and the average years of education of the rural labor force are derived from the China Rural Statistical Yearbook; the proportion of land consolidation area and the input data of agricultural comprehensive development are from the China Financial Yearbook; the urbanization rate, planting structure, multiple cropping index, CF price index, disaster rate, agricultural mechanization level, and agricultural operation scale data are derived from the China Statistical Yearbook. Table 1 shows the descriptive statistical characteristics of the variables.

It can be seen from Figure 2 that from 2005 to 2017, the proportion of land consolidation areas in China increased year by year, and it showed a rapid upward trend after the implementation of the HSFC policy. At the same time, after the performance of the HSFC policy, the growth trend of CF use per unit area slowed down. After reaching its peak in 2015, it began to show a declining trend. The factors affecting the amount of CF are very complicated. To more accurately study the relationship between HSFC policies and the amount of CF, relevant control variables need to be added. This paper conducts an empirical analysis of this.

TABLE 2 Baseline estimation results.

Variable	Ordinary standard error	Robust standard error	Bootstrap sampling 1000 times
	(1)	(2)	(3)
$Lcap \times I^{post}$	−0.089***	−0.089***	−0.089***
	(0.013)	(0.024)	(0.024)
Urban	0.001	0.001	0.001
	(0.002)	(0.004)	(0.005)
LnLabor	0.128***	0.128	0.128
	(0.033)	(0.081)	(0.084)
Edu	−0.008	−0.007	−0.008
	(0.020)	(0.033)	(0.033)
Struc	−0.007***	−0.007***	−0.007***
	(0.001)	(0.002)	(0.002)
Mcrop	−0.392***	−0.392***	−0.392***
	(0.032)	(0.067)	(0.076)
LNFprice	−0.056	−0.056	−0.056
	(0.089)	(0.064)	(0.068)
Disaster	0.001*	0.001*	0.001*
	(0.001)	(0.001)	(0.001)
Cons	6.036***	6.036***	6.036***
	(0.515)	(0.717)	(0.751)
Provincial effects	Yes	Yes	Yes
Year effect	Yes	Yes	Yes
R-squared	0.6851	0.6851	0.6851
Sample size	403	403	403

Note: ***, **, and * indicate significance at the 1%, 5%, and 10% statistical significance levels, respectively, and the standard errors are in parentheses corresponding to the regression coefficients.

4 Empirical results and analysis

4.1 Baseline regression results

Before the baseline regression, the variance inflation factor test found that the VIF values of each explanatory variable were lower than 4.21, so the multicollinearity problem between explanatory variables could be excluded. According to Formula 1, the effect of the implementation of the HSFC policy on the amount of CF per unit area is estimated. The results are shown in Table 2. Table 2 column (1)–(3) is the estimation results of the common standard errors, the robust standard errors, and the standard errors obtained by Bootstrap self-help random sampling for 1000 iterations. In the case of three standard misestimations, the estimated coefficients of the HSFC policy on the amount of CF per unit area have passed the 1% significance level test, indicating that the model estimation results have good robustness. At the same time, the coefficient of the HSFC policy variable is negative, meaning that the HSFC policy can significantly reduce the amount of CF per unit area. Under the same other conditions, the estimated coefficient of the HSFC policy is −0.089, which indicates that the implementation of the HSFC policy has reduced the amount of CF per unit area by 8.9% on average and has a significant policy effect. Accordingly, Hypothesis 1 is verified. In addition, considering that this paper focuses on the causal relationship between HSFC policy and CF use per unit area, there is little discussion on control variables.

4.2 Parallel trend test and dynamic impact of policy

The continuous DID model's premise is that it needs to pass the parallel trend test. Although the previous graphic can preliminarily test the parallel trend, to more accurately judge whether the HSFC policy meets the parallel trend hypothesis before implementation, this paper tests it through the econometric model in Formula (2). Figure 3 depicts the changing trend of the estimated coefficient. It can be found that before the implementation of the HSFC policy, the estimated coefficient β_t generally showed a downward trend, and the confidence interval of the impact coefficient included the value of 0. Therefore, it can be judged that there is no systematic difference in the estimated coefficients

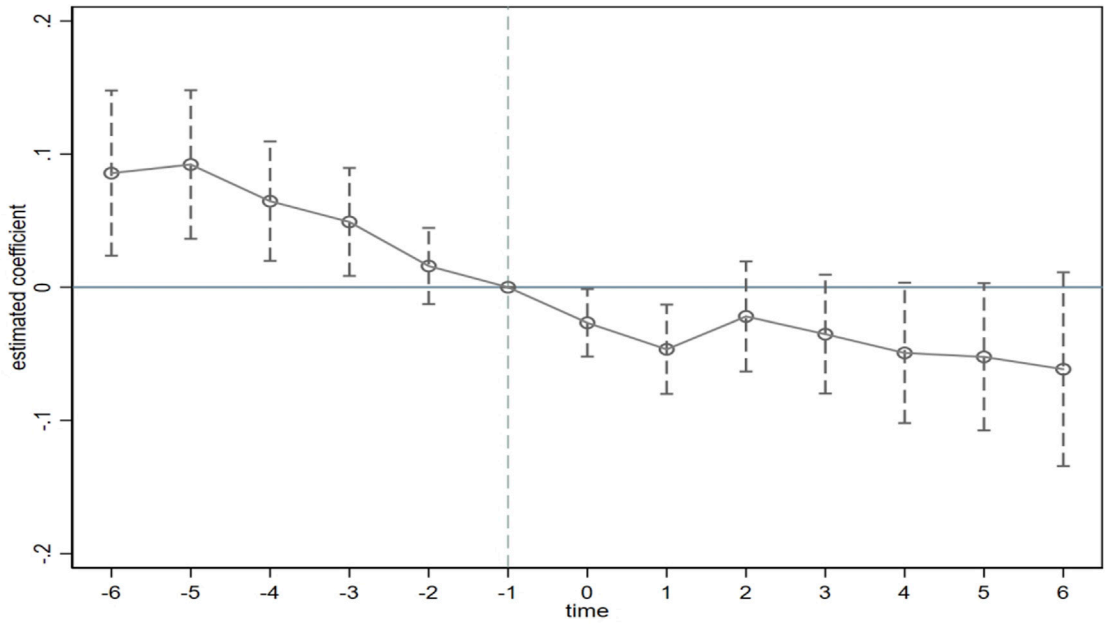

FIGURE 3
Parallel trend test and dynamic effect.

TABLE 3 Dynamic impact estimation results.

Variable	Coefficient St.Er	Variable	Coefficient St.Er
Lcap × 2005	0.086 (0.089)	*Lcap × 2015*	−0.049***(0.016)
Lcap × 2006	0.092 (0.075)	*Lcap × 2016*	−0.052***(0.017)
Lcap × 2007	0.065 (0.049)	*Lcap × 2017*	−0.062***(0.022)
Lcap × 2008	0.049 (0.030)	X_{it}	Yes
Lcap × 2009	0.016 (0.014)	*Cons*	6.126***(0.710)
Lcap × 2011	−0.027**(0.012)	*Provincial effects*	Yes
Lcap × 2012	−0.047***(0.016)	*Year effect*	Yes
Lcap × 2013	−0.022**(0.010)	*R-squared*	0.7008
Lcap × 2014	−0.035***(0.012)	*Sample size*	403

The italic values represents the high standard farmland construction in different years, and the number is the influence coefficient of the high standard farmland construction policy on the reduction of chemical fertilizer in different years.

between the years before the implementation of the HSFC policy and the parallel trend test passed. At the same time, it shows that the HSFC proposed in 2011 can be regarded as a quasi-natural experiment and can be estimated using the continuous DID model.

Table 3 reports the dynamic estimation results of the impact of the implementation of HSFC policies on the amount of CF per unit area. From the first year before the implementation of the HSFC policy, the estimated coefficient has changed to a negative number. The reason is that the implementation of the HSFC policy can be pre-judged. In 2010, the Central No. 1 Document proposed vigorously building high-standard farmland, causing some provinces to respond in advance. It is not difficult to understand why the effect of HSFC policy on CF reduction can be observed in the first year before the implementation.

In addition, the estimated coefficients were not significant before the implementation of the HSFC policy. In contrast, the estimated coefficients passed the significance test and were negative in the year and after the policy implementation. Before the implementation of the HSFC policy, the estimated coefficient shows a general downward trend, indicating that the policy's effect on CF reduction is continuous.

Specifically, the effect of the HSFC policy on CF reduction showed a positive trend of decreasing first and then increasing. The estimated coefficients in the current year and the first year of the implementation were −0.027 and −0.047, respectively, with a significant decrease. In the second year (2013) after the implementation of the HSFC policy, the estimated coefficient increased significantly (−0.022). Starting from 2013, the estimated coefficient of the HSFC policy showed a steady downward trend and reached the lowest value (−0.062) in the sixth year (2017) after the implementation. The estimated coefficient of the fifth year (2016) of the implementation of the HSFC policy (−0.052). Overall, this shows that the HSFC policy is sustainable.

4.3 Robustness tests

In order to ensure the robustness of the model estimation results, this paper draws on the research of Acemoglu et al. (2019), Zhang et al. (2019), and Zhu et al. (2020), trying to consider the missing variables and the continuity of the economic and social environment, change the policy implementation time point, eliminate other policy interference,

TABLE 4 Robustness tests.

Variable	Considering missing variables and the continuity of the economic and social environment	Changing the policy implementation time point	Eliminate other policy interference	Replacing the core explaining variables	Eliminating municipalities
	(1)	(2)	(3)	(4)	(5)
$Lcap \times I^{post}$	−0.085***	—	−0.077***	—	−0.088***
	(0.022)		(0.023)		(0.027)
$Lcap \times I^{post2008}$	—	−0.059	—	—	—
		(0.043)			
$Ainve \times I^{post}$	—	—	—	−0.046**	—
				(0.018)	
X_{it}	Yes	Yes	Yes	Yes	Yes
Cons	6.142***	4.332***	5.094***	5.808***	6.246***
	(0.989)	(0.812)	(0.713)	(0.548)	(0.669)
Provincial effects	Yes	Yes	Yes	Yes	Yes
Year effect	Yes	Yes	Yes	Yes	Yes
R-squared	0.6203	0.7165	0.7017	0.6421	0.6877
Sample size	372	186	310	403	351

Note: ***, **, and * indicate significance at the 1%, 5%, and 10% statistical significance levels, respectively, and the standard errors are in parentheses corresponding to the regression coefficients.

replace core explanatory variables, and eliminate municipalities. The results are shown in Table 4.

4.3.1 Considering the missing variables and the continuity of the economic and social environment

By introducing *per capita* GDP into the control variables and lagging it with the CF price index for one period, the impact of missing variables and the continuity of the economic and social environment on the estimation results is controlled. The estimation results are shown in Column (1) of Table 4. The interaction term $Lcap \times I^{post}$ still significantly negatively affects the amount of CF per unit area at 1%, and the previous baseline estimation results are still valid.

4.3.2 Changing the policy implementation time point

This paper selects the sample data before the policy implementation (i.e., 2005–2010) and takes 2008 as the time point of policy implementation for the placebo test. The estimated results are shown in Column (2) of Table 4. The results show that the estimated coefficient of the interaction term $Lcap \times I^{post2008}$ on the amount of CF per unit area is negative but insignificant. Therefore, it can be considered that other policies have no effect before implementing the HSFC policy. This again verifies the robustness of the previous baseline estimation results.

4.3.3 Eliminating other policy interference

In 2015, the Ministry of Agriculture (now the Ministry of Agriculture and Rural Affairs) issued the 'Zero Growth Action Plan for Chemical Fertilizer Use by 2020'to guide the reduction of CF use in agricultural production in various regions, which will inevitably have an impact on the amount of CF used per unit area. Therefore, this paper verifies whether the baseline estimation results are robust by eliminating the data after 2015, and the estimation results are shown in Column (3) of Table 4. Considering the interference of the zero growth policy of CF, the HSFC policy still has a significant adverse effect on the amount of CF per unit area at the level of 1%.

4.3.4 Replacing core explanatory variables

The input of comprehensive agricultural development is also the main basis for measuring the degree of HSFC. If there is a causal relationship between the implementation of HSFC policies and the CF reduction, then whether it is the proportion of land consolidation area or the interaction of virtual variables between the input of comprehensive agricultural development and the time point of policy implementation will not change the basic conclusions of this paper. The results in Column (4) of Table 4 show that the negative impact of the interaction term $Ainve \times I^{post}$ after replacing the core explanatory variables on the amount of CF per unit area is significant at the 5% level, and the estimated coefficient is −0.046. This again confirms the robustness of the pre-conclusion.

4.3.5 Elimination of samples from municipalities directly under the central government

Considering that the cities differ from the general provinces regarding administrative power, economic level, and agricultural development, this paper further narrows the sample range. It excludes the data from four samples Beijing, Tianjin, Shanghai, and Chongqing. Table 4 Column (5) is its estimation result. The

TABLE 5 Mechanism analysis: effect of mechanization and scale on CF reduction.

Variable	*LnFertilizer*	*Mech*	*Scale*	*LnFertilizer*	
	(1)	(2)	(3)	(4)	(5)
$Lcap \times I^{post}$	−0.089***	0.065***	0.010**	−0.081**	−0.062**
	(0.013)	(0.015)	(0.004)	(0.037)	(0.028)
Mech	—	—	—	−0.072***	—
				(0.026)	
Scale	—	—	—	—	−0.094***
					(0.030)
X_{it}	Yes	Yes	Yes	Yes	Yes
Cons	6.036***	15.603***	4.233***	5.967***	6.342***
	(0.515)	(9.499)	(0.631)	(0.609)	(0.545)
Provincial effects	Yes	Yes	Yes	Yes	Yes
Year effect	Yes	Yes	Yes	Yes	Yes
R-squared	0.6851	0.5317	0.6152	0.5625	0.6876
Sample size	403	403	403	403	403

Note: ***, **, and * indicate significance at the 1%, 5%, and 10% statistical significance levels, respectively, and the standard errors are in parentheses corresponding to the regression coefficients.

estimated coefficient of the HSFC policy is still significantly negative at the statistical level of 1%. It is very close to the estimated value of the baseline model, indicating that the previous baseline regression results are still robust.

4.4 Mechanism analysis

The empirical results above show that the HSFC policies promote CF reduction. Based on the previous theoretical analysis, this part analyzes the specific mechanism of action from the perspectives of agricultural mechanization level and agricultural operation scale. Table 5 reports the results of the mechanism analysis.

The results of Column (2) in Table 5 show that the implementation of the HSFC policy has a significant positive impact on the agricultural mechanization level, with a coefficient of 0.065, which has passed the 1% significance level test. It shows that implementing the HSFC policy is conducive to improving the agricultural mechanization level. Compared with Column (4), it can be seen that when the mediating variable of agricultural mechanization level is added to the model, the significance of the estimated coefficient of the HSFC policy on the amount of CF per unit area has decreased, from the original significant at the 1% level to the significant at the 5% level. The estimation coefficient of the HSFC policy on the amount of CF per unit area has increased. The agricultural mechanization level has partially mediated the HSFC policy's promotion of CF per unit area. This shows that the HSFC policies promote CF reduction by improving the agricultural mechanization level. In summary, the research Hypotheses 2 and Hypotheses 3 are verified.

The results of Column (3) in Table 5 show that the implementation of the HSFC policy has a significant positive impact on the agricultural operation scale, with a coefficient of 0.010, which has passed the 5% significance level test, indicating that the implementation of the HSFC policy is conducive to improving the agricultural operation scale. In Column (5), after adding the agricultural operation scale as a control variable to the regression equation, the HSFC policy significantly negatively affects the amount of CF per unit area at the level of 5%. At the same time, the estimated coefficient of the HSFC policy on the amount of CF per unit area has increased. The agricultural operation scale has partially mediated the HSFC policy's promotion of CF per unit area. Therefore, the HSFC policies promote CF reduction by increasing the agricultural operation scale. In summary, research Hypotheses 4 and Hypotheses 5 are verified.

4.5 Heterogeneity tests

4.5.1 Location heterogeneity

Considering China's vast territory, there are obvious regional differences. In order to further analyze the regional differences in CF reduction by the HSFC policies, this paper divides 31 provinces from the perspective of natural geographical location and food production functional areas.

Table 6 reports the estimation results of regional heterogeneity of the HSFC policies on CF use per unit area. Table 6 Column (1)–(3) reports the estimation results of the HSFC policy on the amount of CF per unit area in the natural geographical location dimension. The results showed that the effect of the HSFC policy on the amount of CF per unit area was the strongest in the eastern region, followed by the central region, and the weakest in the western region. The estimation coefficient of the HSFC policy in the western region was insignificant. The reason is that the economic development level in the eastern and central regions is better than western region. After the policy implementation, the

TABLE 6 Location heterogeneity.

Variable	Natural geographical location			Functional zone of grain production	
	(1)Eastern region	(2)Central region	(3)Western region	(4) Major grain-producing areas	(5)Non-major grain-producing areas
$Lcap \times I^{post}$	−0.094***	−0.064**	−0.061	−0.106***	−0.059**
	(0.025)	(0.024)	(0.035)	(0.027)	(0.033)
X_{it}	Yes	Yes	Yes	Yes	Yes
Cons	7.536***	6.287***	3.856***	6.073***	5.421***
	(0.629)	(1.041)	(1.186)	(1.514)	(0.895)
Provincial effects	Yes	Yes	Yes	Yes	Yes
Year effect	Yes	Yes	Yes	Yes	Yes
R-squared	0.8326	0.7708	0.7684	0.6541	0.7555
Sample size	143	104	156	169	234

Note: ***, **, and * indicate significance at the 1%, 5%, and 10% statistical significance levels, respectively, and the standard errors are in parentheses corresponding to the regression coefficients.

TABLE 7 Distribution heterogeneity.

Variable	0.1quantile	0.25quantile	0.5quantile	0.75quantile	0.9quantile
	(1)	(2)	(3)	(4)	(5)
$Lcap \times I^{post}$	−0.074***	−0.072***	−0.078***	−0.076***	−0.061***
	(0.013)	(0.013)	(0.019)	(0.013)	(0.010)
X_{it}	Yes	Yes	Yes	Yes	Yes
Cons	7.691***	7.245***	7.139***	6.838***	6.530***
	(0.520)	(0.548)	(0.781)	(0.512)	(0.416)
Provincial effects	Yes	Yes	Yes	Yes	Yes
Year effect	Yes	Yes	Yes	Yes	Yes
Pseudo R^2	0.9003	0.8836	0.8729	0.8745	0.8859
Sample size	403	403	403	403	403

Note: ***, **, and * indicate significance at the 1%, 5%, and 10% statistical significance levels, respectively, and the standard errors are in parentheses corresponding to the regression coefficients.

transformation of medium and low-yield fields and the construction of high-standard farmland demonstration projects are better, the land consolidation area accounts for a relatively high proportion, and the agricultural scale and agricultural mechanization are easier to achieve. In the western region, although the HSFC policies help improve agricultural production conditions to encourage CF reduction, the relatively backward economic development level will weaken farmland transfer and agricultural machinery demand, which weakens the CF reduction effect of the HSFC policy to a certain extent. Columns (4) and (5) reported the estimated results of the HSFC policies on the amount of CF per unit area in the dimension of grain production functional areas. The results showed that the HSFC policy significantly affected the amount of CF per unit area in the major grain-producing regions compared with the non-major grain-producing regions. The reason is that the natural endowment of the main grain-producing areas is better than non-major grain producing areas, such as richer cultivated land resources, more fertile soil, and flatter terrain, which is conducive to the realization of agricultural scale operation and convenient application of agricultural machinery, and the main producing areas have obtained more financial input and transfer payment. Farmland construction standards are higher, and the effect is better, thus effectively promoting CF reduction.

4.5.2 Distribution heterogeneity

Considering that in the samples with different CF use per unit area, the effect of the HSFC policy on CF use per unit area may be different. Further, the panel quantile model tests the policy effect under different quantiles of CF use per unit area. The results are shown in Table 7. In general, the marginal effect of the implementation of the HSFC policy on the reduction of CF use passed the 1% significance level at each quantile. It showed a trend of increasing first and then decreasing. Starting from the 0.5 quantiles, this marginal effect gradually reduced, and the estimated coefficient

was the largest at the 0.9 quantiles. The possible reasons are as follows: on the one hand, in areas with low CF use per unit area, the potential of CF reduction is small, so the promotion of the HSFC policies on CF reduction is small; on the other hand, for provinces with relatively high CF use per unit area, the inertia of farmers' high fertilization behavior is strong, and the path dependence of agricultural production mode leads to the relatively limited CF reduction effect of the HSFC policy. This shows that CF reduction also needs to find coordinated measures other than the HSFC policies for provinces with relatively high CF use per unit area.

5 Conclusion and recommendations

Based on the panel data of 31 provinces in China from 2005 to 2017, this paper empirically analyzes the impact of the high standard farmland construction (HSFC) policies on chemical fertilizer (CF) reduction using continuous DID and mediating models. It reveals the internal logic and empirical evidence of CF reduction. The main conclusions are as follows: Firstly, the baseline regression results show that the HSFC policy implementation significantly promotes CF reduction. The parallel trend test analysis finds that this promoting effect is persistent, and the pre-conclusion is still valid under multiple robustness tests such as considering missing variables and the continuity of the economic and social environment, changing the policy implementation time point, eliminating other policy interference, replacing core explanatory variables, and eliminating municipalities. Secondly, from the perspective of the mechanism of action, the HSFC policy can promote CF reduction by improving the agricultural mechanization level and expanding the agricultural operation scale. Finally, the heterogeneity analysis found that the promotion effect of policy implementation on CF reduction was more evident in the eastern and central regions, and the promotion effect was more robust in the main grain-producing areas than in the non-major grain-producing areas. In the dimension of CF application distribution, the effect of CF reduction brought by the HSFC policy showed a trend of increasing first and then decreasing with the increase of quantiles. Among them, it was the highest at the 0.5 quantile and the lowest at the 0.9 quantile.

This paper puts forward the following suggestions based on the above research conclusions. First, continue to promote the HSFC in an orderly manner. The HSFC is conducive to improving agricultural economic benefits and has the self-realization mechanism of CF reduction. We should change the single idea of reducing CF by promoting new scientific fertilization technology and take the HSFC as an essential way to encourage CF reduction and realize the high-quality development of agriculture. Second, expanding the agricultural operation scale and improving the agricultural mechanization level should be the essential content of the future HSFC policy. Relevant government departments should continue to take measures such as flat ridges, consolidation, and centralized contiguous operations. At the same time, the government should increase financial support for large-scale households and agricultural machinery purchases, reduce farmers' financial pressure, promote agricultural-scale operation and mechanization, and promote CF reduction. Third, increase the HSFC in the western and non-major grain-producing areas. The HSFC policy has achieved positive results in the eastern and central regions and major grain-producing provinces, which can significantly reduce the amount of CF used in the central and east regions and major grain-producing areas. In the future, the government should strengthen the HSFC policies to implement in the western region and non-major grain-producing areas, and expand the positive impact of the HSFC policies on CF reduction and high-quality development. Fourth, combined with the regional economic and social development, the government should explore the HSFC mode according to local conditions. For example, in the high-quantile area of CF use, attention should be paid to changing the concept of fertilization in the process of HSFC, and increasing the promotion of new scientific fertilization technologies, thereby increasing the space for CF reduction in HSFC.

Due to limited research resources and objective conditions, this paper also has the following deficiencies, which need to be further improved in future studies. First, limited by the availability of data, our study data are only updated to 2017 and may not be able to assess recent policy effects. Second, this paper takes rural agricultural production areas in China as the research object. Whether the research conclusion is applicable to rural areas in other countries remains to be further tested.

Data availability statement

The original contributions presented in the study are included in the article/Supplementary material, further inquiries can be directed to the corresponding author.

Author contributions

YL: Data curation, Writing–original draft. WL: Software, Writing–review and editing, Funding acquisition. XZ: Investigation, Validation, Writing–review and editing. HQ: Writing, Methodology, Software, Writing–reviewing and editing.

Funding

The authors declare financial support was received for the research, authorship, and or publication of this article. This study was financially supported by the National Natural Science Foundation of China (71934003, 72263017), the National Social Science Foundation Youth Program of China (22CGL027), Jiangxi Modern Agricultural Sericulture Industry Technology System Project (JXARS-23) and the Jiangxi Provincial Forestry Bureau (Innovation Special Project [2023] No. 9).

Acknowledgments

The authors thank referees for their helpful comments.

Conflict of interest

The authors declare that the research was conducted in the absence of any commercial or financial relationships that could be construed as a potential conflict of interest.

Publisher's note

References

Abbruzzini, T. F., Davies, C. A., Toledo, F. H., and Cerri, C. E. P. (2019). Dynamic biochar effects on nitrogen use efficiency, crop yield and soil nitrous oxide emissions during a tropical wheat-growing season. *J. Environ. Manag.* 252, 109638. doi:10.1016/j.jenvman.2019.109638

Acemoglu, D., Naidu, S., Restrepo, P., and Robinson, J. A. (2019). Democracy does cause growth. *J. political Econ.* 127 (1), 47–100. doi:10.1086/700936

Bhatt, M. S., and Bhat, S. A. (2014). Technical efficiency and farm size productivity—micro level evidence from Jammu & Kashmir. *Int. J. Food Agric. Econ. (IJFAEC)* 2, 27–49. doi:10.22004/ag.econ.190809

Chen, X., and Liu, T. (2023). Can agricultural socialized services promote the reduction in chemical fertilizer? Analysis based on the moderating effect of farm size. *Int. J. Environ. Res. Public Health* 20 (3), 2323. doi:10.3390/ijerph20032323

Chen, Y., and Zhou, L. A. (2007). The long-term health and economic consequences of the 1959–1961 famine in China. *J. health Econ.* 26 (4), 659–681. doi:10.1016/j.jhealeco.2006.12.006

Delgado, M. S., and Florax, R. J. (2015). Difference-in-differences techniques for spatial data: Local autocorrelation and spatial interaction. *Econ. Lett.* 137, 123–126. doi:10.1016/j.econlet.2015.10.035

Fortson, J. G. (2009). HIV/AIDS and fertility. *Am. Econ. J. Appl. Econ.* 1 (3), 170–194. doi:10.1257/app.1.3.170

Guo, J., Li, C., Xu, X., Sun, M., and Zhang, L. (2022). Farmland scale and chemical fertilizer use in rural China: New evidence from the perspective of nutrient elements. *J. Clean. Prod.* 376, 134278. doi:10.1016/j.jclepro.2022.134278

Han, J., Dong, Y., and Zhang, M. (2021). Chemical fertilizer reduction with organic fertilizer effectively improve soil fertility and microbial community from newly cultivated land in the Loess Plateau of China. *Appl. Soil Ecol.* 165, 103966. doi:10.1016/j.apsoil.2021.103966

Holden, S., and Yohannes, H. (2002). Land redistribution, tenure insecurity, and intensity of production: A study of farm households in southern Ethiopia. *Land Econ.* 78 (4), 573–590. doi:10.2307/3146854

Hu, Y., Li, B., Zhang, Z., and Wang, J. (2022). Farm size and agricultural technology progress: Evidence from China. *J. Rural Stud.* 93, 417–429. doi:10.1016/j.jrurstud.2019.01.009

Hu, Y., and Zhang, Z. (2018). The impact of agricultural machinery service on technical efficiency of wheat production. *China Rural. Econ.* (5).

Huang, J., Xu, C. C., Ridoutt, B. G., Wang, X. C., and Ren, P. A. (2017). Nitrogen and phosphorus losses and eutrophication potential associated with fertilizer application to cropland in China. *J. Clean. Prod.* 159, 171–179. doi:10.1016/j.jclepro.2017.05.008

Ju, X. T., Xing, G. X., Chen, X. P., Zhang, S. L., Zhang, L. J., Liu, X. J., et al. (2009). Reducing environmental risk by improving N management in intensive Chinese agricultural systems. *Proc. Natl. Acad. Sci.* 106 (9), 3041–3046. doi:10.1073/pnas.0813417106

Krugman, P. (1994). The myth of Asia's miracle, *Foreign Aff.*, 73, 62–78.

Kumar, R., Kumar, R., and Prakash, O. (2019). "The impact of chemical fertilizers on our environment and ecosystem," in *Research trends in environmental sciences* (Wuhan, China: Scientific Research Publishing).

Li, B., and Zeng, Q. (2022). The effect of land right stability on the application of fertilizer reduction technologies—evidence from large-scale farmers in China. *Sustainability* 14 (13), 8059. doi:10.3390/su14138059

Li, X., and Shang, J. (2021). Decision-making behavior of fertilizer application of grain growers in Heilongjiang Province from the perspective of risk preference and risk perception. *Math. Problems Eng.* 2021, 1–8. doi:10.1155/2021/6667558

Liang, Z. H., Zhang, L., and Zhang, J, B. (2021). Land consolidation and fertilizer reduction: Quasi-natural experimental evidence from China's well-facilitated capital farmland construction. *Chin. Rural. Econ.* 4, 123–144.

LiLiSun, Y. F. X. H., and Wang, S. (2019). Ecological compensation standards for paddy fields based on the control of chemical fertilizer application-Lishui District, Nanjing as an example. *Acta Ecol. Sin.* 39. doi:10.5846/stxb201809172020

Lin, J. Y. (1992). Rural reforms and agricultural growth in China, *The American economic review*, 82. 34–51.

LiNansekiTakeuchiSongChen, D. T. S. M. T., and Zhou, H. (2012). Farmers' behaviors, perceptions and determinants of fertilizer application in China: Evidence from six eastern provincial–level regions. *Journal- Fac. Agric. Kyushu Univ.* 57 (1), 245–254. doi:10.5109/22078

Liu, J., Xu, Q., and Zhou, T. (2022). Role of mechanization: The impact of the cropland use scale on fertilizer reduction. *Front. Environ. Sci.* 10, 1053715. doi:10.3389/fenvs.2022.1053715

Liu, Y., Zou, L., and Wang, Y. (2020). Spatial-temporal characteristics and influencing factors of agricultural eco-efficiency in China in recent 40 years. *Land Use Policy* 97, 104794. doi:10.1016/j.landusepol.2020.104794

Nunn, N., and Qian, N. (2011). The potato's contribution to population and urbanization: Evidence from a historical experiment. *Q. J. Econ.* 126 (2), 593–650. doi:10.1093/qje/qjr009

Peng, J., Zhao, Z., and Chen, L. (2022a). The impact of high-standard farmland construction policy on rural poverty in China. *Land* 11 (9), 1578. doi:10.3390/land11091578

Peng, J., Zhao, Z., Liu, D., Wang, J., Song, W., Lu, X., et al. (2022b). Impact of agricultural mechanization on agricultural production, income, and mechanism: Evidence from hubei province, China. *Front. Environ. Sci.* 10, 53. doi:10.1038/s41368-022-00207-y

Pu, L., Zhang, S., Yang, J., Yan, F., and Chang, L. (2019). Assessment of high-standard farmland construction effectiveness in liaoning province during 2011–2015. *Chin. Geogr. Sci.* 29, 667–678. doi:10.1007/s11769-019-1061-z

Sarkar, A. (2020). Agricultural mechanization in India: A study on the ownership and investment in farm machinery by cultivator households across agro-ecological regions. *Millenn. Asia* 11 (2), 160–186. doi:10.1177/0976399620925440

Song, W., Wu, K., Zhao, H., Zhao, R., and Li, T. (2019). Arrangement of high-standard basic farmland construction based on village-region cultivated land quality uniformity. *Chin. Geogr. Sci.* 29, 325–340. doi:10.1007/s11769-018-1011-1

Tian, M., Zheng, Y., Sun, X., and Zheng, H. (2022). A research on promoting chemical fertiliser reduction for sustainable agriculture purposes: Evolutionary game analyses involving 'government, farmers, and consumers'. *Ecol. Indic.* 144, 109433. doi:10.1016/j.ecolind.2022.109433

Wan, L. X., and Yang, Guo. (2023). Influence pathways and effects of agricultural mechanization on the application of chemical fertilizers. *Chin. J. Eco-Agriculture* 31 (4), 643–653. doi:10.12357/cjea.20220686

Wang, X. Y., Zhao, S. D., Zheng, X. F., Wang, Z. H., and He, G. (2021). Effects of straw returning and nitrogen application rate on grain yield and nitrogen utilization of winter wheat. *Sci. Agric. Sin.* 54, 5043–5053. doi:10.3864/j.issn.0578-1752.2021.23.010

Wang, Y., Li, G., Wang, S., Zhang, Y., Li, D., Zhou, H., et al. (2022). A comprehensive evaluation of benefit of high-standard farmland development in China. *Sustainability* 14 (16), 10361. doi:10.3390/su141610361

Wen, Z., and Ye, B. (2014). Analyses of mediating effects: The development of methods and models. *Adv. Psychol. Sci.* 22 (5), 731. doi:10.3724/sp.j.1042.2014.00731

Wu, H., Hao, H., Lei, H., Ge, Y., Shi, H., and Song, Y. (2021b). Farm size, risk aversion and overuse of fertilizer: The heterogeneity of large-scale and small-scale wheat farmers in Northern China. *Land* 10 (2), 111. doi:10.3390/land10020111

Wu, H., Li, J., and Ge, Y. (2022). Ambiguity preference, social learning and adoption of soil testing and formula fertilization technology. *Technol. Forecast. Soc. Change* 184, 122037. doi:10.1016/j.techfore.2022.122037

Wu, X., Zhang, T., Zhao, J., Wang, L., Yang, D., Li, G., et al. (2021a). Variation of soil bacterial and fungal communities from fluvo-aquic soil under chemical fertilizer reduction combined with organic materials in North China Plain. *J. Soil Sci. Plant Nutr.* 21, 349–363. doi:10.1007/s42729-020-00365-0

Wu, Y., Xi, X., Tang, X., Luo, D., Gu, B., Lam, S. K., et al. (2018). Policy distortions, farm size, and the overuse of agricultural chemicals in China. *Proc. Natl. Acad. Sci.* 115 (27), 7010–7015. doi:10.1073/pnas.1806645115

Xiang, T., Malik, T. H., Hou, J. W., and Ma, J. (2022). The impact of climate change on agricultural total factor productivity: A cross-country panel data analysis, 1961–2013. *Agriculture* 12 (12), 2123. doi:10.3390/agriculture12122123

Xu, Q., Zhu, P., and Tang, L. (2022). Agricultural services: Another way of farmland utilization and its effect on agricultural green total factor productivity in China. *Land* 11 (8), 1170. doi:10.3390/land11081170

Yan, H., Du, W., Zhou, Y., Luo, L., and Niu, Z. E. (2022). Satellite-based evidences to improve cropland productivity on the high-standard farmland project regions in Henan Province, China. *Remote Sens.* 14 (7), 1724. doi:10.3390/rs14071724

Yang, C., Zeng, H., and Zhang, Y. (2022). Are socialized services of agricultural green production conducive to the reduction in fertilizer input? Empirical evidence from rural China. *Int. J. Environ. Res. Public Health* 19 (22), 14856. doi:10.3390/ijerph192214856

Ye, F., Wang, L., Razzaq, A., Tong, T., Zhang, Q., and Abbas, A. (2023). Policy impacts of high-standard farmland construction on agricultural sustainability: Total factor productivity-based analysis. *Land* 12 (2), 283. doi:10.3390/land12020283

Zhang, G. J., Tong, M. H., Li, H., and Chen, F. (2019). Economic growth effects and policy effectiveness assessment of pro-poor reform pilot zones. *China Ind. Econ.* 8, 136–154. doi:10.19581/j.cnki.ciejournal.2019.08.008

Zhou, S., Qing, C., He, J., and Xu, D. (2023). Impact of agricultural division of labor on fertilizer reduction application: Evidence from western China. *Int. J. Environ. Res. Public Health* 20 (5), 3787. doi:10.3390/ijerph20053787

Zhu, B., Zhang, M., Huang, L., Wang, P., Su, B., and Wei, Y. M. (2020). Exploring the effect of carbon trading mechanism on China's green development efficiency: A novel integrated approach. *Energy Econ.* 85, 104601. doi:10.1016/j.eneco.2019.104601

frontiers | Frontiers in Environmental Science

TYPE Original Research
PUBLISHED 17 October 2023
DOI 10.3389/fenvs.2023.1261295

OPEN ACCESS

EDITED BY
Hualin Xie,
Jiangxi University of Finance and Economics, China

REVIEWED BY
Bruna Almeida,
NOVA University of Lisbon, Portugal
Sandeep Samantaray,
National Institute of Technology Srinagar, India

*CORRESPONDENCE
Wenfu Peng,
pwfzh@126.com

RECEIVED 19 July 2023
ACCEPTED 06 October 2023
PUBLISHED 17 October 2023

CITATION
Ning L, Peng W, Yu Y, Xiang J and Wang Y (2023), Quantifying vegetation change and driving mechanism analysis in Sichuan from 2000 to 2020.
Front. Environ. Sci. 11:1261295.
doi: 10.3389/fenvs.2023.1261295

Quantifying vegetation change and driving mechanism analysis in Sichuan from 2000 to 2020

Lina Ning[1,2], Wenfu Peng[1,2]*, Yanan Yu[1,2], JiaYao Xiang[1,2] and Yong Wang[3]

[1]The Institute of Geography and Resources Science, Sichuan Normal University, Chengdu, China, [2]Key Lab of Land Resources Evaluation and Monitoring in Southwest, Ministry of Education, Chengdu, China, [3]School of Geographical Sciences, Southwest University, Chongqing, China

Vegetation cover is a crucial indicator of biodiversity and ecological processes, but there are still uncertainties about the factors driving changes in vegetation. In this study, we conducted a comprehensive analysis of vegetation cover changes in Sichuan Province from 2000 to 2020 using Formation Vegetation Cover (FVC) derived from MODIS13Q1 data. Our results revealed a consistent increase in vegetation FVC, rising from 0.506 to 0.624 over the 21-year period, with an annual growth rate of 0.0028. The turning point in this growth occurred in 2006. Of significance, the expansion of vegetation covered a substantial portion, accounting for 84.76%, while the decrease constituted 13%. Elevation proved to be an effective explanatory factor, with a coefficient of 0.417, indicating its role in explaining vegetation cover changes. It is important to note that FVC trends and averages exhibited distinct patterns concerning elevation, land use, population density, topography, and soil type, while their correlation with meteorological factors was relatively weak. Concurrently, the increase in construction and urban development had a negative impact on vegetation cover.

KEYWORDS

GeoDetectors, human activities, sichuan province, spatial and temporal dynamics, vegetation cover

1 Introduction

Surface vegetation, a cornerstone of Earth's terrestrial ecosystem, serves as a vital indicator of ecosystem health and interconnects various natural elements like the atmosphere and soil (Du et al., 2015; Kong et al., 2018; Zhao et al., 2018). In recent decades, global changes have led to significant shifts in vegetation cover at regional and continental scales (Kotharkar et al., 2016; Pang et al., 2017). This has spurred a critical need to comprehensively study long-term changes in vegetation cover to better understand spatial and temporal dynamics in terrestrial ecosystems. Such understanding is crucial for maintaining ecosystem equilibrium in the face of environmental changes over the past century (Fang et al., 2018). Remote sensing offers a valuable means to monitor vegetation cover dynamics with high precision and frequency across different spatial and temporal scales (Piao et al., 2003; Jalonen et al., 2014). Formation Vegetation Cover (FVC) is adept at tracking changes in ground-level vegetation (Zhang et al., 2003). For instance, Du et al. (2015) noted a consistent increase in vegetation activity in Xinjiang during spring, summer, and autumn over the past 3 decades. Zhao et al. (2019) further supported this observation, documenting a yearly rise in vegetation cover from 2000 to 2014. Notably, He's work highlighted the significant impact of farmland-to-forest initiatives on vegetation

dynamics. Additionally, a strong correlation was found between cumulative afforestation efforts and vegetation cover in the Yan'an and Yulin regions from 2000 to 2013. In a separate study, Peng et al. (2019) conducted a geographic analysis of natural factors influencing vegetation dynamics in Sichuan from 2000 to 2015. This research revealed key factors driving vegetation growth, enriching our understanding of the interaction between natural factors and the mechanisms behind vegetation change. It is worth noting that many of these studies relied on the GIMMS dataset, which, despite its long availability, has limitations due to its coarse resolution. This limitation may result in the loss of critical spatial details at the regional level. Furthermore, acquiring detailed Landsat satellite imagery at a large scale demands substantial computational resources and time, which led to the selection of the MODIS dataset with higher resolution. The computation of vegetation cover was carried out using the Google Earth Engine (GEE) platform, a powerful cloud-based computational facility designed for processing and analyzing extensive spatial datasets (Mutanga, O. and Kumar, 2019). This platform enables efficient monitoring of vegetation cover changes through high-resolution imagery, despite its limited temporal scope (Kumar, L. and Mutanga, O., 2018).

Moreover, it is imperative to acknowledge that the intricate causative linkages between influential factors and the dynamics of vegetation cover exhibit a multifaceted and non-linear character (Zhang et al., 2018). Preceding scholarly inquiries have conventionally resorted to correlation and residual analyses in their pursuit of unraveling the driving forces governing vegetation changes (Zhao et al., 2021; Jiang et al., 2022). However, these conventional approaches often fall short in elucidating the nuanced, non-linear interdependencies among multiple impact factors, notably those entwined with anthropogenic influences and climate fluctuations. In response to these inherent limitations, non-linear methodologies have been employed as an indispensable toolset to disentangle the intricate tapestry of driving mechanisms underlying changes in vegetation cover (Jiang et al., 2022). Foremost among these methodologies are Geodetectors, which represent spatially-focused analytical methods adept at discerning the spatial variances inherent in these dynamics and unveiling their causative underpinnings (Wang et al., 2017). Notably, a multitude of studies have effectively applied Geodetectors methodologies across various scales and encompassing a diverse array of influential factors, yielding comprehensive insights into the driving forces steering alterations in vegetation cover (Huo et al., 2021). Hence, predicated on the intrinsic spatial heterogeneity characterizing geographical phenomena, Geodetectors models emerge as a compelling and nuanced approach, well-suited to furnishing cogent explanations for the manifold transformations in vegetation cover.

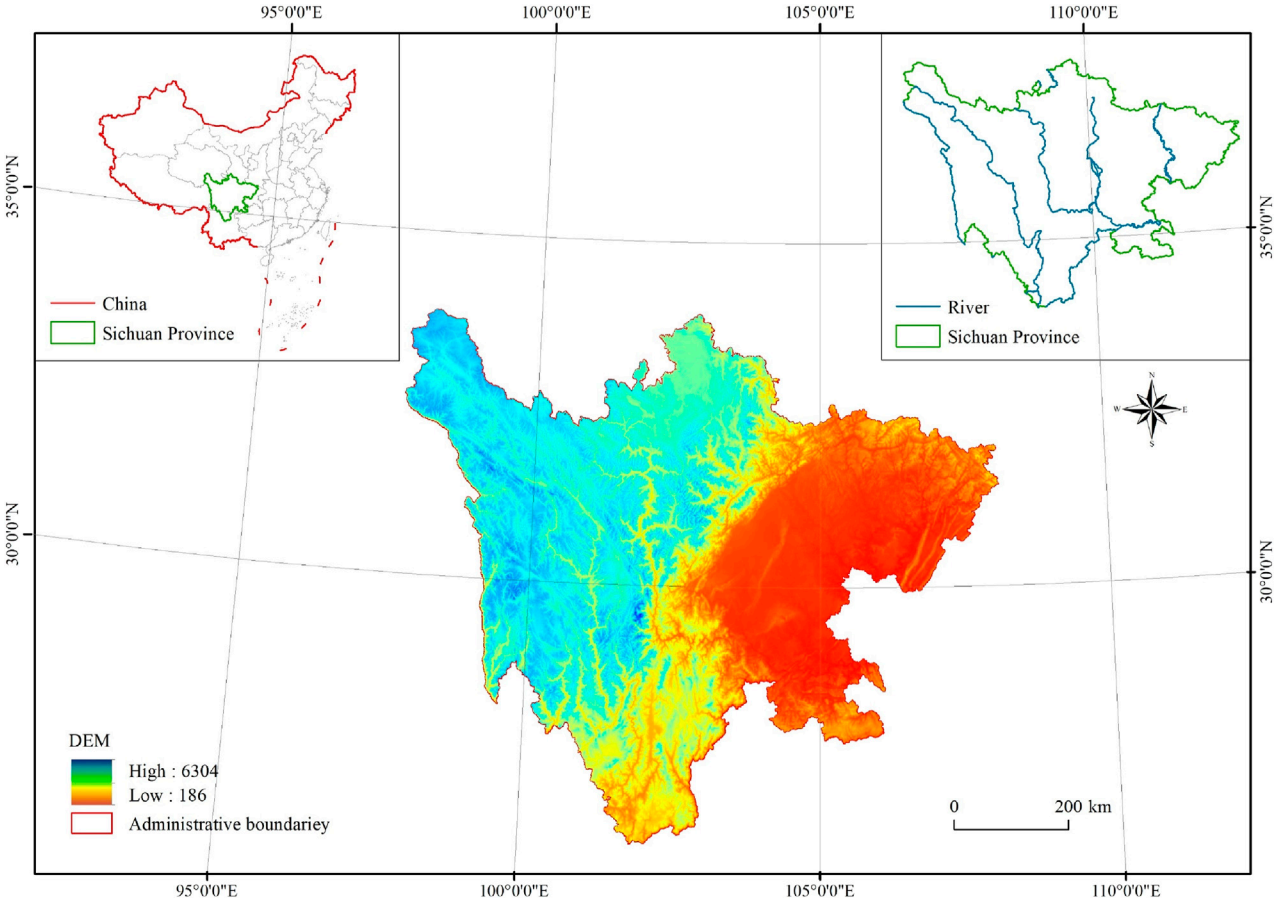

FIGURE 1
Elevation map of study area.

Sichuan Province, situated in the upper reaches of the Yangtze River, holds strategic significance as a vital water source and ecological protector within the Yangtze River Basin. Given its climatic diversity and substantial variations in topography across different regions, Sichuan Province exhibits notable disparities in surface vegetation cover and ecological conditions. This study utilizes remote sensing data from MODIS, processed through the Google Earth Engine (GEE) platform. Employing various analytical methods, including the image element dichotomous model, coefficient of variation analysis, and Geodetectors, it aims to identify complex patterns and temporal changes in vegetation cover across Sichuan Province. The study also explores the primary factors driving these changes. The results are significant for advancing ecological restoration efforts in the region and providing guidance for the preservation of the local environment.

2 Study area

Located in the southwest region of inland China, Sichuan Province spans a vast area of 485,000 square kilometers and is situated between 26°03′-34°19′N latitude and 97°21′-108°12′E longitude, predominantly covering the upper reaches of the Yangtze River (Figure 1). The province's landscape exhibits significant variations from east to west, characterized by a complex and diverse topography. Residing in the transitional zone between the Qinghai-Tibetan Plateau, representing the initial terrain step of the Chinese mainland, and the middle and lower reaches of the Yangtze River Plain, constituting the third step, Sichuan Province boasts an extensive range of elevations, featuring a prominent west-to-east elevation gradient. Its terrain comprises mountains, hills, plains, basins, and plateaus. Notably, Sichuan Province experiences three major climatic zones. In central Sichuan, the Sichuan Basin is characterized by a humid central subtropical climate. Meanwhile, the mountains in southwest Sichuan exhibit a semi-humid subtropical climate, while northwest Sichuan is characterized by an alpine plateau climate (Wang, H, X and Liu, C, M.; 2000). Furthermore, the province is home to numerous rivers that primarily form part of the extensive Yangtze River system, with major tributaries including the Yalong, Min, and Dadu Rivers. Lastly, the natural vegetation of Sichuan Province encompasses eight vegetation types, 18 phyla groups, and 48 group groups, contributing to its relatively rich biological resources and unique ecological value.

3 Materials and methods

3.1 Data

The data sources and processing of the article are shown in Table 1.

3.2 Image element dichotomous model

This model operates on the idea that an image's surface can be divided into two parts–one with vegetation and one without (Figure 2) (He et al., 2023; Xu et al., 2023). It suggests that the spectral information captured by remote sensors is a blend of these two parts, with their importance determined by their relative surface areas within the image.

TABLE 1 Data source and preprocessing.

Data sources	Source	Spatial resolution	Preprocessing
MOD13A1	USGS (United States Geological Survey) https://earthexplorer.usgs.gov/	250 m	Maximum value synthesis method to obtain 2000–2020 average data
Vector extent of the study area	National Centre for Basic Geographic Information (https://www.ngcc.cn/)	-	-
DEM	USGS (United States Geological Survey) https://earthexplorer.usgs.gov/	90 m	Projection, resampling
Slope, aspect, elevation	DEM	-	-
Temperature, precipitation	Data Centre for Resource and Environmental Sciences, Chinese Academy of Sciences (https://www.resdc.cn/)	1 km	Kriging interpolation
Soil Map of the People's Republic of China 1: 1 Million	Data Centre for Resource and Environmental Sciences, Chinese Academy of Sciences (https://www.resdc.cn/)	1 km	-
Geomorphological Atlas of the People's Republic of China (1:1 million)	Data Centre for Resource and Environmental Sciences, Chinese Academy of Sciences (https://www.resdc.cn/)	1 km	-
Vegetation Atlas of China 1:1,000,000	Data Centre for Resource and Environmental Sciences, Chinese Academy of Sciences (https://www.resdc.cn/)	1 km	-
Remote sensing monitoring data on the status of land use in China	Data Centre for Resource and Environmental Sciences, Chinese Academy of Sciences (https://www.resdc.cn/)	1 km	reclassify
Population density, GDP data	Sichuan Statistical Yearbook	-	-

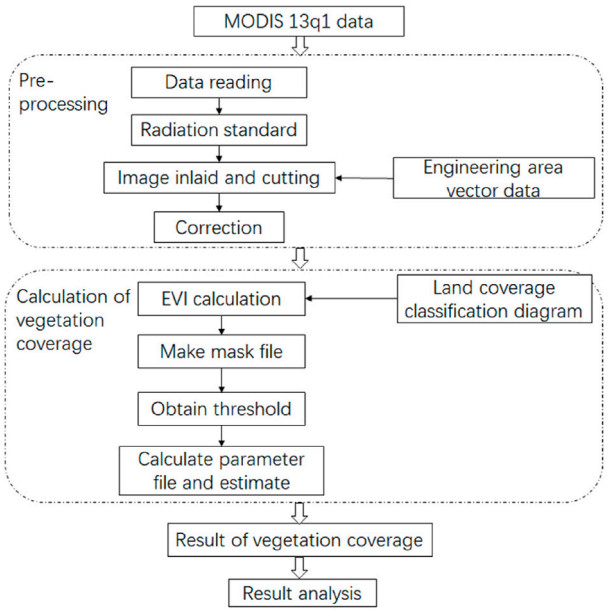

FIGURE 2
Flowchart of the image element dichotomous model.

For example, vegetation cover can be seen as the weight assigned to the vegetation component based on its area relative to the total image area. (Kalisa et al., 2019; Li et al., 2023). Its calculation formula is

$$FVC = (EVI - EVI_{soil}) / (EVI_{veg} - EVI_{soil}) \quad (1)$$

The Enhanced Vegetation Index (EVI), which adjusts for the absorption of red light by residual aerosols by comparing red and blue light transmission through the aerosol, offers a more accurate representation of vegetation changes (Wu et al., 2020).

3.3 Coefficient of variation

The coefficient of variation CV, also known as the coefficient of dispersion, is a normalised measure of the degree of dispersion of a probability distribution (Deng et al., 2017; Kinjal C and Ankit T, 2023). The coefficient is a dimensionless quantity that does not need to be referenced to the mean of the data, so when comparing the stability of vegetation cover, the ratio of the standard deviation to the mean (relative value) can be used for comparison (He et al., 2023). It is calculated as:

$$C_v = \sigma / \mu \quad (2)$$

where *s* is the standard deviation and μ is the mean.

3.4 Trend analysis

The Theil-Sen Median and Mann-Kendall tests are non-parametric statistical methods introduced (Hirsch and Slack., 1984). The Theil-Sen Median is adept at identifying trends and quantifying changes in a time series but does not independently determine the statistical significance of these trends. In contrast, the Mann-Kendall test is employed to assess the statistical significance of temporal trends in a time series, and the Kendall test specifically evaluates the significance of these trends. The combination of these two non-parametric methods has become a common approach in remote sensing for analyzing trends in time series data (De Jong et al., 2011; Gocic and Trajkovic, 2013).

3.4.1 The Theil-Sen median

The Theil-Sen median method, also known as Sen slope estimation, is a robust, non-parametric statistical approach to trend analysis (Xie et al., 2022; Tabari et al., 2011; Xiang et al., 2023). The method is computationally efficient, insensitive to measurement error and niche data, and suitable for trend analysis of long time series data (Yue et al., 2002; Li et al., 2020). Its calculation formula is:

$$\beta = \text{Median}\left(\frac{FVC_j - FVC_i}{j - i}\right) \forall j > i \quad (3)$$

If β is greater than zero, it indicates an increasing trend in vegetation cover, and *vice versa* for a decreasing trend.

3.4.2 Mann-Kendall (MK)

The Mann-Kendall (MK) test is a non-parametric time series trend test (Wang et al., 2019; He et al., 2022) that does not require measurements to follow a normal distribution, is unaffected by missing values and outliers, and is suitable for testing whether long time series data are indeed significant (Wang et al., 2010; Li et al., 2020; Guo and Bryan, 2022). However, it is not applicable to detect sequences with multiple mutation sites. The procedure is as follows: for a sequence xt = x1, x2, . . . , xn., first determine the relationship between the magnitude of xi and xj (set to S) for all pairs of values (xi,xj,j > i). Make the following assumptions: the data in the HO series are random, i.e., there is no significant trend; there is an upward or downward trend in the H1 series (Li and Song, 2022). The test statistic S is calculated as:

$$S = \sum_{i=1}^{n-1} \sum_{j=i+1}^{n} \text{sgn}(x_j - x_i) \quad (4)$$

where sgn () is the sign function, calculated as:

$$\text{sgn}(x_j - x_i) \begin{cases} +1 & x_j - x_i > 0 \\ 0 & x_j - x_i = 0 \\ -1 & x_j - x_i < 0 \end{cases} \quad (5)$$

The trend test is performed with the test statistic Z. The calculation of the Z-value is as follows:

$$Z = \begin{cases} \frac{S}{\sqrt{\text{Var}(S)}} & (S > 0) \\ 0 \quad (S = 0) & \\ \frac{S+1}{\sqrt{\text{Var}(S)}} & (S < 0) \end{cases} \quad (6)$$

where var is computed by the formula

$$\text{Var}(S) = \frac{n(n-1)(2n+5)}{18} \quad (7)$$

where n is the number of data in the sequence; m is the number of nodes (repeating data groups) in the sequence.

TABLE 2 Mann-kendall test trend categories.

β	Z	Trend type	Trend features
$\beta \geq 0.0005$	$\|Z\| \geq 1.96$	5	Significant improvement
$\beta \geq 0.0005$	$\|Z\| < 1.96$	4	Slight improvement
$\|\beta\| < 0.0005$	$\|Z\| < 1.96$	3	Stable and unchanged
$\beta < -0.0005$	$\|Z\| < 1.96$	2	Slight degradation
$\beta < -0.0005$	$\|Z\| \geq 1.96$	1	Severe degradation

Again, a bilateral trend test was used to find the critical value Z1-α/2 in the normal distribution table at the given significance level. if |Z| = Z1-α/2, the original hypothesis was accepted, i.e., the trend was not significant, and if |Z|>Z1-α/2, the original hypothesis was rejected, i.e., the trend was considered significant. This paper refers to the trend classification of Yuan et al. (2013), where if the significance level is $\alpha = 0.05$, the critical value is Z1-α/2 = ±1.96, then the absolute value of Z is greater than 1.96, indicating that the trend has passed the significance test at the 95% confidence level. The method of distinguishing the significance of the trends is shown in Table 2.

3.4.3 Pettitt

The Pettitt test, a statistical technique employed for identifying the inflection point within a time series, discerns pronounced shifts in the trend exhibited by the sequence over an extended temporal span (Radu et al., 2022; Zhao et al., 2023). A notable advantage intrinsic to this method lies in its independence from the constraint of adhering to specific probability distributions within the sample sequence (Carla et al., 2023). A Pettitt mutation test yielding a statistic K value below the 0.05 significance threshold serves as compelling evidence of a substantively significant mutation point within the sequence under consideration (Karen et al., 2019).

$$\begin{gathered} S = \sum_{i=1}^{k} ri \quad k = 1, 2, 3, \ldots, n \\ if\left(x_i - x_j\right) > 0; sgn\left(x_i - x_j = 1\right) \\ if\left(x_i - x_j\right) = 0; sgn\left(x_i - x_j = 0\right) \\ if\left(x_i - x_j\right) < 0; sgn\left(x_i - x_j = -1\right) \end{gathered} \tag{8}$$

If moment t_0 satisfies $kt_0 = max\, sk$, then t_0 is a mutation point.

$$P = 2\, exp\left[-6kt_0^2\left(n^3 + n^2\right)\right] \tag{9}$$

If the statistic $P < 0.05$, it means that the mutation point at the moment of t_0 is a significant mutation.

3.5 Geographical

Geographical detectors can either test for spatial heterogeneity of a single variable or detect possible causal relationships between two variables by testing them (Song et al., 2020; Zhang et al., 2020). It consists of four main components: factor detection, interaction detection, risk zone detection and ecological detection (Wang et al., 2016; Wang et al., 2017; Huang et al., 2023). In this paper, the interaction detection tool and the Geodetector interaction detection tool were selected to analyse the influence of vegetation cover drivers in Sichuan Province.

Factor detection: detection of the spatial heterogeneity of Y (FVC); and detection of how much of the spatial heterogeneity of attribute Y is explained by a given factor X (each detection factor) (Lei et al., 2023). Using the q-value metric, the expressions are:

$$q = 1 - \frac{\sum_{h=1}^{L} N_h \sigma_h^2}{N\sigma^2} = 1 - \frac{SSW}{SST} \tag{10}$$

$$SSW = \sum_{h=1}^{L} N_h \sigma_h^2 \tag{11}$$

$$SST = N\sigma^2 \tag{12}$$

where: h = 1, . . . , L is the classification or partition of the variable Y or the factor X, N_h and N are the number of cells in layer h and the total area respectively, and σ_h^2 and σ^2 are the variance of the Y values in layer h and the total area respectively. SSW and SST are the sum of the within-stratum variance and the total area-wide variance, respectively. q has a value range [0,1], with larger values indicating a greater spatial differentiation of Y. If the stratification is generated by the independent variable X, a larger value of q indicates a stronger explanatory power of the independent variable X for the attribute Y, and *vice versa*.

Interaction detection: different detection factors were used for two-by-two interactions on FVC. The type of interaction between factors was determined by comparing the interaction q-values with the single factor q-values, and the interaction was judged as shown in Table 3.

3.6 Correlation analysis

Correlation analysis refers to the analysis of the variable elements relevant to each influence factor, and calculates the correlation coefficient between each influence factor and FVC on a frame-by-frame basis to measure the closeness of the correlation of each factor (Liu et al., 2020). Its calculation formula is:

$$R_{xy} = \frac{\sum_{i=1}^{n}\left(x_i - \bar{y}\right)\left(y_i - \bar{y}\right)}{\sqrt{\sum_{i=1}^{n}\left(x_i - \bar{x}\right)\sum_{i=1}^{n}\left(y_i - \bar{y}\right)}} \tag{13}$$

Where: R_XY is the correlation coefficient between the two variables, between 1 and -1, where 1 indicates a perfectly positive correlation between the variables, 0 indicates no correlation, and −1 indicates a perfectly negative correlation; x_i is the meteorological factor in year i; $\bar{x}$ is the mean of the vegetation cover over the years; $\bar{y}$ is the mean of the correlation factors over the years; and i is the number of samples.

4 Results and discussion

4.1 Spatial and temporal variation of vegetation cover

This study aimed to examine the inter-annual variation trend of vegetation fractional cover (FVC) across Sichuan Province spanning

TABLE 3 Types of interaction between two independent variables on the dependent variable.

Judgments based	Interaction	Judgments based	Interaction
$q(X_1 \cap X_2) < \text{Min}(q(X_1)), q(X_1)$	Non-linear weakening	$q(X_1 \cap X_2) = q(X_1) + q(X_2)$	Independent
$\text{Min}(q(X_1), q(X_2)) < q(X_1 \cap X_2) < \text{Max}(q(X_1), q(X_2))$	Single factor non-linear attenuation	$q(X_1 \cap X_2) > q(X_1) + q(X_2)$	Non-linear independence
$q(X_1 \cap X_2) > \text{Max}(q(X_1), q(X_2))$	Two-factor enhancement		

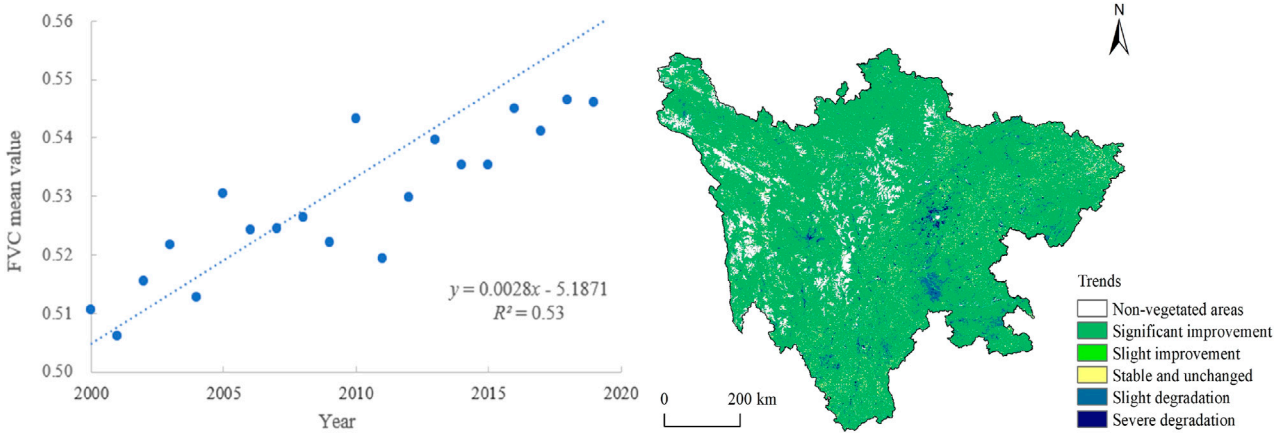

FIGURE 3
Interannual variation and trend of vegetation FVC in Sichuan Province from 2000 to 2020.

from 2000 to 2020. The investigation revealed a consistent upward trend in FVC, as evidenced by an average growth rate of 0.0028/a over the past 21 years. Strikingly, the mean value of FVC reached its nadir at 0.5061 in 2001, subsequently exhibiting a gradual increase over time and reaching its highest point of 0.6244 in 2020, representing an overall growth of 81.05% during the 21-year period under investigation.

Figure 3 effectively depicts the trends of vegetation cover changes observed within the study area. The graphic indicates that 84.76% of the region exhibited significant or slight improvement in vegetation cover from 2000 to 2020, while 13.23% of the total area experienced various degrees of degradation. Notably, these degraded areas were primarily concentrated in Chengdu City, Yibin City, and other scattered regions, which can be attributed to the rapid urban expansion that has occurred within these regions. As a result, there has been a conversion of land for construction purposes, leading to a corresponding reduction in vegetated areas. However, it is important to acknowledge the significant strides that have been made towards improving vegetation cover within Sichuan Province, which can be attributed to various efforts such as land restoration, afforestation, and the implementation of ecological construction projects. These positive trends are also attributable to relevant policies aimed at promoting ecological conservation and restoration, including the conversion of cultivated land back to forest and grassland.

The average value of vegetation FVC in Sichuan Province during 2000–2020 is 0.60. The spatial distribution of vegetation cover in Sichuan Province shows the characteristics of high in the east and low in the west, high in the south and low in the north, with the eastern region dominated by the Sichuan Basin, with low elevation and extensive deciduous forests; the southern region dominated by the Mountainous areas, with low elevation and extensive deciduous forests.

The coefficient of variation, a measure of spatial variability, ranged from 0 to 0.93 across Sichuan Province's study area. Based on the prevailing situation of vegetation cover fluctuations, the coefficient of variation was categorized into five distinct classes (refer to Figure 4; Table 4): low fluctuation (<0.05), relatively low variability (0.05≤CV < 0.10), medium variability (0.10≤CV < 0.15), relatively high variability (0.15≤CV < 0.2), and high variability (≥0.2). The mean coefficient of variation determined for the province was 0.1167 (<0.15), indicating a relatively steady rate of variation. However, considerable spatial differences were noted in the degree of variation. High and relatively high variability accounted for 10% of the region and were predominantly evident in districts and counties around Shiqu County and Chengdu City. The low vegetation cover and high variability observed in these regions may be attributed to rapid socio-economic development in the past 2 decades, leading to extensive land use changes and recurrent human activities. Conversely, areas with lower variation accounted for 10% of the total area and were mainly concentrated in Batang County, Derong County, Ganzi County, and Shiqu County. These regions are characterized by high mountain plateaus with moderately low vegetation cover, high altitudes, and colder climatic conditions. Overall, the spatial variability of vegetation cover in Sichuan Province exhibits a complex pattern that reflects the combined influence of geographical and anthropogenic factors on vegetation dynamics across various regions within the province.

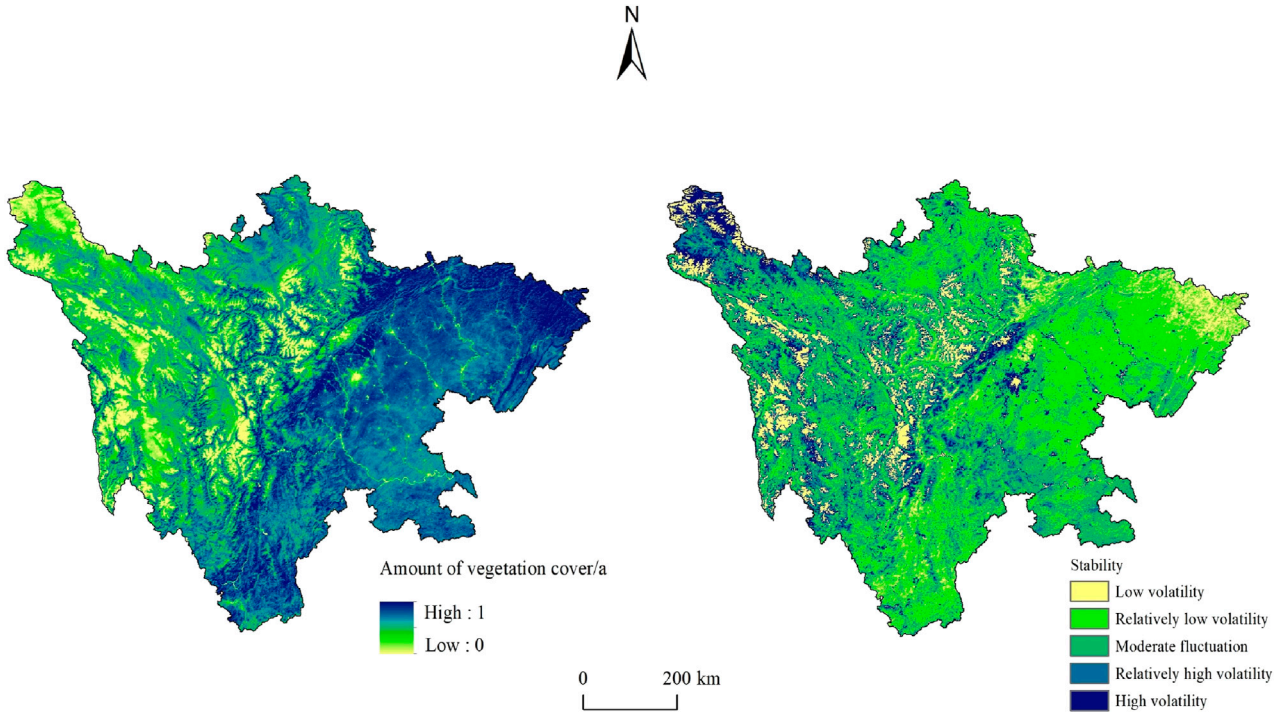

FIGURE 4
Spatial distribution of vegetation cover and stability in Sichuan Province from 2000 to 2020.

TABLE 4 Classification table of coefficient of variation of vegetation cover in Sichuan Province.

Fluctuation level	CV value	Number of pixels	Area percentage (%)
Minimum fluctuation	< 0.05	57,083	10
Low volatility	0.05 ≤ CV < 0.10	202,376	35
Moderate fluctuation	0.10 ≤ CV < 0.15	196,972	35
high volatility	0.15 ≤ CV < 0.2	58,512	10
Maximum fluctuation	≥ 0.2	52,081	10

Figure 5 provides additional insights by indicating that the inception of vegetation cover mutation was observed as early as 2006. The findings suggest a bifurcation in the temporal evolution of vegetation mutation, broadly categorized into two distinct phases. The initial phase spans from 2000 to 2010, predominantly manifesting in the southeastern sector of the nation and the western expanse of the Sichuan Plateau. Subsequently, the second phase, commencing from 2010 onward, is characterized by its prevalence in the northern and southwestern regions of the country, as well as within the transitional zone bridging the Sichuan Basin and the Yunnan-Guizhou Plateau.

4.2 Drivers of vegetation cover change

In order to probe the impact of various geographical factors on vegetation coverage dynamics in Sichuan Province, a total of 11 pertinent variables were selected for investigation across 4,862 sampling points in the province through Geodetector detection.

Geodetector analysis were employed to calculate and scrutinize the q-values of each geographic factor (Figure 6), subsequently appraising the impact of these factors on vegetation FVC in Sichuan Province. It has been observed that elevation, soil type, and landform type exhibit q-values exceeding 0.3, consequently indicating their remarkable contribution towards the elucidation of changes in vegetation cover and their identification as chief driving forces. Notably, elevation boasts the highest q-value of 0.417, signifying its unparalleled influence over vegetation cover variations. Coupled with this, other geographic factors, including vegetation type, temperature, population density, GDP, precipitation, and land use type, have demonstrated significant explanatory power with q-values greater than 0.05, although they are considered secondary drivers. Conversely, slope and slope direction manifest weaker explanatory capabilities, indicative of their minimal impact on the study area's vegetation cover

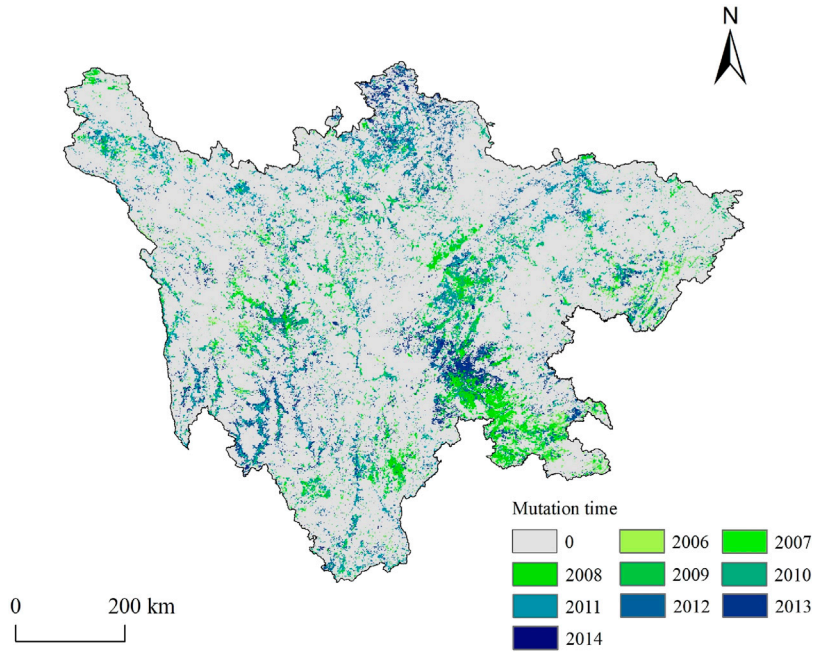

FIGURE 5
Analysis of FVC mutations, 2000–2020.

changes. In general, geological landforms, comprising of elevation, soil type, and landform type, have exerted the most substantial impact on the integration of vegetation cover changes. Moreover, a thorough investigation of vegetation cover dynamics based on plateau and plain areas reveals the provision of additional insights into vegetation cover dynamics from an elevation perspective through slope, slope orientation, precipitation, and temperature. The relatively low explanatory power of population density, GDP, and land use type may be attributed to frequent ecological engineering measures implemented in the study area, the overall positive trend in vegetation cover growth observed in Sichuan Province, and significant improvements in vegetation cover recovery. Ultimately, the study highlights the preeminent role played by geological landforms, particularly elevation, in shaping vegetation cover dynamics in Sichuan Province, whilst other factors such as vegetation type, temperature, precipitation, and land use contribute collectively to the overall understanding of vegetation cover changes.

The detection of spatial changes in vegetation cover relating to diverse drivers imparts insights into whether the explanatory power of the individual drivers is increasing, decreasing or fluctuating. The Geodetector tool effectively discloses the interplay of detection factors responsible for vegetation cover changes. Figure 7 illustrates the results of the factor interaction detection, revealing a mutually reinforcing and non-linear relationship between the influence of detection factors on vegetation cover in Sichuan Province. Specifically, 1) among natural factors, there is a two-factor amplification of slope with altitude and land use type, and a non-linear amplification with other interacting factors. Additionally, there is a non-linear amplification of slope direction with all other interacting factors. 2) Among human factors, there is a two-factor enhancement of GDP with vegetation type and population density, and a non-linear enhancement with other interaction factors. Moreover, there is a non-linear enhancement of land use type with slope direction, and a two-factor enhancement with other interaction factors.

All interactions between factors exhibited q-values surpassing those of individual factors, indicating that the super positioning of multiple factors results in an increased explanatory power of vegetation cover. Notably, crucial drivers displaying a heightened influence on the spatial distribution of vegetation cover in Sichuan Province encompass elevation ∩ vegetation type (q = 0.540), elevation ∩ GDP (q = 0.539), elevation ∩ population density (q = 0.506), and elevation ∩ land use type (q = 0.501). Notably, elevation, as the foremost driver, possesses the highest explanatory power for vegetation cover's spatial distribution in Sichuan Province when interacting with other detection factors. The human activity factor's explanatory power is markedly elevated after interplaying with geological and geomorphological factors.

4.3 Geomorphological factors

Figure 8 illustrates the discernible trend and mean of FVC for each landform, indicating the highest growth rate of 0.0187/a in the Plain category, while Extremely undulating mountainous hills display the lowest growth rate at 0.0046/a. Hills cover boasts the highest mean FVC value of 0.6865, whereas Extremely undulating mountainous hills demonstrate the lowest mean FVC value of 0.1547. Moreover, the FVC trends and means across every soil type disclose that Man-Made soils exhibit the largest trend with a growth rate of 0.0165/a, whereas High-Mountain-Soils showcase the smallest trend at 0.0076/a. The mean FVC value is notably higher for

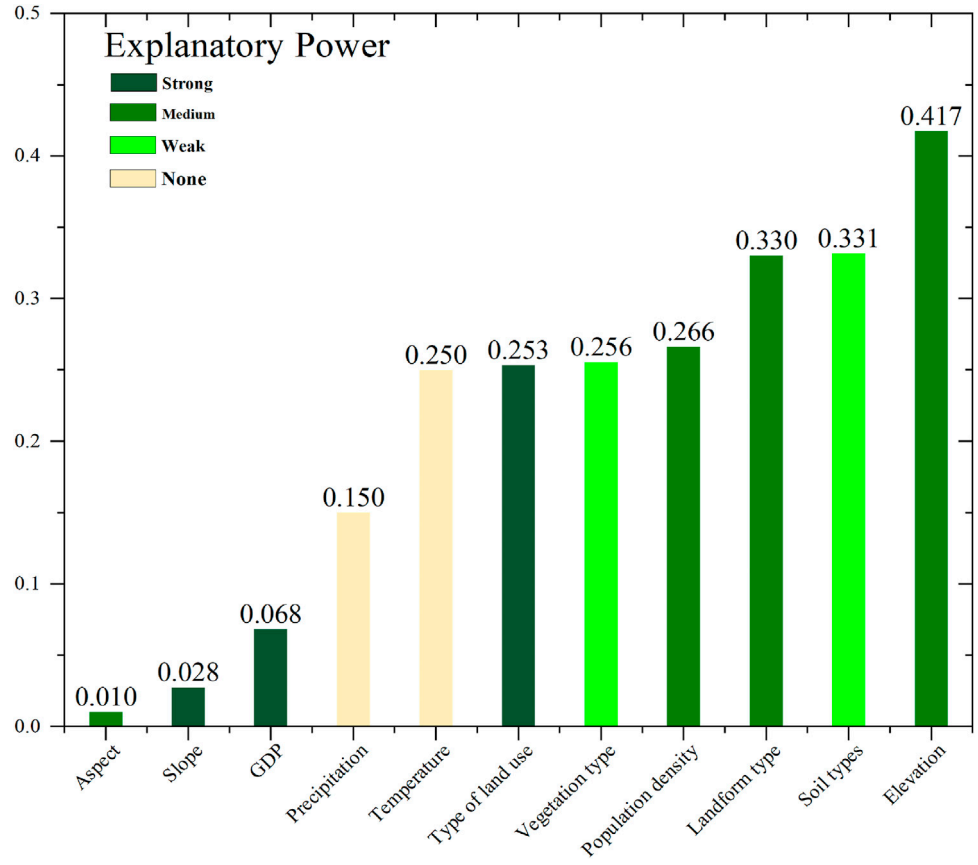

FIGURE 6
Detection factor (q) value from 2000 to 2020.

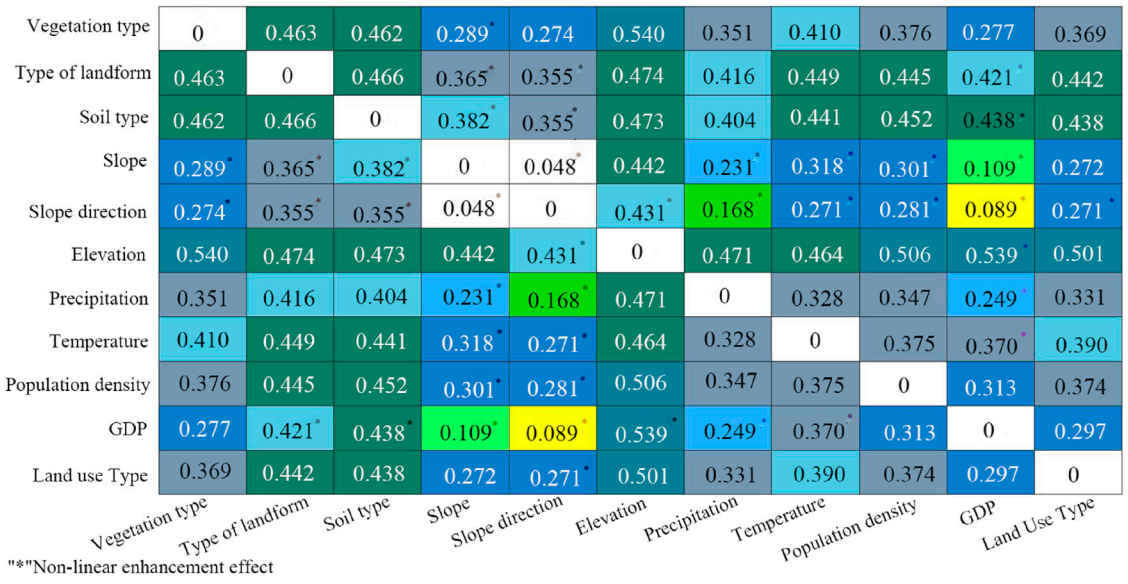

FIGURE 7
Interactive explanatory power of detection factors in Sichuan Province from 2000 to 2020 (q).

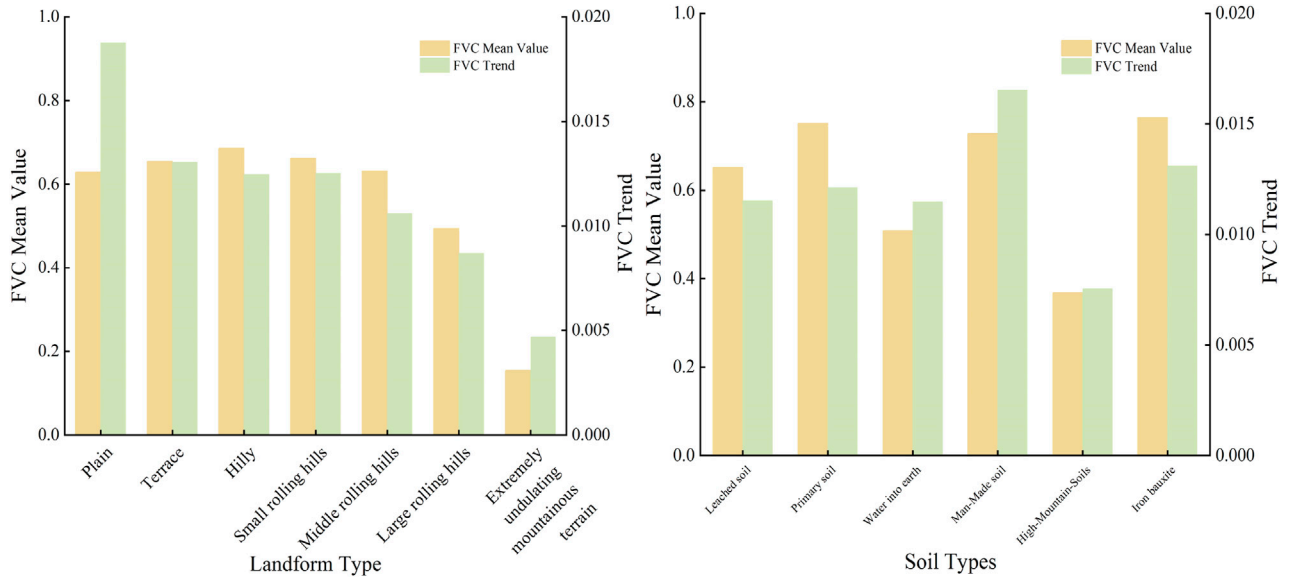

FIGURE 8
Relationship between vegetation FVC trend, mean value, landform type and soil type in Sichuan Province.

Iron bauxite soils, registering a value of 0.7642, while High-Mountain-Soils record the lowest mean FVC value of 0.3686.

4.4 Climatic factors

The majority of areas revealed non-significant correlation coefficients between vegetation FVC and both temperature and air temperature, with an increased proportion of areas displaying negative correlation between vegetation FVC and air temperature and precipitation compared to those exhibiting positive correlation (as portrayed in Figure 9; Table 5). Additionally, the relevance of this article is classified by reference to Xie [0]. Notably, the spatial range of the temperature correlation coefficient spans from −0.948 to 0.940, wherein 40.20% and 59.80% of the area correspondingly displays positive and negative correlation with vegetation FVC. Furthermore, 1.52% and 2.55% of the area exhibit significant positive and negative correlation, respectively, and are more widely dispersed across the study area than those for precipitation. In contrast, the spatial extent of the precipitation correlation coefficient ranges from −0.926 to 1, with 41.06% and 58.94% of the area reflecting positive and negative correlation, respectively, and only 0.79% and 1.30% of the area exhibiting significant positive and negative correlation, respectively.

4.5 Topographical factors

The analysis involved computing the mean vegetation cover and its changing trend within elevation zones at 100-m intervals (Figure 10). The results reveal a bifurcated trend in the evolution of Formation Vegetation Cover (FVC). In the initial stage, spanning from 0 to 3,300 m, the trend exhibits fluctuations followed by an increase with rising altitude. Subsequently, in the second stage, commencing above 3,300 m, the FVC change trend reaches its zenith growth rate at 3,300 m, registering a rate of 0.0138/a. Beyond this altitude, the trend experiences a substantial deceleration, gradually approaching stability. The average FVC value demonstrates an ascent followed by a descent, with its peak at 0.8165 occurring at an elevation close to 1,000 m above sea level. As elevation increases, the average FVC steadily diminishes, ultimately converging toward zero.

4.6 Human activity factor

Examining the FVC trends and means at all population density levels depicted in Figure 10, it is discernible that the most significant trend appears within densely populated areas, exhibiting a growth rate of 0.0142/a. Conversely, sparsely populated areas display the lowest growth rate of 0.094/a. Moreover, the mean FVC value is notably higher for moderately populated areas, registering a value of 0.7527, whilst extremely sparse regions reflect the lowest mean FVC value of 0.4396.

Upon scrutinizing the alterations in land use types that have transpired in Sichuan Province, as illustrated in Table 6, a clear preponderance of forest and construction lands is discernible. Between 2000 and 2020, the areas for forest land, water sources, construction land, and idle land have substantially augmented, while cultivated land and grassland exhibit noteworthy decline. Notably, arable land and grassland are the primary land conversion categories for forest land, accounting for a transferred area of 21,357.74 km^2 and 36,173.38 km^2, respectively. Furthermore, the chief conversion category for construction land is arable land, with an area of transferred land amounting to 3,731.06 km^2.

The influence of land cover on vegetation FVC is perceptible in the composite trend of FVC variation resulting from land use conversion, as presented in Table 7. The conducted investigation unveils that the overall growth rate of vegetation cover for

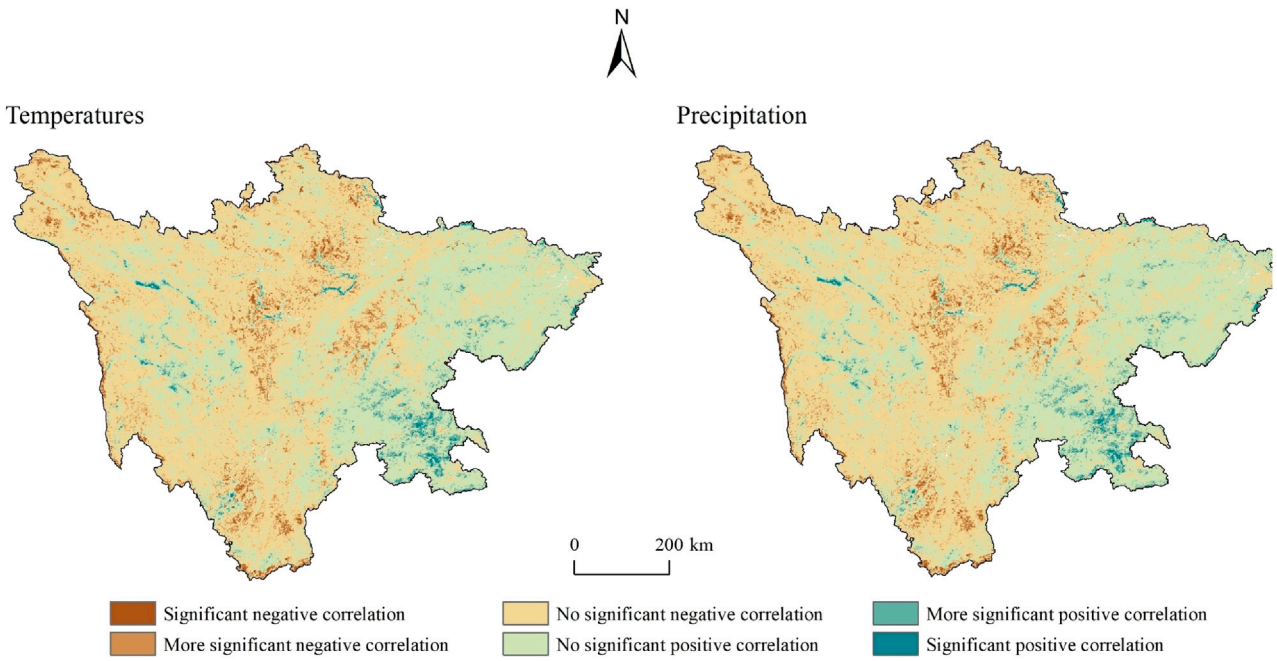

FIGURE 9
Classification of vegetation FVC and climatic factors correlation coefficient in Sichuan Province from 2000 to 2020.

TABLE 5 Distribution of area associated with FVC interannual variation of vegetation and climatic factors in Sichuan Province/%.

Level of correlation	Correlation coefficient	Temperature	Precipitation
Significant negative correlation**	<-0.606	2.55	1.30
Significant negative correlation*	−0.606— − 0.482	5.19	4.29
No significant negative correlation	−0.482—0	52.06	53.35
No significantly positively correlated	0—0.482	35.59	37.58
significantly positively correlated*	0.482—0.606	3.09	2.69
significantly positively correlated**	>0.606	1.52	0.79

*Denotes $p < 0.05$.
** denotes $p < 0.01$.

watersheds, unused, and construction lands in 2020 is considerably inferior in comparison to the growth rate of grassland, forest land, and cropland. Remarkably, the area that has reverted back to forest and grassland in Sichuan Province over the course of 21 years attains 28,359.30 km^2, correlating with a total growth rate of 317.62/a. Furthermore, the vegetation cover of unused land has rapidly expanded to 16,375.22 km^2, corresponding to a total growth rate of 183.40/a, whilst urban expansion encompasses an area of 5,664.73 km^2 with a total growth rate of 63.45/a.

Between 2000 and 2020, a marked increase in vegetation cover throughout Sichuan Province has been observed, consistently supported by the recent findings of Xu et al. (2022) and Zhu et al. (2022). The spatial distribution of vegetation exhibits an uneven pattern, with higher values concentrated in the eastern and southern regions, while lower values are found predominantly in the western and northern provinces. Nevertheless, overall vegetation cover has shown a relatively stable trend, with more pronounced fluctuations detected in the western Sichuan Plateau and Chengdu City. Areas experiencing degradation are concentrated primarily in Chengdu, Yibin, and scattered locations in their adjacent regions. Notably, Chengdu, as a provincial capital and an economic center, is densely populated, with a significant proportion of available land (94.2%) converted into urban areas. The dominant vegetation type in Chengdu consists of cultivated vegetation, including food crops, fruit forests, and other economically-driven artificial forests. However, human activities significantly influence vegetation cover in this region (Li et al., 2019). The rapid growth of urban areas and population has led to the conversion of a significant portion of land into urban development, consequently reducing vegetation coverage (Ma et al., 2023). This aligns with findings from previous research.

The trends and mean values of FVC change exhibit distinct patterns in relation to elevation, land use, population density, geomorphological type, and soil type (Jiang et al., 2021). Notably,

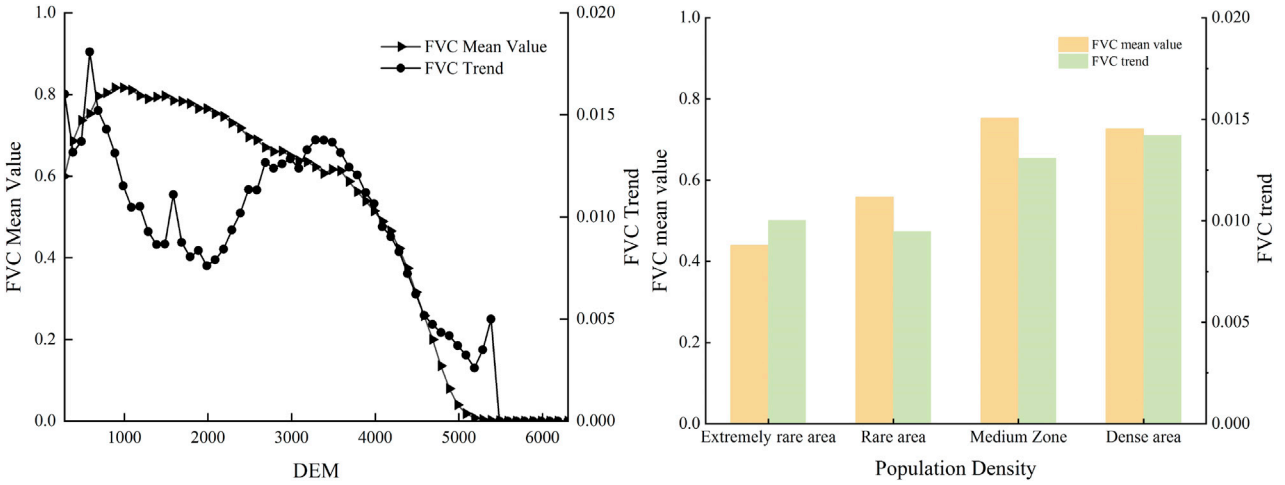

FIGURE 10
Relationship between vegetation FVC trend, mean value, elevation and population density in Sichuan Province.

TABLE 6 Transfer matrix of land use type change in Sichuan Province, 2000–2020/km².

		2020						
		Cultivated land	Woodland	Grassland	Waters	Construction land	Unused land	Total
2000	Cultivated land	87,940.21	21,357.74	7,001.56	1,645.93	3,731.06	59.73	121,736.23
	Woodland	19,745.76	109,541.52	32,268.28	592.83	421.03	1,344.56	163,913.98
	Grassland	7,660.86	36,173.38	121,092.45	720.24	385.24	7,513.04	173,545.21
	Waters	1,307.77	279.78	512.95	853.83	207.34	138.65	3,300.31
	Construction land	1,147.19	186.47	79.87	90.41	918.18	-	2,422.11
	Unused land	72.03	1,113.10	7,389.05	208.11	1.90	7,873.07	16,657.26
	Total	117,873.82	168,651.99	168,344.16	4,111.34	5,664.73	16,929.05	481,575.09

"-" indicates no value.

TABLE 7 Proportion of vegetation cover change area of land use type in Sichuan Province from 2000 to 2020.

		2020						
		Cultivated land	Woodland	Grassland	Waters	Construction land	Unused land	Total
2000	Cultivated land	984.93	239.21	78.42	18.43	41.79	0.67	1,363.45
	Woodland	221.15	1,226.87	361.40	6.64	4.72	15.06	1835.84
	Grassland	85.80	405.14	1,356.24	8.07	4.31	84.15	1943.71
	Waters	14.65	3.13	5.75	9.56	2.32	1.55	36.96
	Construction land	12.85	2.09	0.89	1.01	10.28	-	27.13
	Unused land	0.81	12.47	82.76	2.33	0.02	88.18	186.56
	Total	1,320.19	1888.90	1885.45	46.05	63.45	189.61	5,393.64

"-" indicates no value.

there is a negative correlation between vegetation FVC and both temperature and air temperature, with a relatively weak direct correlation (Li et al., 2012; Xu et al., 2018; Du et al., 2019). It is worth mentioning that as afforestation policies have evolved, the correlation between vegetation growth and climate has diminished (Huang et al., 2020). Wu et al. (2020) have observed that changes in the Enhanced Vegetation Index are minimally correlated with meteorological factors but strongly associated with artificial ecological engineering, signifying that ecological engineering initiatives are the predominant drivers of such variations. The year 2006 marks a pivotal juncture when sudden shifts in vegetation cover occurred. Prior to this year, thermal factors played a substantial role, but post-2006, active interventions like afforestation and terrain modification diminished the influence of vegetation. In studies of vegetation change, it is crucial to monitor human activities that impact vegetation growth to varying degrees (Zhang et al., 2017; Al-bukhari et al., 2018). Additionally, alterations in land use patterns serve as a tangible reflection of human activity. Over the course of 21 years, the area dedicated to returning farmland to forests and grasslands in Sichuan Province expanded to 28,359.30 km^2 translating to a notable annual growth rate of 317.62/a. This trend underscores the effectiveness of policies promoting land conversion to forests and grasslands, afforestation endeavors, and desert management in fostering increased vegetation cover within Sichuan Province.

To summarize, the vegetation fractional cover (FVC) in Sichuan Province is influenced by a complex interplay of multiple factors. This study employed geographic probes and correlation analysis to reveal an overall increasing trend in vegetation cover within the province. Notably, elevation, landform type, and soil type were identified as dominant factors that promoted vegetation growth and exerted significant effects on vegetation FVC. The study also introduced a dichotomous image model based on MOD13Q1 data, which proved to be a relatively simple, intuitive, and efficient approach for analyzing vegetation patterns.

This study employed the higher-resolution MODIS dataset, which spans from 2000 onwards. While the GIMMS dataset offers long-term data, it has limitations due to its coarser analysis rate. Alternatively, Landsat satellite imagery, which provides more detailed information on a larger scale, demands substantial computational resources and time. To attain detailed, long-term surface data and detect significant vegetation cover changes over the past decades, we utilized the Google Earth Engine (GEE) platform. Moreover, the image element dichotomous model is a remote sensing estimation model. It is not particularly sensitive to the radiatively corrected images within its remote sensing data. However, it exhibits some limitations when applied solely to the distribution of two components: photosynthetic vegetation end-elements and bare soil, especially in specific regions like desertified areas. To enhance our understanding of the distinct driving mechanisms in different regions of Sichuan Province, future research could consider utilizing the image element trichotomous model. This advanced approach would allow for a more comprehensive study of vegetation, addressing uncertainties in specific regions that may arise from the dichotomous model. Ultimately, it would enable a more precise analysis of vegetation cover trends.

5 Conclusion

Utilizing MOD13Q1 data, DEM data, and additional relevant data sources, this study sought to investigate the spatial and temporal dynamics of vegetation cover in Sichuan Province from 2000 to 2020. Further, it explored the driving forces behind these changes by employing the Geodetector model and correlation analysis. The key findings of this research are as follows:

(1) The vegetation Formation Vegetation Cover (FVC) in Sichuan Province displayed a clear pattern from 2000 to 2020, with higher values in the eastern and southern regions and lower values in the western and northern areas. The overall coefficient of variation (CV) was 0.1167, indicating relatively stable changes (CV < 0.15), with the earliest abrupt change occurring in 2006. Approximately 20% of the region exhibited significant fluctuations, primarily concentrated in areas like Shiqu County, Chengdu City, and its neighboring districts and counties. Conversely, about 10% of the area experienced minor fluctuations, mainly in places such as Batang County, Derong County, Ganzi County, and Shiqu County. Regarding the temporal dimension, 84.76% of the vegetation area showed improvement, while 13% experienced degradation. The degradation was primarily observed in Chengdu City, Yibin City, and sporadically in the surrounding areas.

(2) Within the study area, the q-values of elevation, landform type, and soil type were observed to exceed 0.3, suggesting that they predominantly account for changes in vegetation cover. Conversely, the explanatory power of slope and slope direction was insignificant, with q-values less than 0.05, indicating that their influence on vegetation is minimal. Notably, the various factors displayed significant interactions, with q-values indicating interactions surpassing those associated with individual factors. For instance, the most influential interaction was noted between altitude ∩ vegetation type, yielding an impressive explanatory power of 0.540.

(3) The analysis revealed the existence of correlations between each factor and vegetation fractional cover (FVC) across Sichuan Province. Notably, distinct characteristics were observed in relation to the trend and mean of FVC changes and elevation, land use, population density, landform type, and soil type. Additionally, the correlation coefficients of both temperature and air temperature with vegetation FVC exhibited negative correlations, albeit displaying low spatial correlation. These factors were observed to significantly influence the ecological interaction cycle. Intriguingly, shifts in land use were found to be indicative of human activities, with rapid urban expansion increasingly encroaching upon areas previously occupied by vegetation cover, resulting in a corresponding decrease in FVC.

Data availability statement

Publicly available datasets were analyzed in this study. This data can be found here: https://search.earthdata.nasa.gov/search.

Author contributions

LN: Conceptualization, Investigation, Writing–original draft, Writing–review and editing. WP: Conceptualization, Writing–review and editing. YY: Conceptualization, Data curation, Investigation, Writing–review and editing. JX: Formal Analysis, Methodology, Supervision, Writing–review and editing. YW: Writing–review and editing.

Funding

The author(s) declare that no financial support was received for the research, authorship, and/or publication of this article.

Conflict of interest

The authors declare that the research was conducted in the absence of any commercial or financial relationships that could be construed as a potential conflict of interest.

Publisher's note

All claims expressed in this article are solely those of the authors and do not necessarily represent those of their affiliated organizations, or those of the publisher, the editors and the reviewers. Any product that may be evaluated in this article, or claim that may be made by its manufacturer, is not guaranteed or endorsed by the publisher.

References

Al-bukhari, A., Hallett, S., and Brewer, T. (2018). A review of potential methods for monitoring rangeland degradation in Libya. *Pastoralism* 8, 13. doi:10.1186/s13570-018-0118-4

Carla, L. F. D. S., Demetrius, D. D. S., Michel, C. M., Jackson, M. R., Igor, S. D. S. R., Rafael, P. C. L., et al. (2023). Trend analysis and identification of possible periods of change in the occurrence of extreme streamflow events in a tropical basin. *J. S. Am. Earth Sci.* 128, 2023. 104485. doi:10.1016/j.jsames.2023.104485

De, Jong, R., De, Bruin, S., De, Wit, A., Schaepman, M. E., and Dent, D. L. (2011). Analysis of monotonic greening and browning trends from global NDVI time-series. *Remote Sens. Environ.* 115 (2), 692–702. doi:10.1016/j.rse.2010.10.011

Deng, X. Y., Liu, Y., Liu, Z. F., and Yao, J. Q. (2017). Spatial and temporal dynamics of evapotranspiration in the arid zone of northwest China. *Acta Ecol. Sin.* 37 (9), 2994–3008. doi:10.5846/stxb201601270190

Du, J. Q., Qing, F., Fang, S. F., Wu, J. H., He, P., and Quan, Z. J. (2019). Effects of rapid urbanization on vegetation cover in the metropolises of China over the last four decades. *Ecol. Indic.* 107, 105458. doi:10.1016/j.ecolind.2019.105458

Du, J. Q., Shu, J. M., Yin, J. Q., Yuan, X. J., Ahati, J. H., Xiong, S. S., et al. (2015). Analysis on spatio-temporal trends and drivers in vegetation growth during recent decades in Xinjiang, China. *Int. J. Appl. Earth Obs. Geoinf.* 38, 216–228. doi:10.1016/j.jag.2015.01.006

Fang, W., Huang, S. Z., Huang, Q., Huang, G. H., Meng, E., and Luan, J. K. (2018). Reference evapotranspiration forecasting based on local meteorological and global climate information screened by partial mutual information. *J. Hydrol.* 561, 764–779. doi:10.1016/j.jhydrol.2018.04.038

Gocic, M., and Trajkovic, S. (2013). Analysis of changes in meteorological variables using Mann-Kendall and Sen's slope estimator statistical tests in Serbia. *Glob. PlanetaryChange* 100, 172–182. doi:10.1016/j.gloplacha.2012.10.014

Guo, F. Z., and Rasmussen., B. (2022). Predictive maintenance for residential air conditioning systems with smart thermostat data using modified Mann-Kendall tests. *Appl. Therm. Eng.* 222, 119955. 119955. doi:10.1016/j.applthermaleng.2022.119955

He, X., Zhang, F., Cai, Y., Tan, M. L., and Chan, N. W. (2023). Spatio-temporal changes in fractional vegetation cover and the driving forces during 2001-2020 in the northern slopes of the Tianshan Mountains, China. *Environ. Sci. Pollut. Res. Int.* 30 (30), 75511–75531. doi:10.1007/s11356-023-27702-x

He, Y. H. Z., Wang, L., Niu, Z., and Nath, B. W. (2022). Vegetation recovery and recent degradation in different karst landforms of southwest China over the past two decades using GEE satellite archives. *Ecol. Inf.* 68, 101555. doi:10.1016/j.ecoinf.2022.101555

Hirsch, R. M., and Slack, J. R. (1984). A nonparametric trend test for seasonal data withserial dependence. *Water Resour. Res.* 20 (6), 727–732. doi:10.1029/wr020i006p00727

Hu, X. L., Zhang, S. Y., Zhang, J., and Aamir, S. (2023). Efficient CUSUM control charts for monitoring the multivariate coefficient of variation. *Comput. Industrial Eng.* 179, 109159. 109159. doi:10.1016/j.cie.2023.109159

Huang, C. L., Yang, Q. K., Guo, Y. H., Zhang, Y. Q., and Guo, L. N. (2020). The pattern, change and driven factors of vegetation cover in the Qin Mountains region. *Sci. Rep.* 10, 20591. doi:10.1038/s41598-020-75845-5

Huang, S., Yu, L., Cai, D., hu, J., Liu, Z., Zhang, Z., et al. (2023). Predictors of surgery choices in women with early-stage breast cancer in China: a retrospective study. *Ecol. Indic.* 23, 23–28. 16718. doi:10.1186/s12885-023-10510-4

Huo, H., and Sun, C. P. (2021). Spatiotemporal variation and influencing factors of vegetation dynamics based on Geodetector: a case study of the northwestern Yunnan Plateau, China. *Ecol. Indic.* 130, 108005. doi:10.1016/j.ecolind.2021.108005

Jalonen, J., Järvelä, J., Koivusalo, H., and Hyyppä, H. (2014). Deriving floodplain topography and vegetation characteristics for hydraulic engineering applications by means of terrestrial laser scanning. *J. Hydraulic Eng.* 140, 04014056. doi:10.1061/(ASCE)HY.1943-7900.0000928

Jiang, H., Xu, X., Zhang, T., Xia, H., Huang, Y., and Qiao, S. (2022). The relative roles of climate variation and human activities in vegetation dynamics in coastal China from 2000 to 2019. *Remote Sens.-Basel.* 14, 2485. doi:10.3390/rs14102485

Jiang, H. P., Sun, Z. C., Guo, H. D., Weng, Q. H., Du, W. J., Xing, Q., et al. (2021). An assessment of urbanization sustainability in China between 1990 and 2015 using land use efficiency indicators. *npj Urban Sustain* 1, 34. doi:10.1038/s42949-021-00032-y

Kalisa, W., Igbawua, T., Henchiri, M., Ail, S., Zhang, S., Bai, Y., et al. (2019). Assessment of climate impact on vegetation dynamics over East Africa from 1982 to 2015. *Sci. Rep.* 9, 16865. doi:10.1038/s41598-019-53150-0

Karen, R., Ryberg, Glenn, A., Hodgkins, Robert, W., and Dudley, (2019). Change points in annual peak streamflows: method comparisons and historical change points in the United States. *J. Hydrology* 583, 124307. 124307. doi:10.1016/j.jhydrol.2019.124307

Kinjal, C., and Ankit, T. (2023). Neural network systems with an integrated coefficient of variation-based feature selection for stock price and trend prediction. *Expert Syst. Appl.* 219, 2023. 119527. doi:10.1016/j.eswa.2023.119527

Kong, D. X., Miao, C. Y., Borthwick, A. G. L., Lei, X. H., and Li, H. (2018). Spatiotemporal variations in vegetation cover on the Loess Plateau, China, between 1982 and 2013: possible causes and potential impacts. *Environ. Sci. Pollut. Res.* 25, 13633–13644. doi:10.1007/s11356-018-1480-x

Kotharkar, R., and Surawar, M. (2016). Land use, land cover, and population density impact on the formation of canopy urban heat islands through traverse survey in the nagpur urban area, India. *J. Urban Plan. Development-asce* 142, 04015003. doi:10.1061/(ASCE)UP.1943-5444.0000277

Kumar, L., and Mutanga, O. (2018). Google earth engine applications since inception: usage, trends, and potential. *Remote Sens.* 10, 1509–1515. doi:10.3390/rs10101509

Li, A., Wu, J., and Huang, J. (2012). Distinguishing between human-induced and climate-driven vegetation changes: a critical application of RESTREND in inner Mongolia. *Landsc. Ecol.* 27, 969–982. doi:10.1007/s10980-012-9751-2

Li, H. H., and Song, W. (2022). Spatial transformation of changes in global cultivated land. *Sci. Total Environ.* 859, 160194. 160194. doi:10.1016/j.scitotenv.2022.160194

Li, J. K., Yang, Y. T., Zhang, H. R., Huang, A. W., and Gao, Y. M. (2019). Spatial and temporal evolution characteristics of vegetation NPP and analysis of natural and anthropogenic factors in the Qinba Mountains in the past 15 years. *Acta Ecol. Sin.* 39 (22), 8504–8515. doi:10.5846/stxb201807231575

Li, X., Hai, Q., Zhu, Z., Zhang, D., Shao, Y., Zhao, Y., et al. (2023). Spatial and temporal changes in vegetation cover in the three north protection forest project area supported by GEE cloud platform. *Forests* 14, 295. doi:10.3390/f14020295

Li, Y. L., Wang, X. Q., Chen, Y. Z., and Wang, M. M. (2020). Land surface temperature variations and their relationship to fractional vegetation coverage in subtropical regions: a case study in Fujian Province, China. *Int. J. Remote Sens.* 41 (6), 2081–2097. doi:10.1080/01431161.2019.1685714

Liu, H., Jiao, F. S., Yin, J. Q., Li, T. Y., Gong, H. B., Wang, Z. Y., et al. (2020). Nonlinear relationship of vegetation greening with nature and human factors and its forecast-a case study of Southwest China. *Ecol. Indic.* 111, 106009. doi:10.1016/j.ecolind.2019.106009

Ma, B. X., He, C. X., Jing, J. L., Wang, Y. F., Liu, B., and He, H. C. (2023). Attribution of vegetation dynamics in Southwest China from 1982 to 2019. *Acta Geogr. Sin.* 78 (3), 714–728. doi:10.11821/dlxb202303013

Mutanga, O., and Kumar, L. (2019). Google earth engine applications since inception: usage, trends, and potential. *Remote Sens.* 11, 1509–1514. doi:10.3390/rs10101509

Pang, G. J., Wang, X. J., and Yang, M. X. (2017). Using the NDVI to identify variations in, and responses of, vegetation to climate change on the Tibetan Plateau from 1982 to 2012. *Quatern. Int.* 444, 87–96. doi:10.1016/j.quaint.2016.08.038

Peng, W. F., Zhang, D. M., Luo, Y. M., Tao, S., and Xu, X. L. (2019). Geographical detection of natural factors on NDVI changes of vegetation in Sichuan. *Acta Geogr. Sin.* 74 (9), 1758–1776. doi:10.11821/dlxb201909005

Piao, S., Fang, J. Y., Zhao, L. M., Guo, Q. H., Henderson, M., Ji, W., et al. (2003). Interannual variations of monthly and seasonal normalized difference vegetation index (NDVI) in China from 1982 to 1999. *J. Geophys. Res.* 108, 1–13. doi:10.1029/2002JD002848

Radu, G. P., Cristian, V. P., Bogdan, R., Dragoș, A., Mirea, Vasile, D., et al. (2022). Insights into the Phaeozems pedogenesis using total elemental composition analysis. *A case study north-eastern Romania, Geoderma* 409, 115604. doi:10.1016/j.geoderma.2021.115604

Song, Y. Z., Wang, J. F., Ge, Y., and Xu, C. D. (2020). An optimal parameters-based geographical detector model enhances geographic characteristics of explanatory variables for spatial heterogeneity analysis: cases with different types of spatial data. *GIS Sci. Remote Sens.* 57 (5), 593–610. doi:10.1080/15481603.2020.1760434

Wang, H. X., and Liu, C. M. (2000). The meaning of crop water use efficiency and progress of research. *Adv. Water Sci.* 11 (1), 99–104.

Wang, J. B., Zhao, J., Li, C. H., Zhu, Y., Kang, C. Y., and Gao, C. (2019). Spatial and temporal patterns of anthropogenic impacts on vegetation cover in China from 2001-2015. *Acta Geogr. Sin.* 74 (3), 504–519. doi:10.11821/dlxb201903008

Wang, J. F., and Xu, C. D. (2017). Instrumental networking and social network building: how horizontal networking and upward networking create social capital. *Acta Geogr. Sin.* 72, 116–134. doi:10.3724/sp.j.1041.2017.00116

Wang, J. F., Zhang, T. L., and Fu, B. J. (2016). A measure of spatial stratified heterogeneity. *Ecol. Indic.* 67, 250–256. doi:10.1016/j.ecolind.2016.02.052

Wang, J., Li, X., Christakos, G., Liao, Y., Zhang, T., Gu, X., et al. (2010). Geographical detectors-based health risk assessment and its application in the neural tube defects study of the heshun region, China. *Int. J. Geogr. Inf. Sci.* 24 (1), 107–127. doi:10.1080/13658810802443457

Wu, Y. D., Ma, Y., Wu, H. R., Xiao, Y., and Li, H. (2020). Spatial and temporal evolution characteristics and driving forces of vegetation index in Sichuan Province based on MODIS-EVI index. *Soil Water Conservation Res.* 27 (05), 230–236+243+2. doi:10.13869/j.cnki.rswc.2020.05.031

Xiang, J. Y., Peng, W. F., Tao, S., Yin, Y., and Liu, H. S. (2023). Effectiveness and influencing factors of vegetation restoration in Sichuan Province, 2000-2019. *Acta Ecol. Sin.* 43 (04), 1596–1609. doi:10.5846/stxb202106071505

Xie, H., Tong, X. J., Li, J., Zhang, J. R., Liu, P. R., and Yu, P. Y. (2022). Changes of NDVl and EVI and their responses to climatic variables in the Yellow River Basin during the growing season of 2000 2018. *Acla Ecol. Sin.* 42 (11). doi:10.5846/stxb202104271108

Xu, Q. L., Li, W. H., Liu, J., and Wang, X. (2023). A geographical similarity-based sampling method of non-fire point data for spatial prediction of forest fires. *For. Ecosyst.* 10, 100104. doi:10.1016/j.fecs.2023.100104

Xu, S. Q., Yu, Z. B., Yang, C. G., Ji, X. B., and Zhang, K. (2018). Trends in evapotranspiration and their responses to climate change and vegetation greening over the upper reaches of the Y ellow River Basin. *Agric. For. Meteorol.* 263, 118–129. doi:10.1016/j.agrformet.2018.08.010

Xu, Y., Huang, W. T., Dou, S. Q., Guo, Z. D., Li, X. Y., Zheng, Z. M., et al. (2022). Response of vegetation NDVI to climate change and human activities in Southwest China from 2000 to 2020. *Environ. Sci.* 43 (06), 3230–3240. doi:10.13227/j.hjkx.202108107

Yuan, L. H., Jiang, W. G., Shen, W. M., Liu, Y. H., Wang, W. J., Tao, L. L., et al. (2013). Spatial and temporal variation of vegetation cover in the Yellow River Basin from 2000 to 2010. *Acta Ecol. Sin.* 33 (24), 7798–7806. doi:10.5846/stxb201305281212

Yuan, L., Cao, J., Wang, D., Yu, D., Liu, G., and Qian, Z. C. (2023). Regional disparities and influencing factors of high quality medical resources distribution in China. *Int. J. Equity Health* 22, 8. doi:10.1186/s12939-023-01825-6

Yue, S., Pilon, P., and Cavadias, G. (2002). Power of the Mann-Kendall and Spearman's rho tests for detecting monotonic trends in hydrological series. *J. Hydrology* 259 (1/4), 254–271. doi:10.1016/S0022-1694(01)00594-7

Zhang, K., Lü, Y., Fu, B., and Li, T. (2018). The effects of restoration on vegetation trends: spatiotemporal variability and influencing factors. *Earth Env. Sci. T R. SO* 109, 473–481. doi:10.1017/S1755691018000518

Zhang, K., Lv, Y. H., Fu, B. J., Yin, L. X., and Yu, D. D. (2020). Impacts of vegetation cover changes on ecosystem services and their thresholds in the Loess Plateau. *Acta Geogr. Sin.* 75 (5), 949–960. doi:10.11821/dlxb202005005

Zhang, L., Karthikeyan, R., Bai, Z. K., and Srinivasan, R. (2017). Analysis of streamflow responses to climate variability and land use change in the Loess Plateau region of China. *CATENA* 154, 1–11. doi:10.1016/j.catena.2017.02.012

Zhang, Y. X., Li, X. B., and Chen, Y. H. (2003). A review of multi-scale remote sensing and field measurement methods for grassland vegetation cover. *Adv. Earth Sci.* 18 (1), 1673–4831. doi:10.3321/j.issn:1001-8166.2003.01.012

Zhao, A. Z., Zhang, A. B., Liu, J. H., Feng, L. L., and Zhao, Y. L. (2019). Assessing the effects of drought and "Grain for Green" program on vegetation dynamics in China's Loess Plateau from 2000 to 2014. *CATENA* 175, 446–455. doi:10.1016/j.catena.2019.01.013

Zhao, J. Y., Li, J. J., Zuo, L. L., Liu, G. H., and Su, X. K. (2023). Interaction dynamics of multiple ecosystem services and abrupt changes of landscape patterns linked with watershed ecosystem regime shifts. *Ecol. Indic.* 150, 110263. 110263. doi:10.1016/j.ecolind.2023.110263

Zhao, L., Dai, A., and Dong, B. (2018). Changes in global vegetation activity and its driving factors during 1982–2013. *Agric. For. Meteorol.* 249, 198–209. doi:10.1016/j.agrformet.2017.11.013

Zhao, Y., Feng, Q., and Lu, A. (2021). Spatiotemporal variation in vegetation coverage and its driving factors in the Guanzhong Basin, NW China. *Ecol. Inf.* 64, 101371. doi:10.1016/j.ecoinf.2021.101371

Zhu, F. L., Yang, H., Xie, S. Y., Ma, M. G., and Xia, J. (2022). Topographic differentiation of vegetation cover in Sichuan Province based on MODIS-EVI, 2000-2020. 37 (05), 58–68. doi:10.11721/cqnuj20220509

frontiers | Frontiers in Environmental Science

TYPE Original Research
PUBLISHED 23 October 2023
DOI 10.3389/fenvs.2023.1241781

OPEN ACCESS

EDITED BY
Hualin Xie,
Jiangxi University of Finance and Economics, China

REVIEWED BY
Haibin Chen,
Northwest A&F University, China
Shanzhong Qi,
Shandong Normal University, China

*CORRESPONDENCE
Xiaozheng Zheng,
zhengxz@xauat.edu.cn

RECEIVED 17 June 2023
ACCEPTED 12 October 2023
PUBLISHED 23 October 2023

CITATION
Yang S and Zheng X (2023), Spatio-temporal relationship between carbon emission and ecosystem service value under land use change: a case study of the Guanzhong Plain Urban Agglomeration, China.
Front. Environ. Sci. 11:1241781.
doi: 10.3389/fenvs.2023.1241781

Spatio-temporal relationship between carbon emission and ecosystem service value under land use change: a case study of the Guanzhong Plain Urban Agglomeration, China

Shuo Yang and Xiaozheng Zheng*

School of Public Administration, Xi'an University of Architecture and Technology, Xi'an, China

Changes in land use restructuring significantly impact carbon emissions and the provision of ecosystem service value (ESV). This study focuses on the Guanzhong Plain Urban Agglomeration, and accounts for carbon emissions and ecosystem service values caused by land use in the years 2000, 2005, 2010, 2015, and 2020. Carbon sources, carbon sinks, net carbon emission intensity, and ESV intensity were introduced as research variables and the spatial and temporal divergence and correlation patterns between them were examined. The results show that: 1) The carbon emission intensity of land use in the Guanzhong Plain Urban Agglomeration has increased significantly over the study period, showing a distribution pattern of high intensity in the centra regions and low intensity in the surrounding regions. Construction land was identified as the largest carbon source. 2) The overall ESV follows an increasing trend, with the total value increasing from 215,263.7 million to 216,776.2 million. The distribution of ESV intensity is low in the central regions and high in the surrounding regions, and significant changes were observed in the ESV loss and gain intensity of farmland and water body. 3) Carbon emissions and ESV show a significant negative spatial correlation, and both are dominated by low-high and high-low aggregation patterns. A spatial spillover effect of carbon emissions on ESV was observed. Through the correlation analysis of carbon emissions and ESV, theoretical support is provided for promoting regional low-carbon green development and eco-economic synergistic development.

KEYWORDS

land use change, carbon emissions, ecosystem service value, spatial autocorrelation, Guanzhong Plain Urban Agglomeration

1 Introduction

Ecosystems provide nearly all the elements of human wellbeing in the natural resource domain as well as ecological goods and services through a variety of ecological processes, which are typically distinguished by the ecosystem service value (ESV); therefore, humans have come to rely on ecosystems as the service providers that enable a high quality of life (Leemans and De Groot, 2003). In addition to accelerated urbanization and economic construction achievements, China's energy consumption, water use, land use, and other

demands have also increased. This has displaced agricultural land and other ecological land, has increased the scarcity of resources, and has splintered the overall continuous natural ecological landscape. Resulting ecological issues are the heat island effect and greenhouse effect, which in turn affect the carbon cycle and carbon emissions, which impede the beneficial effects of ecosystems and ultimately reduce China's ability to maintain a healthy environment. China's sustainable development is threatened by low ecological carrying capacity, which seriously challenges the development of regional ecological security.

The use of land resources, which carry different ecosystems, changes the ability of ecosystems to deliver services. Land use change is one of the most direct drivers of the carbon cycle in terrestrial ecosystems and a significant contributor to changes in ecosystem services. Urban agglomerations are a major source of power and growth centers in China's urbanization process. At the same time, construction land is the most important place for fossil fuel use, thus identifying the combustion of fossil fuels and carbon emissions in urban agglomerations as the two main sources of carbon emissions that exert an immediate impact on the function of the regional ecosystem services. China's carbon emissions are far higher than those of other countries due to the constraints imposed by such factors as the extensive economic growth mode, irrational energy utilization structure, low energy development technology, low level of energy equipment management, and pressure from population growth. These pressures intensify because of the gradually increasing intensity of land development and utilization in local areas. China has produced the greatest global total carbon emissions in recent years, and its emissions are still increasing. In September 2020, at the United Nations General Assembly, President Xi Jinping stated that "China will increase its autonomous national contribution, adopt stronger policies and measures, strive to peak CO_2 emissions by 2030, and work towards achieving carbon neutrality by 2060" (Xi, 2020). To promote the integrated high-quality development and synergistic management of both regional economies and ecological environments in urban aggregations, it is important to examine the spatial relationship between ESV and land carbon emissions under land use change.

On the one hand, since the 1990s, Chinese as well as international research on carbon emissions has been growing. Total emissions have been measured at various geographic scales, including national, provincial, municipal, and regional scales; moreover, multiple perspectives have been discussed, including carbon intensity, risk, efficiency, the regional carbon cycle, the relationship between energy consumption and carbon emissions, the decoupling effect of carbon emissions and economic growth, influences, and the regional carbon cycle (Larsen et al., 2011; Forman, 2015; Zhao et al., 2018; Li et al., 2019; Yang et al., 2022a). On the other hand, research on ESV has been gradually deepened by Xie et al. and Wang et al. in response to research of academics like Constanza et al. and the United Nations Millennium Ecological Assessment Program on the assessment of ecosystems and ecological wellbeing (Costanza et al., 1997; Xie et al., 2003; Li et al., 2013; Leemans and De Groot, 2003; Scholte et al., 2015; Wang et al., 2014). For national, provincial, municipal, district (county), watershed, and numerous ecological types, the accounting of ESV is conducted from the perspectives of service supply-demand balance relationship, the relationship between ecological environment and economy and society, and ecological spatial distribution (Davidson et al., 2019; Xue et al., 2022; Liu et al., 2023a; Liu et al., 2023b). The development of urban agglomerations, in particular, has altered natural ecosystems into ecosystems that are human-dominated and human-nature coupled. This has become the main factor that drives changes in ecosystem services in urban agglomeration destinations. The mechanisms of interaction between ecological compensation policies, standards, and wellbeing can be uncovered by studying the functions and values of ecosystems as well as the ecological footprint and ecological carrying capacity (Chen et al., 2017; Cai et al., 2021; Ouyang et al., 2021; Zhang et al., 2022a; Yang and Su, 2022; Pan et al., 2023). Reducing carbon emissions is an indispensable condition for realizing the goal of "carbon peaking and carbon neutrality", and is one of the most important ways to consolidate and enhance the protection of ecosystems. Terrestrial ecosystems also play an important role in the process of carbon neutralization. Taken together, there are two aspects of existing research that could be improved. The first is reflected in the lack of analysis of theoretical issues. Most studies discuss methods and processes for accounting for carbon emissions and ESV. Based on the changes in urban socio-economic activities carried by the land, the land-use structure is adjusted and redistributed, affecting the total amount of carbon emissions, which in turn changes the functions and values affecting the ecosystem provision. There is a relative lack of analysis and organization of this theoretical issue. The second shortcoming is mainly in the specific research process. Few quantitative examinations of the intensity of carbon emissions have been based on geographic information system method and land use data, and most research has employed yearbook data to evaluate carbon emissions. Studies on urban agglomerations in less developed areas of western China, especially those that include ecologically complex and fragile areas, are rare compared to studies on developed regions or traditional administrative boundaries. Most studies have merely considered carbon emissions or ESV alone, with fewer studies linking the two and analyzing their spatial aggregation. Using this information as a foundation, this paper analyzes the theoretical issue of carbon emissions affecting ESV. In this paper, based on land use, carbon emissions and ESV are assessed at two scales (administrative division and grid method under geographic information system data), and the relationship between their spatial aggregation is also examined. The spatial differentiation and problems of the carbon emissions and ESV are discussed and estimated to provide the support and references needed to optimize the ecological security pattern, alleviate the contradiction between regional economic development and ecological protection, and promote regional synergistic development.

The Guanzhong Plain Urban Agglomeration (GPUA) is the only urban agglomeration in the national plan that is clearly strategically positioned as an inland ecological civilization construction pioneer area. This area is of great significance for urban integration, economic and social development, as well as for the construction of an ecological security barrier in northwest China. It also has significant academic value. The GPUA is located in the inland area of northwest China, an area with a fragile ecological background. As a consequence of the ongoing expansion of urban construction land, the GPUA will predictably expand from the Guanzhong Plain to numerous complex natural ecosystem source areas such as the

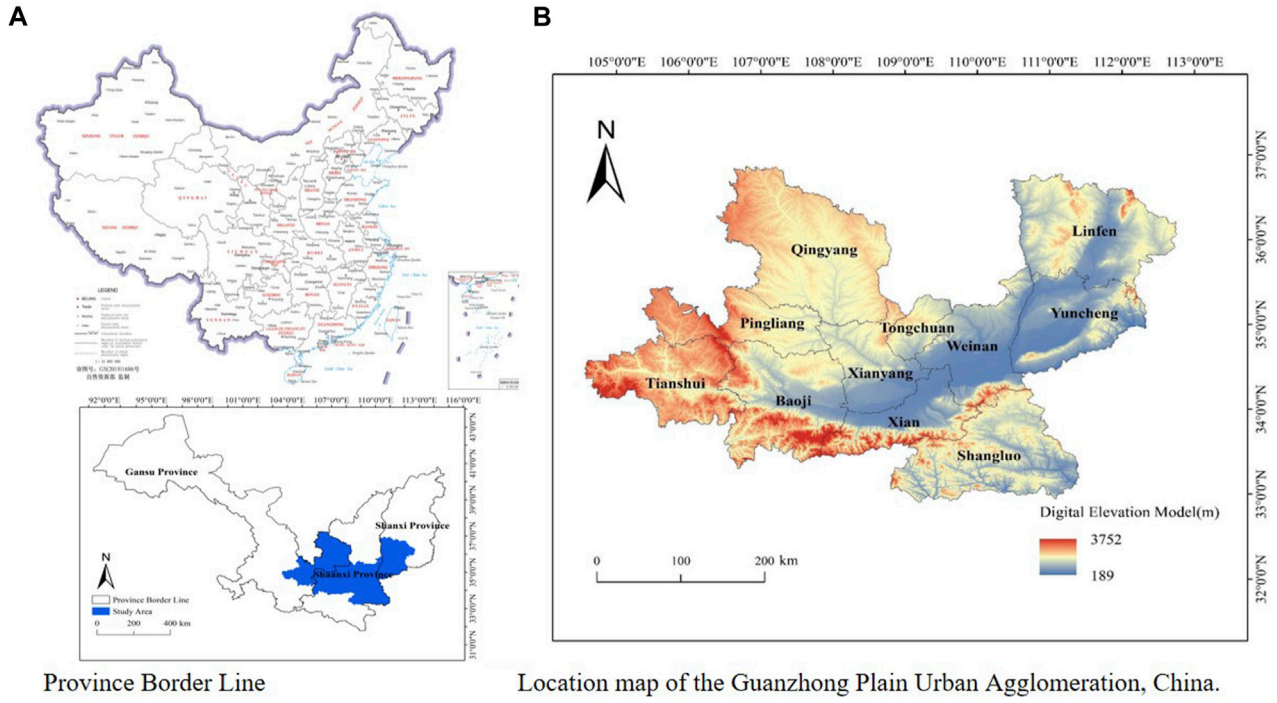

FIGURE 1
Location map of the GPUA, China. **(A)** Province Border Line. **(B)** Location map of the Guanzhong Plain Urban Agglomeration, China.

Qinba Mountains, loess hills, and gullies. As a result, the intensity of land use, carbon emissions, and the deterioration of the ecological environment will increase. The scientific question to be addressed in this study is how carbon emissions and ESV can contribute to the realization of ecologically and economically synergistic sustainable development in ecologically fragile areas under the background of "carbon peak and carbon neutrality". Specific questions include: 1) What are the spatial differentiation characteristics and change trends of land use restructuring and carbon emission and ESV respectively? 2) What is the spatial and temporal clustering relationship between carbon emission intensity and ESV intensity?

2 Materials and methods

2.1 Study area

The Guanzhong Plain Urban Agglomeration (104°34′–112°34′E, 33°34′–36°56′N), centered around Xi'an, is located in the inland area of northwest China and is the second largest urban agglomeration in western China. This urban agglomeration covers an area of 107,000 km^2 and belongs to the warm temperate continental monsoon climate zone, bordered by the Qinling Mountains in the south and the Yellow River in the east, situated between the Qinba Mountains and the Loess Plateau. In 2020, the GPUA had a resident population of 38.87 million and a regional GDP of CNY 2.2 trillion.

The Guanzhong Plain Urban Agglomeration Development Plan officially delineated the planning area of the GPUA. This area includes Xi'an, Baoji, Xianyang, Tongchuan, Weinan, and Shangluo City (Shangzhou District, Luonan County, Danfeng County, and Zhashui County) in Shaanxi Province; Yuncheng City (except Pinglu County and Quanqu County) and Linfen City (Yaodu District, Houma City, Xianfen County, Huozhou City, Quwo County, Yicheng County, Hongdong County, and Fushan County) in Shanxi Province; as well as Tianshui City and Pingliang City (Kongdong District, Huating County, Jingchuan County, Chongxin County, and Lingtai County) and downtown Qingyang (Xifeng District) in Gansu Province. Because of data availability, this study uses the municipal area as the boundary, including the city-wide areas of Shangluo, Yuncheng, Linfen, Pingliang, and Qingyang. The study area is shown in Figure 1.

2.2 Data sources

1) Vector boundaries of the study area were obtained from the 1: 1 million National Basic Geographic Database of the National Geographic Information Resource Catalog Service System (https://www.webmap.cn/); (2)Land use data at a spatial resolution of 30 m were obtained from the Resource Environment and Science Data Center of the Chinese Academy of Sciences. These data are based on the Landsat series of satellite images and were generated through human-computer interaction and manual visual interpretation (https://www.resdc.cn/). According to the land use classification standard of the Chinese Academy of Sciences, the study area is divided into six primary types, namely, farmland, woodland, grassland, water body, construction land, and unused land. Social and economic data as well as energy consumption data ranging from 2001 to 2021 were

obtained from the *"Gansu Province Statistical Yearbook"* (2001–2021), *"Shaanxi Province Statistical Yearbook"* (2001–2021), *"Shanxi Province Statistical Yearbook"* (2001–2021), *"China City Statistical Yearbook"* (2001–2021), and statistical bulletins of cities and towns from 2000 to 2020. Food price data were obtained from the *"National Compilation of Information on Costs and Benefits of Agricultural Products"* (2001–2021).

3 Research methods

3.1 Land use type transfer matrix

The land use transfer matrix reflects the quantitative transfer status of each land use type in the form of a two-dimensional matrix over a 20-year period. This matrix is used to visualize the quantity and direction of changes between time periods and land use types.

$$S_{ij} = \begin{bmatrix} S_{11} & S_{12} & \cdots & S_{1n} \\ S_{21} & S_{22} & \cdots & S_{2n} \\ \cdots & \cdots & \cdots & \cdots \\ S_{n1} & S_{n2} & \cdots & S_{nn} \end{bmatrix} \tag{1}$$

where, S_{ij} is the land area that is transferred from land use i to land use j; n is the number of land classes; i is the land use type at the beginning of the study period; j is the land use type at the end of the study period.

3.2 Land use dynamics model

The dynamism model is expressed by calculating the average annual rate of change in the quantity of a particular land use type in the region at the end of the study period and at the beginning of the study period. The degree of single land use dynamic is mainly used to reflect changes in specific land use types in the study area, indicating the rate of change and the magnitude of change in different land use types over time. The calculation formula is:

$$K = \frac{U_b - U_a}{U_a} \times \frac{1}{T} \tag{2}$$

where, K > 0 means that the land scale of the type is expanding, K < 0 means that the land scale is shrinking, U_a、U_b are the number of single land use/cover types at the beginning and the end of the study period, respectively; T is the length of the study time period, and when the time period is set to 1 year, the attitude of the single land use dynamics is the annual rate of change of the utilization/cover type of the land.

Comprehensive land use dynamics responds to the rate of change in the overall type of land use in the study area over a given period of time, responding to comprehensive regional land use changes. The calculation formula is:

$$LC = \frac{\sum_{i=1}^{n} \Delta LU_{i-j}}{2\sum_{i=1}^{n} LU_i} \times \frac{1}{T} \times 100\% \tag{3}$$

Where, LC is the comprehensive land use dynamics, LU_i is the area of type i land use type at the beginning of the study, ΔLU_{i-j} is the absolute value of the area of type i land use type converted to non-type i land use type during the study period; T is the study period, and n is the number of land use types.

3.3 Carbon emission measurement

The carbon emissions in the study area were calculated by multiplying the area and carbon emission factors of each land type and then summing the results. The main land types that can be directly measured for carbon emissions are types of carbon sink land, including woodland, grassland, water body, and unused land; these are measured based on the carbon emission factors obtained by previous studies. The direct carbon emission calculation formula is:

$$E_l = \sum e_i = \sum S_i \times \delta_i \tag{4}$$

where, E_l denotes direct carbon emissions; e_i denotes carbon emissions from different site types; S_i and δ_i denote the area of the site type and the carbon emission factors, respectively. In this study, the carbon emission coefficients of each land type were determined based on the research results of Cai et al. (2005), Fang et al. (2007), Duan et al. (2008), and Lai (2010). Table 1

Carbon emissions from construction land originate from fossil energy consumed in the production process. Because energy consumption varies greatly among different regions, indirect measurement is used to calculate it. The total carbon emissions from construction land are estimated indirectly by accounting for energy consumption of oil, coal, natural gas, and electricity, combined with data obtained from the China Energy Statistics Yearbook and the 2006 IPCC Guidelines for National Greenhouse Gas Emissions Inventories. The formula for calculating carbon emissions from construction land is as follows:

$$E_\varphi = \sum e_i = \sum_{i=1}^{n} m_i \times \beta_i \times \theta_i \tag{5}$$

where, E_φ represents the total carbon emissions from construction land; e_i represents the carbon emissions generated by energy source i; m_i is the consumption of various fossil energy fuels; β_i is the standard coal conversion factor of energy sources; θ_i is the carbon emission factor of each energy source. Table 2

The carbon emission intensity is determined by the area of each land use type and the carbon emission factor, where a larger carbon emission intensity means a larger carbon emission from each grid. The calculation formula is:

$$C_{RI} = \sum_{i}^{n} \frac{S_i P_i}{S} \tag{6}$$

where, C_{RI} is the carbon emission intensity; S_i and P_i are the area of gridded land type and carbon emission coefficient, respectively; S is the total area of the gridded network.

3.4 Ecosystem service value

In reference to the results of Xie et al. (2015), in this study, the ESV equivalent factor of one standard unit of ESV was defined as one-seventh of the economic value of natural food production per unit area of farmland per year nationwide. ESV correction and accounting were performed. Xie et al. (2015) corrected the ESV

TABLE 1 Carbon emission factors by land use type.

Land use types	Carbon emission factors (t/hm²·a)	
Farmland	0.372	Cai et al. (2005)
Woodland	−0.644	Fang et al. (2007)
Grassland	−0.022	Fang et al. (2007)
Water body	−0.253	Duan et al. (2008)
Unused land	−0.005	Lai (2010)

TABLE 2 Energy conversion standard coal factor and carbon emission factor by type of energy.

Energy types	Discount factors for standard coal	Carbon emission factors
Raw Coal (Coal)	0.7143	0.7559
Coke	0.9714	0.855
Gasoline	1.4714	0.5538
Kerosene	1.4714	0.5714
Diesel	1.4571	0.5921
Fuel oil	1.4286	0.6185
Natural gas	1.33	0.4483
Electricity	0.1229	0.2132

TABLE 3 Equivalent factors of ESV.

Ecosystem classification	Secondary type	Farmland	Woodland	Grassland	Water body	Unused land
Supply service	Food production	0.85	0.31	0.1	0.8	0
	Raw material production	0.4	0.71	0.14	0.23	0
	Water supply	0.02	0.37	0.08	8.29	0
Reconciliation service	Gas regulation	0.67	2.35	0.51	0.77	0.02
	Climate regulation	0.36	7.03	1.34	2.29	0
	Environmental purification	0.1	1.99	0.44	5.55	0.1
	Hydrological regulation	0.27	3.51	0.98	102.24	0.03
Support service	Soil conservation	1.03	2.86	0.62	0.93	0.02
	Nutrient maintenance	0.12	0.22	0.05	0.07	0
	Biodiversity	0.13	2.6	0.56	2.55	0.02
Cultural service	Aesthetic landscape	0.06	1.14	0.25	1.89	0.01

equivalent factor table adapted to the actual situation in China, which is more suitable for the actual application in China, as shown in Table 3. Based on Table 3, this study utilizes the following methods to make corrections to match the actual social development and regional characteristics of the GPUA.

The calculation formula is as follows:

$$D = \frac{1}{7} \times \sum_{i=1}^{n} \frac{P_i G_i}{S_i} \tag{7}$$

where, D is the ESV for a standard equivalent factor; P_i is the unit price of crop category i; G_i is the yield of crop category i; S_i is the planted area of crop category i.

The ESV coefficient is calculated by the formula:

$$VC_j = \sum E_{ji} \times D \tag{8}$$

where, VC_j denotes the coefficient of ESV of the jth land; E_{ji} is the equivalent factor of the ESV of the ith land use ecological service

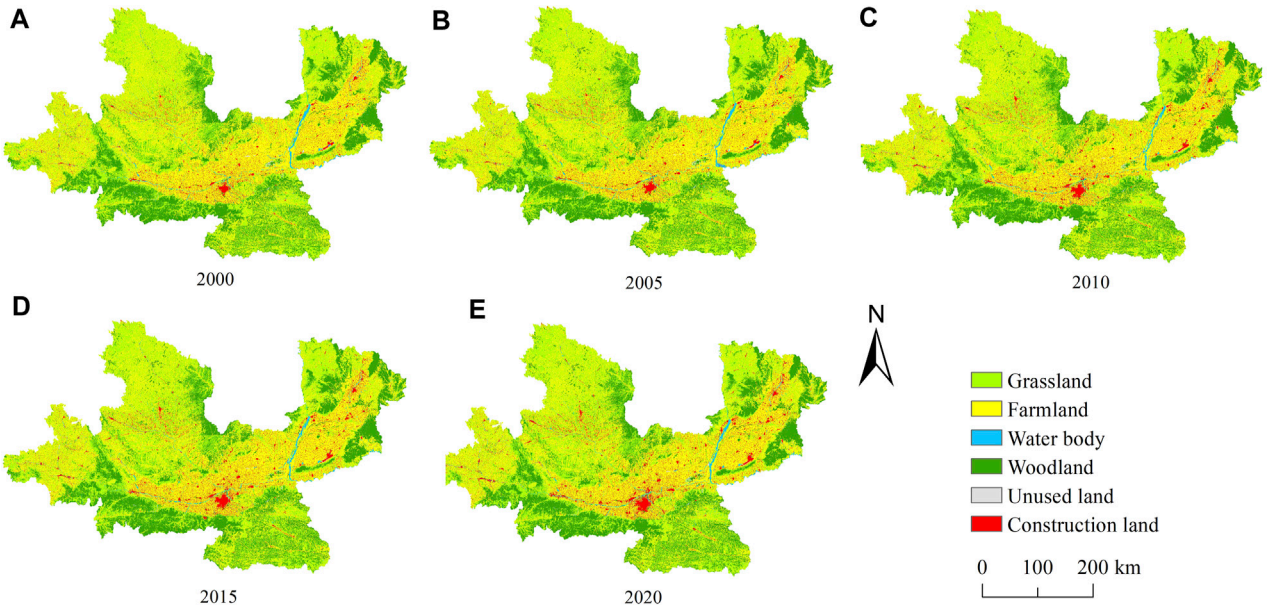

FIGURE 2
Land use changes in the GPUA over the study period. **(A)** 2000, **(B)** 2005, **(C)** 2010, **(D)** 2015, **(E)** 2020.

function of the *j*th land; D represents the value of a standard equivalent factor.

3.5 Bivariate spatial autocorrelation analysis

The spatial clustering and dispersion between carbon emission intensity and ESV intensity was examined using the bivariate Moran's index. The calculation formula is as follows:

$$I = \frac{\sum_{i=1}^{n}\sum_{j=1}^{n} W_{ij}(x_i - x)\left(x_j - \bar{x}\right)}{S^2 \sum_{i=1}^{n}\sum_{j=1}^{n} W_{ij}} \quad (9)$$

$$I_i = \frac{x_i - \bar{x}}{S^2}\sum_{j=1}^{n} W_{ij}\left(x_j - \bar{x}\right) \quad (10)$$

where, I and I_i denote the global Moran's I and local Moran's I of carbon emissions and ESV intensity, respectively. The Moran's I index should be in the range of [−1,1]. When Moran's I index is greater than 0, it indicates the existence of spatial positive correlation, when Moran's I index is less than 0, it indicates the existence of spatial negative correlation of agglomeration effect, and when Moran's I is equal to 0, it indicates the non-existence of spatial relationship. Where, n represents the number of spatial grid units; x_i and x_j are the attribute values of cell grids i and j, respectively; S^2 is the variance. The bivariate LISA clustering diagram can illustrate the degree of association between the two at a certain significance level. This is mainly used to examine ESV and carbon emissions in the study area in terms of their spatial location, as well as to find the correlation and difference between both variables.

4 Results

4.1 Land use change analysis

Figure 2 shows the land use types of the GPUA from 2000 to 2020. According to the land use classification standard, the GPUA is dominated by farmland, grassland, and woodland, which together account for about 94.7% of the total land area in 2020. In terms of the 2020 land use structure, for example, farmland accounts for about 39.9% of the total land area of the region, grassland accounts for about 33% of the total land area of the region, and woodland accounts for about 21.8% of the total land area of the region. The GPUA has a beneficial geographical location. The northern part of the urban agglomeration is a loess hilly and ravine area with relatively high vegetation coverage and rich grassland and forest resources. The central part consists of the Guanzhong Plain and the Fenwei Plain and is adjacent to the Weihe River water system, which is suitable for agricultural development. The southern part depends on the Qinling Mountains, which have good ecological diversity. During the period of 2000–2020, farmland decreased by 3,872.546 km^2 in total, which is the main category of land transferal. Construction land is the land type that increased the most, with an increase of 2002.442 km^2, whereas grassland increased by 892.98 km^2, woodland increased by 890.77 km^2, and water body and unused land increased by 67.351 km^2 and 19.003 km^2, respectively. To more intuitively understand the structural characteristics of land use change in the GPUA during this period, a land use transfer matrix was used to calculate land use dynamics. The land use transfer matrix was constructed and the land use dynamic attitude was calculated. The specific results are shown in Tables 4, 5. Overall, unused land has the highest land use motivation, followed by water body and construction land. Unused land and water body are smaller because of their land

TABLE 4 Land use dynamics in the GPUA.

Types		2000–2005	2005–2010	2010–2015	2015–2020
Single land use dynamic attitude	Farmland	−0.33%	−0.46%	−0.06%	−0.46%
	Woodland	0.30%	−0.01%	−0.01%	−0.01%
	Grassland	0.04%	0.32%	0.00%	0.32%
	Water body	1.68%	1.72%	0.17%	1.72%
	Construction land	1.67%	1.64%	0.72%	1.64%
	Unused land	−1.24%	8.91%	−2.56%	8.91%
Comprehensive land use dynamic attitude		0.14%	0.16%	0.03%	0.19%

TABLE 5 Land use transfer matrix for the GPUA.

Periods	Types	2020						
		Farmland	Woodland	Grassland	Water body	Construction land	Unused land	Total (km^2)
2000	Farmland	61607.137	805.749	3724.272	231.531	2212.084	24.307	68605.081
	Woodland	369.481	33318.434	662.822	14.221	55.792	10.318	34431.068
	Grassland	2206.467	1166.475	48937.062	51.787	139.740	21.090	52522.622
	Water body	146.864	10.015	46.891	1232.455	36.638	13.987	1486.850
	Construction land	389.774	16.014	31.058	8.593	4387.668	0.537	4833.644
	Unused land	12.811	5.150	13.498	15.614	4.164	120.052	171.289
	Total	64732.535	35321.838	53415.602	1554.201	6836.086	190.292	162050.554

use area, while construction land increased more because of areas that were transferred in. Although the overall situation from 2000 to 2020 showed an increase in the areas of all land types (except for the largest area of transferred out farmland), the transfer-in attitude of woodland showed a slight decrease after 2005. The change in the transfer attitude of grassland was clearly slower than that of construction land. From 2000 to 2020, the largest amount of land that was transferred out was farmland, and the main transfer directions were grassland, construction land, and woodland. With the continuous promotion of the project of returning farmland to forest and grass and the project of soil erosion control in the northern loess hills and ravines, the degree of vegetation cover increased year by year. Moreover, wasteland and bare land were gradually transformed into grasslands and forests. According to *the China Forestry and Grassland Statistical Yearbook*, during the period of 2000–2020, the forest coverage rate of Shanxi Province increased from 13.3% to 20.5%; the forest coverage rate of Shaanxi Province increased from 32.6% to 43.1%; the forest coverage rate of Gansu Province increased from 6.7% to 11.3%. The prevention of soil erosion and the return of cultivated land to forest and grassland made great achievements. During this period, the GPUA expanded rapidly: construction land increased, population increased, urbanization expanded rapidly, regional arable land was annexed, and the intensity of land development and utilization also increased. The expansion met the demand for rapid economic expansion and development of this region.

4.2 Carbon emissions analysis

In this study, the carbon emissions of urban land use in the GPUA are measured via carbon emissions, carbon sources/sinks, and net carbon emissions of each category. The dynamic change characteristics of each indicator in 2000–2020 are analyzed, and the results are shown in Table 6; Figure 3. As shown in Table 6, the overall net carbon emissions from land use in the GPUA followed a significant growth trend from 40,815.272 × 10^4 t in 2000 to 352,655.178 × 10^4 t in 2020. The growth trend of carbon emissions from construction land is basically consistent with the growth trend of net carbon emissions from land use, and carbon emissions from construction land have become the main source of the growth of net carbon emissions. The farmland area gradually decreased over the study period, and accordingly, the carbon emissions from cultivated land followed a decreasing trend from 289.77 × 10^4 t in 2000 to 273.407 × 10^4 t in 2020. Carbon sinks followed a first decreasing and then increasing trend during the study period. Woodland was the main source of carbon sequestration, and the carbon sequestration capacities of grassland and water body were relatively low. The carbon sequestration capacity of woodland showed a small increase over 2000–2010 and was more stable from 2010 to 2020. The carbon sequestration effect of grassland and water body remained basically unchanged during the study period. Unused land showed a decreasing trend from 2000 to 2015 and a significant increase from 2015 to 2020, which matches the trend of carbon sink changes.

TABLE 6 Accounting results of carbon emissions from land use in the GPUA.

Years	Farmland (10^4 t)	Woodland (10^4 t)	Grassland (10^4 t)	Water body (10^4 t)	Construction land (10^4 t)	Unused land t)	Carbon source (10^4 t)	Carbon sink (10^4 t)	Net carbon emissions (10^4 t)
2000	289.770	−221.913	−11.570	−3.769	40848.478	−85.724	41138.248	−322.976	40815.272
2005	284.942	−225.276	−11.594	−4.086	83228.922	−80.425	83513.864	−321.381	83192.483
2010	280.654	−227.977	−11.580	−3.593	176986.601	−75.576	177267.255	−318.726	176948.529
2015	279.827	−227.824	−11.582	−3.624	266385.152	−65.894	266664.979	−308.924	266356.055
2020	273.407	−227.655	−11.767	−3.935	352720.370	−95.243	352993.778	−338.6	352655.178

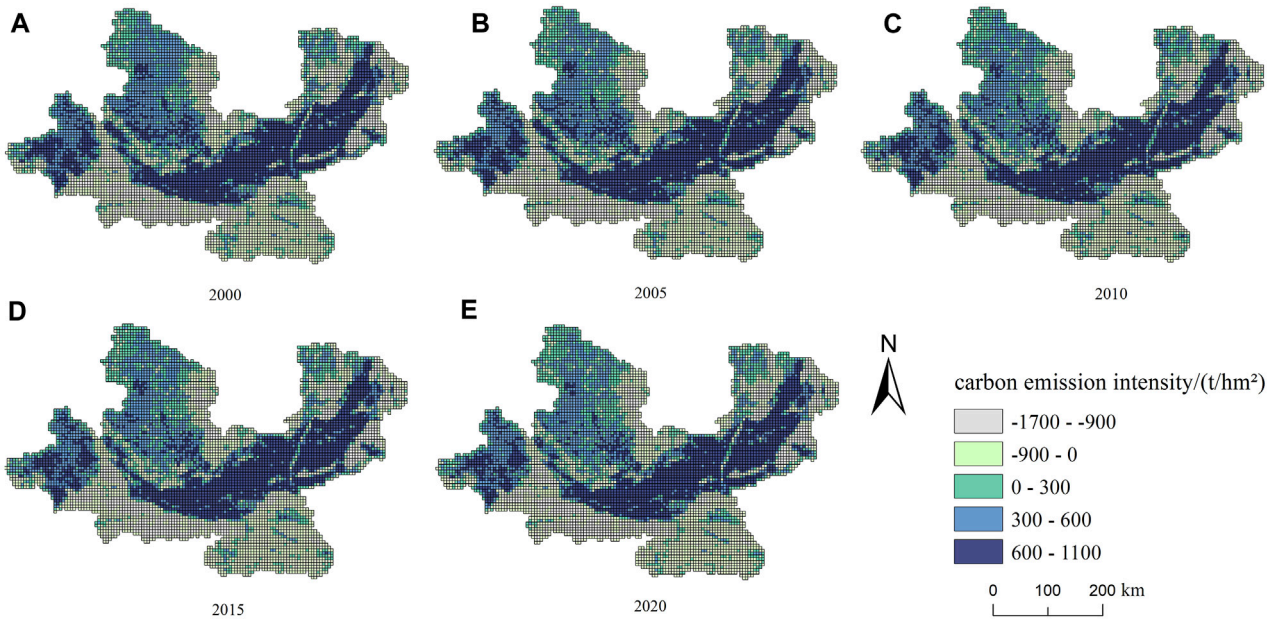

FIGURE 3
Carbon emission intensity in the GPUA. **(A)** 2000, **(B)** 2005, **(C)** 2010, **(D)** 2015, **(E)** 2020.

Analyzing the data in terms of carbon source/sink composition showed that carbon emissions from construction land were the most important carbon source, accounting for 99.30%–99.92% of the total carbon source and increasing significantly year by year. As one of these carbon sources, the contribution rate of carbon emissions from farmland was significantly smaller than that of construction land, but the area share was high. Carbon emissions per hectare of construction land represent the carbon intensity and energy consumption structure of construction land as a land use category in each study year. The average carbon emission intensity of construction land in the study area in 2000, 2005, 2010, 2015, and 2020 were 843.725 t/hm^2, 1586.923 t/hm^2, 2898.595 t/hm^2, 4211.434 t/hm^2, and 5153.703 t/hm^2. The carbon emissions of construction land in 2020 were about six times of those in 2000. This result highlights the great potential for carbon emission reduction on construction land. Regarding the carbon emissions composition of carbon sinks, woodland and grassland are the main carbon sinks, together accounting for about 98.5% of the total carbon sinks. However, woodland and grassland, which cover 54.8% of the land area of the study area, have an extremely important carbon sequestration capacity, while water body and unused land have lower carbon sequestration capacities. Because of the great gap between the amount of carbon sources and carbon sinks, under the integrated regional eco-economic development strategy, the GPUA has begun to focus on controlling carbon sources and increasing carbon sinks to maintain ecosystem services and functions.

Because of differences in the class structure and development level in this urban agglomeration, to analyze the change of carbon emissions more intuitively and enhance comparability, the carbon emission intensity index was analyzed in depth. This index was divided into five intervals of −1700 to −900, −900 to 0, 0 to 300, 300 to 600, and 600 to 1100, and the results are shown in Figure 3. The maximum value of carbon emission intensity in the GPUA decreased from 1053.24 (2000) to 1048.66 (2020). This indicates that ecological and environmental quality issues have attracted attention during the development of urban agglomerations and the uncontrolled brutal development pattern of relying on energy

TABLE 7 Ecosystem service value coefficients of the GPUA (CNY/hm^2·a).

Primary type	Secondary type	Farmland	Woodland	Grassland	Water body	Construction land	Unused land
Supply service	Food production	1433.982	354.710	207.635	850.007	0.000	12.977
	Raw material production	317.942	817.564	304.964	473.668	0.000	38.932
	Water supply	25.954	423.922	168.704	7059.601	0.000	25.954
Reconciliation service	Gas regulation	1154.972	2690.608	1070.620	1732.457	0.000	142.749
	Climate regulation	603.440	8045.869	2829.031	3821.788	0.000	129.772
	Environmental purification	175.192	2340.223	934.359	5937.073	0.000	402.293
	Hydrological regulation	1940.093	5013.528	2069.865	82061.376	0.000	272.521
Support service	Soil conservation	674.815	3274.582	1304.209	2102.308	0.000	168.704
	Nutrient maintenance	201.147	250.893	103.818	162.215	0.000	12.977
	Biodiversity	220.613	2980.432	1187.415	6761.125	0.000	155.726
Cultural service	Aesthetic landscape	97.329	1306.372	525.577	4295.456	0.000	64.886

and expanding land has been restrained. High values of carbon emission intensity were mostly distributed in the central, western, and northwestern parts of the urban agglomeration. In addition, the trend of spatial differentiation shows a distribution pattern of high intensity in the central region and low intensity in the surrounding regions, which is roughly similar to the distribution of land use structure of farmland and grassland. High altitude and slope areas are rich in ecological resources, and these areas also feature low land development, well-protected ecosystems, and low carbon emission intensity. High intensity carbon emission areas are mainly located on the banks of the Weihe and Yellow River as well as in the Guanzhong Plain. These areas are mainly influenced by the expansion of urban and rural settlements and changes in the scale of agricultural production land. The development of agriculture and the expansion of the scope of urban settlements have led to a high degree of land development. The high intensity of human activities has directly led to the problem of high carbon emissions from land use, which is difficult to circumvent.

4.3 Ecosystem service value accounting results

To apply coefficient correction to the actual production capacity of the Guanzhong Plain Urban Agglomeration, the grain yield correction method was used. According to the yield of major grain crops, sown area, and grain purchase price in the study area from 2000 to 2020, the coefficient of ESV of the GPUA was obtained by combining the land use type and the corresponding ecosystem. The results are shown in Table 7.

The total ESV of the GPUA from 2000 to 2020 showed fluctuating changes and an overall increasing trend. The total value increased from 215,263.7 million yuan to 216,776.2 million yuan, which represents an increase of 0.700% (Table 8). Judging from the ESV of each land type, woodland, grassland, and farmland are the main contributors to the total ESV, accounting for 44.674%, 26.160%, and 21.144%, respectively. Among them, ESV contributed by farmland decreased year by year, from 21.836% to 20.459%. The remaining land types showed an overall increasing trend. The functional structure of land use indicates that during the period of 2000–2020, farmland decreased by a total of 3872.546 km^2, while construction land was the main category of increase, increasing by 2002.442 km^2. At 67.351 km^2, the increase in the water area was less. However, the increase in ESV added during the study period reached 4.403%, indicating that water bodies have high ESV intensity and are also the main contributors to the total ESV. Water bodies are also the main contributing land type and hold a very important ecological status. The interconversion among land classes is also an important reason for the fluctuation of total ESV during the study period.

To visually analyze the spatial distribution characteristics of ESV in the study area, while avoiding the influence of the edge area of the study area, a 5 km × 5 km grid was created for an equally spaced sampling of the study area based on 30 m resolution land use data. The study area was divided into 6934 units, and the ESV intensity results of each study unit were identified. The results are shown in Figure 4. In this study, the calculated ESV intensity was divided into four zones, I, II, III, and IV, and the range of values defined for the four zones corresponded to: 0–20, 20–35, 35–55, and >50. The ESV intensity of the GPUA showed a distribution trend of low in the central regions and high in the surrounding regions. The grid in the low ESV intensity range is mainly caused by the relatively uniform spatial distribution and high proportion of farmland and construction land, accounting for about 22.45% of the total grid area. The Guanzhong Plain area is suitable for agricultural development, the scope of urban settlements expands, the ecological and environmental effects are low, and negative effects are difficult to avoid. Areas at high altitude, slopes, and Yellow River and Weihe River basin areas are rich in ecological resources, their ecosystems are more complete, and the positive ecological environment effect is significant; moreover, the value of services available is high, accounting for about 44.71% and 23.61% in zones II and III, respectively, and for about 9.22% in the high ESV intensity zone. Overall, the distribution range of low-intensity areas has been gradually shrinking and transforming into II intervals, and the overall ESV intensity of the GPUA has increased.

TABLE 8 Ecosystem service values and changes in the GPUA over the study period.

Land type	ESV (billion·hm²)					2000–2010 Amount of change/rate of change	2010–2020 Amount of change/rate of change	2000–2020 Amount of change/rate of change
	2000	2005	2010	2015	2020			
Farmland	470.051	462.219	455.264	453.922	443.507	−14.787/-3.15%	−11.757/-2.58%	−26.544/-5.65%
Woodland	947.566	961.923	973.456	972.807	972.083	25.890/2.73%	−1.373/-0.14%	24.517/2.59%
Grassland	563.061	564.196	563.556	563.629	572.625	0.495/0.09%	9.069/1.61%	9.564/1.70%
Water body	171.714	186.127	163.667	165.077	179.274	−8.047/-4.69%	15.607/9.54%	7.56/4.40%
Construction land	0	0	0	0	0	0	0	0
Unused land	0.245	0.230	0.216	0.188	0.272	−0.029/-11.84%	0.056/25.93%	0.027/11.02%
Total	2152.637	2174.695	2156.159	2155.623	2167.762	3.522/0.16%	11.603/0.54%	15.125/0.700%

TABLE 9 Bivariate global Moran's I for the GPUA in 2000–2020.

Year	Moran's I	p	z
2000	−0.5317	<0.001	−99.99
2005	−0.5111	<0.001	−97.54
2010	−0.5467	<0.001	−102.24
2015	−0.5436	<0.001	−101.01
2020	−0.5248	<0.001	−00.04

4.4 Bivariate global autocorrelation

To examine the interaction between carbon emission intensity and ESV intensity, the spatial correlation pattern was identified by bivariate spatial autocorrelation. The Moran's I index was negative in all years with a *p*-value of less than 0.001 (shown in Table 9). This result indicates the existence of a negative spatial correlation between land-use carbon emission intensity and ESV intensity in the study area, i.e., the ESV intensity followed a decreasing trend with increasing land-use carbon emission intensity.

The bivariate local autocorrelation LISA agglomeration map shows that between 2000 and 2020, the high and high agglomerations are concentrated in the Yellow River and Weihe River basins; low and high agglomerations are mainly concentrated in the surrounding areas with higher slopes and topography, such as the Qinling Mountains in the south and the Loess Plateau area in the west. These areas have low land opening intensities, low carbon emission intensities, better ecological backgrounds, and higher values of ecosystem services available. These factors are consistent with the regional distribution pattern of low carbon

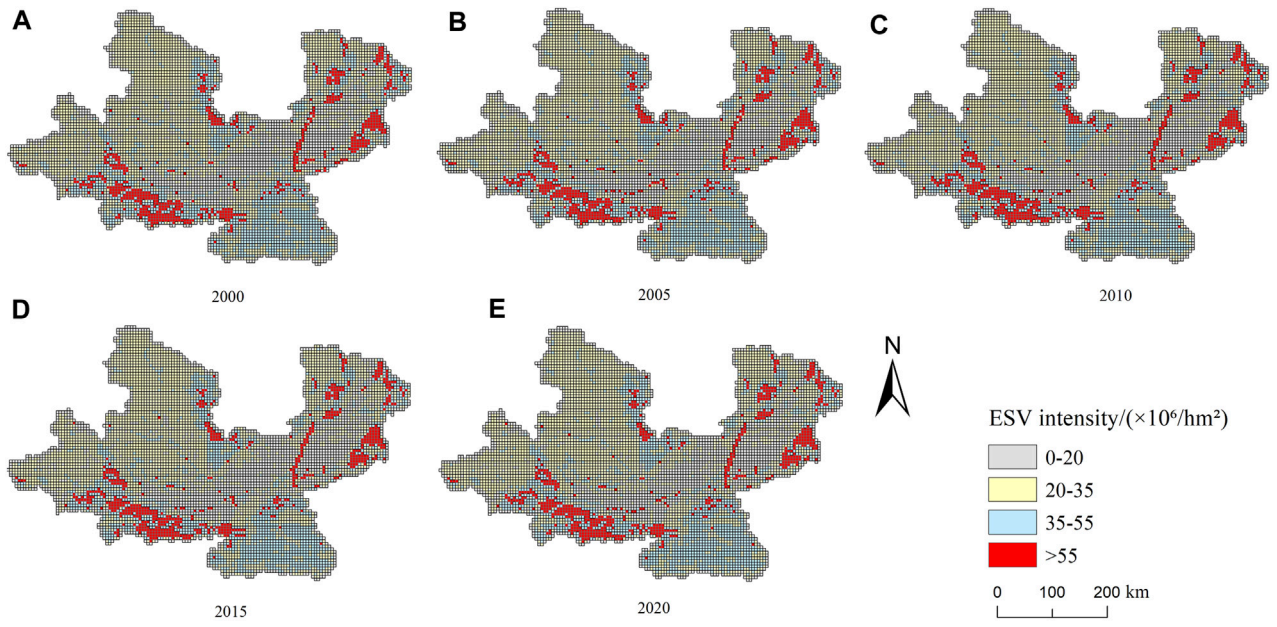

FIGURE 4
Ecosystem service value intensity of the GPUA. **(A)** 2000, **(B)** 2005, **(C)** 2010, **(D)** 2015, **(E)** 2020.

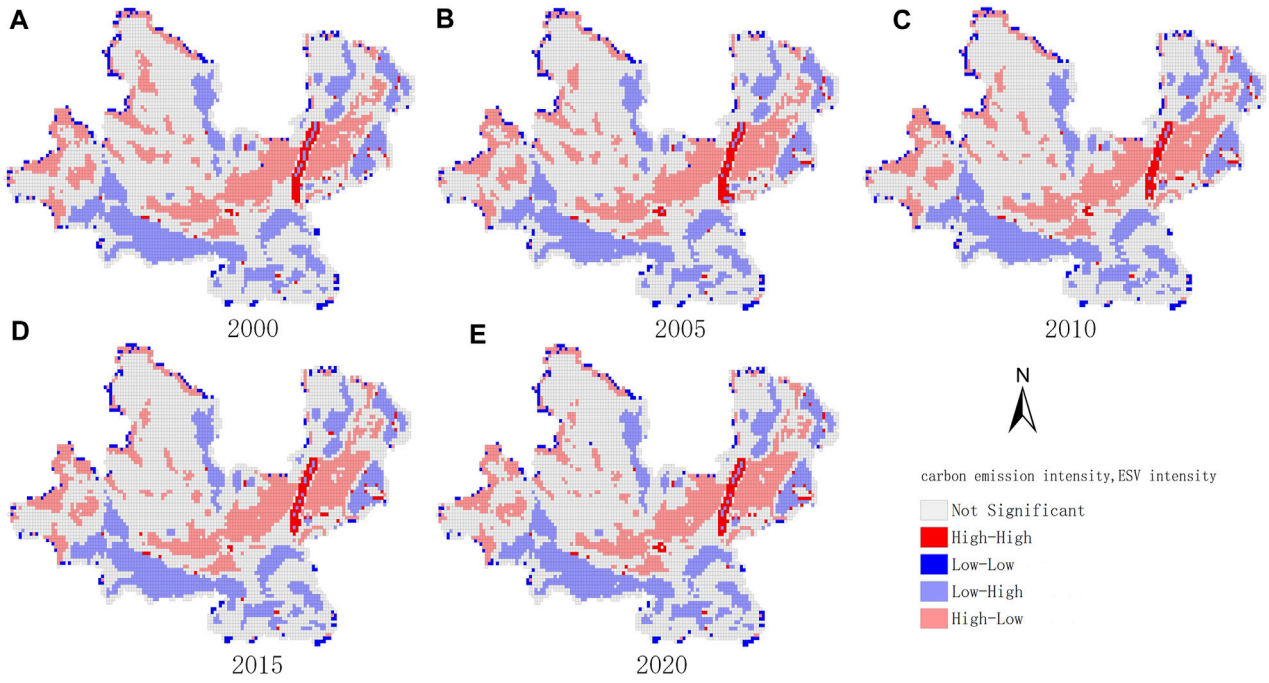

FIGURE 5
Bivariate spatial agglomeration diagram. **(A)** 2000, **(B)** 2005, **(C)** 2010, **(D)** 2015, **(E)** 2020.

emission intensity and high ESV intensity, and present roughly the same spatial distribution trend as woodland and grassland. Figure 5 shows that over the study period, the number of high and high aggregation areas in the Guanzhong Plain increased and the area expanded, while the area of high and low aggregation areas in the northwestern part of the study area decreased. This is probably the result of the increasing intensity of ecosystem service provisioning caused by the structural adjustment of land use functions and the gradual implementation of the policy of returning farmland to forests and grassland in loess hills and gullies. The construction land covers a small area, has a high carbon emission coefficient, and is a carbon source, resulting in high carbon emission intensity in local areas. The coefficient is much higher than that of the surrounding farmland, and thus, the grid area with a high proportion of cultivated land area together with the construction land forms a high–low agglomeration area. In the marginal areas of urban agglomeration zoning, low–low agglomeration areas show a scattered distribution.

5 Discussion

5.1 Distribution and causes of changes in carbon emissions and ESV based on changes in land use structure

Land use is the most direct expression of the interaction between human activities and natural ecosystems. The structure of land use is not only an important part of basic land use units, quantitative characteristics, and spatial layout, but also the core basis of regional ecosystem macro control. Land use change affects the carbon cycle process of terrestrial ecosystems by changing the original land cover type and the socio-economic activities it carries. With the acceleration of the urbanization rate of the GPUA, the development and utilization of land are gradually enhanced, and construction land is the most important application site for fossil fuels. The significant expansion of the areas of construction land causes a shrinkage of the carbon sink area and an expansion of the carbon source area, which directly or indirectly causes changes in carbon emissions and carbon sequestration and affects the supply capacity of ecosystem services. The total carbon emissions from land use in the study area increased significantly from 2000 to 2020, and the carbon emissions from construction land exceeded net carbon emissions. The main reason for this phenomenon is that the development of rapid urbanization has led to significant changes in land use structure. The GPUA, with Xi'an at the core, is rapidly promoting urban construction and social development, thus facilitating the process of industrial construction and service construction. The output value of secondary and tertiary industries accounts for about 90% of the regional GDP. The carbon sequestration capacities of woodland and grassland play an important role in ecological improvement and protection, and these land use types account for a large proportion of the land use area. The maximum carbon emission intensity within the study area decreased from 2000 to 2020, which is generally consistent with the findings of previous related studies (Cao et al., 2021; Zhang et al., 2022b; Wu et al., 2022; Zhao et al., 2023).

From 2000 to 2020, the total value of ESV shows a fluctuating growth trend of "rapid increase–rapid decrease–slow decrease–rapid increase", including two significant change periods from 2000 to

2010 and from 2015 to 2020. This differs from the results of previous research related to the Guanzhong Plain Urban Agglomeration (Yang et al., 2022b). The higher ESV values were distributed in the southern and western and northwestern edges of the study area, in the Qinba Mountains and along the Yellow River, enabled by the positive effect of forest cover and water conservation on ESV intensity. The rapid increase in the total ESV value in 2005 may have been due to the transfer of forest land area as the largest increase during the study period. The implementation of the project of returning farmland to forest and grassland and the erosion control project provide a good start for the restoration of ecosystem service functions. In 2018 China promulgated *The Guanzhong Plain Urban Agglomeration Development Plan*, which specifies ecological environmental protection as a task and prerequisite for the construction of city clusters. This provides policy support for the rapid growth of ecosystem service values and the implementation of ecological protection and restoration projects from 2015 to 2020 (Guo et al., 2022; Wang et al., 2022).

5.2 Carbon emission intensity and ESV intensity distribution and optimization strategies under the spatial agglomeration

The spatial agglomeration of carbon emission intensity and ESV intensity shows a significant negative correlation effect. On production land and living land such as arable land and construction land, the central region of the GPUA generates a large amount of greenhouse gas pollution and emissions due to carrying a large number of human production and living behaviors, and clustering the development and utilization of resources in agriculture, industry and services. Human behavior is also a consumption of ecosystem functions, so it makes the value provided by terrestrial ecosystems impaired, showing a spatial agglomeration distribution pattern of high carbon emission intensity–low ESV intensity. In the southwestern part of the GPUA, the southern hinterland, and part of the northeastern part of the GPUA, i.e., the area with a large distribution of ecological land such as forests and grasslands, a low carbon emission intensity-high ESV intensity distribution pattern is shown. This is in line with the functions of natural ecology such as woodland and grassland in performing soil and water conservation, climate regulation, or other functions. At the same time, a series of man-made ecological projects, such as the government's establishment of the Qinling Protected Area and the introduction of the *Outline of the Plan for the Ecological Protection and High-Quality Development of the Yellow River Basin*, have made an important contribution to the ecological environment of the region. How to reduce the total amount of carbon emissions from land use and carbon sources and improve the level of urban ESV is the breakthrough direction for the future green development of the city and the realization of long-term synergistic development of ecology and economy.

The above changes in land use structure and function yield corresponding changes in total carbon emissions and ESV, leading to ecosystem instability. However, it is worth noting that farmland has a weak ecological carrying capacity, and when making changes to utilization strategies, it is important to pay attention to regional food security and farmland red line restrictions, to not develop and transfer out uncontrollably. The GPUA should prioritize the ecological security pattern in the development process, and the governments of Gansu, Shaanxi, and Shanxi provinces should do a good job of coordinating the division of labor based on the consideration of ecological value coordinated with social and economic value. The three provinces should work together to protect the ecological barrier areas, ensure the smooth flow of ecological corridors, and consolidate the green foundation for the high-quality development of the urban agglomeration (Chen et al., 2022; Yang et al., 2022c). This study complements the relevant research results on carbon emissions and ESV under land use change, and using the GPUA as a case study, proposes strategies to promote integrated regional ecological-economic development, which helps to improve the practicality and completeness of the research results.

6 Conclusion

(1) During the period of 2000–2020, the following land use types accounted for the largest proportion of the GPUA: farmland accounted for about 39.9% of the total land use area; grassland accounted for about 33% of the total land use area; and woodland accounted for about 21.8% of the total land use area. Farmland was the main and largest transfer-out category; grassland and woodland were the main transfer-in categories; and construction land and water body had the largest annual average rate of change.

(2) From 2000 to 2020, the total ESV in the GPUA increased overall and showed corresponding fluctuations with the transformation of each category. The ESV intensity at the grid scale showed a distribution pattern of low in the central regions and high in the surrounding regions. The ESV intensity was significantly lower than in the surrounding areas with high altitude, slope, and abundant ecological and water resources.

(3) The net carbon emissions from land use showed growing carbon emissions year by year. The amount of carbon sources far exceeded the amount of carbon sinks, and the average carbon emission from construction land increased from 843.725 t/hm^2 in 2000 to 5153.703 t/hm^2 in 2020, which is an increase of about six times. Construction land is the largest carbon emission source, and there is great potential for carbon emission reduction from construction land. The overall carbon emission intensity distribution is high in the centra regions and low in the surrounding regions, and the trend is basically opposite to the ESV intensity distribution.

(4) Quantitative and spatial statistical analyses of carbon emission intensity and ESV intensity of land use in the GPUA showed a significant negative spatial agglomeration effect and a spatial spillover effect of carbon emission intensity on ESV intensity.

Compared with most previous studies, this study innovatively analyzed the total amount and temporal and spatial evolution of carbon emissions and ESV based on the functional transformation of land use structure. And the study also analyzed the spatial

agglomeration effect of carbon emission intensity and ESV intensity from the perspective of carbon emission intensity and ESV intensity, and explored whether carbon emission intensity affects the distribution of ESV intensity. In this study, administrative regions are crossed and a specific urban agglomeration is selected. This urban agglomeration features clear strategic positioning as an inland ecological civilization construction pioneer zone in the national plan. By using two calculation scales and methods, this study measures the carbon emissions, carbon emission intensity, and total ESV values and intensity in the study area more comprehensively. This study helps to enrich the existing research results on ecological and environmental quality in the GPUA, thus complementing the framework and perspectives of ESV and carbon emissions related studies. The purposes of this study were to examine the relationship between carbon emission intensity and ESV intensity and their spatial aggregation in the study area from 2000 to 2020, to provide a theoretical basis for the coordinated development of regional ecology and the economy, and to optimize the spatial layout of the national land. As with any research, this study is subject to limitations, which provide avenues for future research. Currently, only carbon emissions from construction land are considered when calculating land carbon emissions, while industrial production processes and waste carbon emissions are not considered. When determining carbon emission factors for different land types, a certain amount of error emerges when drawing on previous studies to obtain carbon emission factors for each examined category. ESV is measured using the unit area value equivalent factor method and grain prices and yields are applied for factor corrections. This approach can affect the accuracy of the ESV assessments because of different correction methods and the reliance of this method on the equivalent factor. Moreover, in the ESV calculation process, the value equivalent of construction land is set to 0, but with the increasing proportion of artificial green spaces and ecological landscape layout of construction land, whether this coefficient remains at 0 is worthy of further discussion and debate. Therefore, future research should explore the impact of these issues on ecosystems in a more focused manner to provide more detailed and scientific guidance for the governance of local ecological security.

Data availability statement

The original contributions presented in the study are included in the article/supplementary material, further inquiries can be directed to the corresponding author.

Author contributions

XZ: conceptualization, conceptualization, methodology, formal analysis, investigation, data curation, writing–original draft. SY: methodology, validation, supervision, writing–review and editing, funding acquisition. All authors contributed to the article and approved the submitted version.

Funding

This research was supported by the National Social Science Foundation of China's Western Region Project: Research on Accounting for the Value of Different Types of Ecological Products in Northwest China and Paths to Realization (23XTJ006).

Conflict of interest

The authors declare that the research was conducted in the absence of any commercial or financial relationships that could be construed as a potential conflict of interest.

Publisher's note

References

Cai, W., Jiang, W., Du, H., Chen, R., and Cai, Y. (2021). Assessing ecosystem services supply-demand (Mis)Matches for differential city management in the yangtze river delta urban agglomeration. *Int. J. Environ. Res. Public Health* 18, 8130. doi:10.3390/ijerph18158130

Cai, Z. C., Kang, G. D., Tsuruta, H., and Mosier, A. (2005). Estimate of CH4 emissions from year-round flooded rice fields during rice growing season in China. *Pedosphere* 15, 66–71. doi:10.1007/s10705-004-5083-1

Cao, Y., Kong, L., Zhang, L., and Ouyang, Z. (2021). The balance between economic development and ecosystem service value in the process of land urbanization: a case study of China's land urbanization from 2000 to 2015. *Land Use Policy* 108, 105536. doi:10.1016/j.landusepol.2021.105536

Chen, J., Wang, S. S., and Zou, Y. T. (2022). Construction of an ecological security pattern based on ecosystem sensitivity and the importance of ecological services: a case study of the Guanzhong Plain urban agglomeration, China. *Ecol. Indic.* 136, 108688. doi:10.1016/j.ecolind.2022.108688

Chen, X., Chen, Y., Shimizu, T., Niu, J., Nakagami, K. I., Qian, X., et al. (2017). Water resources management in the urban agglomeration of the Lake Biwa region, Japan: an ecosystem services-based sustainability assessment. *Sci. Total Environ.* 586, 174–187. doi:10.1016/j.scitotenv.2017.01.197

Costanza, R., D'Arge, R., De Groot, R., Farber, S., Grasso, M., Hannon, B., et al. (1997). The value of the world's ecosystem services and natural capital. *Nature* 387, 253–260. doi:10.1038/387253a0

Davidson, N. C., Van Dam, A. A., Finlayson, C. M., and Mcinnes, R. J. (2019). Worth of wetlands: revised global monetary values of coastal and inland wetland ecosystem services. *Mar. Freshw. Res.* 70, 1189–1194. doi:10.1071/mf18391

Duan, X., Wang, X., Lu, F., and Ouyang, Z. (2008). Current status and potential of carbon sequestration in wetland ecosystems in China. *J. Ecol.* 02, 463–469. doi:10.3321/j.issn:1000-0933.2008.02.002

Fang, J., Guo, Z., Pu, S., and Chen, A. (2007). Estimation of carbon sinks of terrestrial vegetation in China from 1981 to 2000. *China Sci. Ser. D Earth Sci.* 06, 804–812. doi:10.1360/zd2007-37-6-804

Forman, R. T. (2015). "Launching landscape ecology in America and learning from Europe," in *History of landscape ecology in the United States* (New York, NY: Springer).

Guo, X. M., Fang, C. L., Mu, X. F., and Chen, D. (2022). Coupling and coordination analysis of urbanization and ecosystem service value in Beijing-Tianjin-Hebei urban agglomeration. *Ecol. Indic.* 137, 108782. doi:10.1016/j.ecolind.2022.108782

Lai, L. (2010). *Carbon emission effects of land use in China*. Doctor. Nanjing: Nanjing University.

Larsen, F. W., LondoñO-Murcia, M. C., and Turner, W. R. (2011). Global priorities for conservation of threatened species, carbon storage, and freshwater services: scope for synergy? *Conserv. Lett.* 4, 355–363. doi:10.1111/j.1755-263x.2011.00183.x

Leemans, R., and De Groot, R. (2003). *Millennium Ecosystem Assessment: ecosystems and human well-being: a framework for assessment*. Washington: World Resources Institute.

Li, Y.-N., Cai, M., Wu, K., and Wei, J. (2019). Decoupling analysis of carbon emission from construction land in Shanghai. *J. Clean. Prod.* 210, 25–34. doi:10.1016/j.jclepro.2018.10.249

Li, Y., Luo, Y., Liu, G., Ouyang, Z., Zheng, H., Dai, F., et al. (2013). Impacts of land use change on ecosystem service functions: an example from Miyun Reservoir watershed. *J. Ecol.* 33 (03), 726–735. doi:10.1016/j.taap.2013.07.029

Liu, F., Qin, T., Liu, S., Wang, H., and Nie, H. (2023a). Spatial response of urban land use change and ecosystem service value in the lower reaches of the Yangtze River: a case study of Tongling, China. *Front. Environ. Sci.* 11, 535. doi:10.3389/fenvs.2023.1137442

Liu, L., Zheng, L., Wang, Y., Liu, C., Zhang, B., and Bi, Y. (2023b). Land use and ecosystem services evolution in danjiangkou reservoir area, China: implications for sustainable management of national projects. *Land* 12, 788. doi:10.3390/land12040788

Ouyang, X., Tang, L., Wei, X., and Li, Y. (2021). Spatial interaction between urbanization and ecosystem services in Chinese urban agglomerations. *Land Use Policy* 109, 105587. doi:10.1016/j.landusepol.2021.105587

Pan, Y., Dong, F., and Du, C. (2023). Is China approaching the inflection point of the ecological Kuznets curve? Analysis based on ecosystem service value at the county level. *J. Environ. Manag.* 326, 116629. doi:10.1016/j.jenvman.2022.116629

Scholte, S. S. K., Van Teeffelen, A. J. A., and Verburg, P. H. (2015). Integrating socio-cultural perspectives into ecosystem service valuation: a review of concepts and methods. *Ecol. Econ.* 114, 67–78. doi:10.1016/j.ecolecon.2015.03.007

Wang, D., Li, Y., Zheng, H., and Ouyang, Z. (2014). Surfactants present complex joint effects on the toxicities of metal oxide nanoparticles. *J. Ecol.* 34, 70–75. doi:10.1016/j.chemosphere.2014.03.010

Wang, K., Ouyang, X., He, Q. Y., and Zhu, X. (2022). Impact of urban land expansion efficiency on ecosystem services: a case study of the three major urban agglomerations along the yangtze river economic belt. *Land* 11, 1591. doi:10.3390/land11091591

Wu, H., Qiu, Y., Yin, L., Liu, S., Zhao, D., and Zhang, M. (2022). Effects of China's land-intensive use on carbon emission reduction: a new perspective of industrial structure upgrading. *Front. Environ. Sci.* 10, 2386. doi:10.3389/fenvs.2022.1073565

Xi, J. (2020). The general debate of the 75th session of the united Nations general assembly. *Bull. State Counc. People's Repub. China* 28, 5–7.

Xie, G., Lu, C., Leng, Y., Zheng, D., and Li, S. (2003). Valuation of ecological assets on the qinghai-tibet plateau. *J. Nat. Resour.* 02, 189–196. doi:10.11849/zrzyxb.2003.02.010

Xie, G., Zhang, C., Zhang, C., Xiao, Y., and Lu, C. (2015). The value of ecosystem services in China. *Resour. Sci.* 37 (09), 1740–1746.

Xue, X., Chen, Z. J., Wang, S. F., Feng, Z. Y., Duan, Y. C., and Zhou, Z. B. (2022). Value entropy: a systematic evaluation model of service ecosystem evolution. *Ieee Trans. Serv. Comput.* 15, 1760–1773. doi:10.1109/tsc.2020.3016660

Yang, J. X., Ma, X., Zhao, X. Y., and Li, W. Q. (2022a). Spatiotemporal of the coupling relationship between ecosystem services and human well-being in Guanzhong Plain Urban agglomeration. *Int. J. Environ. Res. Public Health* 19, 12535. doi:10.3390/ijerph191912535

Yang, J., Zhang, M., Duo, L., Xiao, S., and Zhao, Y. (2022c). Spatial pattern of land use carbon emissions and carbon balance zoning in Jiangxi Province. *Environ. Sci. Res.* 35, 2312–2321. doi:10.13198/j.issn.1001-6929.2022.05.04

Yang, S., and Su, H. (2022). Multi-scenario simulation of ecosystem service values in the Guanzhong Plain Urban agglomeration, China. *Sustainability* 14, 8812. doi:10.3390/su14148812

Yang, Y., Zhang, Y. Y., Yang, H., and Yang, F. Y. (2022b). Horizontal ecological compensation as a tool for sustainable development of urban agglomerations: exploration of the realization mechanism of Guanzhong Plain urban agglomeration in China. *Environ. Sci. Policy* 137, 301–313. doi:10.1016/j.envsci.2022.09.004

Ye, H., Song, Y. Y., and Xue, D. Q. (2022). Multi-scenario simulation of land use and habitat quality in the Guanzhong Plain Urban agglomeration, China. *Int. J. Environ. Res. Public Health* 19, 8703. doi:10.3390/ijerph19148703

Zhang, C. Y., Zhao, L., Zhang, H. T., Chen, M. N., Fang, R. Y., Yao, Y., et al. (2022b). Spatial-temporal characteristics of carbon emissions from land use change in Yellow River Delta region, China. *Ecol. Indic.* 136, 108623. doi:10.1016/j.ecolind.2022.108623

Zhang, L., Fang, C., Zhu, C., and Gao, Q. (2022a). Ecosystem service trade-offs and identification of eco-optimal regions in urban agglomerations in arid regions of China. *J. Clean. Prod.* 373, 133823. doi:10.1016/j.jclepro.2022.133823

Zhao, C., Liu, Y., and Yan, Z. (2023). Effects of land-use change on carbon emission and its driving factors in Shaanxi Province from 2000 to 2020. *Environ. Sci. Pollut. Res.* 30, 68313–68326. doi:10.1007/s11356-023-27110-1

Zhao, J., Chen, Y., Ji, G., and Wang, Z. (2018). Residential carbon dioxide emissions at the urban scale for county-level cities in China: a comparative study of nighttime light data. *J. Clean. Prod.* 180, 198–209. doi:10.1016/j.jclepro.2018.01.131

frontiers | Frontiers in Environmental Science

TYPE Original Research
PUBLISHED 30 October 2023
DOI 10.3389/fenvs.2023.1294180

OPEN ACCESS

EDITED BY
Hua Lu,
Jiangxi University of Finance and Economics, China

REVIEWED BY
Jian Hou,
Henan Agricultural University, China
Long Cheng,
Shandong University, China
Xiaoya Zhu,
Soochow University, China

*CORRESPONDENCE
Lei Xu,
xulei09@163.com
Shi Yin,
shyshi0314@163.com

RECEIVED 15 September 2023
ACCEPTED 06 October 2023
PUBLISHED 30 October 2023

CITATION
Ma L, Guo F, Hu H, Guo Y, Xu L and Yin S (2023), Analysis of temporal and spatial evolution characteristics and influencing factors of land use transformation in Hebei Province from the perspective of supply and demand.
Front. Environ. Sci. 11:1294180.
doi: 10.3389/fenvs.2023.1294180

Analysis of temporal and spatial evolution characteristics and influencing factors of land use transformation in Hebei Province from the perspective of supply and demand

Lijun Ma[1], Fengyu Guo[2], Hao Hu[1], Yu Guo[1], Lei Xu[1]* and Shi Yin [3]*

[1]College of Land and Resources, Hebei Agricultural University, Baoding, China, [2]College of Urban and Rural Construction, Hebei Agricultural University, Baoding, China, [3]College of Economics and Management, Hebei Agricultural University, Baoding, China

This study focuses on the counties and districts of Hebei Province as the research unit. It adopts a supply-demand perspective to analyze the spatial-temporal evolution characteristics of farmland utilization transformation in the province, investigate the coordination of this transformation, and explore the influencing factors. The weight of indicators is calculated using the entropy weighting method and Analytic Hierarchy Process The comprehensive evaluation model is then applied to calculate the supply-demand transformation index of farmland utilization in Hebei Province for the years 2005, 2010, 2015, and 2020. Furthermore, the spatial-temporal evolution characteristics are analyzed using the kernel density estimation method. The coupling coordination degree model is selected to explain the relationship between the supply-demand transformation of farmland utilization. Finally, the influencing factors are analyzed using the geographical detector model. The research findings are as follows: 1) The supply-demand transformation index of farmland utilization in Hebei Province has shown an increasing trend during the study period. The standard deviation of the supply transformation index has increased over time, while the demand transformation index has increased at a faster rate. High-density supply transformation is concentrated in the southeast, particularly in the eastern part of Shijiazhuang. Conversely, the northwest exhibits a low-density supply transformation. High-density demand transformation is observed in urban areas across the province, with a significant expansion from 2010 to 2015. 2) There is a strong correlation between the supply and demand transformation of farmland utilization. The coupling coordination degree has gradually improved from 2005 to 2015, transitioning from rapid to stable growth. The level of coupling coordination has shifted from imbalance to coordination. The mountainous areas in the northwest of Hebei Province exhibit relatively lower coupling coordination degrees, while the plains in the southeast demonstrate higher levels. 3) The supply transformation of farmland utilization is closely correlated with the natural environment, particularly elevation and topography. On the other hand, the demand transformation is closely associated with socio-economic development, with a scarcity of supply driving an increase in the demand transformation index. Industrial developed areas show a higher intensity of

demand for farmland utilization. 4) To ensure the sustainable utilization of farmland while meeting food production needs, it is crucial to enhance contiguous farmland and mechanization levels, promote the integration of agriculture and tourism, establish an ecological barrier around Beijing-Tianjin, and optimize the ecological compensation mechanism for farmland. The above findings provide valuable insights into farmland utilization transformation and suggest important strategies for its sustainable development.

KEYWORDS

transformation of land use, supply and demand, spatiotemporal evolution, influencing factors, Hebei Province

1 Introduction

The study on the transformation of land use is derived from the analysis of the spatiotemporal evolution of forest land by Mather and Grainger. Both cultivated land and forest land belong to the land system, and the transformation between cultivated land and forest land is an important component of land use transformation (Grainger, 1995; Lu et al., 2020; Ma et al., 2022). The transformation of cultivated land use is based on the transformation of land use, and it is a change in the way of cultivated land use driven by multiple factors such as natural conditions, economic level, and regional development policies. Long and Li pointed out that the transformation of land use corresponds to the stage of social development, and cultivated land is the core element of rural transformation and development (Li, 2002; Long et al., 2019). The research system of the transformation of cultivated land use includes the explicit changes in the quantity of cultivated land, the implicit changes in the nature of cultivated land, the changes in the structure of cultivated land, and the transformation of the functions of cultivated land. The comprehensive changes in multiple factors cause the transformation of the cultivated land system (Long and Li, 2006; Song et al., 2014). Extensive research has been conducted at home and abroad on the transformation of cultivated land use, involving various fields such as economy, society, and management in terms of research content, methods, and scales. Under the background of information utilization of cultivated land, the coordinated development of agricultural production and ecological security is the future development trend. Conducting research on the influencing factors of the transformation of cultivated land use helps to explore the minimal limiting factors and enhance the supply capacity of cultivated land.

The transformation of cultivated land use involves multiple aspects such as agricultural production, economic development, food security, and ecosystems. Research on the transformation of cultivated land use continues to deepen in areas such as agricultural development, rural construction, and farmers' income growth. Lv et al. analyzed the characteristics of farmland utilization transformation from both spatial and functional perspectives (Lv et al., 2022). Improving the quality of arable land through measures such as fallow cultivation is an international trend. Kong pointed out that the goal of arable land use protection transformation is the security of arable land resources, and explored the policy system for arable land protection transformation (Kong et al., 2021). It is crucial to protect the quantity, quality, and ecology of cultivated land in the process of transformation of cultivated land utilization. Kuang et al. analyzed the correlation between green transformation of cultivated land and socio-economic development based on changes in cultivated land structure (Kuang et al., 2021). The research content on the coupling and coordination relationship of farmland use transformation is mostly combined with rural development, covering the correlation between farmland use transformation and food production (Sun, 2018), the marginal effects of rural economic development and farmland use transformation (Lu et al., 2019), and the multi-functional coupling and coordination scheduling of farmland (Du et al., 2021). The research on the spatiotemporal evolution of cultivated land use transformation is mostly based on the temporal changes in dimensions, which can be divided into continuous time changes and phased time changes from a time scale. Continuous changes can be used for mutation point detection, and phased changes have stronger operability, making comparative analysis more significant (Jiang et al., 2022).

The research on the driving factors of farmland utilization transformation mainly includes two aspects: firstly, the selection of relevant influencing factors' indicators, and secondly, the comprehensive impact of macro policies and micro effects. The classification system for the influencing factors of cultivated land use is extensive, which can be divided into the conditions of cultivated land itself, farmers' cultivated land methods, and agricultural policy guidance based on the main body. Overall, natural conditions are the core elements that affect the transformation of cultivated land use. Li divided the influencing factors of cultivated land use transformation into two categories: formation driving and development driving, with natural factors leading the formation driving force and social and economic factors leading the development driving force (Li, 2017). Yang et al. pointed out that natural factors are the core influencing factors of farmland utilization transformation, such as altitude, precipitation, and geological disasters (Yang et al., 2018). Under similar natural conditions, the transformation of cultivated land use is greatly influenced by planting conditions, labor force changes, and farmers' behavior. Zhang et al. pointed out that changes in urbanization rate lead to changes in farmers' income and expenditure structure, labor force changes affect the value of cultivated land, and changes in input factors and planting structure affect the function of cultivated land (Zhang et al., 2021). Tang et al. analyzed the driving mechanism of transformation between highway infrastructure and farmland utilization, and found that the occupation of farmland by infrastructure construction leads to a decrease in the number of farmland. The construction project has

the function of attracting employment and increasing the income of surrounding residents (Tang et al., 2021).

The research methods for farmland utilization transformation can be divided into qualitative and quantitative analysis. Quantitative analysis methods often use evaluation methods to describe the process of farmland utilization transformation, and construct evaluation models for comprehensive analysis from aspects such as changes in farmland area, farmland products, and farmland input. Based on relevant indicators of farmland, farmland utilization changes are reflected (Niu et al., 2020). The evaluation method has strong operability and is easy to compare and analyze the correlation between explicit transformation, implicit transformation, green transformation, and efficiency transformation of cultivated land. There is a strong correlation between the transformation of farmland use and farmland use policies. Changes in land, labor force, and means of production during the process of socio-economic development cause changes in farmers' behavior. Scholars such as Song, based on the theory of induced production substitution, quantitatively analyze structural changes in farmland planting, labor force, and investment at the provincial level, and analyze the laws of farmland use transformation in conjunction with the stages of socio-economic development (Song and Li, 2019). The transformation of cultivated land utilization has strong regional characteristics, and there are convergence and spillover effects in the regional cultivated land planting structure. The analysis of influencing factors should fully consider geographical spatial characteristics (Lu et al., 2021; Song and Xin, 2021). The qualitative analysis method is often based on policy guidance, and constructs a theoretical framework for the transformation of farmland utilization systems from multiple perspectives such as farmland development and consolidation, changes in planting behavior, changes in farmland production and management, and modern agricultural development (Du et al., 2022).

Taking administrative divisions as the basic research unit has the advantages of strong operability and heterogeneity, and the research scale should be matched with the research content. For example, research on the transformation of cultivated land use such as paddy fields and drylands is mostly conducted at the national or provincial level (Xie et al., 2022). There are many studies focusing on the watershed as the research area to analyze the influencing factors of farmland use transformation: Chen takes the Sichuan Basin as the research area to analyze the relationship between farmland function transformation and economic and social development (Chen, 2022). An et al. used Dongting Lake County as the research area to analyze the characteristics and influencing factors of multifunctional transformation of arable land (An et al., 2022). Gai used the Songhua River Basin as the research area to calculate the carbon emissions during the transformation process of arable land use (Gai et al., 2022). The transformation of cultivated land use is the result of the joint action of cities and rural areas. Conducting research on the transformation of cultivated land use in urban agglomerations can contribute to the development of urban-rural integration. Fu et al. used the Beijing Tianjin Hebei urban agglomeration as a research unit to explore the explicit and implicit changes in cultivated land use (Fu et al., 2020). Jin et al. analyzed the characteristics and influencing factors of farmland utilization transformation in the Pearl River Delta urban agglomeration from the perspectives of structure, function, and efficiency (Jin and Wang, 2022).

The connotation of cultivated land utilization supply originates from land supply, which can be divided into two categories: natural supply and economic supply. Economic supply refers to the benefits obtained by relying on natural supply, and the natural supply of cultivated land can be increased through land remediation and other methods. The economic supply of cultivated land emphasizes the efficiency of cultivated land utilization, with human beings as the main body and serving people. The connotation of the demand for arable land utilization is the direct or indirect demand for arable land resources for socio-economic development, and the demand for arable land products is higher in areas with high population density. The demand for social development of arable land is reflected in both social stability and agricultural population security. Regions with large urban-rural income disparities have low stability. The ecological needs of cultivated land include the need to improve the living environment and the need for aesthetic appreciation (He, 2019; Zhou et al., 2020). The connotation of supply and demand for arable land use is the organic unity of the arable land use system. Based on the changes in the connotation of supply and demand for arable land use, research points out the connotation of the supply and demand transformation of arable land use: the supply and demand transformation of arable land use is a change in the natural attributes of arable land to provide services. The transformation of demand for arable land utilization is a phased change in arable land required for human activities. The research on the supply and demand transformation of arable land utilization aims to enhance the supply capacity of arable land, which is a new way to achieve sustainable development of arable land, promote stable economic and social operation, and guide macroeconomic policy regulation.

In summary, research on the transformation of arable land use is rich in content. Most studies explore the path of arable land use transformation by combining regional natural environment and development trends. The transformation of arable land use based on the perspectives of arable land protection and green utilization is gradually improving, and there are few studies on arable land use transformation from the perspective of supply and demand. The research methods for the transformation of cultivated land use are rich, and quantitative analysis methods are often used to construct models for calculating the transformation of cultivated land use. The theory of induced production substitution can reflect the relationship between structure and function. The material quality method intuitively reflects changes in input and output of cultivated land. The comprehensive evaluation method has strong operability and is helpful in analyzing the coupling and coordination characteristics of the arable land subsystem. The process of arable land utilization is a coupling development of multiple systems such as nature, society, economy, and ecology, with strong correlation between subsystems. The research on the coupling coordination relationship of arable land utilization transformation focuses on the coupling between the functions of arable land systems, the coupling of arable land structure transformation, arable land spatial transformation, and arable land function transformation, as well as the coupling of external quantitative characteristics and internal influencing factors of arable

land, lacking provincial and regional coordination Coupling analysis of supply and demand for arable land use at different scales such as city and county levels. The influencing factors of farmland utilization transformation are mostly selected from natural and human activities, and there is a decay effect overall. With the improvement of agricultural technology, the influence of natural factors gradually decreases, while the influence of economic and social factors increases rapidly. There is a lack of research on influencing factors from the perspective of supply and demand.

In the current context of promoting integrated urban-rural development and modernizing agriculture and rural areas, a crucial issue we face is finding new driving forces for land use transformation. It is imperative to facilitate the orderly development of land use transformation and promote rational development and utilization of land resources. Taking a supply and demand perspective, it is essential to establish an evaluation index system for land use transformation, employ a kernel density estimation model to analyze the spatio-temporal evolution characteristics of land use supply and demand transformation, utilize a coupling coordination model to examine the correlation of land use supply and demand transformation, and investigate the influencing factors by selecting natural environment and socio-economic indicators. These approaches will provide new research ideas for measuring the levels of land use supply and demand transformation. This study expands the analysis of land use transformation from the supply and demand perspective, establishes an analytical framework for studying the influencing factors of land use transformation, and conducts a comprehensive examination of the transformation of land use in Hebei Province. This research contributes to exploring the changes and influencing factors of land use transformation in Hebei Province, identifying areas with production and ecological advantages, alleviating population, food, and environmental pressures in the region, ensuring the sustainable utilization of land resources, promoting the adjustment of the agricultural industrial structure, facilitating the development and protection of regional land resources, providing a scientific basis for agricultural production, and offering insights for the rational utilization and formulation of land protection policies. Overall, this study provides valuable insights and guidance for promoting sustainable land use and achieving balanced regional development in Hebei Province.

2 Research area and data source

2.1 Research area

Hebei Province is located between longitude 113°27′ to 119°50′ east and latitude 36°05′ to 42°40’ north. The terrain in the southeast and northwest is significantly different, and the east is connected to the Bohai Sea. To the west is the Taihang Mountains, mostly mountainous areas with large elevation differences. The southern region is a plain area with low terrain undulation. To the north, there are the Bashang Plateau and the Yanshan Mountains, with a wide plateau adjacent to the mountains. Hebei Province has a temperate continental monsoon climate with good light and heat conditions, suitable for crop growth. Winter is cold and dry, and rainfall is mostly concentrated in summer, resulting in less total water resources. Hebei Province includes 11 prefecture level cities, with 167 districts and counties under its jurisdiction. There are a large number of districts and counties, with a smaller area in the southeast and sparsely populated areas in the northwest. Hebei Province has a high population density and a large agricultural population, with a rural population of 28.45 million by the end of 2022. Hebei Province is a major grain producing province in China, and the southeastern plain is an important grain producing area. In 2022, the total grain output was 38.6506 million tons, and the total power of agricultural machinery increased by 1.88% year-on-year. There are significant differences in arable land resources among cities, with dry land being the main cultivated land.

2.2 Data sources

The 30 m resolution land use status data of Hebei Province in 2005, 2010, 2015, and 2020, based on Landsat TM and Landsat 8 remote sensing data interpretation. DEM digital elevation data is sourced from the geospatial data cloud platform (http://www.gscloud.cn). Vegetation coverage data is sourced from the Land Product Processing and Distribution Data Center (https://lpdaac.usgs.gov). County population, effective irrigation area, grain sowing area, total grain output, *per capita* net income of rural residents, total retail sales of consumer goods, total industrial output value, and *per capita* vegetable consumption in urban and rural areas are all sourced from the 2006 to 2021 “Hebei Rural Statistical Yearbook”, “Hebei Economic Yearbook”, “China County Statistical Yearbook”, and “China Statistical Yearbook”. The socio-economic data of some municipal districts are obtained through statistical yearbooks and statistical bulletins of each city.

3 Research methods

3.1 Calculation of the supply and demand transformation index of cultivated land use in Hebei Province

3.1.1 Evaluation index system for the transformation of cultivated land use and supply

The utilization supply of cultivated land refers to the ability of cultivated land to provide services and support. With reference to relevant literature, the transformation level of cultivated land utilization supply can be reflected from four aspects: the supply of cultivated land quantity, the supply of cultivated land production, the supply of social security, and the supply of cultivated land ecology. Based on this, 11 indicators are selected for quantitative analysis, using counties and districts in Hebei Province as the research units to construct an evaluation index system for the transformation of cultivated land utilization supply (He, 2019). The ratio of sloping cultivated land refers to the ratio of the area of cultivated land with a slope greater than 15 degrees to the total area of cultivated land. The higher the ratio of sloping cultivated land, the greater the difficulty in farming. The land development rate refers to the ratio of the total area of cultivated land to the total area of land. The chemical load of cultivated land refers to the ratio of fertilizer application amount to the area of cultivated land. Taking into account the regional characteristics of cultivated land utilization, the carbon sequestration of cultivated land is calculated based on the yield of six crops, including wheat, corn,

TABLE 1 Evaluation index system of cultivated land use supply transformation.

Factor layer	Indicator layer	Entropy weight method weight	Analytic hierarchy process weights	Comprehensive weight	Unite
Supply of cultivated land quantity	Land reclamation rate	0.061	0.059	0.060	—
	Proportion of sloping farmland	0.027	0.073	0.050	—
	Irrigated Area	0.113	0.114	0.114	hm^2
Farmland production supply	the acreage sown in grain crops	0.103	0.081	0.092	hm^2
	total grain output	0.135	0.091	0.113	kg
	Crop planting area	0.100	0.095	0.097	hm^2
Social security supply	Gross Agricultural Product	0.180	0.208	0.194	Ten thousand yuan.
	Agricultural, forestry, animal husbandry, and fishery practitioners	0.094	0.139	0.116	Person
Ecological supply of cultivated land	Carbon sequestration in arable land	0.159	0.034	0.096	kg
	Chemical load on cultivated land	0.020	0.042	0.031	kg/hm^2
	Pesticide application rate	0.008	0.065	0.037	kg

soybeans, oil crops, cotton, and vegetables. Detailed calculation formulas can be found in relevant literature (Gu and Zha, 2012; Chen et al., 2016). The remaining indicators are directly obtained through statistical yearbooks. The evaluation index system for the transformation of arable land use supply is shown in Table 1.

3.1.2 Index system for evaluating the transformation of cultivated land use demand

The transformation of land utilization demand is the change in land resources required by human social activities. The consumption of agricultural products directly reflects the demand for arable land, while the changes in arable land caused by human activities indirectly reflect the demand for arable land. By referring to relevant literature and focusing on factors such as farmers, population, social development, and policies, 11 indicators were selected from five aspects: grain consumption demand, rural development demand, national economic demand, social construction demand, and ecological civilization demand, to construct an evaluation index system for the transformation of land utilization demand in counties and districts in Hebei Province. The grain demand is estimated by multiplying the total population of the county by the *per capita* grain consumption. The vegetable consumption is calculated by multiplying the population by the *per capita* vegetable consumption, separately for urban and rural areas, and then summing them up. The population density is the ratio of the total population of the research unit to its administrative area. The *per capita* net income of rural residents, total agricultural machinery power, balance of urban and rural savings deposits, and total retail sales of consumer goods are obtained directly from statistical yearbooks. The proportion of construction land area is the ratio of the area used for construction to the total land area. The proportion of arable land to ecological land is the ratio of the arable land area to the ecological land area. The higher the proportion, the stronger the regional demand for arable land landscape ecology. Ecological land includes farmland, gardens, forests, and water areas. Please see Table 2 for the evaluation index system of land utilization demand transformation.

3.1.3 Calculation of the supply and demand transformation index for cultivated land use

Referring to existing research, entropy method and Analytic Hierarchy Process are selected from both subjective and objective aspects to comprehensively determine the weights. Adopting range standardization method for dimensionless processing. In the evaluation index system for the transformation of arable land use and supply, the proportion of sloping arable land, pesticide application amount, and arable land chemical load are negative indicators, while the rest are positive indicators. The evaluation index system for the transformation of cultivated land use demand is all positive indicators. Use the comprehensive index method to calculate the transformation index of arable land use supply and demand, respectively (Wei et al., 2022).

$$W1 = \mu W2 + (1 - \mu)W3 \quad (1)$$

$$F = \sum_{i=1}^{n} KiWi \quad (2)$$

In the formula, W_1 is the comprehensive weight, W_2 is the entropy method weight, W_3 is the weight of the Analytic Hierarchy Process, μ takes a value of 0.50, n is the number of evaluation units, K_i is the standardized value, F is the comprehensive score.

3.2 Kernel density estimation model

The utilization of arable land exhibits spillover effects in terms of supply and demand, and to investigate the correlation between different counties, the kernel density estimation method is applied to analyze the spatial evolution characteristics of arable land utilization transformation (Yin and Kang, 2022). The kernel density estimation method simulates probability distribution zones in space and uses the spatial analysis function of ArcGIS software to describe the kernel density changes in the transformation of arable land use supply and demand. The formula is as follows:

TABLE 2 Evaluation index system of cultivated land use demand transformation.

Factor layer	Indicator layer	Entropy weight method weight	Analytic hierarchy process weights	Comprehensive weight	Unite
Food consumption demand	Grain demand	0.044	0.051	0.048	kg
	Vegetable consumption	0.046	0.049	0.048	kg
	population density	0.119	0.053	0.086	Person/hm^2
Rural development needs	Per capita net income of rural residents	0.078	0.105	0.092	Ten thousand yuan.
	Total power of agricultural machinery	0.068	0.110	0.089	KW
National economic needs	Balance of urban and rural savings deposits	0.172	0.107	0.140	Ten thousand yuan.
	Total retail sales of social consumer goods	0.165	0.095	0.130	Ten thousand yuan.
Social construction needs	Proportion of construction land area	0.056	0.107	0.082	—
	Rural residential area	0.040	0.107	0.074	hm^2
Ecological civilization demand	rural power consumption	0.182	0.140	0.161	Millions of kilowatt-hours
	Proportion of arable land to ecological land	0.029	0.075	0.052	—

$$k(x) = \frac{1}{nh}\sum_{i=1}^{n} k\left(\frac{x - xi}{h}\right) \tag{3}$$

In the formula, k(x) is the kernel density function, n is the number of evaluation units, h is the search radius, x_i is the transformation index of arable land use supply and demand, which determines the sample point location based on the centroid of the evaluation unit.

3.3 Coupling coordination model

In order to analyze the correlation between supply and demand of cultivated land use, the study is based on the transformation index of supply and demand of cultivated land use. The coupling coordination degree model is used to analyze the development coordination level of the supply and demand system of cultivated land use, and the calculation results are charted and expressed using ArcGIS software (Zhang Y. et al., 2023). The coupling coordination degree reflects the strength of the coupling relationship, and the formula is as follows:

$$C = \sqrt{\frac{F1 \times F2}{\left[(F1 + F2)/2\right]^2}} \tag{4}$$

$$T = \alpha \times F1 + \beta \times F2 \tag{5}$$

$$D = \sqrt{C \times T} \tag{6}$$

In the equation, C is the coupling degree, and the result interval is 0–1, F_1 is the transformation index of farmland utilization supply, F_2 is the transformation index of arable land use demand, T is the weighted sum of the supply and demand transformation index for arable land use, α and β is the undetermined coefficient, with a value of 0.50, D refers to coupled co scheduling.

3.4 Geographic detectors

The factors affecting the transformation of land utilization supply and demand include natural environment and socio-economic factors. A study based on the Geographical Detector Model examines six indicators selected from both the natural environment and socio-economic perspectives, analyzing the degree of influence of these factors on the transformation of land utilization supply and demand (Wang and Xu, 2017; Guo et al., 2023). The formula is as follows:

$$q = 1 - \frac{1}{N\sigma^2}\sum_{h=1}^{L} N_h \sigma_h^2 \tag{7}$$

In the equation, q represents the explanatory power of the factors influencing the transformation of supply and demand in cultivated land use, which is positively correlated with the degree of impact, h is the number of layers, Nh refers to the number of units within a layer, N is the total number of units, σ_h^2 refers to the variance of layer h, σ^2 refers to the variance of the entire region.

4 Results and analysis

4.1 Characteristics of the spatiotemporal pattern of farmland utilization transformation in Hebei Province

The research analyzes the spatiotemporal evolution pattern of cultivated land utilization transformation in Hebei Province using a 5-year time frame. The ArcGIS software is employed to visualize the transformation scores of cultivated land utilization supply and

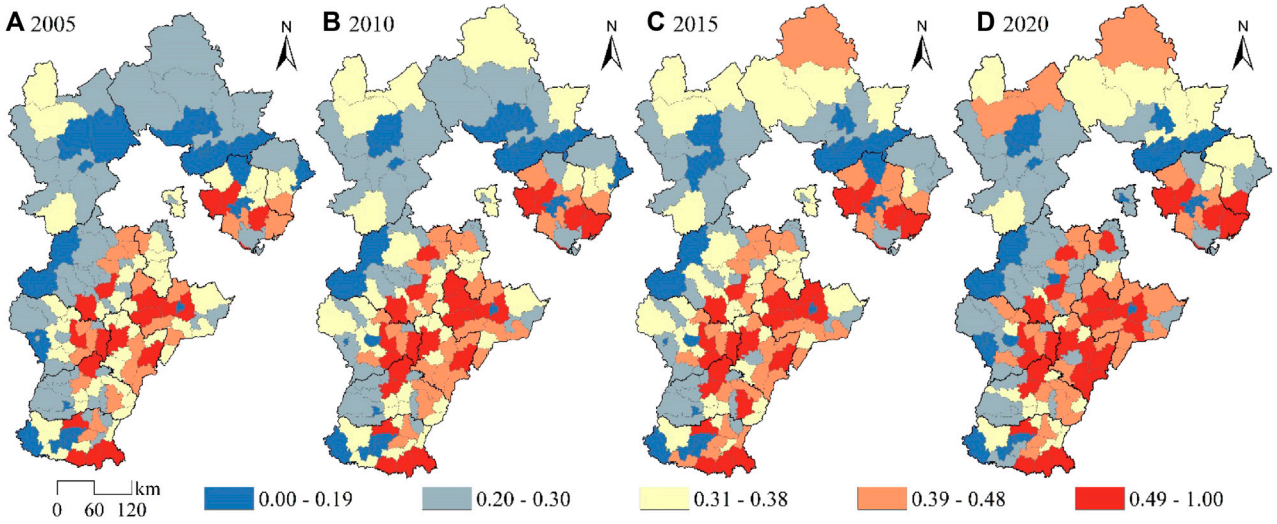

FIGURE 1
Spatio-temporal evolution pattern of cultivated land use supply transformation index.

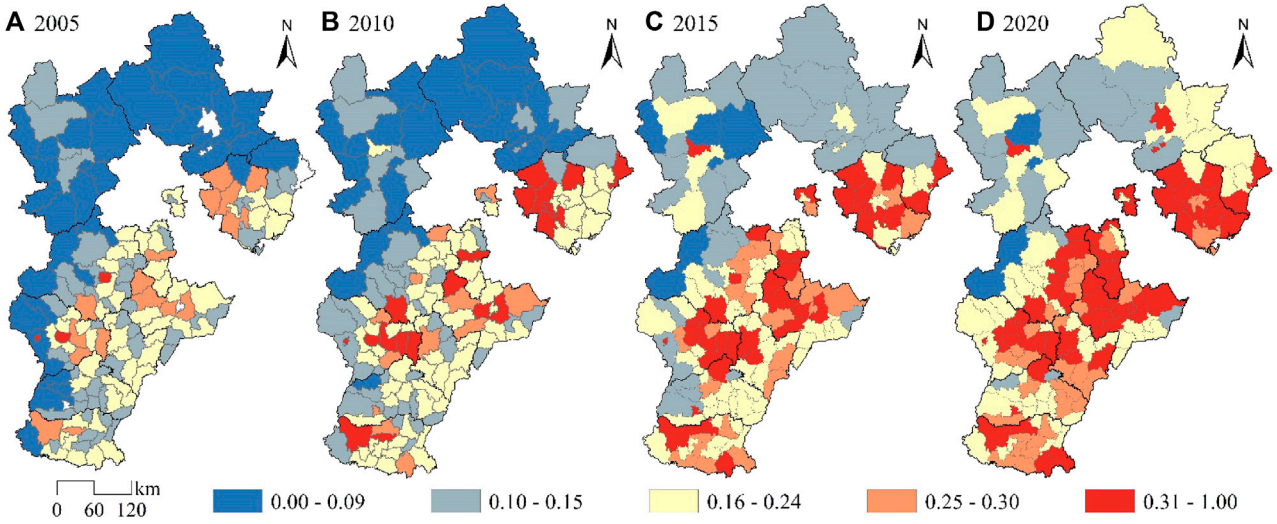

FIGURE 2
Spatio-temporal evolution pattern of cultivated land use demand transformation index.

demand. The transformation index of cultivated land utilization supply and demand is divided into five levels based on the index magnitude. The spatiotemporal pattern characteristics of cultivated land utilization supply and demand transformation are analyzed using time series analysis. The results of the classification can be seen in Figure 1 and Figure 2.

4.1.1 Temporal evolution characteristics of farmland utilization and supply transformation

During the research period, the transformation index of land utilization supply and demand in Hebei Province showed an upward trend. The greatest increase in the transformation index occurred between 2005 and 2010. Moreover, the standard deviation of the transformation index of land utilization supply and demand has been increasing year by year, indicating that the differences in land supply capacity among various districts and counties have been continuously expanding.

(1) The index of transformation in the utilization of cultivated land supply showed a growing trend from 2005 to 2010. The transformation index of cultivated land utilization and supply in Luanzhou, Leting, and Zunhua of Tangshan City increased rapidly. With the gradual improvement of cultivated land production conditions, the total agricultural production value and total grain yield increased. The region is relatively close to Beijing and Tianjin, with well-developed transportation

conditions, which is conducive to the production, circulation, and sales of cultivated land crops. The junction of Hengshui City, Xingtai City, and Shijiazhuang City is a high-value area for the transformation index of cultivated land use and supply. The supply capacity of cultivated land in areas such as Jizhou and Fucheng in Hengshui City has improved rapidly. This area is located in the Hebei Plain area, with good water and thermal conditions for cultivation. The transformation index of cultivated land use and supply in areas adjacent to Hengshui City, such as Wuqiao and Nangong, has increased significantly.

(2) From 2010 to 2015, the transformation index of cultivated land utilization and supply in Chengde City grew at the fastest rate, with a significant increase in the supply capacity of cultivated land in areas such as Weichang, Fengning, Longhua, and Pingquan. The region is short of water resources, with little change in effective irrigation area, and a significant increase in the ecological supply capacity of cultivated land. The agglomeration degree of the transformation index of farmland utilization and supply in the western districts and counties of Handan City has increased, and the pattern of east-west differentiation is significant. From the perspective of the quantity supply of farmland, the proportion of slope farmland in the eastern mountainous areas far exceeds that in the western plains. There are many saline alkali lands in coastal areas such as Huanghua in the eastern part of Cangzhou City, making development difficult. The main crops such as corn in Hejian, Xianxian, and Cangxian in the eastern part have high yields, and the transformation of arable land utilization and supply refers to long-term high levels.

(3) The growth rate of the transformation index of arable land utilization and supply from 2015 to 2020 has slowed down, and the agglomeration of arable land supply capacity in the southeastern part of Hebei Province is relatively high. The grain planting area in Huanghua and Dongguang in Cangzhou has increased significantly, and the yield of arable land has been increased through planting salt alkali tolerant plants and soil improvement techniques. The ancient cities of Hengshui, such as Zaoqiang and Wuyi, have a large agricultural population, with rural residents mainly relying on agriculture for their income and strong ability to guarantee arable land. The natural conditions at the junction of Shijiazhuang and Hengshui are similar, and the supply capacity of arable land is strong. Baoding City, Shijiazhuang City, Xingtai City, and Handan City are located in the western Taihang Mountains, with high labor costs. The distribution of arable land in the mountainous areas is scattered, and the degree of fragmentation is low. The growth rate of the transformation index of arable land utilization and supply is relatively low.

4.1.2 Temporal evolution characteristics of farmland utilization demand transformation

During the research period, the transformation index of land utilization demand in Hebei Province exhibited significant growth. The eastern part of Hebei Province experienced a higher increase in the transformation index of land utilization demand. The most substantial increase in the transformation index occurred between 2010 and 2015. Compared to the transformation of land utilization supply, the transformation of land utilization demand is more influenced by policy adjustments and exhibits more pronounced agglomeration effects. The changes in land utilization demand within evaluation units are more drastic, while the external effects of land utilization demand between evaluation units are stronger.

(1) From 2005 to 2010, the transformation index of arable land use demand showed a relatively low range of changes, with some districts and counties experiencing significant growth in arable land use demand. Rural residents in Jinzhou, Gaocheng, and Xinji in the western part of Shijiazhuang City experienced significant income growth, while agricultural development also led to an increase in rural residents' consumption levels, resulting in an increased demand for arable land for rural development. The increase in urbanization construction speed occupies the arable land space around the city, and the demand for the quantity of arable land resources increases. The primary and secondary industries in Fengnan, Fengrun, and Yutian in the western part of Tangshan City have developed rapidly, and the demand for rations, industrial grains, and feed has increased. The low demand for arable land utilization in districts and counties of Handan City has undergone significant changes, such as Wu'an City and Congtai District. During this period, the arable land area in Handan City continued to grow.

(2) The transformation index of cultivated land use demand from 2010 to 2015 showed significant differences: the population in the eastern part of Hebei Province flowed from rural areas to urban areas, and population mobility was a direct factor in the growth of cultivated land use demand. The demand for cultivated land increased faster in urban areas with higher population density and surrounding areas, such as Shijiazhuang and Baoding urban areas. Langfang City undertakes the population of Beijing and Tianjin, while Tangshan City undertakes some industries. The population and industries have increased the regional price level, and the economic demand for arable land has increased. The growth rate of the demand transformation index for arable land utilization in the northwest of Hebei Province is relatively low, and the growth rate is relatively fast. For example, in the municipal districts of Zhangjiakou City, Xuanhua, and Yuxian, there is unemployment while economic development, and the demand for employment protection for arable land is outstanding and perfect.

(3) The transformation index of land utilization demand in the eastern counties of Hebei Province from 2015 to 2020 has further improved, forming a significant high-value agglomeration zone from Tangshan to Shijiazhuang. This region is mostly plains and has well-developed transportation conditions in terms of location. There is a large income gap between urban and rural areas, requiring the guarantee of land resources to ensure social stability. The growth of the transformation index of land utilization demand in Xingtai City and Handan City is concentrated in the eastern region, such as Nong and Weixian. The agricultural mechan level in Botou, Cxian, and Hejian of Cangzhou City is relatively high, with large areas of rural settlements. The adaptability of agricultural labor and mechanization level is strong, and

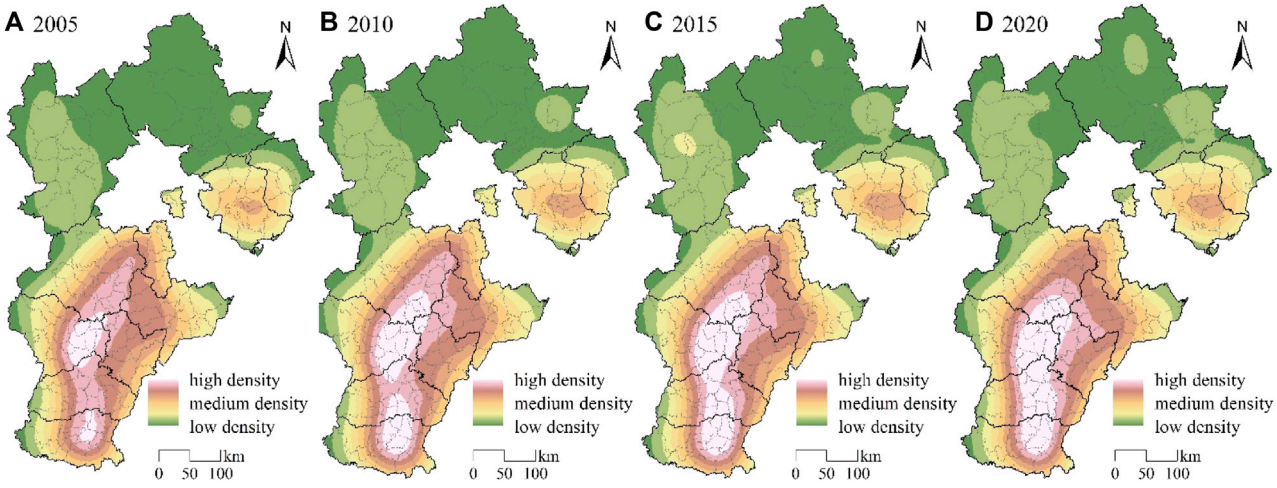

FIGURE 3
Kernel density estimation of cultivated land use supply transformation index.

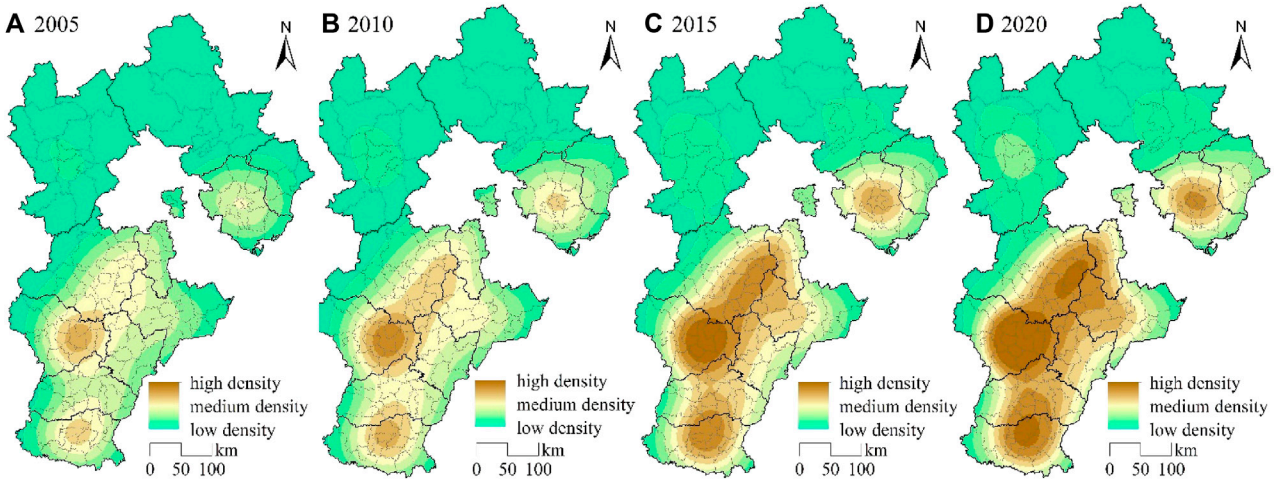

FIGURE 4
Kernel density estimation of cultivated land use demand transformation index.

there is a higher demand for rural development based on land production.

4.1.3 Distribution of nuclear density in the transformation of cultivated land use and supply

To analyze the spatial evolution characteristics of land utilization supply and demand transformation, and to explore the development trends and factors influencing the spatial changes in land utilization transformation, a kernel density estimation model is selected. Formula (3) is used to calculate the kernel density of land utilization supply and demand transformation in Hebei Province. The natural break classification method is applied to classify the kernel density of land utilization supply and demand transformation into low-density, medium-density, and high-density areas. The analysis of the spatial patterns of land utilization supply and demand transformation is conducted by examining the area and spatial changes of the density zones. Please refer to Figure 3 and Figure 4 for the kernel density maps of land utilization supply and demand transformation in Hebei Province.

During the research period, the overall distribution of the nuclear density of cultivated land use supply transformation was high in the south and low in the north. The center of the high-density area was in the eastern part of Shijiazhuang City, while the medium density area was mainly distributed at the edge of Tangshan City and the high-density area. Chengde City had the lowest nuclear density of cultivated land use supply transformation, followed by Zhangjiakou City.

(1) From 2005 to 2010, there was little change in the total area of high-density areas, with core areas such as the intersection of

Shijiazhuang, Baoding, and Hengshui experiencing a growth in nuclear density. The area of high-density areas at the intersection of Handan and Xingtai in the south slightly expanded. The medium density area is widely distributed in Tangshan City, Cangzhou City, the western part of Baoding City, and the western part of Shijiazhuang City. The area has a wide distribution range, high environmental advantage, and potential improvement ability in arable land utilization and supply. The proportion of low-density areas is the largest, and the farming infrastructure in northern Hebei Province is weak, lacking irrigation water sources, making it suitable for the combined development of planting and animal husbandry.

(2) The improvement direction of the transformation index of arable land use and supply from 2010 to 2015 is mainly in the southeast, with relatively small changes in the number of high-density areas and counties in Xingtai City. Affected by the spillover effect of Shijiazhuang City in the north and Handan City in the south, the supply capacity of arable land use has been enhanced. The range of changes in medium density areas is relatively small, mainly distributed in transitional areas with significant changes in arable land supply capacity. The range of medium density areas has slightly decreased compared to the previous period, and some medium density areas have been transformed into high-density areas. The potential of arable land in this area is gradually developed, and agriculture and tourism are integrated in the western mountainous areas. The area of low-density areas in Chengde and Qinhuangdao cities expanded, and the supply capacity of arable land gradually stabilized during this period.

(3) The density area of the transformation index of cultivated land use and supply from 2015 to 2020 showed relatively small changes, while the area of high-density areas increased significantly compared to the initial stage of the study. In terms of space, it covers Shijiazhuang, Baoding, Hengshui, Cangzhou, Xingtai, and Handan cities. The soil texture of this area is suitable for cultivated land, and the terrain is flat, forming a belt shaped area with advantages in cultivated land use and supply. There are scattered expansion patches in the low-density area, and the transformation index of arable land utilization and supply in some districts and counties has increased. For example, the paddock in Chengde City has a significant advantage in the development of the aquaculture industry, with multiple pastures serving as an ecological barrier in the north. Sightseeing agriculture and characteristic agricultural product processing industry are gradually developing.

4.1.4 Core density distribution of farmland utilization demand transformation

The overall distribution of cultivated land use demand transformation density areas is high in the south and low in the north. The southern high-density areas are constantly expanding with the urban area as the core, while the transformation index of cultivated land use demand in the northern low-density areas is gradually increasing. Overall, the change in the area of low-density areas is relatively small.

(1) From 2005 to 2010, the high-density areas had a relatively large circle area, and the radiation effect of the transformation of arable land use demand was relatively low. This indicates that the degree of dispersion of the transformation index of arable land use demand in districts and counties was high, and the degree of mutual influence was weak. During this period, the degree of large-scale utilization of arable land was low, with agricultural grain as the main demand for arable land and low level of agricultural mechanization. The medium density area in the eastern part of Baoding City has evolved into a high-density area, with a small and densely populated county area and a significant transformation in demand for arable land utilization. Low density areas are widely distributed in Zhangjiakou and Chengde cities, with significant differences from medium density areas.

(2) From 2010 to 2015, the area of high-density areas in the transformation of arable land use demand significantly expanded. The development of high-density areas was influenced by Beijing and Tianjin, with Shijiazhuang City as the core and expanding towards the northeast. The spillover effect of nuclear density in the eastern part of Shijiazhuang City, which has a high demand for arable land use, on the surrounding areas was significant. The tourism industry in Zhangjiakou urban area, Xuanhua, and Wanquan is developing in combination with agriculture and animal husbandry, transitioning from low density areas to medium density areas. The overall development direction is mainly towards the south, and the overall utilization level of arable land, forest land, and grassland is increasing.

(3) From 2015 to 2020, there was a significant expansion of high-density areas. The core high-density areas include the downtown area of Shijiazhuang, Xiong'an New Area, and economically developed counties, indicating a close connection between changes in land demand and economic development. The demand for cultivated land has shifted from agricultural product demand to the needs of social stability and rural development. The medium-density area in the southeast plain of Hebei Province gradually decreased during this period, mainly concentrated in the coastal cities of Cangzhou and Qinhuangdao. Qinhuangdao has witnessed rapid development in fisheries and tourism, and it has a relatively small total population in the region. The low-density areas in Zhangjiakou and Chengde transitioned into medium-density areas, and the expansion of demand is focused on the flat southern counties.

4.2 Spatial correlation of farmland utilization transformation in Hebei Province

There are differences between the direction and speed of transformation of land utilization supply and demand in Hebei Province. A coupling coordination model is selected for analysis, and the coupling coordination degree of land utilization supply and demand transformation is calculated using Formula (6). The spatial correlation between the transformation of land utilization supply and demand in Hebei Province from 2005 to 2020 is explored. The lowest value of the coupling coordination degree of land utilization supply and demand in Hebei Province is 0.21, and the highest value is 0.79. Divided by intervals of 0.10, the coupling coordination

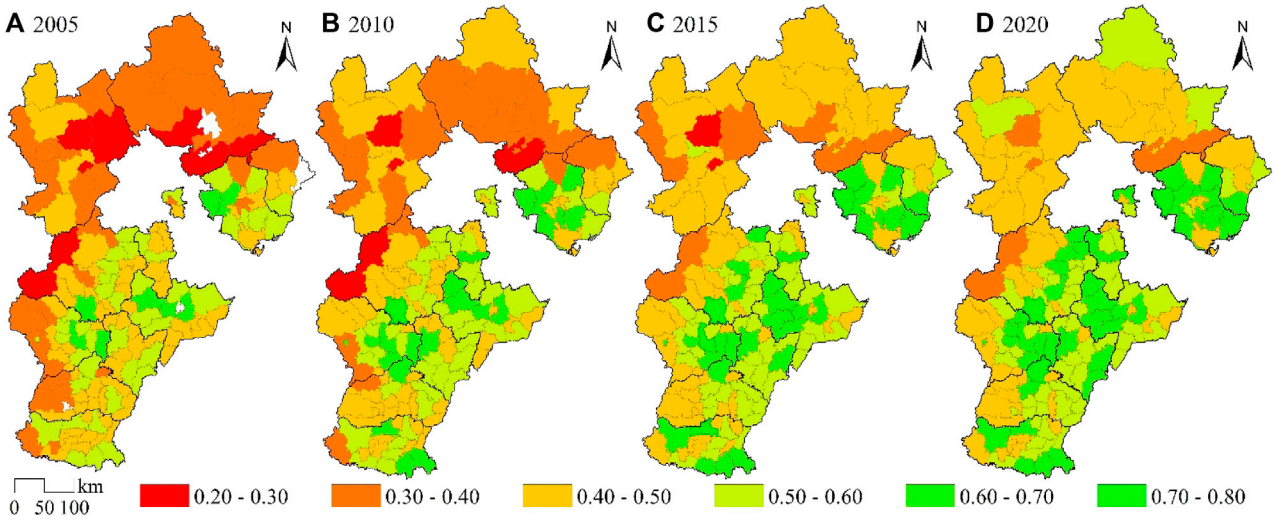

FIGURE 5
Coupling and coordination degree of cultivated land use supply and demand transformation.

degree of land utilization supply and demand is classified into six levels: moderate imbalance, mild imbalance, imminent imbalance, precarious coordination, primary coordination, and intermediate coordination, as shown in Figure 5.

(1) In 2005, the average coupling coordination degree of land utilization supply and demand transformation was 0.45, indicating mild imbalance. From the perspective of the coupling coordination degree, there is a strong correlation between land utilization supply and demand systems. The number of counties in imminent imbalance is the highest, with a total of 66 counties, accounting for 42.58% of the total. The second highest is precarious coordination, with a total of 40 counties, accounting for 25.80% of the total. The transformation index of land utilization supply and demand is low, and there are no counties in the intermediate coordination level. In terms of spatial distribution, primary coordination and intermediate coordination of land utilization supply and demand transformation are mainly concentrated in Shijiazhuang, Baoding, Cangzhou, and Tangshan. The level of land utilization supply and demand is relatively low, with most counties having a higher land utilization supply transformation index than demand. The coupling coordination degree of land utilization supply and demand transformation in Zhangjiakou and Chengde is lower than that in surrounding areas, with mainly mild and imminent imbalances, and a few counties with developed agriculture and animal husbandry are in moderate imbalance, such as Chicheng, Xinglong, and Kuancheng.

(2) In 2010, the average coupling coordination degree of land utilization supply and demand transformation was 0.48, with an overall improvement compared to 2005. During this period, the land production capacity increased, the transformation index of land utilization demand continued to grow, and the gap between land utilization supply and demand narrowed. From the perspective of the coupling coordination degree, there were 19 counties in mild imbalance, accounting for 12.26%, a decrease of 11 compared to 2005. The number of counties in imminent coordination remained unchanged. There were 46 counties in precarious coordination, accounting for 29.68%. In terms of spatial distribution, most counties in Hengshui and Handan were in precarious coordination. Primary coordination was mainly concentrated in Tangshan and Cangzhou, such as Fengrun, Yutian, Renqiu, Hejian, and Cangxian, with large administrative areas and rich resources. The transformation of land utilization supply and demand was synchronous. The climatic and natural conditions in Shijiazhuang and Baoding are similar, and there is a significant difference in the coupling coordination degree between eastern and western counties. Most eastern counties are in precarious coordination, while western counties are in imminent imbalance.

(3) In 2015, the average coupling coordination degree of land utilization supply and demand transformation was 0.52, transitioning from mild imbalance to precarious coordination. The growth rate of the transformation index of land utilization demand was faster than that of supply, indicating a relatively balanced index. From the perspective of the coupling coordination degree, the number of counties in imminent imbalance decreased to 59, accounting for 38.06%, and the number of counties in precarious coordination increased to 55, accounting for 35.48%. In terms of spatial distribution, a gradually improving northwest-southeast spatial pattern was formed. The mountainous areas in the northwest of Hebei Province have lower land utilization demand, and the improvement of land supply capacity is affected by labor migration. The southeast of Hebei Province has a rapid growth in land utilization demand, and the coupling coordination degree gradually develops towards intermediate coordination. The number of counties in moderate imbalance and mild imbalance decreased. Fuping, Xinglong, and Laiyuan counties changed from moderate imbalance to mild imbalance.

These three areas have a small population density and limited agricultural labor resources, which restrict the speed of land utilization transformation in the region.

(4) In 2020, the average coupling coordination degree of land utilization supply and demand transformation was 0.54, further improving compared to 2015. The land protection policies in Hebei Province were continuously improved. From the perspective of the coupling coordination degree, there were no counties in moderate imbalance, and the number of counties in imminent imbalance and precarious coordination changed slightly, with 53 and 56 counties respectively. The number of counties in primary coordination changed significantly, increasing from 27 to 37, accounting for 23.87%. This indicates a gradual transformation in land utilization supply and demand towards high supply and high demand. In terms of spatial distribution, the coupling coordination degree of land utilization supply and demand steadily increased. The largest increase in the coupling coordination degree occurred between 2010 and 2015, transitioning from rapid rise to stable improvement. Combined with the index of land utilization supply and demand transformation, land utilization demand grew faster. The development differences in industries among the counties in Hebei Province led to heterogeneity in land demand. Soil conditions, water resources, and climate types should be fully considered to mitigate conflicts between land and other land types.

4.3 Analysis of factors influencing the transformation of cultivated land use in Hebei Province

The study selects three indicators from the perspective of natural environment: elevation, terrain undulation, and vegetation coverage. From the perspective of social economy, three indicators are selected: road mileage, urbanization rate, and total industrial output value. The factor detection function of geographic detectors is used to explore the influencing factors of the supply-demand transformation of farmland utilization. According to formula (7), the q value and significance of each influencing factor and the supply-demand transformation of farmland utilization are calculated, The higher the q value, the stronger the influence ability of this factor. The q value and significance of the transformation of arable land use supply and demand are shown in Table 3 and Table 4.

(2) From 2005 to 2020, the q-value of terrain fluctuation decreased from 0.35 to 0.26. Areas with lower terrain fluctuation were mainly distributed in the southeastern plain region and the northern plateau. Terrain fluctuation reflects the water, fertilizer, air, and thermal conditions of an area. The southeastern counties of Hebei Province had lower soil organic matter content. Improving soil physical and chemical properties is an effective measure to enhance the potential productivity of farmland. It is necessary to explore advantageous agricultural areas, utilize modern machinery in the agricultural production process, focus on the development of water-saving agriculture, and improve the quality of soil and water resources in order to promote the utilization and development of farmland and green areas (Zeng et al., 2022; Zeng, 2023).

(3) From 2005 to 2020, the q-value of vegetation coverage and the transformation of land utilization supply increased and then decreased, with significant enhancement after 2010. Regions with higher vegetation coverage were mostly areas with large forest and grassland areas. Vegetation coverage is strongly related to land utilization policies. The implementation of policies for converting cultivated land into forests and grasslands has effectively increased vegetation coverage, contributing to the construction of an ecological barrier around Beijing and Tianjin. Sloping farmland, which is difficult to develop and has low cultivation efficiency, should be planned for conversion into forests and grasslands. This will improve the regional ecological civilization level while also considering the rights and interests of farmers to enhance the social security supply capacity of cultivated land (Zhang P. et al., 2023).

(4) From 2005 to 2020, the urbanization rate was significantly correlated with the transformation of land utilization supply at a confidence level of 0.01. The q-value of the urbanization rate increased significantly after 2010, indicating that urbanization construction affects land supply capacity. Conflicts between urban construction land, residential land, and cultivated land have persisted for a long time. It is necessary to coordinate the utilization of construction land and cultivated land, reduce abandoned and fallow farmland in rural areas (Yu and Yin, 2023), and simultaneously enhance grain income and prioritize the cultivation of food crops to prevent non-food utilization of cultivated land and improve the food production capacity of cultivated land in order to ensure food security.

(5) From 2005 to 2020, the q-value of highway mileage initially decreased and then increased, and it was significantly correlated with the transformation of land utilization supply at a confidence level of 0.01, stabilizing at 0.29 overall. Highway mileage reflects the level of regional transportation development. Regional transportation costs and transportation time affect the prices of agricultural products. Improving transportation conditions and reducing transportation costs contribute to the circulation and further processing of agricultural products. Improving rural roads facilitates the circulation of agricultural products, the development of distinctive agricultural brands, and the enhancement of the added value of agricultural products.

4.3.1 Analysis of factors influencing the transformation of cultivated land use and supply in Hebei Province

Elevation and terrain undulation are the main natural factors affecting the transformation of arable land use and supply, and natural terrain is the primary factor limiting the transformation of arable land use and supply. The vegetation coverage gradually increased significantly after 2005. During the research period, there was a significant correlation between road mileage and urbanization rate and the transformation of arable land use supply at a confidence level of 0.01, while there was no

TABLE 3 Explanatory power and significance of influencing factors of cultivated land use supply transformation.

Influence factor	2005	2010	2015	2020
Elevation	0.35	0.33	0.30	0.30
	***	***	***	***
Relief	0.35	0.32	0.29	0.26
	***	***	***	***
Vegetation coverage	0.20	0.26	0.25	0.23
	*	***	***	***
Road	0.29	0.28	0.26	0.29
	***	***	***	***
Urbanization rate	0.25	0.25	0.29	0.33
	***	***	***	***
Total industrial output value	0.12	0.09	0.11	0.09

Note: *, * * and * * * indicate significant correlation at confidence levels of 0.1, 0.05, and 0.01, with null values indicating no significant correlation.

TABLE 4 Explanatory power and significance of influencing factors of cultivated land use demand transformation.

Influence factor	2005	2010	2015	2020
Elevation	0.44	0.45	0.38	0.32
	***	***	***	***
Relief	0.38	0.30	0.24	0.17
	***	***	**	*
Vegetation coverage	0.07	0.05	0.07	0.21
				**
Road	0.15	0.12	0.10	0.09
Urbanization rate	0.22	0.21	0.26	0.18
	**	**	***	**
Total industrial output value	0.28	0.40	0.39	0.33

Note: *, * * and * * * indicate significant correlation at confidence levels of 0.1, 0.05, and 0.01, with null values indicating no significant correlation.

significant correlation between total industrial output value and the transformation of arable land use supply. Analyzing the trend of q value changes in the transformation of arable land use supply from a factor perspective:

(1) From 2005 to 2015, the q value of elevation and arable land use supply transformation decreased from 0.35 to 0.30. With the development of modern agricultural technology, the impact of elevation gradually decreases, indicating that the degree of limitation of elevation on arable land use supply transformation has decreased. The supply of arable land can be improved through land consolidation, land reclamation, and other methods. Hebei Province has a high altitude difference, and the areas with higher elevations are mostly distributed in the Yanshan and Taihang Mountains. The terrain in this area is complex and not suitable for the use of modern agricultural machinery and large-scale utilization of arable land. The development and utilization of arable land are mostly based on households, and there are phenomena of abandonment and non grain cultivation of arable land. Therefore, it is necessary to strengthen land circulation and promote the rational utilization of arable land resources.

4.3.2 Analysis of factors influencing the transformation of cultivated land use demand in Hebei Province

The driving factors for the transformation of arable land use demand include multiple levels such as food consumption, population mobility, land use conflicts, and economic development. Elevation, terrain undulation, urbanization rate, and total industrial output value are significantly correlated with the transformation of arable land use demand. Terrain conditions

are the core factor limiting the transformation of demand for arable land use, causing differences in natural resources and economic development, thereby affecting the supply and demand level of arable land use in counties. Labor force is the core element of the agricultural industrial structure, indirectly affecting demand from the supply side.

(1) The correlation between elevation and the transformation of cultivated land use demand is strong. During the research period, the q value of elevation decreased from 0.44 to 0.32. Areas with higher elevations have greater difficulty in development and lower intensity of cultivated land use demand. The q value of terrain undulation decreases significantly, and the correlation with the transformation of arable land use demand is becoming weaker. It is the main limiting factor for the growth of arable land use demand at small scales such as urban areas. Regions with high terrain undulation have lower population agglomeration and density, lower demand for arable land resources, and flat terrain areas are suitable for urban construction and agricultural production. Urban construction and rural development require support from arable land resources, and the demand for arable land resources is high.
(2) The urbanization rate is significantly correlated with the transformation of farmland utilization demand, with the highest q value of 0.26 in 2015. The areas with higher urbanization rates are mostly municipal districts and surrounding areas. The population siphon effect is stronger in areas with higher urbanization rates. The increase in urbanization rates leads to a decrease in the proportion of agricultural population, and the transformation of labor forces leads to a scarcity of supply growth, indirectly affecting the demand for farmland utilization. The industrial structure of Hebei Province is in the process of transformation and development, gradually transitioning from being dominated by the secondary industry to being dominated by the tertiary industry. It is necessary to optimize the industrial structure, protect the ecological environment, and achieve the integrated development of agriculture and other industries.
(3) There is a positive correlation between the demand for farmland utilization and transportation conditions. The districts and counties with higher road mileage in Hebei Province are mostly located in Chengde City and Zhangjiakou City, which have larger administrative areas. The districts and counties with smaller administrative areas in the southeast of Hebei Province have lower road mileage, and the correlation between road mileage and farmland utilization demand is relatively low. The transportation advantage areas in Hebei Province are mostly located in Shijiazhuang, Tangshan, and Langfang. There is a high flow of people and industries in the Beijing Tianjin and surrounding areas. This area should pay attention to the circulation and complementarity of agricultural products, plan the use of arable land, and meet the needs of regional arable land use.
(4) The total industrial output value reflects the development level of the secondary industry in the region and is an important influencing factor for the transformation of farmland utilization demand. The q value first increases and then decreases, reaching a peak of 0.40 in 2010. The intensity of farmland utilization demand in industrial developed areas is high, with metal smelting as the main industry in Hebei Province. The proportion of agricultural and sideline food processing industry and food manufacturing industry is relatively low. While promoting agricultural industrialization, it should ensure the income of farmers. Promote the rational utilization of arable land resources in the process of urbanization and agricultural modernization, pay attention to the protection of the three in one system of arable land, broaden the channels for supplementing arable land, and improve the balance between supply and demand of arable land utilization.

5 Conclusion

During the research period, the supply and demand transformation index of arable land use in Hebei Province showed an upward trend. The agglomeration degree of the transformation index of cultivated land use supply in the southeast of Hebei Province is high, while the transformation index of cultivated land use supply in the northwest is relatively low. The transformation index of demand for arable land utilization has undergone significant changes. The demand for arable land in urban areas and surrounding areas with high population density has grown faster, and the demand for arable land has gradually transformed from agricultural products to social stability and rural development. At the same time as economic development, the ability to provide basic support for arable land has been enhanced. The overall distribution of the core density of supply and demand transformation for arable land use in Hebei Province is high in the southeast and low in the northwest. The improvement direction of the arable land use supply transformation index is mainly in the southeast, and the expansion trend of the density area of arable land use demand transformation is obvious. The dispersion degree of the arable land use demand transformation index between districts and counties is high.

The supply and demand system of cultivated land utilization in Hebei province has a strong correlation, and the coupling coordination of supply and demand of cultivated land utilization has steadily increased from 2005 to 2015. From 2015 to 2020, the coupling coordination has transformed from rapid growth to stable improvement, transitioning from imbalance to coordination at the provincial level, and gradually transforming toward high supply and high demand of cultivated land utilization. There is a significant spatial pattern differentiation in the coupling coordination of supply and demand for cultivated land utilization in Hebei province, with a overall spatial pattern of gradual improvement from northwest to southeast. The coupling coordination of the transformation of supply and demand of cultivated land utilization in the mountainous areas of the northwest is relatively low, and the improvement of land supply capacity is influenced by both labor migration and geographic environment. The southeast has seen rapid growth in demand for cultivated land utilization, and the level of coupling coordination has gradually increased.

The transformation of supply of cultivated land utilization in Hebei province is strongly correlated with the natural environment,

and elevation and topographical fluctuation are the primary factors influencing the transformation of land supply. Highway mileage is significantly correlated with the transformation of land supply of cultivated land utilization, and improving transportation conditions and reducing transportation costs contribute to the development of the agricultural land industry. The transformation of demand for cultivated land utilization is closely related to social and economic development (Yin et al., 2022), and areas with flat terrain are suitable for urban construction and agricultural production. Urban construction and rural development require the support of land resources. Areas with higher urbanization rates have a greater population agglomeration, and the scarcity of supply stimulates the growth of the index of transformation of demand for cultivated land utilization. The total industrial output value is an important influencing factor for the transformation of demand for cultivated land utilization, and areas with developed industries such as Tangshan have a higher intensity of demand for cultivated land utilization. In the process of industrialization, urbanization, and agricultural modernization, attention should be paid to the protection of the three-dimensional cultivated land, expanding the ways of supplementary land, and improving the balance of supply and demand for cultivated land utilization.

Cultivated land utilization needs to ensure the current supply of grain production and meet the rigid demand for land utilization, while also adopting measures such as fallow rotation to enhance land productivity and achieve sustainable utilization of cultivated land. The southeastern part of Hebei province has flat terrain, and the level of contiguous cultivated land and mechanization should be improved. The support system for agricultural mechanization policies should be improved, and the comprehensive mechanization of the crop production process should be promoted to prevent non-food land utilization. The priority order of land utilization should be clarified to ensure the cultivated area for basic food crops. The northern part of Hebei province has a favorable natural environment, and the integration of agriculture and tourism should be promoted. Measures such as developing leisure agriculture, improving public facilities, and enhancing service levels should be taken to promote the integration of agriculture and tourism. In the western part of Hebei province, efforts should be made to build an ecological barrier around Beijing and Tianjin, carry out rural fallow trials, coordinate the arrangement of land retirement, afforestation, and grass planting, and optimize the ecological compensation mechanism for cultivated land.

Data availability statement

The raw data supporting the conclusion of this article will be made available by the authors, without undue reservation.

Author contributions

LM: Conceptualization, Supervision, Writing–original draft, Writing–review and editing. FG: Software, Visualization, Writing–original draft, Writing–review and editing. HH: Methodology, Software, Validation, Writing–original draft, Writing–review and editing. YG: Formal Analysis, Investigation, Methodology, Writing–original draft, Writing–review and editing. LX: Formal Analysis, Funding acquisition, Project administration, Writing–original draft, Writing–review and editing. SY: Conceptualization, Methodology, Resources, Writing–original draft, Writing–review and editing.

Funding

The authors declare financial support was received for the research, authorship, and/or publication of this article. This research was funded by 2022 Annual Research Project on Development of Social Sciences in Hebei Province (20220303087); Research Project on Basic Scientific Research Funds of Provincial Universities in Hebei Province (KY2022100); Research Project on Humanities and Social Sciences in Universities in Hebei Province (SQ2023207).

Conflict of interest

The authors declare that the research was conducted in the absence of any commercial or financial relationships that could be construed as a potential conflict of interest.

Publisher's note

All claims expressed in this article are solely those of the authors and do not necessarily represent those of their affiliated organizations, or those of the publisher, the editors and the reviewers. Any product that may be evaluated in this article, or claim that may be made by its manufacturer, is not guaranteed or endorsed by the publisher.

References

An, Y., Tan, X., Li, Y., Zhou, Z., Yu, H., and Ren, H. (2022). Study on the spatiotemporal evolution characteristics and influencing factors of cultivated land function in the Dongting Lake area. *Geogr. Sci.* 42 (7), 1272–1282.

Chen, L., Hao, J., Wang, F., Yin, Y., Gao, Y., Duan, W., et al. (2016). Research on carbon fixation function of cultivated land in the huanghuaihai plain based on carbon cycle. *Resour. Sci.* 38 (6).

Chen, L. (2022). The spatial scale characteristics and driving mechanisms of the transformation of cultivated land use function: an investigation of the jialing River Basin in sichuan province. *Res. Soil Water Conservation* 05, 327–335+342.

Du, G., Chai, L., and Li, Y. (2022). Theoretical analysis and research framework of farmland utilization system. *Prog. Geogr. Sci.* 2022.

Du, G., Guo, K., and Yu, F. (2021). Suggestions for the transformation and regulation of cultivated land utilization function in reclamation areas of heilongjiang province. *Res. Agric. Mod.* 42 (4), 589–599.

Fu, H., Liu, Y., Sun, H., and Zhou, G. (2020). Spatiotemporal characteristics and dynamic mechanism of cultivated land use transition in the Beijing-Tianjin-Hebei region. *Prog. Geogr. Sci.* 39 (12), 1985–1998. doi:10.18306/dlkxjz.2020.12.003

Gai, Z., Zhan, W., Wang, H., and Du, G. (2022). Research on the spatiotemporal differentiation characteristics and formation mechanism of carbon emissions from farmland utilization transformation. *J. Agric. Mach.* 07, 187–196.

Grainger, A. (1995). The forest transition: an alternative approach. *Area* 1995, 242–251.

Gu, J., and Zha, L. (2012). A study on the dynamic changes of crop carbon storage in the wanjiang urban belt. *Resour. Environ. Yangtze River Basin* 21 (12), 1507–1513.

Guo, J., Zhang, Y., Zhang, Z., Hou, L., and Zeng, W. (2023). Land use change and its driving mechanism in the mountainous and canyon areas of southeastern Tibet based on geographic detectors. *J. China Agric. Univ.* 28 (4), 210–226.

He, S. (2019). "Research on multifunctional evaluation and use zoning of cultivated land based on multisource information," (Hangzhou, China: Zhejiang University). Doctoral dissertation.

Jiang, M., Li, Z., Li, J., and Liu, X. (2022). Detection and spatiotemporal characteristics of abrupt changes in farmland utilization transformation: a case study of Dongchuan District, Kunming City. *Chin. Land Sci.* 2022.

Jin, Y., and Wang, F. (2022). Analysis of the spatiotemporal evolution characteristics and influencing factors of farmland utilization transformation in the Pearl River Delta. *Res. Soil Water Conservation* 2022.

Kong, X., Wang, J. S., and Yang, H. (2021). Upregulation of lncRNA DARS-AS1 accelerates tumor malignancy in cervical cancer by activating cGMP-PKG pathway. *J. Soc. Sci. Hunan Normal Univ.* 50 (3), 1–11. doi:10.1002/jbt.22749

Kuang, B., Fan, B., and Lu, X. (2021). The spatiotemporal differentiation characteristics and influencing factors of green transformation efficiency in farmland utilization in China. *Trans. Chin. Soc. Agric. Eng.* 37 (21).

Li, Q. (2017). *Research on the characteristics and mechanisms of farmland utilization transformation in the middle reaches of the Yangtze River*. Wuhan: China University of Geosciences.

Li, X. (2002). Explanation of land use change. *Prog. Geogr. Sci.* 03, 195–203.

Long, H., Hua, D., and Wang, J. (2019). Research progress and prospects on the coupling of land use transformation and rural transformation development. *ACTA Geogr. SIN.* 74 (12).

Long, H., and Li, X. (2006). The Transformation of Cultivated Land and Land Consolidation in China: Research progress and framework. *Prog. Phys. Geogr.* 5, 67–76.

Lu, H., Hu, L., Zheng, W., Yao, S., and Qian, L. (2020). Impact of household land endowment and environmental cognition on the willingness to implement straw incorporation in China. *J. Clean. Prod.* 262, 121479. doi:10.1016/j.jclepro.2020.121479

Lu, H., Xie, H., Lv, T., and Yao, G. (2019). Determinants of cultivated land recuperation in ecologically damaged areas in China. *Land Use Policy* 81, 160–166. doi:10.1016/j.landusepol.2018.10.052

Lu, X., Wang, H., Tang, Y., and Jiang, X. (2021). A Study on the Spatial Spillover Effect of the Transformation of Cultivated Land Utilization on Farmers' Income in Hubei Province. *resour. environ. Yangtze River Basin* 30 (7), 1757–1767.

Lv, T., Fu, S., Zhang, X., Wu, G., Hu, H., and Tian, J. (2022). Assessing cultivated land–use transition in the major grain-producing areas of China based on an integrated framework. *Land* 11 (10), 1622. doi:10.3390/land11101622

Ma, L., Xu, S., Guo, F., Xu, L., and Yin, S. (2022). Spatial differentiation and influencing factors of rural-area multi-functionality in Hebei province based on a spatial econometric model. *Front. Environ. Sci.* 10, 773259. doi:10.3389/fenvs.2022.773259

Niu, S., Fang, B., Cui, C., and Huang, S. (2020). Analysis of the spatiotemporal pattern and path of farmland utilization transformation from the perspective of rural revitalization - taking the Huaihai Economic Zone as an example. *J. Nat. Resour.* 35 (8), 1908–1925.

Song, H., and Xin, L. (2021). Research on the differentiation characteristics and influencing factors of cultivated land use intensity in China. *Trans. Chin. Soc. Agric. Eng.* 37 (16).

Song, X., and Li, X. (2019). Theoretical explanation and empirical study on the transformation of regional cultivated land utilization function. *J. Geogr.* 74 (5), 992–1010.

Song, X., Wu, X., and Ouyang, Z. (2014). Discussion on the research path of cultivated land transformation. *Geogr. Res.* 33 (3).

Sun, Y. (2018). A study on the coupling relationship between the transformation of cultivated land use and grain yield in shaanxi province. *China's Agric. Resour. zoning* 39 (7), 14–20.

Tang, Y., Lu, X., and Zhang, X. (2021). Research on the impact and threshold effect of highway infrastructure construction on the transformation of cultivated land use. *Chin. Land Sci.* 35 (1), 59–68.

Wang, J., and Xu, D. (2017). Geographic detectors: principles and prospects. *J. Geogr.* 72 (1).

Wei, X., Lin, L., Luo, P., Wang, S., Yang, J., and Guan, J. (2022). Analysis of the spatiotemporal pattern and driving forces of multifunctional coupling and coordinated development of cultivated land. *Trans. Chin. Soc. Agric. Eng.* 38 (4).

Xie, S., Yin, G., Lou, Y., and Wei, W. (2022). Analysis of the "water drought differentiation" pattern and mechanism of cultivated land use in China from 1990 to 2020. *Land Sci. China* 06, 113–124.

Yang, L., Min, J., and Kong, X. (2018). The transformation of cultivated land in the three gorges reservoir area and its influencing factors. *Resour. Dev. Mark.* 34 (11), 1511–1519.

Yin, S., Wang, Y., and Xu, J. (2022). Developing a conceptual partner matching framework for digital green innovation of agricultural high-end equipment manufacturing system toward agriculture 5.0: a Novel Niche Field Model Combined with Fuzzy VIKOR. *Front. Psychol.* 13, 924109. doi:10.3389/fpsyg.2022.924109

Yin, Z., and Kang, Z. (2022). Advances in kernel density estimation supported by time geography. *Prog. Geogr. Sci.* 41 (01), 64–72. doi:10.18306/dlkxjz.2022.01.006

Yu, Y., and Yin, S. (2023). Incentive mechanism for the development of rural new energy industry: new energy enterprise–village collective linkages considering the quantum entanglement and benefit relationship. *Int. J. Energy Res.* 2023, 1–19. doi:10.1155/2023/1675858

Zeng, J., Chen, X., Cui, R., and Zhao, P. (2022). How does the enterprise green innovation ecosystem collaborative evolve? Evidence from China. *J. Clean. Prod.* 375, 134181. doi:10.1016/j.jclepro.2022.134181

Zeng, J. (2023). Exploring the influence of ecological relationship on knowledge interaction in green innovation cooperation. *Environ. Sci. Pollut. Res.* 2023 (30), 45369–45387. doi:10.1007/s11356-023-25436-4

Zhang, P., Lu, H., Geng, X., and Chen, Y. (2023b). How do outsourcing services affect agricultural eco-efficiency? Perspectives from farmland scale and technology substitution. *J. Environ. Plan. Manag.* 2023, 1–25. doi:10.1080/09640568.2023.2246170

Zhang, W., Zhang, Z., Dong, J., Zhang, H., Gao, F., and Gong, W. (2021). Analysis of the transformation and driving forces of cultivated land use function from a multiscale perspective - taking gansu province as an example. *Geogr. Sci.* 41 (5), 900–910.

Zhang, Y., Dai, Y., Chen, Y., Ke, X., and Yu, X. (2023a). The spatiotemporal evolution and driving factors of multifunctional coupling coordination of cultivated land in China. *J. Agric. Eng.* 35 (07), 244–249. doi:10.3760/cma.j.cn121430-20220815-00745

Zhou, D., Li, S., Wen, W., and Jiang, G. (2020). Multifunctional evaluation and optimization of arable land in Henan Province based on the perspective of supply and demand. *J. Agric. Mach.* 51 (11), 272–281.

frontiers | Frontiers in Environmental Science

TYPE Original Research
PUBLISHED 02 November 2023
DOI 10.3389/fenvs.2023.1258697

OPEN ACCESS

EDITED BY
Hualin Xie,
Jiangxi University of Finance and Economics, China

REVIEWED BY
László Erdős,
Hungarian Academy of Science, Hungary
Maria Villa,
Instituto Politécnico de Bragança, Portugal

*CORRESPONDENCE
Judit Rubio-Delgado,
juditrd@unex.es

†These authors have contributed equally to this work

RECEIVED 14 July 2023
ACCEPTED 12 October 2023
PUBLISHED 02 November 2023

CITATION
Rubio-Delgado J, Schnabel S, Burgess PJ and Burbi S (2023), Reduced grazing and changes in the area of agroforestry in Europe.
Front. Environ. Sci. 11:1258697.
doi: 10.3389/fenvs.2023.1258697

Reduced grazing and changes in the area of agroforestry in Europe

Judit Rubio-Delgado[1*†], Susanne Schnabel[1†], Paul J. Burgess[2†] and Sara Burbi[3]

[1]INTERRA Research Institute, Universidad de Extremadura, Cáceres, Spain, [2]School of Water, Energy and Environment, Cranfield University, Bedfordshire, United Kingdom, [3]Sant'Anna School of Advanced Studies, Pisa, Italy

Agroforestry integrates woody vegetation with crop and/or livestock production to benefit from the ecological and economic interactions. The objective of this paper is to systematically determine the spatial distribution of agroforestry in the EU, and changes in the areas and types of agroforestry from 2009 to 2018. This was achieved using the Land Use/Cover Area Statistical (LUCAS) dataset. Agroforestry was categorised into silvopastoral, silvoarable, agrosilvopastoral, grazed permanent crops, intercropped permanent crops and kitchen gardens systems. In our categorisation of 'agroforestry', sites combing trees and shrubs with understorey grass or forage were required to show evidence of grazing. In 2018, the total area of agroforestry in the EU28 was 114,621 km^2 equivalent to 6.4% of the utilised agricultural area (UAA), and a majority located in the Mediterranean bioregion. Silvopastoral was the most widespread system, representing 81% of the total agroforestry area (5% of UAA), with almost a third of that area present in Spain. An initial analysis of the LUCAS data suggested that the area of agroforestry increased from 2009 to 2012, before declining from 2012 to 2018. However our subsequent analysis suggests that the area of agroforestry in 2009 was underestimated due to a mis-categorisation of some grazing areas. After making corrections, we calculated that the area of agroforestry (using the above definitions) in the EU23 (a full-time sequence for the EU28 is unavailable) declined by 47% between 2009 and 2018. This decline is primarily due to a reduction in outdoor grazing, perhaps driven by reduced livestock numbers and/or permanent livestock housing. The only agroforestry system showing an increase was kitchen gardens (7%). The paper highlights the usefulness of the LUCAS dataset for studying the extent of agroforestry in Europe, but also potential limitations in terms of the consistency of the location of data points and the categorisation of grazing. The paper also argues that although the area of within-field agroforestry may be declining, the drive towards net zero greenhouse gas emissions may be re-establishing the link between increased tree cover and food production at a farm-level.

KEYWORDS

agroforestry, European Union, land use changes, spatial analysis, LUCAS data

1 Introduction

Agroforestry has been defined as 'the practice of deliberately integrating woody vegetation (trees or shrubs) with crop and/or animal systems to benefit from the resulting ecological and economic interactions' (Burgess and Rosati, 2018). In many places, it is a traditional land use system, and it is estimated that globally there is

1 billion ha of agricultural land with more than 10% tree cover (Zomer et al., 2014), i.e., about 7% of the global land area.

In Europe, agroforestry includes a wide diversity of systems such as silvopastoral, silvoarable, and agrosilvopastoral systems, forest farming, home gardens, improved fallow, grazed forests, and intercropped and grazed orchards (Mosquera-Losada et al., 2009; Nerlich et al., 2013; Pantera et al., 2021). Examples of silvopastoral systems in Mediterranean parts of Europe include the *montados* in Portugal and the *dehesas* in Spain where cattle graze beneath cork and holm oaks (Moreno et al., 2018). Other examples include the cork oak forest systems in Sardinia, known as *sugherete*, and valonia oak systems in Greece (den Herder et al., 2015). The combination of fruit trees with crops or grazing livestock is known as streuobst in central Europe (Herzog, 1998). In the boreal forest and subarctic tundra, reindeer husbandry is widespread, estimated to occupy more than 40 million ha of land in Sweden, Norway and Finland (Jernsletten and Klokov, 2002). In some frameworks, agroforestry also includes the integration of woody landscape features on cropland or grassland, such as hedges, windbreaks, and riparian buffer strips (Mosquera-Losada et al., 2009). For example, hedges and scattered trees occupy more than 400,000 ha in France and parts of the UK and Belgium (den Herder et al., 2015), and windbreaks are a common practice in Hungary (Takács and Frank, 2008).

Trees in arable and grassland systems can be an important source not only of food but also of products such as fuelwood, fibre, timber, gums and resins, and craft products. Agroforestry can also provide recreational opportunities, such as hunting and tourism, and mosaic landscapes are often valued for their diversity and attractiveness of the landscape (Fagerholm et al., 2019; Augére-Granier, 2020). There is also widespread recognition of the environmental benefits of agroforestry compared to conventional agricultural systems. Agroforestry systems can improve the soil health of arable systems, as the trees can increase soil organic matter and retain nutrients (Jose et al., 2009). Integrating trees in crop systems can also reduce soil erosion by increasing the permanence of vegetation cover (Jose et al., 2009) and windbreaks and shelterbelts can reduce windspeed (Bartus et al., 2017; Kučera et al., 2020). Trees on arable land can increase rainfall infiltration rates and soil water retention and reduce nitrate leaching (Siriri et al., 2013). In livestock systems, tree canopies can moderate the temperature with benefits for animal welfare, health, and productivity (Atangana et al., 2014). Trees also provide a habitat for arthropods and some species of birds (Jose et al., 2009; Torralba et al., 2016; Santos et al., 2019; Pantera et al., 2021). Trees and shrubs can increase the amount of soil carbon stored in arable systems (Kirby and Potvin, 2007; Upson et al., 2016; Kay et al., 2019) and the biomass carbon stored in crop and grassland systems (Beka et al., 2023). Tölgyse et al. (2023) reported that trees in temperate deciduous forest wood-pastures in Hungary and Romania reduced herbage growth, but this was offset by positive effects in terms of storing carbon and providing shade and microhabitats. In addition, the presence of management can reduce fire risk relative to shrubland systems (Damianidis et al., 2021). For these reasons, agroforestry is recognised as a sustainable climate-smart agriculture option (FAO and ICRAF, 2019) and hence there is interest in its spatial extent.

Initial reports on the extent of agroforestry in Europe were typically based on literature reviews (Herzog, 1998; Eichhorn et al., 2006; Bergmeier et al., 2010). However, since 2006, Eurostat has carried out the Land Use/Cover Area frame Statistical (LUCAS) survey across the European Union every 3 years, which comprises land cover, land use, agro-environmental and soil data determined by field observation at geographically referenced points (Eurostat, 2009). At each LUCAS point, the land cover (LC) and land use (LU) were recorded. Land cover is the type of physical cover of the land around the point and land use is the socio-economic use. An important feature of LUCAS is that it allows multiple land covers, i.e., where there are multiple layers, such as in agroforestry, the recorder can both report a tree layer and a secondary layer composed of crops or grasses. Thus, the LUCAS surveys was used by den Herder et al. (2017) to determine that the total area under agroforestry in the EU (27 member states) in 2012 was 15.4 million ha, equivalent to about 4% of the territorial area or 9% of the Utilised Agricultural Area (UAA). Den Herder et al. (2017) differentiated three main categories of agroforestry: livestock agroforestry (where livestock production is integrated with trees), high value tree agroforestry (where the primary land use was permanent woody crops such as fruit orchards, olive groves, and nut trees combined with grazing or arable/temporal crops), and arable agroforestry (arable crops integrated with trees). Mosquera-Losada et al. (2018) calculated a larger extent of 19.8 million ha in 2012 by also adding the extent of kitchen gardens. Kitchen gardens, also called home gardens, typically refer to fenced plots in residential areas and allotments where a variety of crops are grown for home consumption. Also using the LUCAS database from 2012, Plieninger et al. (2015a) estimated that pastures in open woodlands, and pastures with sparse or cultivated trees (but not necessarily grazed) in the EU covered 20.3 million ha.

Some authors have suggested that the area of agroforestry is decreasing as farmers remove trees from arable systems to enable easier mechanisation (Eichhorn et al., 2006). In addition, for permanent crops such as olives and apples, there has been a move from high-stem trees (which allowed understorey grazing) to trees grown on dwarf rootstocks (Oosterbaan and Kuiters, 2009; Bergmeier et al., 2010). In Germany, in the last 40 years, streuobst of apple and pear trees have also been converted to grasslands, fields and development areas (Bergmeier et al., 2010), with Küpfer and Balko (2010) reporting a 50% decline. A study of the area of orchard meadows for a region in Southwestern Germany suggested a decline from 16% of the area in 1968 to 12% in 2009, an annual loss rate of 1% (Plieninger er al., 2015b). Other cited reasons for the reduced cover of individual trees include poor tree regeneration due to overgrazing, and new pests (Bergmeier et al., 2010).

To our knowledge, there has been no attempt to use LUCAS data from surveys conducted between 2009 and 2018 to investigate whether the area of agroforestry in Europe is increasing, decreasing, or stable. Hence, the aim of this paper is to evaluate the changes that have occurred in agroforestry in Europe, including the following specific objectives: 1) to determine the current extent of different agroforestry systems in the EU using LUCAS data from 2018; 2) to assess the changes in agroforestry from 2009 to 2018 and examine the implications for future trends; 3) to analyse the causes contributing to variations during the study period; 4) to investigate trends in grazing and their relationship with the changes in the different agroforestry systems; and 5) to evaluate the usefulness of LUCAS data for this type of studies.

2 Material and methods

2.1 Description of the LUCAS database

The extent of agroforestry systems in the EU were determined using LUCAS data, which are based on a two-phases sampling strategy (Buck et al., 2015). In the first phase, points are systematically sampled in a regular grid with a spacing of 2 km in the four cardinal directions covering the whole territory of the EU. This survey contains around 1.1 million different points (the so-called master sample or frame) (Eurostat, 2019a). Each point of the first phase sample is photo-interpreted and assigned a pre-defined land cover class: artificial land, cropland, woodland, shrubland, grassland, bare land, water area or wetland (Buck et al., 2015).

From the first phase sample, a second phase sample of points is drawn randomly and proportionally with respect to the assigned land cover class (more detail on the sampling procedure in Buck et al., 2015; Ballin et al., 2018). These points are visited in the field by surveyors, who record land cover, land use and other environmental parameters. Land cover and land use are recorded according to a harmonised classification system. The surveyor also collects information related to the percentage of land cover within a specific window of observation, including the area size, the width of any specific feature, the height of trees, information on land and water management, such as grazing or irrigation (Eurostat, 2019a). Those points which could not be visited for any reason, for example, due to problems of accessibility, are evaluated using office-based photointerpretation (Ballin et al., 2018). Regarding the geographical location, in the first place the coordinates of the theoretical location are established, and once in the field, the coordinates of the real sampling point are measured with a geographical positioning system (GPS). Those points which could not be visited and that are analysed by photointerpretation are assigned the theoretical coordinates. The LUCAS database includes both coordinates, the real and the theoretical ones.

The basic sampling and survey methods have remained the same throughout all surveys. Nevertheless, the goals of the surveys and their implementation in new countries to the survey have changed and have led to different sample point allocations for different land covers (d'Andrimont et al., 2020). Table 1 presents the number of sample points for each EU member state and for the different survey years. The LUCAS 2006 survey was not included in the study because of its small number of points and the few countries included in the sample (Belgium, Czechia, Germany, France, Italy, Luxembourg, Hungary, Netherlands, Poland and Slovakia). Between 2009 and 2015 the number of sample points increased from 234,484 to 338,725, related mainly with an increment of points per previous countries (+78,269), but also with the inclusion of new countries in the survey (+25,972 points: Bulgaria, Cyprus, Croatia, Malta, Romania). Between 2015 and 2018 the total number of points remained almost unchanged, with some countries registering increases and others decreases. For example, the number of points of the Netherlands almost doubled, whilst Portugal registered a decrease.

LUCAS points provide information about the land cover and land use of the sampled plot. To classify different types of agroforestry, we assumed that these systems always had a primary land cover (LC1) comprising a tree or shrub layer, and a secondary land cover (LC2) including other types of covers, such as crops, grass or, even, tree and shrub layers. The land use component of the LUCAS database includes information on whether the point has agricultural, forestry or other land uses. Kitchen gardens, for example, are considered as an individual land use.

Following instructions for surveyors (Eurostat, 2019a), land management could be classified as '*signs of grazing*', '*no signs of grazing*', or '*grazing not relevant*'.'*Signs of grazing*' was recorded when the surveyor observed cattle feeding; cattle infrastructure such as fences, stables, and drinking troughs; and/or dung or cattle trampling. Areas grazed during summer (transhumance) are also considered. If the land cover is suitable for grazing (croplands, woodlands, shrublands, grasslands, wetlands or bare lands) but no signs of grazing are visible, it is marked '*no signs of grazing*'. Finally, if the land cover is not suitable to be grazed (artificial or water areas) it must be assigned as '*grazing not relevant*'. In this way, the selection of certain combinations of primary and secondary land covers, as well as information on land use and management, enabled the identification of agroforestry points and their classification.

The LUCAS surveys in 2009, 2012 and 2015 also included information on woody linear features, which are examined along a 250 m transect running east from the observation point. Agricultural land with woody linear features, although a form of agroforestry, were not included in the present study because the converted length to area requires additional assumptions, and the lack of transect data collected in 2018 prevents a direct comparison between 2009 and 2018.

2.2 Classification of agroforestry systems

Agroforestry systems were classified in six principal classes: kitchen gardens, grazed permanent crops, intercropped permanent crops, silvoarable, silvopastoral, and agrosilvopastoral (Table 2). The classification was completed using the harmonised LUCAS database published by Palmieri et al. (2020). This has the advantage of reducing the complexity and layered nature of the original LUCAS datasets, avoiding inconsistencies and errors between legends and labels from one survey to the next. Furthermore, this harmonization corrected missing internal cross-references in the dataset, which limited the capacity to compute and link the observed variables (d'Andrimont et al., 2020).

Classification criteria were based on the combination of land covers LC1 and LC2, as well as on the presence of grazing and of kitchen gardens. The classification was developed so that the agroforestry classes were mutually exclusive, i.e., each point corresponds to only one single class.

Kitchen gardens are considered a form of agroforestry as they commonly combine temporary crops, permanent crops, and, sometimes, shrubs and grass. In order to avoid duplication, kitchen gardens were identified first and did not contribute to any other agroforestry category.

TABLE 1 Number of sample points of each LUCAS survey for each of 28 European countries over 4 years.

Country	Country code	2009 (EU23)	2012 (EU27)	2015 (EU28)	2018 (EU28)
Austria	AT	4,961	6,469	8,839	8,840
Belgium	BE	1,804	2,446	2,899	3,659
Bulgaria	BG		6,641	7,677	7,678
Croatia	HR			3,532	4,239
Cyprus	CY		1,442	1,726	2,313
Czechia	CZ	4,662	5,514	5,712	5,713
Denmark	DK	2,540	3,442	3,665	3,703
Estonia	EE	2,663	2,200	2,637	2,665
Finland	FI	19,895	13,476	16,116	16,182
France	FR	32,318	38,324	48,188	48,215
Germany	DE	21,113	24,939	26,598	26,777
Greece	EL	7,758	7,821	12,521	12,622
Hungary	HU	5,513	4,637	5,169	5,514
Ireland	IE	4,164	3,484	4,907	4,975
Italy	IT	17,790	20,985	28,693	28,294
Latvia	LV	3,825	4,420	5,374	5,376
Lithuania	LT	3,860	3,889	4,505	4,584
Luxembourg	LU	152	213	251	340
Malta	MT		79	79	79
Netherlands	NL	2,449	2,237	2,521	5,011
Poland	PL	18,487	21,797	22,980	23,086
Portugal	PT	5,423	7,332	9,006	7,168
Romania	RO		14,278	16,720	16,725
Slovakia	SK	2,898	2,455	2,755	2,898
Slovenia	SI	1,203	1,621	1,923	1,922
Spain	ES	29,912	35,377	50,281	45,314
Sweden	SE	26,656	22,420	26,648	26,709
United Kingdom	UK	14,438	12,214	16,803	17,253
Total		234,484	270,152	338,725	337,854

Next, LC1 with woody vegetation were divided in two groups (Table 2): a) permanent crops and b) woodlands, shrublands or grasslands with sparse tree cover.

The permanent crops category includes fruit trees, olive groves, vineyards, nurseries and industrial woody crops. Permanent crops have also been referred to in previous agroforestry studies as high value trees (den Herder et al., 2017) or multipurpose trees (Mosquera-Losada et al., 2018). Names for agroforestry systems involving permanent crops include *streuobst, près vergers*, and fruit-tree meadows or orchards (Mosquera-Losada et al., 2009). In this study, agroforestry systems incorporating permanent crops were categorised into grazed permanent crops and intercropped permanent crops.

The woodlands[1], shrublands[2] or grasslands with sparse tree cover[3] (LC1) were segregated into one of three categories. Grazed areas were classified as silvopastoral, including systems as forest

1 Areas covered by trees with a canopy of at least 10% (Eurostat, 2019b).

2 Areas dominated (at least 10% of the surface) by shrubs and low woody plants normally not able to reach more than 5 m of height. It may include sparsely occurring trees with a canopy below 10% (Eurostat, 2019b).

3 Land predominantly covered by communities of grassland, grass-like plants and forbs including sparsely occurring trees (the tree canopy is between 5% and 10% and the total of the tree + shrub canopy is between 5% and 20% of the area) (Eurostat, 2019b).

TABLE 2 Criteria used to classify the six agroforestry systems used in the analysis (class), based on the primary land cover (LC1) and the secondary land cover (LC2) defined by LUCAS. U = undetermined which means that any combination is possible but is not relevant for classification.

Class	LC1	LC1 code	LC2	LC2 code	Grazing	Land use
Kitchen gardens	U	U	U	U	U	113
Grazed permanent crops	Permanent crops	B71-B83, B84k, B84m, Bx2	U	U	Yes	—
Intercropped permanent crops	Permanent crops	B71-B83, B84k, B84m, Bx2	Temporary crops	B11 -B54, Bx1	No	—
Silvoarable	Woodlands	C10-C33	Temporary crops	B11-B54, Bx1	No	—
	Shrublands	D10-D20				
	Grasslands with sparse tree/shrub cover	E10				
Silvopastoral	Woodlands	C10-C33	Permanent crops Woodlands; Shrublands; Grasslands; Not relevant	B71- B83; B84k, B84m Bx2; D10-D20; E10-E30; 8	Yes	—
	Shrublands	D10-D20				
	Grasslands with sparse tree/shrub cover	E10				
Agrosilvopastoral	Woodlands	C10-C33	Temporary crops	B11-B54, Bx1	Yes	—
	Shrublands	D10-D20				
	Grasslands with sparse tree/shrub cover	E10				

grazing and wood pasture. Tree cover intercropped with temporary crops (LC2) were classified as silvoarable. Finally, silvopastoral systems combined with arable crops (LC2) were classified as agrosilvopastoral systems.

All of the agroforestry practices defined in the above process represent simultaneous agroforestry systems, where the tree and shrub component is present at the same time as the crop and/or livestock component. Sequential systems where, for example, afforested land is rotated with cropland were not considered.

2.3 Data analysis

The current state and spatial distribution of the agroforestry systems were analysed integrating the classified LUCAS points into a Geographical Information System (ArcGIS software by Esri, 2010) together with a layer of biogeographic regions of Europe. In this way, agroforestry classes were not only characterised by countries, but also by European bioclimatic regions (Alpine, Atlantic, Boreal, Black Sea, Continental, Macaronesia, Mediterranean, Pannonian and Steppic) (European Environment Agency, 2016). In addition, a more in-depth analysis on the dominant land covers for each agroforestry class was carried out.

The area of each agroforestry class for each country ($A_{AF,C}$; km^2) was estimated using the methodology described by den Herder et al. (2017), i.e., the number of classified points for that class in each country ($N_{AF,\,C}$) was divided by the total number of LUCAS points surveyed in the country (N_C) and multiplied by the surface area of the country (A_c; km^2) (Equation 1), using data from Eurostat (2013a):

$$A_{AF,C} = \frac{N_{AF,C}}{N_C} A_C \quad (1)$$

Additionally, the proportion of Utilised Agricultural Area (UAA) occupied by agroforestry systems was analysed by country, using data from Eurostat (2013b).

The above analysis was completed using data from the survey years 2009, 2012, 2015 and 2018. These results were then used to determine change between surveys using only countries with data from each of the four survey years, i.e., the 23 countries sampled in 2009 (EU23). Data from the new four countries included in the EU27 (Bulgaria, Cyprus, Malta and Romania; Table 1) were also analysed to find out how the extent of agroforestry changed in these territories between 2012 and 2018.

Additional studies were also completed on changes between the 'grazing', 'not grazed' and 'grazing not relevant' classifications and their relationship with the changes in agroforestry systems. It is important to note that grazing is one of the criteria used to classify silvopastoral, agrosilvopastoral and grazed permanent crops systems, and, therefore, it can be helpful in understanding changes.

Furthermore, we conducted a comprehensive analysis of the variation in the number of sampled points among the different LUCAS surveys (refer to Section 2.1) to determine whether these variations could impact the derived area of each agroforestry type. The objective of this analysis was to identify any disparities in the total number of points sampled in each land cover category (including artificial areas, temporary crops, permanent crops, woodlands, shrublands, grasslands, and other land cover types) across the various LUCAS surveys. Additionally, changes in the proportion of sampled points by land cover were also examined by country.

To explore the possible causes of changes, a more detailed analysis was carried out using common datum points. These are points that have the same geographical location between survey years. This analysis resulted in a smaller dataset as not all points are revisited from one survey to the next. The number of common points obtained by comparing the data from consecutive survey years was 184,603 for 2009–2012, 210,658 for 2012–2015, and 107,909 for 2015–2018. An analysis of the common points between the first and the last survey (2009 and 2018) is not reported because the resulting number of points classified as agroforestry was very low.

3 Results

3.1 Extent and spatial distribution of agroforestry in Europe

In 2018, the estimated surface area occupied by agroforestry in EU28 using the specified definitions was 114,621 km^2, which represented 3% of the total extent and 6% of utilised agricultural land[4] (UAA) (Table 3). In 2018, silvopastoral systems extended over 92,986 km^2 (5% of UAA) equivalent to 81% of the agroforestry area. Kitchen gardens occupied 16,687 km^2, about 15% of the agroforestry area (1% of UAA), and grazed permanent crops covered 3,434 km^2 (about 3% of the agroforestry and 0.2% of UAA). Silvoarable and intercropped permanent crops only covered 676 km^2 and 587 km^2 respectively, representing less than the 1% of the agroforestry and about 0.04% of UAA. Finally, agrosilvopastoral systems only occupied 251 km^2 (0.1% of the agroforestry area) (Table 3).

Spain was the country with the largest area of agroforestry (33,230 km^2), followed by Greece (16,089 km^2) and France (12,103 km^2). These three countries together accounted for 54% of the agroforestry in the EU28 in 2018. The proportions in Italy and Portugal were 8% and 7%, respectively (Table 3). When expressing the surface area occupied by agroforestry systems as a percentage of UAA (Table 3), the highest value of 30% was in Greece. Agroforestry systems occupied more than 20% of UAA in Portugal, and more than 12% in Cyprus, Sweden, Spain, and Slovenia. At the other extreme are countries like Poland, Denmark, Germany, Netherlands, the United Kingdom, Lithuania, and Hungary with less than 3% of their UAA occupied by the six types of agroforestry examined.

3.1.1 Silvopastoral and agrosilvopastoral systems

In 2018, silvopastoral (n = 7,805 points) was the most frequent agroforestry class and Spain was the country with the largest share (34%), followed by Greece (16%), France (11%), Italy (7%) and Portugal (7%). These five countries together represented approximately 61% of the total agroforestry area and 75% of the total silvopastoral area (Table 3). The proportion of European silvopastoral agroforestry in the Atlantic and Continental regions were 14% and 12% respectively (Figure 1; Supplementry Table S1).

The main types of land covers found in silvopastoral systems were broadleaved woodland (38%), followed by grasslands with sparse tree or shrub cover (26%) and shrublands without and with sparse tree cover (17% and 10%, respectively) (Supplementry Table S2). In all biogeographical regions, the dominant land cover was grasslands with sparse tree or shrub cover, except for the Mediterranean region, where broadleaved woodland was dominant (45%). Within broadleaf woodland in the Mediterranean region, 68% of the area was broadleaved evergreen forest and 21% was thermophilous deciduous forest (Supplementry Table S2).

Agrosilvopastoral systems (n = 21 points) were only recorded in Mediterranean regions (Supplementry Table S1), split between Portugal (51%), Spain (45%) and Italy (4%) (Table 3). As there were very few points, agrosilvopastoral systems were added to the silvopastoral total in the remaining temporal analyses.

3.1.2 Silvoarable systems

Silvoarable systems (n = 56 points) were only identified in a small number of European countries, with 48% of the area in Spain and 38% in Portugal. Smaller shares were present in France (4%), Italy (3%), Finland (3%), Hungary (3%) and Austria (1%) (Table 3). Silvoarable was mainly found in the Mediterranean region (88%; Figure 1, Supplementry Table S1), where broadleaved woodlands dominate, in combination with cereal crops.

3.1.3 Grazed and intercropped permanent crops

Agroforestry where permanent crops form the main land cover (n = 344 points) could be associated with grazing or with intercrops, with the area associated with grazing being about six-times greater than the area associated with intercrops. The share of grazed permanent crops was unevenly distributed in the EU within Greece and Romania representing 27% and 19% of its total. Moderate shares are found in Germany (11%), Spain (9%), France (9%), Portugal (7%) and Italy (6%). The remaining countries represented less than 13% of total area (Table 3). The highest amounts of intercropped permanent crops were found in Italy (22%), Spain (19%), Greece (14%) and Portugal (13%). The proportions found in Poland, France, Cyprus, Romania, Austria, Czechia and Croatia were less than 7%, and this class was not found in the rest of the EU28 (Table 3).

By biogeographical regions, permanent crops were more characteristic of Mediterranean (57%) and Continental (30%) areas than the rest of the bioregions (Figure 1, Supplementry Table S1). Predominant crops were olive groves in Mediterranean countries; apple orchards in Alpine, Atlantic, Boreal and Continental areas; and nut orchards in the Pannonian region (Supplementry Table S3). Regarding intercropped permanent crops, cereals were the main temporary crop (41%), followed by fodder crops and dry pulses, vegetables, and flowers, representing 25% and 23%, respectively (data not included).

3.1.4 Kitchen gardens

Kitchen gardens (n = 1,266 points) were identified in all countries, with the largest areas found in Romania (13% of total), followed by Italy (11%), France (10%), Poland (9%), Germany (7%), Hungary (6%), Spain (6%) and Czechia (6%). The highest share of kitchen gardens was found in the Continental bioregion (40% of total), followed by the Mediterranean (20%). Smaller proportions

4 In 2018, following data of Eurostat, the total extent of utilised agricultural land for the EU28 was 1,791,446 km2.

TABLE 3 Area of six agroforestry classes for the survey year 2018, and proportion of agroforestry by country (AF) in relation to total surface area occupied by agroforestry systems in Europe, as well as to utilised agricultural area (UAA) of each country. Data are ordered according to the proportion of AF. GPC = grazed permanent crops, IPC = intercropped permanent crops, ASP = agrosilvopastoral, KG = kitchen gardens.

Country	Area (km^2)							Proportion (%)	
	GPC	IPC	Silvo-arable	Silvo-pastoral	ASP	KG	Total AF	AF	UAA
Spain	324	112	324	31,366	112	994	33,230	29.0	13.7
Greece	908	83	0	14,743	0	355	16,089	14.0	30.4
France	318	40	26	10,091	0	1,629	12,103	10.6	4.2
Italy	203	128	21	6,555	11	1,751	8,669	7.6	6.7
Portugal	244	77	257	6,536	129	579	7,823	6.8	21.8
Romania	656	29	0	4,576	0	2,152	7,412	6.5	5.5
Sweden	17	0	0	4,774	0	218	5,009	4.4	16.7
United Kingdom	14	0	0	3,669	0	184	3,867	3.4	2.3
Bulgaria	101	0	0	2,414	0	549	3,065	2.7	6.1
Germany	361	0	0	1,188	0	1,188	2,737	2.4	1.6
Poland	27	41	0	392	0	1,473	1,932	1.7	1.3
Finland	0	0	21	1,129	0	690	1,840	1.6	8.1
Hungary	17	0	17	304	0	1,012	1,349	1.2	2.5
Czechia	41	14	0	248	0	966	1,270	1.1	3.6
Ireland	0	0	0	1,195	0	14	1,209	1.1	2.7
Austria	19	19	9	816	0	294	1,158	1.0	4.4
Croatia	13	13	0	788	0	240	1,055	0.9	7.1
Slovakia	0	0	0	169	0	761	931	0.8	4.8
Lithuania	43	0	0	85	0	612	741	0.6	2.5
Slovenia	53	0	0	411	0	158	622	0.5	13.0
Latvia	12	0	0	132	0	469	613	0.5	3.2
Belgium	25	0	0	293	0	151	469	0.4	3.5
Denmark	0	0	0	359	0	58	417	0.4	1.6
Netherlands	22	0	0	298	0	22	343	0.3	1.9
Estonia	0	0	0	170	0	119	289	0.3	2.9
Cyprus	16	32	0	152	0	28	228	0.2	17.2
Luxembourg	0	0	0	118	0	13	131	0.1	5.8
Malta	0	0	0	0	0	8	8	0.0	6.9
EU28	3,434	587	676	92,986	251	16,687	114,621	100	6.4
% AF EU28	3.00	0.51	0.59	81.12	0.22	14.56	100	—	—
% EU28	0.08	0.01	0.02	2.08	0.01	0.37	2.56	—	—
% UAA EU28	0.19	0.03	0.04	5.19	0.01	0.93	6.40	—	—

were reported in the Atlantic (13%), Boreal (11%), Pannonian (7%) and Alpine (6%) bioregions (Figure 1; Supplementry Table S1).

Kitchen gardens is a land use where different land covers are combined. Among these kitchen gardens, those with permanent crops (mainly apple trees) combined with grasslands, were predominant (45%). They were mostly located in Alpine, Atlantic, Boreal, Continental, Pannonian, and Black Sea bioregions. In contrast, kitchen gardens where temporary crops (mostly dry pulses, vegetables, and flowers) were the predominant land cover, dominated in the Mediterranean and Steppic bioregions (37%). They were followed by kitchen gardens with permanent crops associated with grasslands (25%) (Supplementry Table S4). Only 2% of kitchen gardens were grazed.

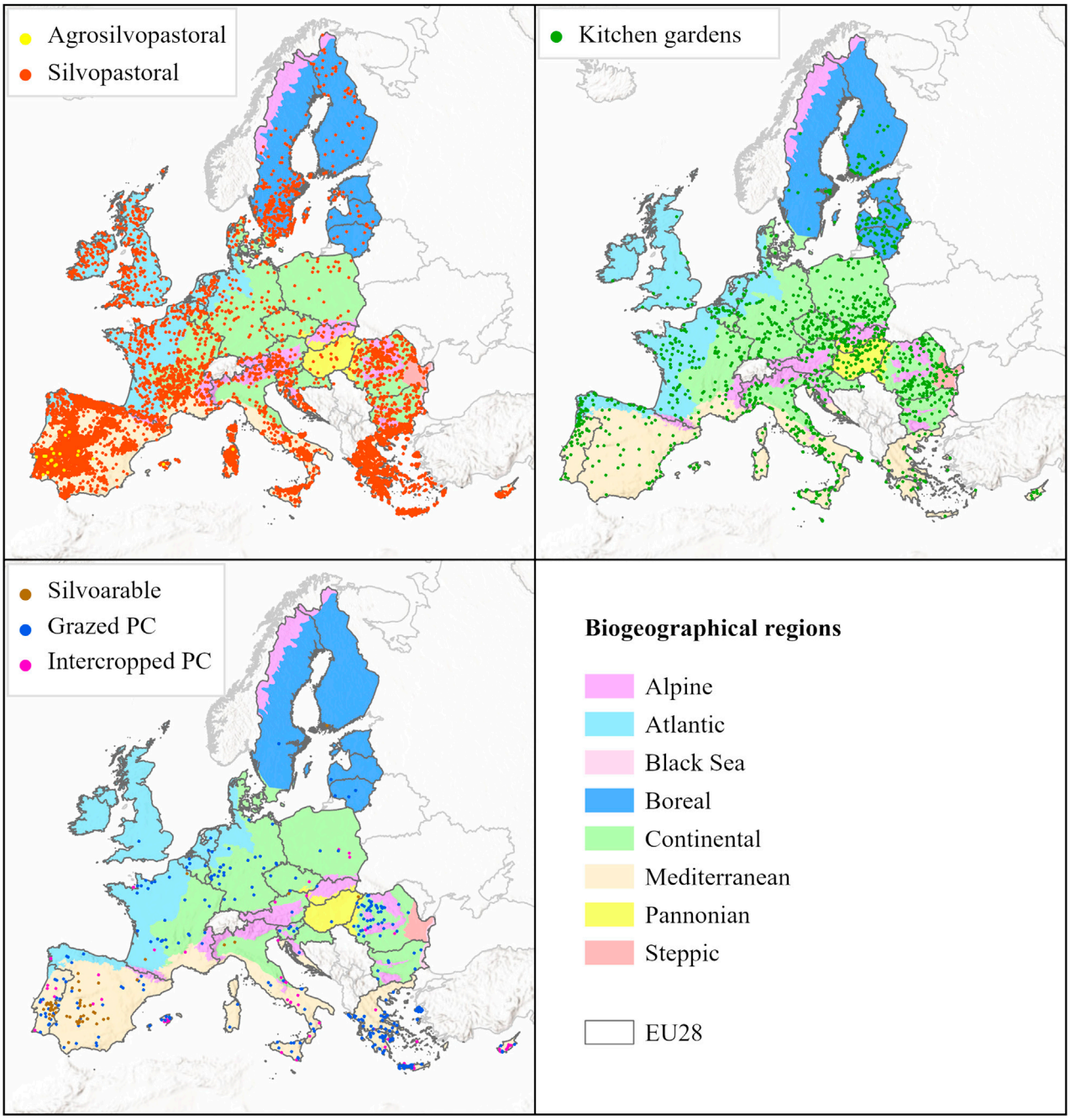

FIGURE 1
Spatial distribution of agroforestry classes in EU28 for the survey year 2018. PC = permanent crops. Bioregion data source: https://www.eea.europa.eu/data-and-maps/data/biogeographical-regions-europe-3.

3.2 Change in the extent of agroforestry

The estimated area of agroforestry systems, based on our initial analysis of the data, increased by 55% between 2009 and 2012, but decreased by 26% from 2012 to 2015, and by 22% from 2015 to 2018. The overall estimated change between 2009 and 2018 was a decrease of 12,278 km^2 or 11% (Table 4). Countries not included in this analysis because they did not belong to the EU23 (Bulgaria, Cyprus, Malta, and Romania) also showed an approximate halving of the agroforestry area from 21,769 km^2 in 2012 to 10,713 km^2 in 2018.

The initial data analysis indicated that the areas of silvopastoral systems, the most common type of agroforestry, increased by 59,782 km^2, i.e., 63%, between 2009 and 2012 (Table 4). By contrast, there was a 27% reduction between 2012 and 2015, and by 25% from 2015 to 2018. The area of grazed permanent crops also increased by 40% between 2009 and 2012, followed by a 32% decline from 2012 to 2015, and a 47% decline from 2015 to 2018 (Table 4). Ungrazed agroforestry land uses, such as intercropped permanent crops, silvoarable and kitchen gardens, also increased from 2009 to 2012, but less than

TABLE 4 Area and proportional area changes of five types of agroforestry system for four surveys or four time periods between 2009 and 2018. Data include only countries (EU23) common for each year. The proportional changes are with respect to the initially stated survey year.

Agroforestry systems	Area (km^2)				Proportional change (%)			
	2009	2012	2015	2018	2009–2012	2012–2015	2015–2018	2009–2018
Grazed PC	5,198	7,287	4,953	2,648	40.2	−32.0	−46.5	−49.1
Intercropped PC	1,103	1,255	566	513	13.8	−54.9	−9.3	−53.4
Silvoarable	752	973	591	676	29.4	−39.3	14.4	−10.0
Silvopastoral	95,293	155,075	113,717	85,307	62.7	−26.7	−25.0	−10.5
Kitchen gardens	12,786	14,086	12,490	13,709	10.2	−11.3	9.8	7.2
Agroforestry	115,132	178,674	132,317	102,854	55.2	−25.9	−22.3	−10.7

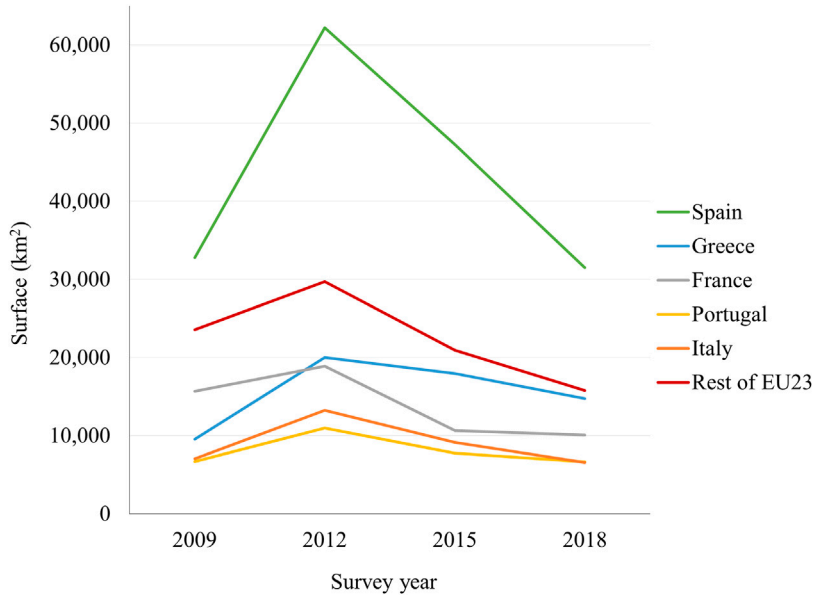

FIGURE 2
Surface extent of silvopastoral systems for survey years 2009, 2012, 2015 and 2018 in EU23.

the two grazed agroforestry types. Intercropped permanent crops showed a decrease of 53% between 2009 and 2018, and the reduction in grazed permanent crops was 49%. Between 2009 and 2018, the area of silvoarable systems was estimated to decline by 10%, whereas the area of kitchen gardens increased by 7% (Table 4).

Figure 2 illustrates the changes which took place between 2009 and 2018 in silvopastoral for selected countries. The surface area occupied by this class in Spain almost doubled between 2009 and 2012 with values of 32,766 and 62,231 km^2, respectively (Supplementry Table S5). The resulting difference of 29,465 km^2 makes up about half of the total increase of silvopastoral agroforestry between these two survey years (59,782 km^2, Table 4). In all other countries silvopastoral agroforestry recorded an increase between 2009 and 2012 and most of them registered a decrease thereafter (2012–2018).

If the period as a whole is considered, marked differences can be observed between EU23 nations (Figure 2), with Greece being the only Mediterranean country where there was a substantial increase in silvopastoral agroforestry (+54%). Other countries recorded a net increase, but this is not readily apparent in Figure 2 because the total extent of silvopastoral was small in Estonia (+233%), Denmark (+136%), Luxembourg (+101%), Austria (+42%), Netherlands (+30%), Sweden (+32%) and Finland (+21%). Non-Mediterranean countries with notable decreases were United Kingdom (−68%), Hungary (−67%), Lithuania (−58%), Slovakia (−44%), Germany (−38%) and France (−36%) (Supplementry Table S5). Overall, these data indicate an increase of silvopastoral systems in some northern European countries, whereas a decrease was generally observed in southern Europe, except for Greece. New member states included in EU27 (Bulgaria, Cyprus, Romania, Malta) also presented a decrease of silvopastoral

TABLE 5 Area and proportional change in the area of agroforestry systems from 2009 to 2018. Data include the EU23 countries sampled in 2009, and the four new countries included in the EU27 in 2012. The proportional differences presented are with respect to the previous survey year. Data are ordered by the change between 2009 and 2018.

Country	Area km^2				Proportional change (%)			
	2009	2012	2015	2018	2009–2012	2012–2015	2015–2018	2009–2018
Denmark	152	224	164	417	47.6	−27.0	154.5	174.4
Estonia	136	268	327	289	96.7	21.9	−11.5	112.3
Luxembourg	68	73	41	131	7.0	−43.4	217.3	92.1
Finland	1,038	1,733	1,008	1,840	67.0	−41.8	82.6	77.3
Belgium	323	514	423	469	59.2	−17.7	10.9	45.3
Greece	11,187	21,974	18,921	16,089	96.4	−13.9	−15.0	43.8
Sweden	3,743	4,909	6,397	5,009	31.2	30.3	−21.7	33.8
Slovenia	472	663	622	622	40.5	−6.2	0.1	31.9
Latvia	473	628	541	613	32.9	−13.9	13.3	29.6
Lithuania	575	839	681	741	46.0	−18.9	8.7	28.8
Netherlands	275	384	311	343	39.9	−19.0	10.2	24.9
Poland	1,789	2,318	2,280	1,932	29.6	−1.6	−15.3	8.0
Austria	1,082	2,178	2,069	1,158	101.3	−5.0	−44.0	7.0
Portugal	8,214	12,981	9,309	7,823	58.0	−28.3	−16.0	−4.8
Spain	35,878	66,164	49,923	33,230	84.4	−24.5	−33.4	−7.4
Slovakia	1,015	1,278	1,068	931	25.9	−16.5	−12.9	−8.3
Italy	10,188	16,842	11,844	8,669	65.3	−29.7	−26.8	−14.9
Czechia	1,540	1,702	1,781	1,270	10.6	4.6	−28.7	−17.5
Ireland	1,512	2,750	1,425	1,209	81.9	−48.2	−15.2	−20.0
Germany	3,607	4,144	3,697	2,737	14.9	−10.8	−26.0	−24.1
Hungary	1,923	1,103	1,206	1,349	−42.6	9.3	11.9	−29.8
France	18,116	21,858	12,865	12,103	20.7	−41.1	−5.9	−33.2
United Kingdom	11,826	13,145	5,414	3,867	11.2	−58.8	−28.6	−67.3
EU23	115,132	178,674	132,317	102,843	55.2	−25.9	−22.3	−10.7
Country		2012	2015	2018		2012–2015	2015–2018	2012–2018
Malta		8	0	8		−100.0	797.5	−0.3
Romania		11,504	7,985	7,412		−30.6	−7.2	−35.6
Bulgaria		9,493	4,323	3,065		−54.5	−29.1	−67.7
Cyprus		764	145	228		−81.0	57.5	−70.1
Total		21,769	12,452	10,713		−42.8	−14.0	−50.8

systems surface between 2012 and 2018 (−59%; Supplementry Table S5).

Regarding kitchen gardens, the countries with the largest share in 2018 showed diverse changes along the study period, with Italy, Poland and Hungary recording an increase of 9%–21%, whereas France, Germany, Spain and Czechia recorded area losses between 11% and 23% for this type of system. Most countries showed increases (Supplementry Table S6).

In the case of grazed and intercropped permanent crops and silvoarable agroforestry, the main changes between 2009 and 2018 took place in countries with the highest share of the area of each practice. Thus, the calculated area of grazed permanent crops decreased in Mediterranean countries such as Spain, Italy, Portugal and Greece, while in Germany an increase of 18% was estimated. The area of intercropped permanent crops declined in Spain, Italy and Portugal by around 70%, but increased by about 25% in Greece.

Finally, silvoarable agroforestry declined by 23% in Spain, whereas an increase of 116% was observed in Portugal.

Overall, in the Mediterranean bioregion, where 64% of agroforestry systems were reported in 2018, between 2009 and 2018 a decrease in agroforestry occurred in countries such as Italy (15%), Spain (7%) and Portugal (5%), while in Greece an increase was registered (44%) (Table 5). Within a country, the greatest proportional declines in agroforestry area were observed in the United Kingdom (−67%), followed by France (−33%), Hungary (−30%), Germany (−24%), Ireland (−20%) and Czechia (−18%) (Table 5). By contrast, the greatest proportional increases in the agroforestry area were recorded in Denmark (174%), Estonia (112%) and Luxembourg (92%) (Table 5), but their overall share of agroforestry systems in 2018 was very low at less than 1% (Table 3). The increase in the agroforestry areas in Sweden, Poland and Finland were associated with an increase in the area of silvopastoral systems and kitchen gardens. Although the area of silvopastoral and silvoarable systems declined in the United Kingdom, France, Germany, Poland and Lithuania, there were increases in the area of grazed or intercropped permanent crops. Spain was the only country that showed a decrease of all types of agroforestry systems.

3.2.1 Analysis of the causes of variations

The observed variations in agroforestry area between 2009 and 2018 could be related to a number of causes. They could be due to the implementation of the survey, such as the number of survey points and the criteria used by the observers in the different surveys, and/or real changes of land cover and land use.

The number of sampled points varied depending on the survey year, both the total number of sampled points and the points per country (see Section 2). An additional analysis was completed to determine if this variation could affect the surface estimation of each agroforestry type. Examining high level categories such as 'woodlands, shrublands and grasslands with sparse tree cover' indicated point number changes of only −4% to −3%, temporary crops showed a variation of about −3% to 3%, and the number of permanent cropping points varied between −2% and 1% (data not presented). The results suggested that sample point number variations did not explain the land use changes in agroforestry.

To examine the causes that generate changes of land cover/land use in agroforestry systems, an analysis was completed using only common points. Table 6 presents the net balance (difference between percentage gains and losses) for the different agroforestry systems, indicating an increase of 10% for the silvopastoral category between 2009 and 2012, and declines of 12% for 2012–2015 and 11% for 2015–2018. These results follow the same trends as observed with the total number of classified points, i.e., an increase of silvopastoral surface from 2009 to 2012, followed by a decrease from 2012 to 2018 (Table 4). Hence the common points analysis shows that the changes observed with the full dataset were also occurring with the common points. The changes in the area of grazed and intercropped permanent crops also showed similar results with those obtained in the analysis with all data since losses were estimated for 2012–2015 and 2015–2018 periods (Table 6).

The proportion of common point numbers relative to the total number of survey points for each survey year and each agroforestry type (Table 7) provides an estimate of the representativeness of the common points analysed. The common points represented more than 62% of the total points for the periods 2009–2012 and 2012–2015. By contrast the common points represented only between 18% and 49% of the total number of points in the 2015–2018 period, suggesting that changes in location could be more significant in this final period. However, even with a lower proportion of common points, the analysis indicates that real changes took place in the area of agroforestry systems.

TABLE 6 Net balance of the number of points of the different agroforestry types between survey years.

	Net balance (%)		
	2009–2012	2012–2015	2015–2018
Silvopastoral	9.7	−12.0	−10.8
Kitchen gardens	−0.7	7.5	6.7
Grazed permanent crops	9.8	−6.2	0
Intercropped permanent crops	1.7	−29.3	−15.6
Silvoarable	0	−6.7	14.6
Total	8.6	−8.9	−8.3

The next step was to examine the reason for changes in the proportion of silvopastoral and grazed permanent crops systems using the common points dataset (Table 8). From 2009 to 2012, for the same land cover, 10% of silvopastoral sites changed from 'grazing not relevant' to 'grazed' compared to only 0.1% of sites changing from 'grazed' to 'grazing not relevant', and our analysis indicates that it is this change that is primarily responsible for the increase in the silvopastoral area from 2009 to 2012. By contrast for the period 2012–2015 the proportion of sites changing from 'grazed' to 'non-grazed' (28%) was greater than the change from 'non-grazed' to 'grazed' (18%). Similar changes were apparent in 2015–2018. In 2012–2015 and 2015–2018, no changes in 'grazing not relevant' were reported for silvopastoral systems. Grazed permanent crops showed similar changes to those for silvopastoral systems, i.e., most gains were linked with changes from 'non-grazed' to 'grazed' and losses were related with the cessation of grazing (Table 8). In general, losses of silvopastoral or grazed permanent crops due to land cover change were relatively small. The question as to whether there were real changes in grazing or changes in methodological criteria is addressed in the next section.

Regarding the ungrazed intercropped permanent crops and silvoarable systems, the main sources of variation were related with changes of temporary crops, i.e., most gains and losses were associated to changes of temporary crops from/to other land cover (data not presented here). In the case of kitchen gardens, the gains and losses were primarily related to changes between land uses, mainly from/to agricultural use (data not presented here).

3.2.2 Analysis of 'grazing' criteria

The area of grazed agroforestry systems (silvopastoral and grazed permanent crops) increased by 73% between 2009 and 2012 and decreased by 43% from 2012 to 2018 (Table 4). In order to determine if the change between 2009 and 2012 was related to the field criteria for detecting grazing, we determined

TABLE 7 Proportion of common points with respect to the total number of points for each survey year.

Analysis of common points	Proportion of common points (%)					
	2009–2012		2012–2015		2015–2018	
Survey years	2009	2012	2012	2015	2015	2018
Silvopastoral	98.7	62.4	77.7	65.7	31.7	38.8
Kitchen gardens	97.3	78.3	89.8	92.2	32.5	33.0
Grazed permanent crops	98.0	70.3	89.6	88.2	18.2	36.1
Intercropped permanent crops	100	76.1	93.2	90.6	49.1	44.4
Silvoarable	100	62.9	84.3	91.2	33.3	44.6
Agroforestry systems	98.7	64.1	88.5	75.1	31.3	38.1

TABLE 8 Proportion of silvopastoral and grazed permanent crops systems in EU23 showing changes between land cover (LC) and grazing status including grazing, grazing not relevant (GNR), and not grazed for three periods.

Balance	Drivers	Proportion of total (%)					
		Silvopastoral			Grazed permanent crops		
		2009–2012	2012–2015	2015–2018	2009–2012	2012–2015	2015–2018
No change		32.1	41.5	36.0	15.7	23.7	19.4
Gain	Same LC, from not grazed	20.9	17.9	22.4	33.5	28.0	31.7
	Same LC, from GNR	10.4	0.0	0.0	4.6	0.0	0.0
	Changed LC maintaining grazing	4.0	3.2	2.3	2.9	3.5	5.8
	Changed LC and not grazed	2.2	2.0	1.9	4.1	2.3	2.9
	Changed LC and GNR	1.3	0.2	0.0	1.8	0.3	0.0
	Other	0.0	0.0	0.0	0.2	0.7	0.0
	Sub-total	38.8	23.3	26.6	47.1	34.8	40.3
Loss	Same LC, to not grazed	21.3	28.3	32.1	31.7	34.5	33.8
	Same LC, to GNR	0.1	0.0	0.0	0.0	0.0	0.0
	Changed LC, maintaining grazing	4.6	4.0	2.5	2.3	2.2	1.4
	Changed LC and not grazed	3.0	2.8	2.7	2.7	4.4	4.3
	Changed LC and GNR	0.1	0.2	0.1	0.0	0.3	0.7
	Other	0.0	0.0	0.0	0.5	0.2	0.0
	Sub-total	29.1	35.3	37.4	37.2	41.5	40.3
Total		100	100	100	100	100	100

the proportion of points categorised as 'grazing', 'not grazed' and 'grazing not relevant' for each period using the complete LUCAS dataset for the EU23 (Figure 3). Between 2009 and 2012, a reduction on the proportion of 'grazing not relevant' (−23%) was associated with an increase in the proportion of points classified as 'grazing' (+2%) and 'not grazed' (+20%). However after 2012, 'grazing not relevant' remained stable, and the 'grazing' area declined back to 9%.

Using common points classified as 'grazing not relevant' between 2009 and 2018, we observed that 7% and 51% of the points classified in 2009 as 'grazing not relevant' changed in 2012 to 'not grazed' and 'grazing' respectively (Table 9). In the two subsequent periods, the proportions changing from 'grazing not relevant' were much lower, and when this occurred, a higher proportion was classified as 'not grazed'. The percentage of points changing from 'grazing not relevant' to 'grazing' was less than 0.5% in both periods.

Instructions in the LUCAS manuals (Eurostat, 2019a) indicate that only the land covers *artificial lands* or *water areas* should be classified as 'grazing not relevant', that is, those land covers not susceptible to be grazed or land covers where there is nothing to be grazed (Eurostat, 2019a). However, in 2009 and 2012 there were many points with land covers that could be grazed such as grasslands, permanent crops, shrublands, temporary crops or woodlands, which

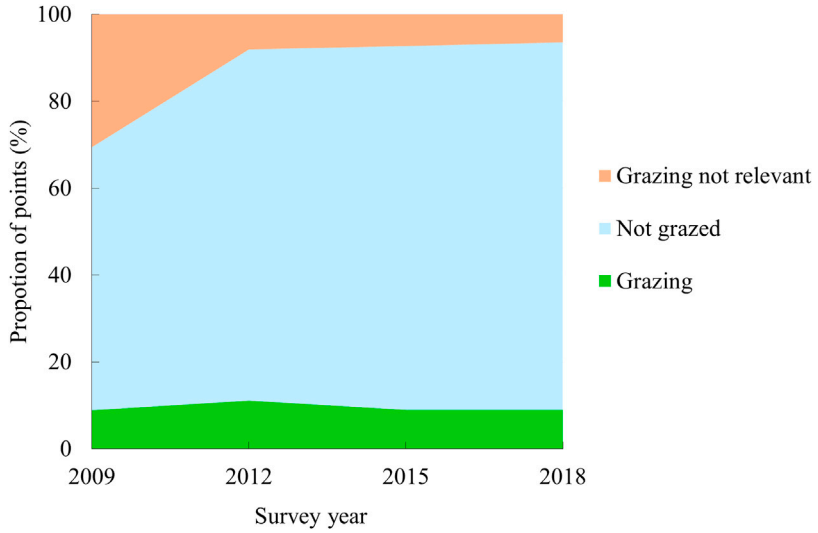

FIGURE 3
Proportion of three grazing classes in the sampled LUCAS data points in 2009, 2012, 2015, and 2018.

TABLE 9 Changes from 'grazing not relevant' to 'grazing' and to 'not grazed' points based on common points for three survey periods.

Survey years	Proportion of 'grazing not relevant' points (%)		
	To grazing	To not grazed	Not changed
2009–2012	7.2	50.8	42.1
2012–2015	0.4	8.6	91.0
2015–2018	0.1	21.3	78.6

were incorrectly classified as 'grazing not relevant' (n = 60,622 points; Supplementry Table S7). This means that these land covers, which could have been 'grazing', 'not grazed' and 'grazing not relevant' in 2009, were incorrectly classified as 'grazing not relevant', and some of these could have been 'grazed' points.

Hence there are grounds to argue that our initial estimate for agroforestry in 2009 is an underestimate, specifically for the grazed classes. Adding back in the 7% of all points that changed from 'grazing not relevant' to 'grazing' between 2009 and 2012 would result in a higher grazed area in 2009 of 570,034 km^2 rather than 344,410 km^2 (Table 9; Figure 4A). Applying this correction results in a more consistent decline in the area of grazing in Europe between 2009 and 2018 (Figure 4A).

Applying a similar correction to the area of silvopastoral agroforestry would increase the area estimate of silvopastoral agroforestry in 2009 from 95,293 km^2 to 172,700 km^2 (Figure 4B). This correction also results in a more consistent decline in the area of silvopastoral agroforestry. The periods after 2012 do not need a correction because no significant changes of 'grazing not relevant' to 'grazing' were identified. The same correction can be applied to grazed permanent crops. In this case, 5% of the points classified in 2012 were related with changes from 'grazing not relevant' to 'grazing' (Table 8). Therefore, the updated area estimated for 2009 was 5,661 km^2 and the increment between 2009 and 2012 was reduced by 12% (Figure 4B). Finally, the total surface of agroforestry systems would also increase in 2009 if we consider the corrected values, occupying an area of 193,002 km^2 instead of 115,132 km^2. In this case, the surface loss of agroforestry between 2009 and 2018 would be 47%.

This reduction in the area of grazing is also evident in official statistics from Spain, Greece and the United Kingdom. In Spain, data from the 2009 and 2020 agricultural census (INEbase, 2011; INEbase, 2022) indicated a 21% reduction in the number of farms with extensive livestock (cattle excluding dairy cows, sheep, goats and pigs), while the number of animal heads increased by 14%. This indicates an increase of the stocking rate, as well as farm abandonment, although farms may also have merged. In Greece, according to data from Hellenic Statistical Authority (2019), between 2009 and 2018 livestock farms (cows, sheep, goats and pigs without differentiating between stabled and extensive cattle) and the number of animals decreased by 37% and 13% respectively, suggesting a reduction in grazing. In the United Kingdom, statistics published by the Government's Department of Environment, Food and Rural Affairs (2022) on land use in agricultural holdings with grazing activities indicated a surface loss between 2009 and 2018 of 2%. These values are not directly comparable with those obtained using LUCAS surveys but they could inform our understanding of the dynamics of the grazed area in Europe between 2009 and 2018.

4 Discussion

The results of this paper are discussed in terms of the challenge of determining the changes in agroforestry area in Europe between 2009 and 2018 and the implications for the use of LUCAS data, as well as the extent of different agroforestry types in 2018 and the implications of previous trends on the anticipated area of agroforestry in Europe in future years. Additionally, the factors that have generated the main changes in the surface area of each

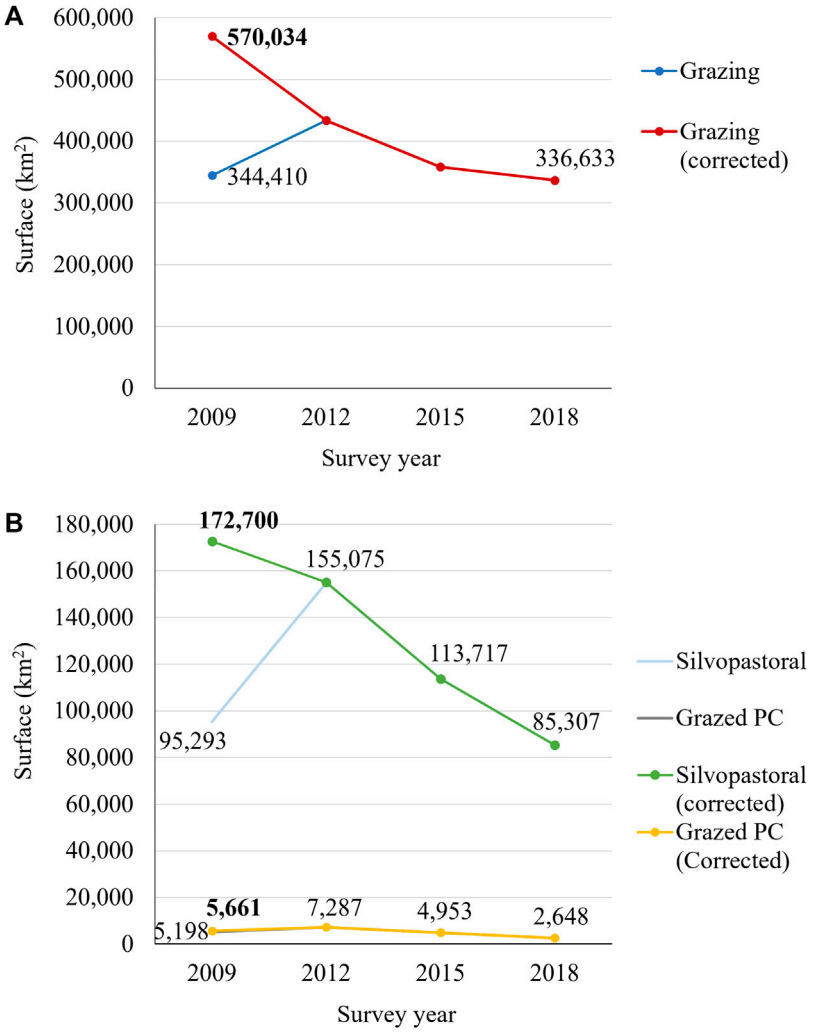

FIGURE 4
Changes of **(A)** the extent of grazing across the EU23, and **(B)** the extent of grazed agroforestry systems between 2009 and 2018 applying the correction of the points classified as grazing not relevant. PC = permanent crops.

agroforestry systems and the current trend to re-establish the link between trees and food production at a farm level are also addressed.

4.1 Changes in the agroforestry area in Europe from 2009 to 2018

An initial analysis of the LUCAS results suggested that the area of agroforestry in the EU23 was 115,132 km^2 in 2009, it then increased by 55% to reach 178,674 km^2 in 2012, before declining by 26% to reach 132,317 km^2 by 2015, and a decline by 22% to reach 102,854 km^2 by 2018. However more detailed analysis suggests that some of these large changes are due to methodological problems in the 2009 LUCAS survey. In 2009, some points were incorrectly classified as 'grazing not relevant'. The guidance for LUCAS indicates that 'grazing not relevant' should only correspond to areas that cannot be grazed, such as urban areas or water bodies. However common point analysis showed that points classified in 2009 as 'grazing not relevant' represented land covers that could be grazed such as woodland and shrubland, and in the following surveys (2012–2018) such areas were either assigned as 'grazing' or 'not grazed'. If a correction to the 2009 data is made, then the updated predicted area of agroforestry in 2009 is 193,002 km^2. This corrected value also results in a more consistent pattern of declining areas of agroforestry between 2009 and 2018, driven primarily by reduced grazing (Figure 4).

The above analysis, suggests that the estimates made by den Herder et al. (2017) for the EU27, using the 2012 data are still valid. Den Herder et al. (2017) estimated the total area occupied by agroforestry (excluding kitchen garden) in the EU27 of 154,000 km^2 using LUCAS data from 2012, and Mosquera-Losada et al. (2018) estimated an area (including kitchen gardens and grazed shrublands without sparse tree cover) of 197,700 km^2 using the same data. Within this study, for the same survey year and for the same countries we calculate an area of 200,443 km^2, including kitchen gardens and grazed shrublands without sparse tree cover in a similar way to Mosquera-Losada et al. (2018). Obviously, both results are similar as identical classes were considered, with the

minor variations probably resulting from the use of a harmonised data set in our study which was not previously available.

4.2 Implications for the analysis of LUCAS data

The above results demonstrate the importance of a consistent method for establishing grazing in the LUCAS dataset. If agroforestry areas are defined as areas where there are ecological and economic interactions between trees or shrubs and either crop and/or animals (Burgess and Rosati, 2018), then some criterion is needed to establish if, for example, the level of grazing is significant. Whilst the criterion for 'grazing not relevant' is relatively clear, judging between 'grazing' and 'no-grazing' is not easy and as demonstrated in this paper, the dividing line can have large effects on the estimated area of agroforestry if grazing is considered a necessary part of agroforestry involving livestock. For example, Jensletten and Klokov (2002) estimated that the area of reindeer husbandry in Northern Europe, which could be considered as agroforestry, was 410,000 km^2, which is about four-times the total area of agroforestry in the EU28 of 114,621 km^2 derived in our study from LUCAS in 2018. In the main, areas of reindeer husbandry in northern Sweden and Finland are not included as the evidence of grazing at individual sample points was insufficient. In addition, as described by den Herder et al. (2017), the level of sampling in mountainous and remote areas tend to be underrepresented in the LUCAS survey.

The analysis highlights that paired samples commonly assessed in 2015 and 2018 represented only 31%–38% of the total number of samples in each year, which means that some of the inter-annual variation could be due to changes in sample point location. This should not be a problem if a land type is common, but it could be important for less abundant land classes. Therefore, whilst analyses of common points are useful, analysis of real land use change could be clearer if LUCAS would maintain consistency in the number and location of the survey points.

4.3 Geographical variations in the total area and change in agroforestry

In 2018, using the LUCAS dataset, we calculated that the six defined agroforestry types in the EU28 (Table 3) occupied 114,621 km^2, which represents 6% of utilised agricultural area (UAA). However, this paper demonstrates a consistent decrease in the area of agroforestry in the EU23 between 2009 and 2018. Although we did not recalculate a change in agroforestry per country between 2009 and 2012 to account for the reclassification of 'grazing not relevant', Spain which accounted for 40% of the EU28 agroforestry area in 2012, represented about 44% of the reduction that occurred between 2012 and 2018 (Table 5). Other than Spain, the two countries demonstrating the greatest loss in agroforestry between 2012 and 2018 were the United Kingdom (−70%) and Ireland (−56%). By contrast between 2012 and 2018, the calculated area of agroforestry increased in Hungary, Luxembourg, and Denmark. Some of the decline in the United Kingdom and Ireland may be related to the increased use of permanent housing for livestock, driven in part in the dairy sector by the greater use of automated milking (Barkema et al., 2015).

4.4 Explaining the decline in silvopastoral systems

Silvopastoral was the most common agroforestry practice accounting for 81% of the agroforestry area and 5% of UAA of the EU28 in 2018. Silvopastoral agroforestry has different compositions depending on bioclimatic conditions. Thus, in the Atlantic bioregion, about 27% of silvopastoral systems comprise grazed shrublands without sparse tree cover, and 32% comprise grassland with sparse trees or shrubs (Supplementry Table S2). In the Continental bioregion, 54% of silvopastoral systems comprise grazed grassland with sparse trees and shrubs (Supplementry Table S2). In Mediterranean areas, broadleaved woodland is the predominant cover (45%) (Supplementry Table S2), offering fodder reserves for livestock during the dry summer months and the shade provided by the trees can extend the growing season of pastures (San Miguel-Ayanz, 2004; Mosquera-Losada et al., 2018).

Almost all EU23 countries lost silvopastoral surfaces between 2009 and 2018. Moreno and Pulido (2009) report a decrease of the area and tree density of dehesas and montados since the second half of the 20th century. This decline could be related with increased mechanisation, stocking rate, death of trees in over-aged stands, farm abandonment associated with land degradation, water scarcity linked to climate change and depopulation associated with migration from rural to urban areas (Moreno and Pulido, 2009; Rodríguez-Rigueiro et al., 2021). An additional effect of the natural expansion of unmanaged forestlands in this region is the increased frequency of forest fires (Rodríguez-Rigueiro et al., 2021).

In Spain, the reduction in the agroforestry is associated with an abandonment of the farms with grazing livestock. The Spanish National Strategy to Combat Desertification (Ministerio para la Transición Ecológica y el Reto Demográfico, 2022) highlights the process of progressive intensification of livestock farms, including the increased use of housing and less use of grazing. In Greece, the use of nomadic flocks has also been reducing associated with urban expansion, land abandonment and the expansion of industrial crops in pastureland, which have led to a progressive increase of forest and shrubland in farmland and consequently an increase of fire risk (Colantoni et al., 2020). In Romania, Hartel et al. (2013) highlighted changes in traditional grazing systems in the Saxon region of Transylvania, such as the use of fire as a method for clearing pastures. They report that poor fire management perhaps resulted in the burning of half of the silvopastoral systems in this area in 2012. In addition, whilst cattle, horses, buffalo and pigs were the dominant livestock in silvopastoral systems in the last century, the majority of silvopastoral systems in 2012 were grazed only by sheep (60%). In Hungary, Varga (2017) reports that silvopastoral practices have been abandoned in recent decades due to the intensification of agriculture and forestry management. In some EU countries, high stocking densities are still supported by some subsidies from the Common Agriculture Policy (CAP) (Delattre et al., 2020). However, in general, establishing the evidence for the observed reduction in grazing at a national level is difficult due to a lack of official statistics about the area of grazing as opposed to grass cover, and this appears to be an important gap in the available evidence. Further research would be useful to address this issue, which is anticipated to have impacts in terms of biodiversity, fire risk and nutrient management.

4.5 Explaining the decline in agroforestry with permanent and arable crops

Permanent crops predominate in Mediterranean regions, where olive groves are the main form of permanent crop (69%) (Supplementry Table S3). According to Sánchez (1995), the presence of livestock within permanent crops allows cheaper weed control than the use of herbicides, and the vegetation provides fodder for cattle. In addition, in grazed permanent crops, yields can be higher than in ungrazed permanent crops (Sánchez, 1995). However despite these advantages, the area of grazed and intercropped permanent crops in the EU23 decreased by 63% from 8,552 km^2 in 2012 to 3,162 km^2 in 2018 (Table 4). The decline in the area of *streuobst* and *près vergers* in northern Europe, *pomaradas* in humid parts of northern Spain, *joualle* in southern France or walnuts intercropped with vegetables in the Italian region of Campania was also reported by Eichhorn et al. (2006). The reasons for the decline include the replacement of high-stem orchards with smaller trees, often on dwarf rootstocks, which supports mechanisation and prevents the integration of livestock. Duarte et al. (2008) highlighted that low profitability is one reason for the abandonment of traditional olive orchards in Mediterranean areas. International competition and imports of fruits and nuts from outside of Europe, such as walnuts from California, changes of land use to artificial areas as well as political measures in favour of more standardised means of production, have also been linked to a decline of permanent crop agroforestry across the EU (Eichhorn et al., 2006). Fungal diseases caused by species in the Botryosphaeriaceae family have also reduced the production of nut crops (such as almond, pistachio and walnut), and olives (Moral et al., 2019).

The reported area of silvoarable agroforestry in Europe is relatively small with a reported decrease from 2012 to 2015, and an increase from 2015 to 2018. This value probably ignores landscape features such a hedgerows and windbreaks which are considered as agroforestry in many frameworks. Historically removal of hedgerows and trees from arable fields have been related to the use of larger arable machinery. Esgalhado et al. (2021) analysed the drivers of land use changes in seven Mediterranean case studies (Portugal, Spain, France, Italy, Malta, Tunisia and Algeria) and found that agricultural intensification was typically associated with the simplification of production systems. The loss of trees has also been associated with the loss of landscape diversity and the loss of some wildlife species (Lasanta et al., 2017), and soil erosion. However, in some locations the need to control soil erosion and minimise water-borne pollution is encouraging farmers to re-integrate trees in cropping systems (Burgess and Rosati, 2018).

4.6 The increase in kitchen gardens

Kitchen gardens account for almost 1% of UAA of the EU28 in 2018 and 15% of the area of agroforestry, being particularly widespread in the Continental and Mediterranean bioregions. This form of agroforestry is associated with urban and peri-urban areas and provides a link between urban areas and local food production (Mosquera-Losada et al., 2018). Unlike other agroforestry practices, kitchen gardens showed a net increase in area in the EU23 from 2009 to 2018. The provision of kitchen gardens can be helpful in allowing local communities to enhance food security particularly during the current context of volatile food prices (Bidar et al., 2020). The large areas of kitchen gardens in central European countries could be related to the traditional use of orchards surrounding houses (Santiago-Freijanes et al., 2018). Urban gardening in cities such as Leipzig in Germany and Lisbon in Portugal is seen as a method to increase socio-ecological resilience (Cabral and Weiland, 2016). By contrast, kitchen gardens are disappearing in Czechia where the practice is negatively associated with the Soviet period (Spilková and Vágner, 2016). Hence the spatial distribution and expansion of this type of agroforestry is clearly related to cultural and political drivers.

4.7 Re-establishing the link between trees and food production at a farm-level

The results demonstrate that reductions in the area of grazing is reducing the area of agroforestry (where there are direct tree-animal interactions). However, as national governments and food producers set increasing priority on achieving net zero greenhouse gas emissions (Costa et al., 2022), there is increasing interest in increasing the area of tree cover on farms to 'inset' (as opposed to offsetting) the greenhouse gas emissions related to food production within the farm (Burgess and Graves, 2022). Because many countries across Europe have targets to increase the area of tree cover, whilst the direct link between trees and crop and/or animal production may be reducing in at a field level, the indirect links between trees and food production may be strengthening at farm level.

5 Conclusion

The analysis in this paper provides to our knowledge the first systematic analysis of how the area of agroforestry in Europe has changed over time, using data collected between 2009 and 2018. It uses a similar definition of the area of agroforestry to that used by den Herder et al. (2017), which specifies that there should be evidence of grazing in silvopastoral areas. The results demonstrate that agroforestry occurs throughout Europe, but the proportion of land occupied by the combination of woody perennials with crops and/or animals is greatest in the Mediterranean region. Silvopastoral systems are the most common form of agroforestry in Europe, accounting for about 81% of the agroforestry area in the EU28 area in 2018. The second most common category was kitchen gardens. An initial analysis of the changes in the area of agroforestry in the EU23 area from 2009 to 2018 suggested that the area of agroforestry increased from 2009 to 2012, and then declined from 2012 to 2018. However more detailed analysis suggests that our initial estimate of the area of agroforestry in 2009 was underestimated to an inconsistent use of the criterion for the 'grazing not relevant' category in LUCAS. With this correction, we propose that the actual pattern is of a consistent decline in the area of agroforestry in the EU23 area from 193,002 km^2 in 2009 to 102,854 km^2 in 2018, primarily related to a decline in silvopastoral systems from 172,700 km^2 to 85,307 km^2 over the same period. Moreover, we argue that a reason for this decline is a reduction in the outdoor grazing of livestock across Europe, partly caused by reduced ruminant numbers in some countries and the increasing permanent housing of livestock indoors. These reported changes in the level of grazing across Europe are worthy

of further research, and could have other implications for biodiversity, fire-risk, and nutrient management.

In addition there has been a reduction in the area of grazed permanent crops due to the replacement of high-stem cultivars with short-stem trees which are more suited for mechanical harvesting and less suitable for the integration of livestock. By contrast, the area of kitchen gardens between 2009 and 2018 showed a net increase. The results demonstrate the usefulness of a consistent and regularly collected land cover and land use dataset, including grazing data, across a wide range of countries to understand the changes occurring in European agriculture. The results also demonstrate the importance in establishing clear criteria for the categorisation of different land uses and cover, and that it may be useful to minimise the inter-annual variation in the geographical location of sampling points. Although the reduction in the area of grazing is reducing the area of in-field agroforestry in Europe, the increasing interest in increasing tree cover on farms to mitigate and adapt to the effects of climate change, may be increasing the interactions between trees and food production at a farm-scale.

Data availability statement

Publicly available datasets were analyzed in this study. This data can be found here: https://ec.europa.eu/eurostat/web/lucas/data/primary-data.

Author contributions

JR-D: Conceptualization, Formal Analysis, Investigation, Methodology, Writing–original draft, Writing–review and editing. SS: Conceptualization, Funding acquisition, Investigation, Methodology, Project administration, Supervision, Writing–original draft, Writing–review and editing. PB: Writing–review and editing. SB: Funding acquisition, Project administration, Supervision, Writing–review and editing.

Funding

The authors declare financial support was received for the research, authorship, and/or publication of this article. This work was supported by the European Union's Horizon 2020 Research and Innovation Programme (grant number 862993) in the framework of the Agroforestry and Mixed farming systems—Participatory research to drive the transition to a resilient and efficient land use in Europe (AGROMIX) project.

Acknowledgments

We also thank the two reviewers for their helpful comments and suggestions that helped us in improving the article.

Conflict of interest

The authors declare that the research was conducted in the absence of any commercial or financial relationships that could be construed as a potential conflict of interest.

Publisher's note

Supplementary material

The Supplementary Material for this article can be found online at: https://www.frontiersin.org/articles/10.3389/fenvs.2023.1258697/full#supplementary-material

References

ArcGIS, and ArcMap, (2010). *ArcGIS® and ArcMap™ (software GIS) version 10.0*. Redlands, CA: Environmental Systems Research Institute, Inc.

Atangana, A., Khasa, D., Chang, S., and Degrande, A. (2014). "Agroforestry for soil conservation," in *Tropical agroforestry*. Editors A. Atangana, D. Khasa, S. Chang, and A. Degrande (Netherlands: Springer), 203–216.

Augére-Granier, M. L. (2020). *Agroforestry in the European union*. European Parliament Research Service. Available at: https://policycommons.net/artifacts/1336911/agroforestry-in-the-european-union/1944452/ (Accessed March 14, 2023).

Ballin, M., Barcaroli, G., Masseli, M., and Scarnó, M. (2018). *Redesign sample for land use/cover area frame survey (LUCAS) 2018*. Luxembourg: Publication office of the European Union. doi:10.2785/132365

Barkema, H. W., von Keyserlingk, M. A. G., Kastelic, J. P., Lam, T. J. G. M., Luby, C., Roy, J. P., et al. (2015). Invited review: changes in the dairy industry affecting dairy cattle health and welfare. *J. Dairy Sci.* 98, 7426–7445. doi:10.3168/jds.2015-9377

Bartus, M., Barta, K., Szatmári, J., and Farsang, A. (2017). Modeling wind erosion hazard control efficiency with an emphasis on shelterbelt system and plot size planning. *Z. für Geomorphol.* 61, 123–133. doi:10.1127/zfg/2017/0406

Beka, S., Burgess, P. J., and Corstanje, R. (2023). Robust spatial estimates of biomass carbon on farms. *Sci. Total Environ.* 861, 160618. doi:10.1016/j.scitotenv.2022.160618

Bergmeier, E., Petermann, J., and Schröder, E. (2010). Geobotanical survey of wood-pasture habitats in Europe: diversity, threats and conservation. *Biodivers. Conserv.* 19, 2995–3014. doi:10.1007/s10531-010-9872-3

Bidar, G., Pelfrêne, A., Schwartz, C., Waterlot, C., Sahmer, K., Marot, F., et al. (2020). Urban kitchen gardens: effect of the soil contamination and parameters on the trace element accumulation in vegetables – a review. *Sci. Total Environ.* 738, 139569. doi:10.1016/j.scitotenv.2020.139569

Buck, O., Haub, C., Woditsch, S., Lindemann, D., Kleinwillinghöfer, L., Hazeu, G., et al. (2015). *Analysis of the LUCAS nomenclature and proposal for adaptation of the nomenclature in view of its use by the Copernicus land monitoring services. EEA/EFTAS. Contract No 3436/B2015/RO-COPERNICUS/EEA.56195*. EEA - European Environment Agency. Available at: https://land.copernicus.eu/user-corner/technical-library/LUCAS_Copernicus_Report_v2-2.pdf.

Burgess, P. J., and Graves, A. (2022). *The potential contribution of agroforestry to net zero objectives. Report for the woodland trust*. Bedfordshire: Cranfield University. Available at: https://dspace.lib.cranfield.ac.uk/handle/1826/18664.

Burgess, P. J., and Rosati, A. (2018). Advances in European agroforestry: results from the AGFORWARD project. *Agrofor. Syst.* 92, 801–810. doi:10.1007/s10457-018-0261-3

Cabral, I., and Weiland, U. (2016). "Urban gardering in Leipzig and Lisbon: A comparative study on governance," in *Growing in cities: interdisciplinary perspectives on*

urban gardening. Conference proceedings. Editor S. Tappert (Basel: University of Applied Science), 66–79.

Colantoni, A., Egidi, G., Quaranta, G., D'Alessandro, R., Vinci, S., Turco, R., et al. (2020). Sustainable land management, wildfire risk and the role of grazing in Mediterranean urban-rural interfaces: a regional approach from Greece. *Land* 9, 21. doi:10.3390/land9010021

Costa, C., Wollenberg, E., Benitez, M., Newman, R., Garner, N., and Bellone, F. (2022). Roadmap for achieving net-zero emissions in global food systems by 2050. *Sci. Rep.* 12, 15064. doi:10.1038/s41598-022-18601-1

Damianidis, C., Santiago-Freijanes, J. J., den Herder, M., Burgess, P. J., Mosquera Losada, M. R., Graves, A., et al. (2021). Agroforestry as a sustainable land use option to reduce wildfires risk in European Mediterranean areas. *Agrofor. Syst.* 95. doi:10.1007/s10457-020-00482-w

d'Andrimont, R., Yordanov, M., Martinez-Sanchez, L., Eiselt, B., Palmieri, A., Dominici, P., et al. (2020). Harmonised LUCAS *in-situ* land cover and use database for field surveys from 2006 to 2018 in the European Union. *Sci. Data* 7, 352. doi:10.1038/s41597-020-00675-z

Delattre, L., Debolini, M., Paoli, J. C., Napoleone, C., Moulery, M., Leonelli, L., et al. (2020). Understanding the relationships between extensive livestock systems, land-cover changes, and CAP support in less-favored mediterranean areas. *Land* 9, 518. doi:10.3390/land9120518

den Herder, M., Burgess, P. J., Mosquera-Losada, M. R., Herzog, F., Hartel, T., Upson, M., et al. (2015). Preliminary stratification and quantification of agroforestry in europe. Milestone report 1.1 for EU FP7 AGFORWARD research project (613520). Available at: https://www.repository.utl.pt/bitstream/10400.5/9194/1/REP-CEF-1-M1_Stratification%20of%20agroforestry.pdf den Herder, M

den Herder, M., Moreno, G., Mosquera-Losada, R. M., Palma, J. H. N., Sidiropoulou, A., Santiago Freijanes, J. J., et al. (2017). Current extent and stratification of agroforestry in the European Union. *Agri. Ecosyst. Environ.* 241, 121–132. doi:10.1016/j.agee.2017.03.005

Department of Environment, (2022). *Food and rural Affairs of United Kingdom government*. Structure of the Agricultural Industry. Available at: https://www.gov.uk/government/collections/structure-of-the-agricultural-industry (Accessed January 30, 2023).

Duarte, F., Jones, N., and Fleskens, L. (2008). Traditional olive orchards on sloping land: sustainability or abandonment? *J. Environ. Manage.* 89, 86–98. doi:10.1016/j.jenvman.2007.05.024

Eichhorn, M. P., Paris, P., Herzog, F., Incoll, L. D., Liagre, F., Mantzanas, K., et al. (2006). Silvoarable systems in europe - past, present and future prospects. *Agrofor. Syst.* 67, 29–50. doi:10.1007/s10457-005-1111-7

Esgalhado, C., Guimaraes, M. H., Lardon, S., Debolini, M., Balzan, M. V., Gennai-Schott, S. C., et al. (2021). Mediterranean land system dynamics and their underlying drivers: stakeholder perception from multiple case studies. *Lands. Urban Plan.* 213, 104134. doi:10.1016/j.landurbplan.2021.104134

European Environment Agency, (2016). *Data from: biogeographical regions*. Available at: https://www.eea.europa.eu/data-and-maps/data/biogeographical-regions-europe-3.

Eurostat, (2013a). *Data from: data browser*. Available at: https://ec.europa.eu/eurostat/databrowser/view/reg_area3/default/table?lang=en.

Eurostat, (2013b). *Data from: data browser*. Available at: https://ec.europa.eu/eurostat/databrowser/view/TAG00025/default/table.

Eurostat, (2009). *LUCAS 2009 (land use/cover area frame survey). Technical reference document C-1. Instructions for surveyors*. European Commission. Available at: https://ec.europa.eu/eurostat/documents/205002/208938/LUCAS+2009+Instructions.

Eurostat, (2019a). *LUCAS 2018 (land use/cover area frame survey). Technical reference document C1. Instructions for surveyors*. European Commission. Available at: https://jeodpp.jrc.ec.europa.eu/ftp/jrc-opendata/LUCAS/LUCAS_harmonised/3_supporting/LUCAS2018-C1-Instructions.pdf.

Eurostat, (2019b). *LUCAS 2018 (land use/cover area frame survey). Technical reference document C3 classification (land cover and land use)*. Available at: https://ec.europa.eu/eurostat/documents/205002/8072634/LUCAS2018-C3-Classification.pdf.

Fagerholm, N., Torralba, M., Moreno, G., Girardello, M., Herzog, F., Aviron, S., et al. (2019). Cross-site analysis of perceived ecosystem service benefits in multifunctional landscapes. *Glob. Environ. Change* 56, 134–147. doi:10.1016/j.gloenvcha.2019.04.002

FAO, and ICRAF, (2019). Agroforestry and tenure. *For. Work. Pap.* (8). Rome.

Hartel, T., Dorresteijn, I., Klein, C., Máthé, O., Moga, C. I., Öllerer, K., et al. (2013). Wood-pastures in a traditional rural region of Eastern Europe: characteristics, management and status. *Biol. Conserv.* 166, 267–275. doi:10.1016/j.biocon.2013.06.020

Hellenic Statistical Authority, (2019). *Livestock surveys*. Available at: https://www.statistics.gr/en/statistics/-/publication/SPK13/- (Accessed January 30, 2023).

Herzog, F. (1998). Streuobst: a traditional agroforestry system as a model for agroforestry development in temperate Europe. *Agrofor. Syst.* 42, 61–80. doi:10.1023/a:1006152127824

Inebase, (2011). *Data from: censo agrario 2009*. Available at: https://www.ine.es/dyngs/INEbase/es/operacion.htm?c=Estadistica_C&cid=1254736176851&menu=resultados&idp=1254735727106#!tabs-1254736194950 (Accessed January 30, 2023).

Inebase, (2022). *Data from: censo agrario 2020*. Available at: https://www.ine.es/dyngs/INEbase/es/operacion.htm?c=Estadistica_C&cid=1254736176851&menu=resultados&idp=1254735727106#!tabs-1254736194950 (Accessed January 30, 2023).

Jernsletten, J. L., and Klokov, K. (2002). *Sustainable reindeer husbandry. Arctic Council 2000-2002*. Centre for Saami Studies: University of TromsØ. Available at: http://www.reindeer-husbandry.uit.no/online/Final_Report/final_report.pdf.

Jose, S. (2009). Agroforestry for ecosystem services and environmental benefits: an overview. *Agrofor. Syst.* 76, 1–10. doi:10.1007/s10457-009-9229-7

Kay, S., Rega, C., Moreno, G., den Herder, M., Palma, J. H., Borek, R., et al. (2019). Agroforestry creates carbon sinks whilst enhancing the environment in agricultural landscapes in Europe. *Land use policy* 83, 581–593. doi:10.1016/j.landusepol.2019.02.025

Kirby, K. R., and Potvin, C. (2007). Variation in carbon storage among tree species: implications for the management of a small-scale carbon sink project. *For. Ecol. Manag.* 246, 208–221. doi:10.1016/j.foreco.2007.03.072

Kučera, J., Podhrázská, J., Karásek, P., and Papaj, V. (2020). The effect of windbreak parameters on the wind erosion risk assessment in agricultural landscape. *J. Ecol. Eng.* 21, 150–156. doi:10.12911/22998993/116323

Küpfer, C., and Balko, J. (2010). Streuobstwiesen in Baden-Württemberg-Wie viele Obstbaüme wachsen im Land und in welchem Zustand sind sie? *Horizonte* 35, 38–41.

Lasanta, T., Arnáez, J., Pascual, N., Ruiz-Flaño, P., Errea, M. P., and Lana-Renault, N. (2017). Space–time process and drivers of land abandonment in Europe. *Catena* 149, 810–823. doi:10.1016/j.catena.2016.02.024

Ministerio para la Transición Ecológica y el Reto Demográfico, (2022). *Estrategia nacional de Lucha contra la Desertificación*. Madrid: Ministerio para la Transición Ecológica y el Reto Demográfico.

Moral, J., Morgan, D., Trapero, A., and Michailides, T. J. (2019). Ecology and epidemiology of diseases of nut crops and olives caused by *Botryosphaeriaceae fungi* in California and Spain. *Plant Dis.* 103, 1809–1827. doi:10.1094/pdis-03-19-0622-fe

Moreno, G., Aviron, S., Berg, S., Crous-Duran, J., Franca, A., García de Jalón, S., et al. (2018). Agroforestry systems of high nature and cultural value in Europe: provision of commercial goods and other ecosystem services. *Agrofor. Syst.* 92, 877–891. doi:10.1007/s10457-017-0126-1

Moreno, G., and Pulido, F. J. (2009). "The functioning, management and persistence of dehesas," in *Agroforestry in Europe: current status and future prospects*. Editors A. Rigueiro-Rodríguez, J. McAdam, and M. Mosquera-Losada (Dordrecht: Springer), 127–160.

Mosquera-Losada, M. R., McAdam, J., Romero-Franco, R., Santiago-Freijanes, J. J., and Riguero-Rodríquez, A. (2009). "Definitions and components of agroforestry practices in Europe," in *Agroforestry in Europe: current status and future prospects*. Editors A. Rigueiro-Rodríguez, J. McAdam, and M. Mosquera-Losada (Dordrecht: Springer), 3–19.

Mosquera-Losada, M. R., Santiago-Freijanes, J. J., Rois-Díaz, M., Moreno, G., den Herder, M., Aldrey-Vázquez, J. A., et al. (2018). Agroforestry in Europe: a land management policy tool to combat climate Change. *Land Use Policy* 78, 603–613. doi:10.1016/j.landusepol.2018.06.052

Nerlich, K., Graeff-Hönninger, S., and Claupein, W. (2013). Agroforestry in Europe: a review of the disappearance of traditional systems and development of modern agroforestry practices, with emphasis on experiences in Germany. *Agrofor. Syst.* 87, 475–492. doi:10.1007/s10457-012-9560-2

Oosterbaan, A., and Kuiters, A. T. (2009). "Agroforestry in The Netherlands," in *Agroforestry in Europe: current status and future prospects*. Editors A. Rigueiro-Rodríguez, J. McAdam, and M. R. Mosquera-Losada (Dordrecht: Springer), 331–341.

Palmieri, A., Reuter, H. I., Joebges, C., Eiselt, B., d'Andrimont, R., Lemoine, G., et al. (2020). *Data from: harmonised LUCAS* in-situ *land cover and use database for field surveys from 2006 to 2018 in the European Union*. European Commission, Joint Research Centre JRC. Available at: https://jeodpp.jrc.ec.europa.eu/ftp/jrc-opendata/LUCAS/LUCAS_harmonised/.

Pantera, A., Mosquera-Losada, M. R., Herzog, F., and den Herder, M. (2021). Agroforestry and the environment. *Agrofor. Syst.* 95, 767–774. doi:10.1007/s10457-021-00640-8

Plieninger, T., Hartel, T., Martín-López, B., Beaufoy, G., Bergmeier, E., Kirby, K., et al. (2015a). Wood-pastures of Europe: geographic coverage, social–ecological values, conservation management, and policy implications. *Biol. Conser.* 190, 70–79. doi:10.1016/j.biocon.2015.05.014

Plieninger, T., Levers, C., Mantel, M., Costa, A., Schaich, H., and Kuemmerle, T. (2015b). Patterns and drivers of scattered tree loss in agricultural landscapes: orchard meadows in Germany (1968-2009). *PLoS ONE* 10, e0126178. doi:10.1371/journal.pone.0126178

Rodríguez-Rigueiro, F. J., Santiago-Freijanes, J. J., Mosquera-Losada, M. R., Castro, M., Silva-Losada, P., Pisanelli, A., et al. (2021). Silvopasture policy promotion in European Mediterranean areas. *PLoS ONE* 16, e0245846. doi:10.1371/journal.pone.0245846

San Miguel-Ayanz, A. (2004) 'Mediterranean European silvopastoral systems', in *Silvopastoralism and sustainable land management. Proceedings of an international congress on silvopastoralism and sustainable management held in Lugo, Spain*, eds. R. M. Mosquera-Losada, A. Rigueiro-Rodríguez, and J. McAdam (Wallingford UK: CABI Publishing), 36–40.

Sánchez, M. (1995). Integration of livestock with perennial crops. *World Anim. Rev.* 82 (1), 50–57.

Santiago-Freijanes, J. J., Mosquera-Losada, M. R., Aldrey-Vázquez, J. A., and Rigueiro-Rodríguez, A. (2018). "Homegardens: agriculture in the city as an agroforestry practice," in *Agroforestry as sustainable land use, proceedings of the 4th European agroforestry conference*. Editors R. M. Mosquera-Losada and N. Ferreiro-Domínguez (Spain: European Agroforestry Federation and University of Santiago de Compostela in Lugo), 122–126.

Santos, P. Z. F., Crouzeilles, R., and Sansevero, J. B. B. (2019). Can agroforestry systems enhance biodiversity and ecosystem service provision in agricultural landscapes? A meta-analysis for the Brazilian Atlantic Forest. *For. Ecol. Manag.* 433, 140–145. doi:10.1016/j.foreco.2018.10.064

Schwartz, N. B., Uriarte, M., Gutiérrez-Vélez, V. H., Baethgen, W., Defries, R., Fernandes, K., et al. (2015). Climate, landowner residency, and land cover predict local scale fire activity in the Western Amazon. *Glob. Environ. Change.* 31, 144–153. doi:10.1016/j.gloenvcha.2015.01.009

Siriri, D., Wilson, J., Coe, R., Tenywa, M. M., Bekunda, M. A., Ong, C. K., et al. (2013). Trees improve water storage and reduce soil evaporation in agroforestry systems on bench terraces in SW Uganda. *Agrofor. Syst.* 87, 45–58. doi:10.1007/s10457-012-9520-x

Spilková, J., and Vágner, J. (2016). The loss of land devoted to allotment gardening: the context of the contrasting pressures of urban planning, public and private interests in Prague, Czechia. *Land Use Policy* 52, 232–239. doi:10.1016/j.landusepol.2015.12.031

Takács, V., and Frank, N. (2008). "The traditions, resources and potential of forest growing and multipurpose shelterbelts in Hungary," in *Agroforestry in Europe: current status and future prospects*. Editors A. Rigueiro-Rodríguez, J. McAdam, and M. R. Mosquera-Losada (Dordrecht: Springer), 415–433.

Tölgyesi, C., Kelemen, A., Bátori, Z., Kiss, R., Hábenczyus, A. A., Havadtői, K., et al. (2023). Maintaining scattered trees to boost carbon stock in temperate pastures does not compromise overall pasture quality for the livestock. *Agric. Ecosyst. Environ.* 351, 108477. doi:10.1016/j.agee.2023.108477

Torralba, M., Fagerholm, N., Burgess, P. J., Moreno, G., and Plieninger, T. (2016). Do European agroforestry systems enhance biodiversity and ecosystem services? A meta-analysis. *Agric. Ecosyst. Environ.* 230, 150–161. doi:10.1016/j.agee.2016.06.002

Upson, M. A., Burgess, P. J., and Morison, J. I. L. (2016). Soil carbon changes after establishing woodland and agroforestry trees in a grazed pasture. *Geoderma* 283, 10–20. doi:10.1016/j.geoderma.2016.07.002

Varga, A. (2017). 'Innovation from the past.' silvopastoral systems in Hungary in the light of Hungarian ethnographic literature. *Acta Ethnogr. Hung.* 62 (1), 135–162. doi:10.1556/022.2017.62.1.7

Zomer, R. J., Trabucco, A., Coe, R., Place, F., van Noordwijk, M., and Xu, J. C. (2014). "Trees on farms: an update and reanalysis of agroforestry's global extent and socio-ecological characteristics," in *Working paper 179. Bogor, Indonesia, world agroforestry Centre (ICRAF) southeast asia regional program*. doi:10.5716/WP14064.PDF

frontiers | Frontiers in Environmental Science

TYPE Original Research
PUBLISHED 16 November 2023
DOI 10.3389/fenvs.2023.1306187

OPEN ACCESS

EDITED BY
Hua Lu,
Jiangxi University of Finance and Economics, China

REVIEWED BY
Haipeng Zhang,
Henan University, China
Yuanjun Li,
Guangzhou Institute of Geography, China

*CORRESPONDENCE
Yong Sun,
sunyong@gzhu.edu.cn
Hongyan Du,
dhy@agri.ac.cn

RECEIVED 03 October 2023
ACCEPTED 03 November 2023
PUBLISHED 16 November 2023

CITATION
Gong J, Du H, Sun Y and Zhan Y (2023), Simulation and prediction of land use in urban agglomerations based on the PLUS model: a case study of the Pearl River Delta, China.
Front. Environ. Sci. 11:1306187.
doi: 10.3389/fenvs.2023.1306187

Simulation and prediction of land use in urban agglomerations based on the PLUS model: a case study of the Pearl River Delta, China

Jing Gong[1], Hongyan Du[1]*, Yong Sun[2,3]* and Yun Zhan[2]

[1]Institute of Data Science and Agricultural Economics, Beijing Academy of Agriculture and Forestry Sciences, Beijing, China, [2]School of Public Administration, Guangzhou University, Guangzhou, China, [3]Institute of Rural Revitalization, Guangzhou University, Guangzhou, China

The Pearl River Delta (PRD) is a highly urbanized region in China that faces significant challenges in land use management. These challenges include the decrease in agricultural and ecological land resulting from rapid urbanization, the effectiveness of government governance, and the trajectory of development, all of which warrant careful research examination. Moreover, existing studies on land use in the PRD predominantly rely on static historical analysis, lacking a multi-scenario simulation approach. This study examines land use in PRD using a Patch-Generating Simulation (PLUS), from 1985 to 2020 to address this gap. Three scenarios were established to simulate potential land use outcomes in the PRD by 2030: spontaneous change, cropland protection, and ecological protection. The findings reveal that cropland, forest, and impervious surfaces are the dominant land use types in the PRD. From 1985 to 2020, the proportion of cropland decreased from 37.63% to 27.40%, with most conversions occurring to impervious surfaces and forest land. The proportion of impervious surfaces increased from 1.81% to 12.57%, primarily from conversions of cropland, forest, and water bodies. Economic development, population growth, accessibility, climatic factors, and topographic conditions were shown to be the primary determinants of land use in the PRD. Modelling results suggest that under the spontaneous change scenario, cropland and ecological land decrease, while impervious surfaces expand significantly, threatening cropland preservation and ecological construction. However, under the cropland protection scenario, the conversion rate of cropland to other land types can be effectively controlled, contributing to efficient preservation. Under the ecological protection scenario, impervious infrastructure encroachment on ecological land can be mitigated, but cropland protection is limited. The study proposes cropland protection and ecological priority policies to optimize the structure of land use, enhance efficiency, and offer policy guidance for the efficient utilization of land resources and the preservation of the ecological environment in the PRD.

KEYWORDS

land use, PLUS model, multiple scenarios, policy simulation, the Pearl River Delta

1 Introduction

The land is a key element in nature and the most basic natural resource and material basis for human survival and development (Kozak et al., 2017; Wang et al., 2023a). Human activities transform different attributes of land to meet the requirements of social development, especially in key urban agglomerations, where rapid urban development is seriously crowding out other land uses, threatening food security and ecological safety. This phenomenon has received considerable attention from researchers in various countries and regions. Urban agglomerations are focal areas for land use/land cover change. However, the patterns and processes of land use change in urban agglomerations differ significantly from those in non-urban areas (Chen et al., 2020). With higher population densities and greater influence of economic and social factors, urban agglomerations experience more pronounced land use changes compared to non-urban regions (Yu et al., 2019). Therefore, it is crucial to use satellite imagery, population census data, and statistical models to analyze the dynamic changes in land use within urban agglomerations. In particular, it is essential to unveil the primary drivers that shape land use change in these areas.

Pearl River Delta (PRD) is one of the most populous urban agglomerations in China, with relatively scarce resources, rapid economic development, and high ecological and environmental pressure (Ouyang et al., 2021). In the context of rapid economic development and accelerated urbanisation, the PRD has experienced dramatic land use, leading to a series of problems such as a reduction in cropland area, ecosystem degradation, and biodiversity loss (Jiao et al., 2019; Li et al., 2023). Therefore, researching land use and its impact mechanisms in the PRD has great theoretical significance and practical value.

In the 1990s, the International Geosphere-Biosphere Programme and the International Human Dimensions Programme on Global Environmental Change jointly proposed the land use programme, making land use a hot topic and a Frontier in the natural and social sciences (Li et al., 2012). Previous studies have identified economic development, population growth and climate change as the main drivers of land use and explored their effects on natural ecosystems (Cai et al., 2011; Liu et al., 2019; Himes et al., 2020). These studies have also revealed that land use can have hidden and adverse impacts on ecosystem services, such as biodiversity, climate regulation and hydrological regulation, leading to various ecological problems (Yu et al., 2010; Li et al., 2017; Pellissier et al., 2017). To support land use planning and ecological protection, some studies have conducted multi-scenario simulations and analyses of land use under different conditions (Liu et al., 2020; Cabral et al., 2021). For instance, Li et al. (2022) used land use images to examine land use change in the PRD, simulated land use under different scenarios and evaluated the corresponding ecosystem service values. This study can help us better understand the environmental consequences of land use choices and formulate more sustainable land use policies.

Model-based analysis methods are very effective for land use studies as they can provide information on the trends and changes in land use in terms of quantity and spatial patterns (Jiao et al., 2019; Sun et al., 2022). However, different quantitative research methods are suitable for different conditions and problems, and they have some differences in the issues they address. Firstly, evaluation models of land use are mainly used to assess land use over a specific period. These models quantify the current situation and characteristics of land use, such as the distribution, area and spatial pattern of land use types, by collecting land use data and relevant indicators, such as the use/cover change transfer matrix, land use dynamics and so on (Chang et al., 2022; Yang et al., 2022). Secondly, causal identification models of land use are used to infer the causes and mechanisms of land use change by analysing the correlation and influence of land use and drivers, such as system dynamics models and regression analysis (He et al., 2022; Jiang et al., 2023). Thirdly, predictive models of land use are used to forecast future trends in land use change. These models are based on historical land use data, drivers and trend analysis, *etc.*, and they use mathematical-statistical models or machine learning algorithms to predict future land use changes, such as Markov chain models, cellular automata models and machine learning models (Genga et al., 2017; Huang et al., 2022; Wang et al., 2023a). However, it has been shown that these models can hardly combine the advantages of both quantitative and spatial pattern prediction (Liang et al., 2021).

The model that integrates quantitative and spatial pattern prediction can reveal more information about the trend of land use change, thus providing more comprehensive guidance for total land use control and local governance and facilitating accurate land use management (Jiao et al., 2019; Liu et al., 2023). The Patch-Generating Simulation (PLUS) is a raster-based CA model (Liang et al., 2021), which can explore the drivers of land expansion and predict the patch-level evolution of land-use landscapes (Zhang et al., 2022; Wang et al., 2023b). This model has several advantages. Firstly, it can consider not only the quantity and spatial distribution of land use types but also the shape and size of land use patches, thus reflecting the spatial pattern of land use better. Secondly, it can analyse the interactions and competition between different land-use types in an integrated way by introducing multiple drivers and constraints, as well as adaptive inertia and competition mechanisms, thus simulating the processes and outcomes of land-use change more accurately. This model can help us better understand the impacts of land use on ecosystems and provide a scientific basis for sustainable land use and environmental protection.

The PRD is strategically positioned within China's territorial spatial development pattern, and is facing the challenge of rapid urbanization and its consequent impact on land use changes, which poses a threat to its sustainable development. To comprehensively understand the evolving trends and devise effective strategies for regulating land use changes in urban agglomeration areas, this study employs a multi-perspective analysis and simulation approach based on the case of the PRD. Specifically, the PLUS model is utilized, which combines the quantitative predictive capabilities of Markov models with the spatial pattern predictive advantages of meta-cellular automata. This model enables an examination of the spatial and temporal dynamics of land use changes and their driving forces in the PRD from 1985 to 2020. It also sets up three scenarios of inertial development, Cropland protection and ecological priority to predict the land use situation in the PRD in 2030. The paper aims to answer the following questions:

TABLE 1 Data information.

Data type	Data name	Time	Resolution (m)	Unit	Data sources
Land use	Land use data	1985–2020	30	—	https://zenodo.org/record/5210928
Nature Factor	DEM	—	90	m	https://www.resdc.cn/
	Slope	—	90	°	DEM-based extraction
	Average annual temperature	1985–2015	1,000	0.1°C	https://www.resdc.cn/
	Average annual precipitation	1985–2015	1,000	0.1 mm	
	Soil type	1995	1,000	—	
	Distance from water	2021	300	m	https://www.openstreetmap.org/
Socio-economic factors	Population density	1990–2015	1,000	People/km^2	https://www.resdc.cn/
	GDP density	1995–2015	1,000	Million/km^2	
	Distance from trunk road	2021	300	m	https://www.openstreetmap.org/
	Distance from motorway				
	Distance from primary road				
	Distance from secondary road				
	Distance from tertiary roads				
	Distance from railway				
	Distance from district and county offices				
	Distance from railway station				
	Distance to bus station				
	Distance from the airport				

What are the trends and factors of land use change in the PRD? What are the future land use trends of urban agglomerations under different scenarios? The projections are intended to provide a reference for the optimal allocation of land resources and a rational land use structure in the PRD. This study applies the PLUS model to reveal the main factors affecting the land use change processes and outcomes in urban agglomerations, and provides decision support for optimizing the allocation and rational utilization of land resources in the Pearl River Delta region.

The remaining sections of the paper are structured as follows: Section 2 provides an overview of the study area and data sources. Section 3 outlines the research methodology employed in this study. Section 4 presents a detailed analysis of the obtained results. Section 5 engages in a comprehensive discussion of the findings. Finally, Section 7 draws conclusions based on the findings and contributions of this paper.

2 Study area and data sources

2.1 Study area

The PRD urban agglomeration is one of China's most significant economic regions and ranks among the largest urban clusters globally (Ouyang et al., 2021; Li et al., 2023). Characterized by a subtropical monsoonal climate, this area benefits from abundant rainfall and well-established water systems. With a robust industrial base, efficient transportation networks, high population density, and remarkable economic vitality, it holds a crucial strategic position as a Frontier of China's reform and opening-up policies. As the economy continues to flourish, the land use patterns within the PRD have been undergoing rapid transformations. In comparison to other prominent urban agglomerations in China, such as the Beijing-Tianjin-Hebei region and the Yangtze River Delta, the PRD exhibits a greater diversity of land use types and faces more pronounced ecological and environmental pressures and challenges. Consequently, the land use changes occurring in this region bear significant implications for both China's and the world's socio-economic development and ecological conservation efforts (Figure 1).

The PRD is located between 112°57′-114°48′E and 21°48′-23°56′N. It covers nine prefecture-level cities and is bordered by the mountains of northern Guangdong to the north, the South China Sea to the south, the border between Fujian, Guangdong and Jiangxi to the east and the Xijiang River basin to the west. The PRD is mainly a plain region, with plains accounting for 70% of the total area. Its topography is high in the north and low in the south, with a low centre and high sides. The western, northern and eastern parts are surrounded by hilly mountains, forming a natural barrier. The southern coastline of the PRD has many islands and is 1,059 km long.

2.2 Data sources and pre-processing

This paper uses land use data, socio-economic data and natural conditions data (Table 1). The land use data are from the CLCD dataset,

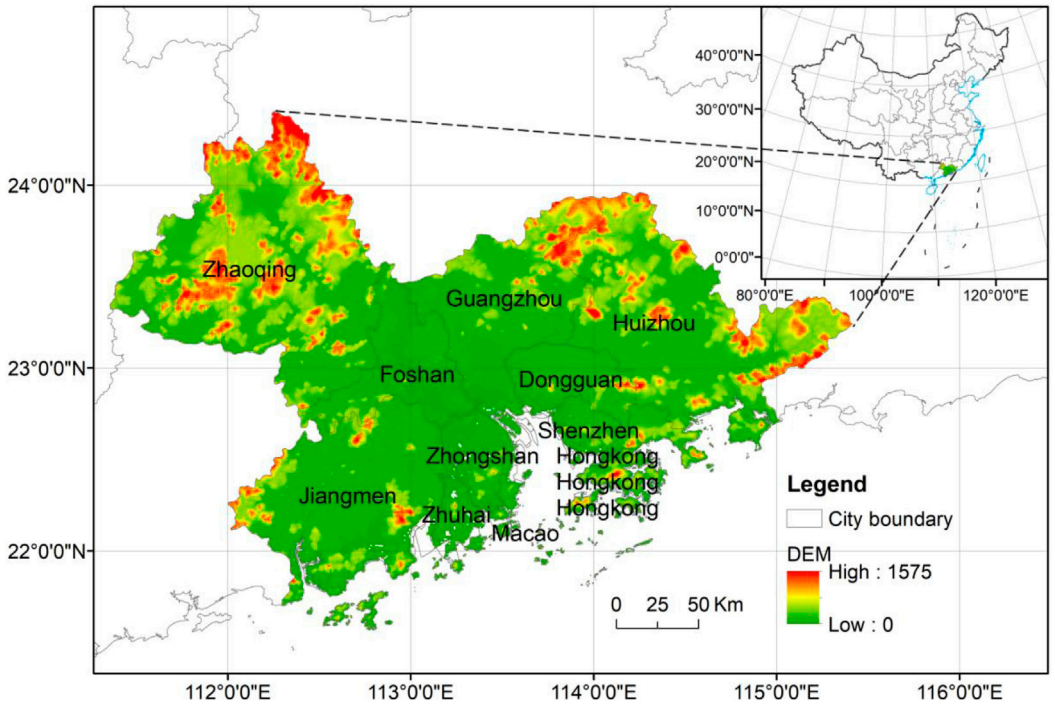

FIGURE 1
Study area.

which was published by Yang Jie and Huang Xin of Wuhan University in Earth System Science Data (Yang and Huang, 2021). This dataset has the advantage of providing 30 m annual land use classification results for 30 years, which is a higher temporal resolution than other products such as GLC_FCS30, Global30, AGLC2000_2015, FROM-GLC10, ESA10 and ESRI10. The dataset divides the land into nine categories: Cropland, Forest, Shrub, Grassland, Water, Sonw/Ice, Barren, Impervious and Wetland. The DEM data is from SRTM (http://srtm.csi.cgiar.org/) and the slope data is derived from DEM. The data on soil type, GDP, population, annual mean temperature and annual precipitation are from the CAS Data Centre for Resource and Environmental Sciences (https://www.resdc.cn/). The data on railways and other transport features are from OSM (https://www.openstreetmap.org/).

3 Research methodology

Our research methodology has two main parts (Figure 2). The first part is a historical analysis of land use in PRD from 1985 to 2020. We use descriptive statistics, land use transfer matrix, and land use dynamic attitudes to analyse the spatial and temporal patterns of land use. The second part is a future simulation of land use using the PLUS model. The year 2030 marks the deadline for the United Nations Sustainable Development Goals, making it a crucial milestone that many studies focus on. With reference to relevant research (Feng et al., 2020; Floreano and de Moraes, 2021; Rahnama, 2021), we examine the impact and driving effects of future variables on land use and compare three scenarios of possible land use change by 2030.

3.1 Study area

3.1.1 Land use transfer matrix

The land use transfer matrix reflects the values and direction of transfer of land use types in a region over the study period. The calculation formula is as follows:

$$S_{ij} = \begin{bmatrix} S_{11} & S_{12} & \cdots & S_{1n} \\ S_{21} & S_{22} & \cdots & S_{2n} \\ \cdots & \cdots & \cdots & \cdots \\ S_{n1} & S_{n2} & \cdots & S_{nn} \end{bmatrix} \quad (1)$$

Where n is the number of land classes, i,j $(i, j = 1, 2, \ldots, n)$ are the land use type at the beginning and end of the land transfer in the study period respectively, S_{ij} is the amount of area converted from i land use type to j land use type.

3.1.2 Land use dynamic attitudes

Land use dynamics quantifies the magnitude and rate of change occurring in each category (Yang et al., 2022), facilitating the study of the overall change and structural dynamics of land use types, with the single land use dynamic attitude as follows:

$$K_i = \frac{U_{bi} - U_{ai}}{U_{ai}} \times \frac{1}{T} \times 100\% \quad (2)$$

Where K_i denotes the single land use dynamic attitude of i land use type during the study period, U_{ai} and U_{bi} are the area at the beginning and end of the study period for i land use type, and T denotes the study period.

TABLE 2 Matrix of land use conversion costs by scenario.

	Spontaneous change scenarios							Cropland protection scenarios							Ecological protection scenarios						
	a	b	c	d	e	f	g	a	b	c	d	e	f	g	a	b	c	d	e	f	g
a	1	1	1	1	1	1	1	1	0	0	0	0	0	0	1	1	1	1	1	1	1
b	1	1	1	1	1	1	1	1	1	1	1	0	1	1	0	1	1	0	0	0	0
c	1	1	1	1	1	1	1	1	1	1	1	1	1	1	0	1	1	0	0	0	0
d	1	1	1	1	1	1	1	1	1	1	1	1	1	1	0	1	1	1	0	0	0
e	1	1	1	1	1	1	1	1	0	1	1	1	1	1	0	0	0	0	1	0	0
f	1	1	1	1	1	1	1	1	1	1	1	1	1	1	1	1	1	1	1	1	1
g	0	0	0	0	0	0	1	0	0	0	0	0	0	1	0	0	0	0	0	0	1

Note: a, b, c, d, e, f, g, and h represent Cropland, Forest, Shrub, Grassland, Water, Barren, and Impervious respectively; where 0 means no conversion allowed, 1 means conversion allowed; rows within the matrix indicate transfer out, columns indicate transfer in.

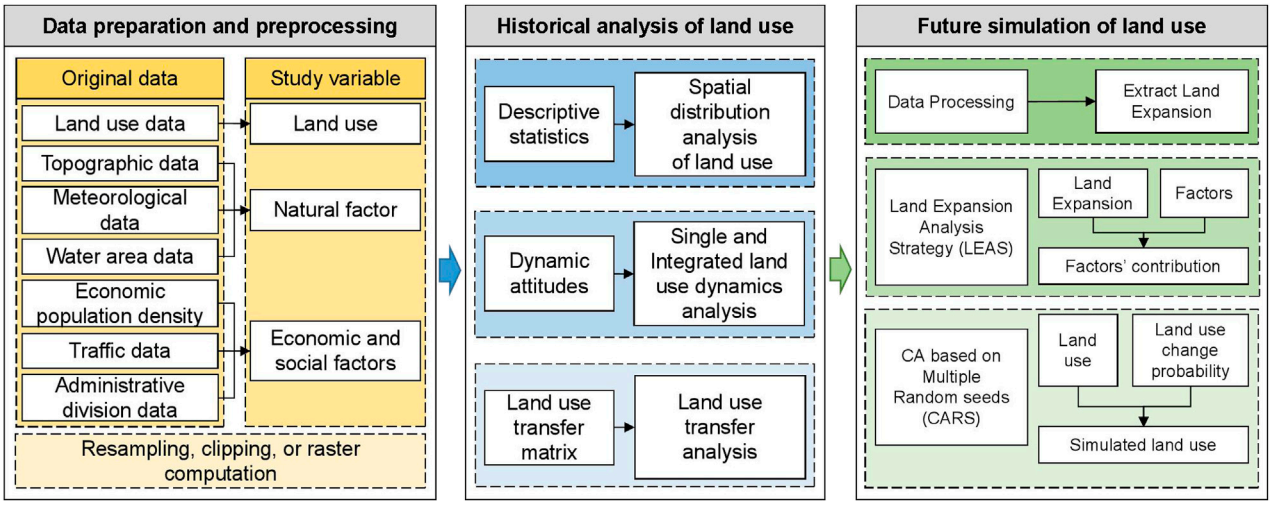

FIGURE 2
Analytical framework.

The expression for the integrated land use dynamic attitude is

$$S = \frac{\sum_{i=1}^{n} |U_{bi} - U_{ai}|}{2 \times \sum_{i=1}^{n} U_{ai}} \times \frac{1}{T} \times 100\% \quad (3)$$

Where S denotes the integrated land use dynamic attitude of i land use type during the study period, U_{ai} and U_{bi} are the area at the beginning and end of the study period for i land use type, and T denotes the study period.

3.2 Scenario setting

To investigate the land use changes in the PRD under different development objectives and concerning relevant studies (Wang et al., 2023a), this paper sets up three scenarios: the inertial development scenario, the cropland protection scenario and the ecological protection scenario. These scenarios are used to predict the spatial pattern of land use in the PRD in 2030. In the ecological protection scenario, the conversion of forest, shrubland, grassland and water to other land types is restricted. The cost of each scenario is shown in Table 2.

4 Analysis of results

4.1 Analysis of spatial and temporal patterns of land use in the PRD

4.1.1 Analysis of spatial distribution characteristics of land use

The PRD primarily encompasses a flat region situated in the lower reaches of the Pearl River. Its topography exhibits higher elevations in the north and lower elevations in the south, resulting in a concave shape with elevated sides. These geographical features significantly influence its land use characteristics (refer to Figure 3). As of 2020, the

TABLE 3 Dynamics Attitudes of land use in the PRD by period 1985–2020 (Unit: %).

		1985–2020	1985–1990	1990–1995	1995–2000	2000–2005	2005–2010	2010–2015	2015–2020
Single land use dynamics	1	−0.78	−0.64	−1.52	−1.01	−1.27	−1.99	−0.55	0.91
	2	−0.06	0.20	−0.05	−0.52	−0.09	0.43	0.14	−0.49
	3	−1.78	−6.30	0.02	2.29	−2.57	−3.26	−4.98	−1.96
	4	−1.71	2.49	14.63	−10.95	11.94	−3.69	−8.34	−7.99
	5	0.48	1.44	3.52	3.99	0.50	0.12	−2.06	−3.27
	7	1.30	−4.67	−5.85	−2.10	−0.57	30.29	1.97	2.35
	8	17.02	3.81	18.66	11.09	6.32	4.23	2.09	2.09
Integrated land use dynamics		0.33	0.24	0.58	0.67	0.46	0.61	0.30	0.48

dominant land use types in the PRD are cropland (27.40%), forest (55.07%) and construction land (12.57%), while grassland, shrub and barren are less common. Urban built-up land is mainly concentrated along the Pearl River Estuary and the Pearl River, forming large and medium-sized cities such as Guangzhou, Shenzhen, Dongguan, Foshan and Zhongshan. The hilly and mountainous areas are the main areas of ecological space, with forests, water bodies and wetlands occupying most of the land. Forests are mainly distributed in the green ecological barrier areas such as Rangke Mountain-Dinghu Mountain in Zhaoqing, Gudou Mountain in Jiangmen and Xiangtou Mountain-Lufushan in Huizhou. Water bodies are mainly distributed in the coastal and inland lakes in the east. Wetlands are mainly distributed in the Pearl River estuary and coastal mudflats.

The PRD has experienced significant changes in land use types. The area of cropland decreased from 37.63% in 1985 to 27.40% in 2020, a decrease of 10.23%. The area share of forest and shrub also decreased slightly, while the area share of grassland, water and barren decreased as well. The area share of impervious increased from 1.81% in 1985 to 12.57% in 2020, an increase of 10.76%, indicating the rapid urbanisation of the PRD, which leads to a reduction in the amount of cropland and natural habitats, which could have adverse impacts on the ecology (Jiao et al., 2019).

4.1.2 Analysis of land use dynamics

Table 3 shows the changes in the various land use types over time. The area share of cropland decreases, while the area share of impervious increases, indicating the acceleration of urbanisation in the PRD. The area share of forest and shrub decreases slightly, while the area share of grassland, water and barren decreases as well. The integrated land use dynamics in the PRD increase overall, and the changes are relatively stable over time, which may indicate the diversification and balanced development of land use types in the PRD.

4.1.3 Analysis of land use transfer

Table 4 shows the main trend of land use transfer in the PRD is the shift from cropland to urban building land and ecological space, reflecting the dual needs of urbanisation and ecological protection. The main features of land use transfer in the PRD by specific types are: Cropland has the largest reduction, with a decrease of about 8,039.44 km^2 and a transfer out of 39.13%, mainly to impervious and forest. This indicates that cropland has been used for urban and construction development or through natural succession in the past decades. Barren has the largest proportion of transfer out, with 96.82% of transfer in, mainly to water and impervious. Impervious has the smallest proportion of transfer out and the largest increase, with an increase of about 5,909.39 km^2. This reflects the accelerated urbanisation and construction activity, with many cropland and other land use types being converted to impervious, leading to a decrease in the ecosystem service of grain production in this region (Liu et al., 2019). Barren has the largest proportion of transfers in, with 97.82% of transfers in, mainly from cropland and water. The forest is the relatively stable type, with less change, mainly within the natural ecological space, reflecting the role of natural succession and anthropogenic disturbance.

4.2 Analysis of the drivers of land use in the PRD based on the PLUS model

Land use change is driven by various factors, including distance from tertiary roads, temperature, and economic development (Figure 4). These drivers can affect the suitability of farmland for agricultural production, the growth and development of crops, and the shift in land use from farming to urbanization. Similarly, changes in forest areas may be attributed to population growth, topographic conditions, and soil types. Shrubland is also impacted by population growth, economic development, and urbanization. Grasslands, on the other hand, may experience a reduction in area due to population growth and changes in precipitation and temperature. Waters are influenced by topographic conditions and changes in temperature and precipitation, while barren areas are affected by accessibility, population growth, and transport and logistics development. Impervious areas are impacted by precipitation, temperature, and topography.

4.3 Analysis of land use in the PRD under multiple scenario modelling

4.3.1 PLUS model accuracy validation

To evaluate the performance of the PLUS model, we used the 2010 land use data to simulate the land use spatial distribution in 2020 and compared it with the actual land use data in 2020

TABLE 4 PRD Land Use Type Transfer Matrix 1985–2020 (Unit: km²).

	a	b	c	d	e	f	g
a	12,503.5146	2064.6873	0.1107	15.3999	997.5753	12.951	4,948.7166
b	2095.2657	27,944.9676	2.9907	13.9455	24.1821	1.3185	593.6274
c	2.0889	11.7729	3.1446	0.3627	0.009	0.0027	0.0648
d	19.395	18.711	0.3402	2.8242	14.8671	0.4221	30.4434
e	327.0996	18.9036	0	2.0268	1,583.9307	2.3895	331.902
f	1.1907	0.0531	0	0.2835	5.4927	0.3825	4.6359
g	7.9254	0.3222	0	0.108	24.5367	0.0522	953.28

Note: a, b, c, d, e, f, g, and h represent Cropland, Forest, Shrub, Grassland, Water, Barren, and Impervious respectively.

(Figure 4). We also sampled the actual land use data, constructed a confusion matrix between the simulated and actual images in 2020, and calculated the overall accuracy and Kappa coefficient. Figure 5 shows that the PLUS model simulation has a high degree of similarity with the actual distribution. However, due to the small area and sample size of Grassland and Barren in the study area, their simulation accuracy is relatively low. Nevertheless, the overall spatial simulation accuracy is high, with an overall accuracy of 0.902052 and a Kappa coefficient of 0.837767. These results indicate that the PLUS model meets the simulation requirements and is suitable for simulating the land use spatial distribution in the PRD.

4.3.2 Multi-scenario simulation analysis

We used the 2020 land use data of the study area as the initial value and applied the CARS module of the PLUS model to simulate the land use in 2030. The CARS module was based on the projected area results of the three scenarios, the land use cost transfer matrix and the neighbourhood weights. We obtained the simulation results of the 2030 land use (Figure 6) and the projected area table (Table 5) for the study area.

Under the Spontaneous change scenario, the impervious area of the PRD increases by 560.68–7,423.35 km² in 2030, expanding from the urban centre to the periphery. Cropland decreases by 56.31 km² compared to 2020, mainly converting to impervious. This scenario poses a serious threat to cropland protection and ecological construction in the study area.

Under the Cropland protection scenario, the impervious area of the PRD increases by 0.65–6,863.32 km² in 2030, which is the lowest expansion among the three scenarios. This scenario effectively controls the growth of impervious areas, but reduces forest by 493.29 km², shrub by 0.57 km² and grassland by 9.38 km² compared to 2020. This scenario also prevents the conversion of cropland to other land types, leading to efficient protection of cropland and food security.

Under the Ecological protection scenario, the forest area of the PRD increases by 62.37–30,121.79 km² in 2030; shrub increases by 2.06 km²; grassland decreases by 7.88 km², which is the smallest decrease among the three scenarios; cropland remains unchanged; water remains unchanged; and impervious increases slightly. This scenario reduces the occupation of ecological land by impervious infrastructure and limits the expansion of impervious areas to some extent, which is beneficial for ecological construction and economic development. However, this scenario does not protect cropland effectively, which may compromise food security in PRD.

The three scenarios reflect the different development orientations of the study area. The economic development scenario aims to accelerate the urbanisation and infrastructure construction in the PRD, resulting in a greater expansion and agglomeration of impervious areas than the other two scenarios. The cropland protection scenario aims to implement the cropland protection system and strengthen food security, resulting in a smaller reduction of cropland and a smaller loss of ecological land than the other two scenarios. It also controls the expansion of impervious areas effectively. The ecological protection scenario aims to consolidate and strengthen ecological protection and restoration efforts, resulting in a more compact distribution of ecological land than the other two scenarios. It also improves the encroachment of impervious areas on ecological land. In any scenario, impervious area expansion is inevitable due to urbanisation and socio-economic progress in the study area. It also shows that in the PRD region, more attention should be paid to the protection of ecological environment while developing the economy (Li et al., 2017).

5 Discussion

Global land use change is confronted with multiple challenges and trends, including population growth, economic globalization, urbanization, agricultural expansion, forestry degradation, desertification, and land degradation, among others (Long et al., 2021). These challenges and trends interact with each other, forming a complex land use system that requires comprehensive analysis and management. In order to achieve the Sustainable Development Goals (SDGs), it is necessary to coordinate land use policies and actions across different scales and sectors, striking a balance between the supply and demand of ecosystem services, protecting and restoring natural capital, and promoting social equity and economic benefits (Zhou et al., 2022; Wei et al., 2023).

Human activities are the direct drivers of land use change, which are also constrained by natural factors and influenced by socio-economic factors (Zhou et al., 2015; Huang et al., 2019; Msofe et al.,

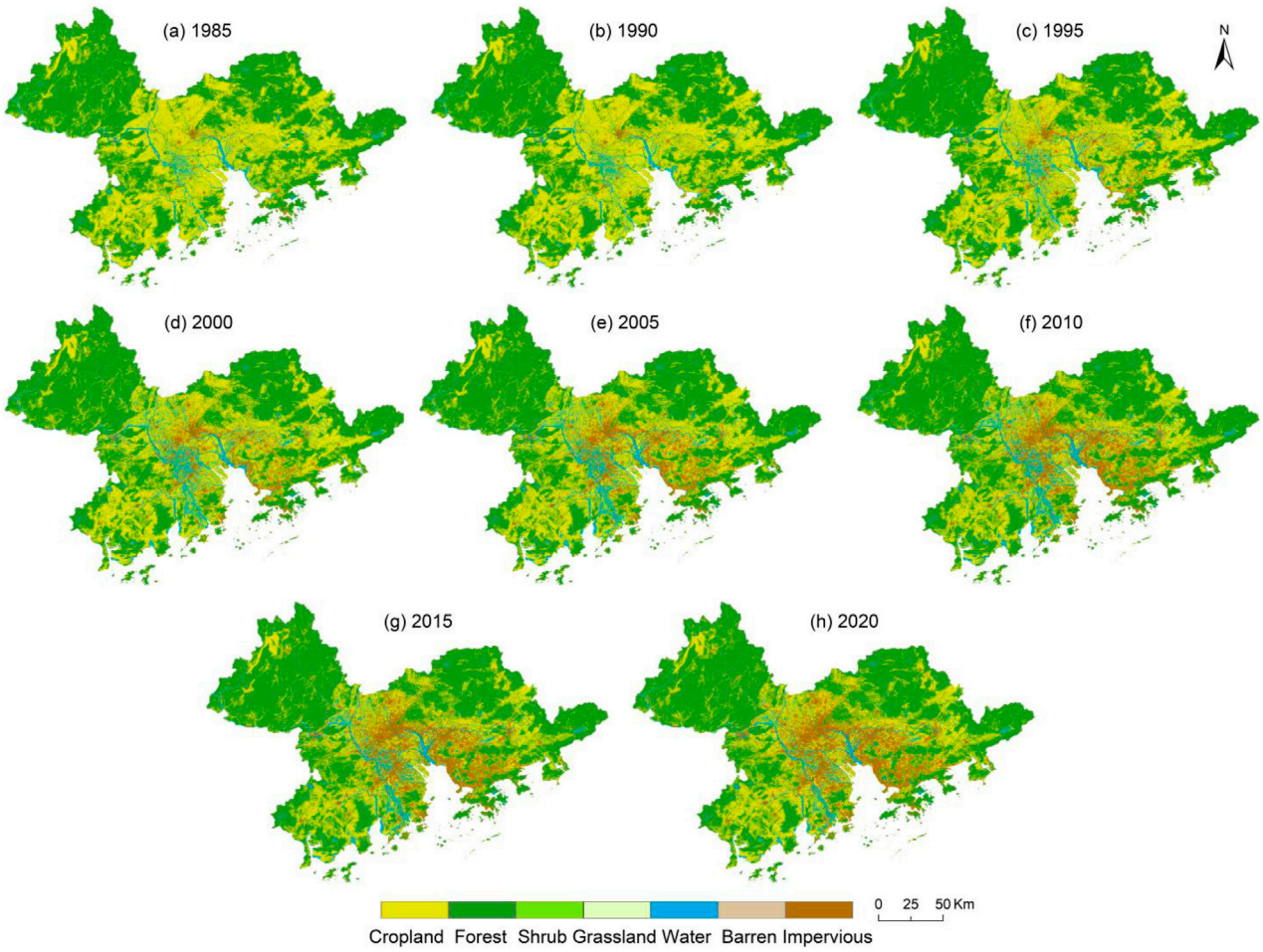

FIGURE 3
Land use distribution in the PRD, 1985–2020. **(A)** 1985. **(B)** 1990. **(C)** 1995. **(D)** 2000. **(E)** 2005. **(F)** 2010. **(G)** 2015. **(H)** 2020.

2019). The demand for a greener environment and the implementation of ecological protection policies are the major drivers for restoring regional ecosystems (Wang et al., 2012; He et al., 2020; Qiu et al., 2022). The PRD is one of the most affluent and dynamic economic regions in China, as well as one of the most densely populated areas. Urbanisation in the PRD is driven by various factors such as economic development, policy support and social demand, leading to changes in land use/cover and ecology (Liu et al., 2019; Zhou et al., 2019). This study analyses the historical changes in land use/cover in the PRD and explores their evolutionary process. It then selects a high-precision model to simulate future land use scenarios. The results of this study can provide decision support for land use planning in the PRD. Most of the converted cropland was transformed into the impervious area and a small part was transformed into a forest under the 'Food for Green' policy. The impervious area expanded along the existing built-up areas (Jiao et al., 2019).

The future land use pattern of the PRD will be influenced by multiple factors, such as economic development, environmental protection and agricultural production. Economic growth drives urbanisation, which increases the demand for impervious areas and may reduce cropland, degrade the environment and threaten food security (Jiao et al., 2019; Li et al., 2020). The PRD was historically an important food production region in China, with agriculture dominating the land use pattern until the 1980s. The rapid urbanisation and industrialisation of the PRD changed the cropland pattern significantly (Jiao et al., 2019; Zhou et al., 2019). Cropland is an important source of food production, and its conservation and rational use are crucial for the sustainable development of agriculture in the PRD. The rapid urbanisation and industrialisation in the PRD also reduced and fragmented the ecological land, such as forest, shrub and grassland, causing ecosystem degradation, atmospheric pollution and water stress (Li et al., 2020; Li et al., 2023). In the future, the PRD needs to optimise its industrial and energy structures, improve land use efficiency, control the scale of impervious areas, and protect cropland and ecological land.

The urban agglomeration represented by the PRD region faces the daunting task of striking a balance between urbanization and sustainability. This challenge arises from the continuous expansion of impervious areas, which leads to the reduction of cropland and ecological land. To promote sustainable development in urban agglomeration, the government needs to control the growth of impervious areas

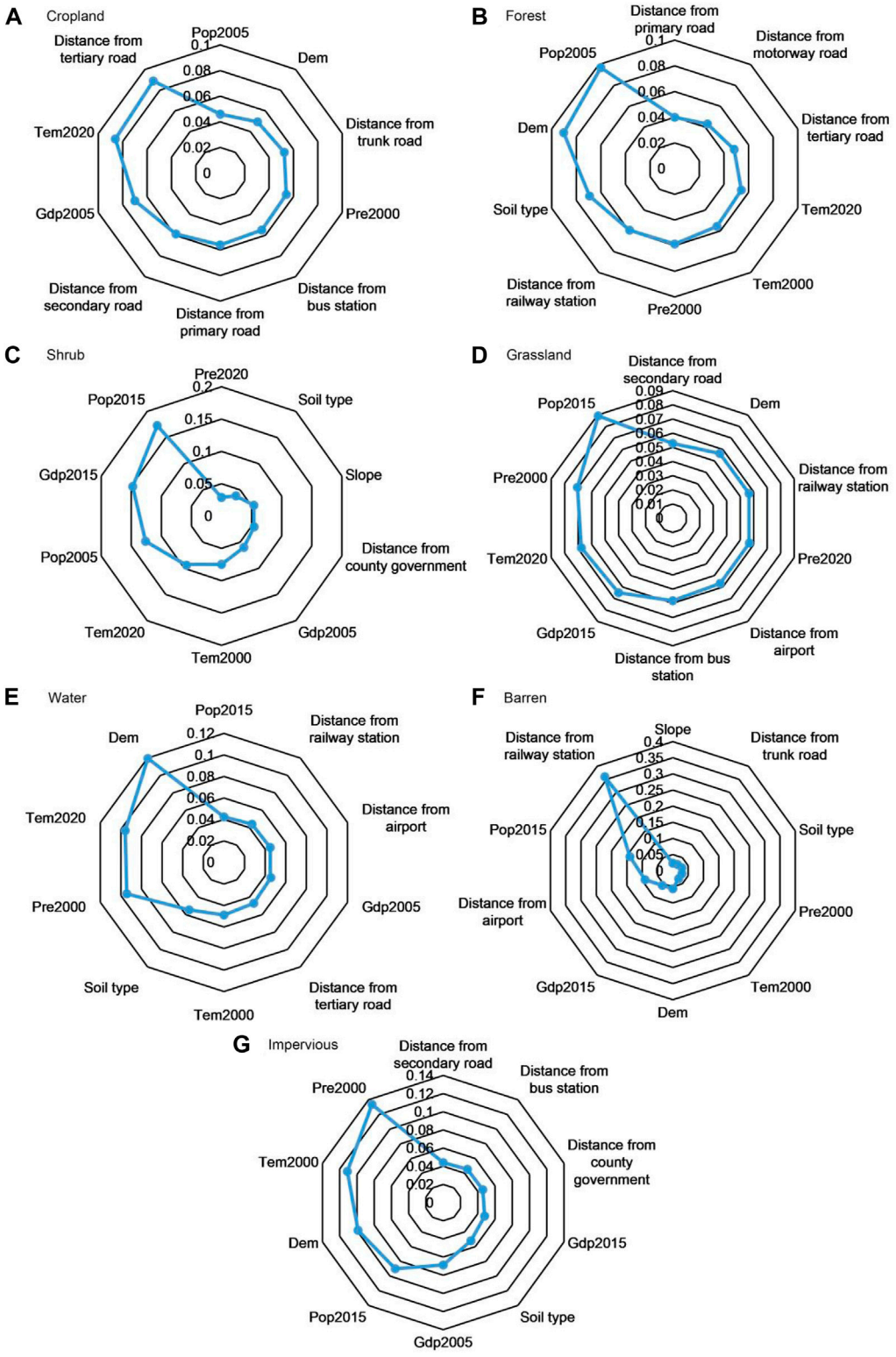

FIGURE 4
Contribution analysis of driving factors. **(A)** Cropland. **(B)** Forest. **(C)** Shrub. **(D)** Grassland. **(E)** Water. **(F)** Barren. **(G)** Impervious.

and protect cropland and ecological land, which are essential for a liveable and sustainable ecological environment. Therefore, it is necessary to conduct land use modelling and scenario analysis based on different development objectives (e.g., regional economy, agricultural production and ecological protection). This approach can simulate different future land use structures and provide multiple perspectives for regional planning decision-makers. Through this approach, we can better predict and assess

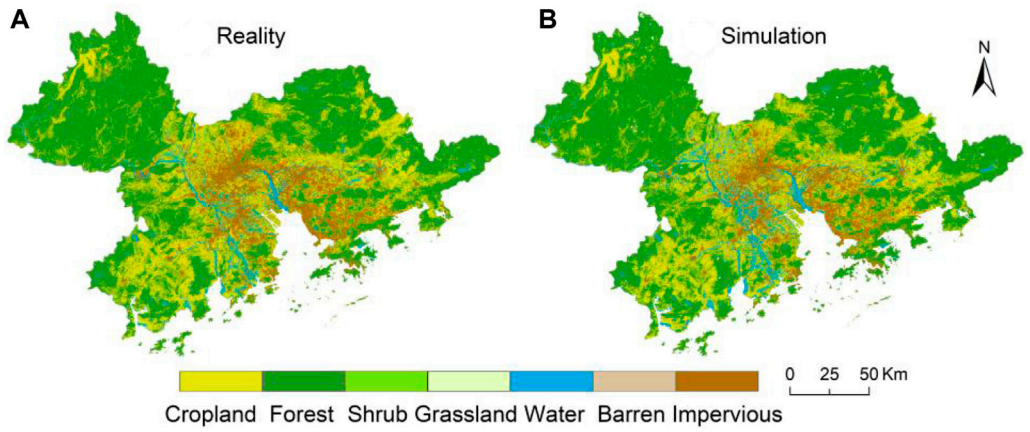

FIGURE 5
Spl comparison of simulated and actual land use in the PRD in 2020. **(A)** Acture land use. **(B)** Simulated land use.

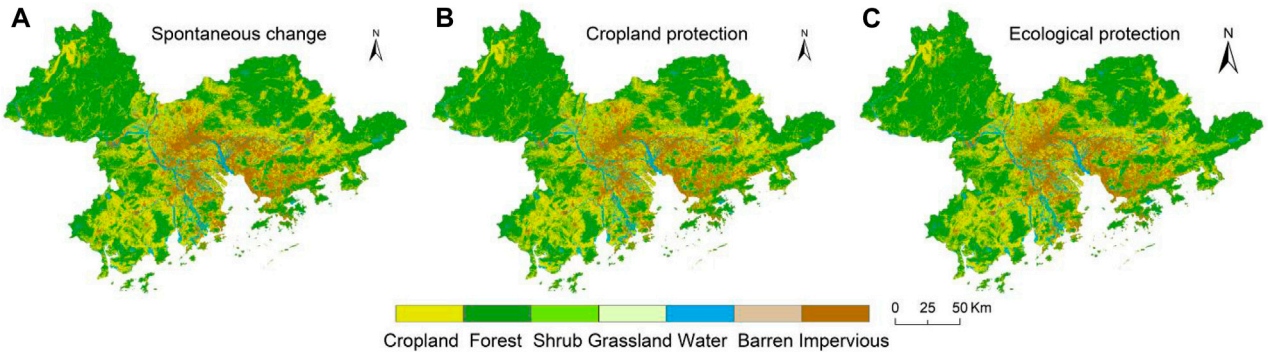

FIGURE 6
Spatial distribution of land use simulations in the PRD under the three scenarios. **(A)** Spontaneous change. **(B)** Cropland protection. **(C)** Ecological protection.

TABLE 5 Projected land use area under three scenarios for the PRD in 2030 (Unit: km^2).

Projects	Cropland	Forest	Shrub	Grassland	Water	Barren	Impervious
2020	14,956.48	30,059.42	6.59	34.95	2,650.59	17.52	6,862.67
Spontaneous change	14,900.17	29,566.13	7.16	25.57	2,650.59	15.24	7,423.35
Cropland protection	15,461.35	29,566.13	6.02	25.57	2,650.59	15.24	6,863.32
Ecological protection	14,900.17	30,121.79	8.64	27.07	2,650.59	15.24	6,864.71

the trends of land use change in urban agglomeration and provide feasible policy recommendations to balance the different objectives and ensure sustainable urban development in the future.

6 Conclusion

This paper analyses the spatial and temporal changes in land use in the PRD from 1985 to 2020 and uses the PLUS model to analyse the drivers of land use expansion for each land type, validate the land use simulation and project the land use under different scenarios for 2030. The main conclusions are.

(1) The main land use types in the PRD are cropland, forest and impervious area, followed by grassland, shrub and barren. The area of cropland decreases from 37.63% in 1985 to 27.40% in 2020, while the area of impervious area increases from 1.81% in 1985 to 12.57% in 2020. The proportion of cropland and natural landscape land decreases as the urbanisation level increases.

(2) The main trend of land use transfer in the PRD is the conversion of cropland to the impervious area and ecological space, reflecting the dual needs of urbanisation and ecological protection. Cropland is the type with the largest decrease, with a reduction of about 8,039.44 km^2 and a transfer out rate of 39.13%, mainly to impervious areas and forest. Impervious area is the type with the smallest transfer out rate and the largest increase, with an expansion of approximately 5,909.39 km^2 and a transfer in the rate of 86.11%, mainly from cropland, forest and water.
(3) According to the driving force analysis, economic development, population growth, accessibility, climatic factors, and topographical conditions are the main drivers of land use change in the PRD. For cropland, the main drivers of change include distance from tertiary roads, temperature, and gross regional product. Population growth, topography, and soil type are the main drivers of forest change, while population growth and gross regional product are the main drivers of shrubland change. Population numbers, precipitation, and temperature drive grassland change, while topography, temperature, and precipitation are the main drivers of water change. For barren land, distance to rail stations and airports and population growth are significant drivers, while precipitation, temperature, and topography affect impervious surfaces.
(4) The PLUS model simulation meets the requirements with an overall accuracy of 0.902052 and a Kappa coefficient of 0.837767. In the Spontaneous Change scenario, there is a significant decrease in cropland and ecological land, while impervious areas expand by 560.68 km^2 from the urban center to the periphery. This expansion poses a severe threat to cropland protection and ecological construction. The Cropland protection scenario prevents cropland conversion to other types, increasing cropland area by 504.87 km^2 compared to 2020 and ensuring food security efficiently. The Ecological protection scenario limits the occupation of ecological land by impervious infrastructure and other areas, restricting the expansion of impervious areas to some extent. The forest area increases by 62.37 km^2, promoting ecological construction and economic development. However, this scenario may not effectively protect cropland, potentially compromising food security in PRD.

This study analyzes the historical land use in the PRD and uses the PLUS model to simulate future land use structures under different scenarios. The PLUS model integrates the differential impacts of road networks on land use changes and controllable conversion rates under different scenarios. The simulation results reveal the spatial patterns of regional land use changes under different scenarios and propose effective regulatory pathways. However, this study has certain limitations. Firstly, the parameter settings of the PLUS model are subjective. Furthermore, the transfer cost matrix and neighborhood weight values are adjusted based on the existing land use structure and previous research experience in the study area, which may introduce errors.

Future research should explore a more objective and quantitative method for parameterization. When assessing the impact of land use changes on the ecological environment, a multidimensional, multiscale, and multi-indicator approach should be adopted to comprehensively reflect the impact of land use changes on ecosystem services, biodiversity, carbon emissions, and other aspects. In formulating land use planning and management strategies, the impact of land use changes on regional sustainable development under different scenarios should be fully considered to balance the relationship between urbanization, agricultural production, and ecological protection, and achieve the optimal allocation and rational utilization of land resources.

Data availability statement

The raw data supporting the conclusion of this article will be made available by the authors, without undue reservation.

Author contributions

JG: Writing–original draft, Writing–review and editing. HD: Writing–review and editing. YS: Writing–original draft, Writing–review and editing. YZ: Writing–review and editing.

Funding

The author(s) declare financial support was received for the research, authorship, and/or publication of this article. This research was funded by the Science and Technology Innovation Capacity Building Project of Beijing Academy of Agriculture and Forestry Sciences, grant number KJCX20230501; the Collaborative Innovation Platform Construction Project of Beijing Academy of Agriculture and Forestry Sciences, grant number KJCX201913; the Guangdong Provincial Philosophy and Social Science Planning Project, grant number GD23XGL067.

Acknowledgments

We thank the journal editor and reviewers.

Conflict of interest

The authors declare that the research was conducted in the absence of any commercial or financial relationships that could be construed as a potential conflict of interest.

Publisher's note

References

Cabral, P., Campos, F. S., David, J., and Caser, U. (2021). Disentangling ecosystem services perception by stakeholders: an integrative assessment based on land cover. *Ecol. Indic.* 126, 107660. doi:10.1016/j.ecolind.2021.107660

Cai, Y. P., Huang, G. H., Wang, X., Li, G. C., and Tan, Q. (2011). An inexact programming approach for supporting ecologically sustainable water supply with the consideration of uncertain water demand by ecosystems. *Stoch. Environ. Res. Risk Assess.* 25 (5), 721–735. doi:10.1007/s00477-011-0477-5

Chang, X. Q., Xing, Y. Q., Wang, J. Q., Yang, H., and Gong, W. S. (2022). Effects of land use and cover change (LUCC) on terrestrial carbon stocks in China between 2000 and 2018. *Resour. Conservation Recycl.* 182, 106333. doi:10.1016/j.resconrec.2022.106333

Chen, K. Q., Long, H. L., Liao, L. W., Tu, S. S., and Li, T. T. (2020). Land use transitions and urban-rural integrated development: theoretical framework and China's evidence. *Land Use Policy* 92, 104465. doi:10.1016/j.landusepol.2020.104465

Feng, Y. J., Chen, S. R., Tong, X. H., Lei, Z. K., Gao, C., and Wang, J. F. (2020). Modeling changes in China's 2000-2030 carbon stock caused by land use change. *J. Clean. Prod.* 252, 119659. doi:10.1016/j.jclepro.2019.119659

Floreano, I. X., and de Moraes, L. A. F. (2021). Land use/land cover (LULC) analysis (2009-2019) with google Earth engine and 2030 prediction using markov-CA in the rondonia state, Brazil. *Environ. Monit. Assess.* 193 (4), 239. doi:10.1007/s10661-021-09016-y

Genga, B., Zhengb, X. Q., and Fua, M. C. (2017). Scenario analysis of sustainable intensive land use based on SD model. *Sustain. Cities Soc.* 29, 193–202. doi:10.1016/j.scs.2016.12.013

He, J., Shi, X. Y., Fu, Y. J., and Yuan, Y. (2020). Evaluation and simulation of the impact of land use change on ecosystem services trade-offs in ecological restoration areas, China. *Land Use Policy* 99, 105020. doi:10.1016/j.landusepol.2020.105020

He, S. T., Wang, D. J., Zhao, P., Chen, W. L., Li, Y., Chen, X. Q., et al. (2022). Dynamic simulation of debris flow waste-shoal land use based on an integrated system dynamics-geographic information systems model. *Land Degrad. Dev.* 33 (12), 2062–2075. doi:10.1002/ldr.4298

Himes, A., Puettmann, K., and Muraca, B. (2020). Trade-offs between ecosystem services along gradients of tree species diversity and values. *Ecosyst. Serv.* 44, 101133. doi:10.1016/j.ecoser.2020.101133

Huang, L. S., Wang, B., Niu, X., Gao, P., and Song, Q. F. (2019). Changes in ecosystem services and an analysis of driving factors for China's Natural Forest Conservation Program. *Ecol. Evol.* 9 (7), 3700–3716. doi:10.1002/ece3.4925

Huang, Z. H., Li, X. J., Du, H. Q., Mao, F. J., Han, N., Fan, W. L., et al. (2022). Simulating future LUCC by coupling climate change and human effects based on multi-phase remote sensing data. *Remote Sens.* 14 (7), 1698. doi:10.3390/rs14071698

Jiang, R. Y., Xie, C. K., Man, Z. H., Afshari, A., and Che, S. Q. (2023). LCZ method is more effective than traditional LUCC method in interpreting the relationship between urban landscape and atmospheric particles. *Sci. Total Environ.* 869, 161677. doi:10.1016/j.scitotenv.2023.161677

Jiao, M. Y., Hu, M. M., and Xia, B. C. (2019). Spatiotemporal dynamic simulation of land-use and landscape-pattern in the Pearl River Delta, China. *Sustain. Cities Soc.* 49, 101581. doi:10.1016/j.scs.2019.101581

Kozak, J., Gimmi, U., Houet, T., and Bolliger, J. (2017). Current practices and challenges for modelling past and future land use and land cover changes in mountainous regions. *Reg. Environ. Change* 17 (8), 2187–2191. doi:10.1007/s10113-017-1217-2

Li, B. W., Yang, Z. F., Cai, Y. P., Xie, Y. L., Guo, H. J., Wang, Y. Y., et al. (2022). Prediction and valuation of ecosystem service based on land use/land cover change: a case study of the Pearl River Delta. *Ecol. Eng.* 179, 106612. doi:10.1016/j.ecoleng.2022.106612

Li, L., Huang, X. J., Wu, D. F., and Yang, H. (2023). Construction of ecological security pattern adapting to future land use change in Pearl River Delta, China. *Appl. Geogr.* 154, 102946. doi:10.1016/j.apgeog.2023.102946

Li, Q., Zhang, X. F., Liu, Q. F., Liu, Y., Ding, Y., and Zhang, Q. (2017). Impact of land use intensity on ecosystem services: an example from the agro-pastoral ecotone of central inner Mongolia. *Sustainability* 9 (6), 1030. doi:10.3390/su9061030

Li, R. P., Guan, Q. F., and Merchant, J. (2012). A geospatial modeling framework for assessing biofuels-related land-use and land-cover change. *Agric. Ecosyst. Environ.* 161, 17–26. doi:10.1016/j.agee.2012.07.014

Li, Z. T., Li, M., and Xia, B. C. (2020). Spatio-temporal dynamics of ecological security pattern of the Pearl River Delta urban agglomeration based on LUCC simulation. *Ecol. Indic.* 114, 106319. doi:10.1016/j.ecolind.2020.106319

Liang, X., Guan, Q. F., Clarke, K. C., Liu, S. S., Wang, B. Y., and Yao, Y. (2021). Understanding the drivers of sustainable land expansion using a patch-generating land use simulation (PLUS) model: a case study in Wuhan, China. *Comput. Environ. Urban Syst.* 85, 101569. doi:10.1016/j.compenvurbsys.2020.101569

Liu, M. H., Chen, H. Y., Qi, L. I., and Chen, C. (2023). LUCC simulation based on RF-CNN-LSTM-CA model with high-quality seed selection iterative algorithm. *Appl. Sci-Basel.* 13 (6), 3407. doi:10.3390/app13063407

Liu, W., Zhan, J. Y., Zhao, F., Yan, H. M., Zhang, F., and Wei, X. Q. (2019). Impacts of urbanization-induced land-use changes on ecosystem services: a case study of the Pearl River Delta Metropolitan Region, China. *Ecol. Indic.* 98, 228–238. doi:10.1016/j.ecolind.2018.10.054

Liu, Y. B., Hou, X. Y., Li, X. W., Song, B. Y., and Wang, C. (2020). Assessing and predicting changes in ecosystem service values based on land use/cover change in the Bohai Rim coastal zone. *Ecol. Indic.* 56, 117, 106004. doi:10.1016/j.ecolind.2019.106004

Long, H. L., Zhang, Y. N., Ma, L., and Tu, S. S. (2021). Land use transitions: progress, challenges and prospects. *Land* 10 (9), 903. doi:10.3390/land10090903

Msofe, N. K., Sheng, L. X., and Lyimo, J. (2019). Land use change trends and their driving forces in the kilombero valley floodplain, southeastern Tanzania. *Sustainability* 11 (2), 505. doi:10.3390/su11020505

Ouyang, Y. R., Cai, Y. P., Xie, Y. L., Yue, W. C., and Guo, H. J. (2021). Multi-scale simulation and dynamic coordination evaluation of water-energy-food and economy for the Pearl River Delta city cluster in China. *Ecol. Indic.* 130, 108155. doi:10.1016/j.ecolind.2021.108155

Pellissier, V., Mimet, A., Fontaine, C., Svenning, J. C., and Couvet, D. (2017). Relative importance of the land-use composition and intensity for the bird community composition in anthropogenic landscapes. *Ecol. Evol.* 7 (24), 10513–10535. doi:10.1002/ece3.3534

Qiu, S. J., Peng, J., Zheng, H. N., Xu, Z. H., and Meersmans, J. (2022). How can massive ecological restoration programs interplay with social-ecological systems? A review of research in the South China karst region. *Sci. Total Environ.* 807, 150723. doi:10.1016/j.scitotenv.2021.150723

Rahnama, M. R. (2021). Forecasting land-use changes in Mashhad Metropolitan area using Cellular Automata and Markov chain model for 2016-2030. *Sustain. Cities Soc.* 64, 102548. doi:10.1016/j.scs.2020.102548

Sun, Y., Du, H. Y., Liu, B. Y., Kanchanaroek, Y., Zhang, J. F., and Zhang, P. (2022). Evolutionary game analysis for grassland degradation management, considering the livelihood differentiation of herders. *Land* 11 (10), 1776. doi:10.3390/land11101776

Wang, J., Chen, Y. Q., Shao, X. M., Zhang, Y. Y., and Cao, Y. G. (2012). Land-use changes and policy dimension driving forces in China: present, trend and future. *Land Use Policy* 29 (4), 737–749. doi:10.1016/j.landusepol.2011.11.010

Wang, J. B., Wu, Y. F., and Gou, A. P. (2023b). Habitat quality evolution characteristics and multi-scenario prediction in Shenzhen based on PLUS and InVEST models. *Front. Environ. Sci.* 11, 11. doi:10.3389/fenvs.2023.1146347

Wang, Q. Z., Guan, Q. Y., Sun, Y. F., Du, Q. Q., Xiao, X., Luo, H. P., et al. (2023a). Simulation of future land use/cover change (LUCC) in typical watersheds of arid regions under multiple scenarios. *J. Environ. Manag.* 335, 117543. doi:10.1016/j.jenvman.2023.117543

Wei, C. J., Meng, J. J., Zhu, L. K., and Han, Z. Y. (2023). Assessing progress towards sustainable development goals for Chinese urban land use: a new cloud model approach. *J. Environ. Manag.* 326, 116826. doi:10.1016/j.jenvman.2022.116826

Yang, H. F., Zhong, X. N., Deng, S. Q., and Nie, S. N. (2022). Impact of LUCC on landscape pattern in the Yangtze River basin during 2001-2019. *Ecol. Inf.* 69, 101631. doi:10.1016/j.ecoinf.2022.101631

Yang, J., and Huang, X. (2021). The 30 m annual land cover dataset and its dynamics in China from 1990 to 2019. *Earth Syst. Sci. Data* 13 (8), 3907–3925. doi:10.5194/essd-13-3907-2021

Yu, G. M., Zeng, Q., Yang, S., Hu, L. M., Lin, X. W., Che, Y., et al. (2010). On the intensity and type transition of land use at the basin scale using RS/GIS: a case study of the Hanjiang River Basin. *Environ. Monit. Assess.* 160 (1-4), 169–179. doi:10.1007/s10661-008-0666-y

Yu, J. Q., Zhou, K. L., and Yang, S. L. (2019). Land use efficiency and influencing factors of urban agglomerations in China. *Land Use Policy* 88, 104143. doi:10.1016/j.landusepol.2019.104143

Zhang, J. B., Zhu, H. R., Zhang, P. Y., Song, Y. P., Zhang, Y., Li, Y. Y., et al. (2022). Construction of gi network based on mspa and PLUS model in the main urban area of zhengzhou: a case study. *Front. Environ. Sci.* 10, 10. doi:10.3389/fenvs.2022.878656

Zhou, M., Ma, Y. X., Tu, J. T., and Wang, M. C. (2022). SDG-oriented multi-scenario sustainable land-use simulation under the background of urban expansion. *Environ. Sci. Pollut. Res.* 29 (48), 72797–72818. doi:10.1007/s11356-022-20904-9

Zhou, R. B., Lin, M. Z., Gong, J. Z., and Wu, Z. (2019). Spatiotemporal heterogeneity and influencing mechanism of ecosystem services in the Pearl River Delta from the perspective of LUCC. *J. Geogr. Sci.* 29 (5), 831–845. doi:10.1007/s11442-019-1631-0

Zhou, S., Huang, Y. F., Yu, B. F., and Wang, G. Q. (2015). Effects of human activities on the eco-environment in the middle Heihe River Basin based on an extended environmental Kuznets curve model. *Ecol. Eng.* 76, 14–26. doi:10.1016/j.ecoleng.2014.04.020

frontiers | Frontiers in Environmental Science

TYPE Original Research
PUBLISHED 16 November 2023
DOI 10.3389/fenvs.2023.1227682

OPEN ACCESS

EDITED BY
Hualin Xie,
Jiangxi University of Finance and Economics, China

REVIEWED BY
Lucian Sfica,
Alexandru Ioan Cuza University, Romania
Dongrui Han,
Shandong Academy of Agricultural Sciences, China

*CORRESPONDENCE
Haisheng Cai,
chs@jxau.edu.cn

RECEIVED 23 May 2023
ACCEPTED 30 October 2023
PUBLISHED 16 November 2023

CITATION
Zhang Y, Cai H, Zhu T, Guo X, Zeng J and Huang L (2023), Impact of land use changes on the land surface thermal environment in Nanchang, Jiangxi province, China.
Front. Environ. Sci. 11:1227682.
doi: 10.3389/fenvs.2023.1227682

Impact of land use changes on the land surface thermal environment in Nanchang, Jiangxi province, China

Yujia Zhang[1,2,3], Haisheng Cai[1,2,3]*, Taifeng Zhu[1,2,3], Xigen Guo[1,2,3], Jiaxi Zeng[4] and Liang Huang[4]

[1]Jiangxi Province Natural Resources Utilization Science, Technology and Management Innovation Research Base, Jiangxi Agricultural University, Nanchang, Jiangxi, China, [2]Key Laboratory of Agricultural Resources and Ecology in Poyang Lake Watershed of Ministry of Agriculture and Rural Affairs in China, Jiangxi Agricultural University, Nanchang, Jiangxi, China, [3]Selenium-rich Agricultural Industry Development Research Centre, Jiangxi Agricultural University, Nanchang, Jiangxi, China, [4]Jiangxi Institute of Territorial Spatial Survey and Planning, Nanchang, Jiangxi, China

Throughout human history, human activities have resulted in land use and land cover changes (LUCC) and can have a direct impact on the land surface thermal environment (LSTE). In the existing studies, the holistic nature of changes in land use and land cover (LULC) has been neglected in favor of focusing on the interactions between different LULC types and the land surface thermal environment. This study used ArcGIS Pro 3.0, ENVI 5.3, and SPSS software to construct a contribution index model and stepwise regression equation to investigate the relationship between LULC type, structure, and pattern changes and LSTE changes in Nanchang City, Jiangxi Province, China, from 1990 to 2020. The findings revealed that 1) rapid urbanization has led to a surge in the area of built-up land and a decrease in the area of arable land in Nanchang; between 1990 and 2020, the area of built-up land in Nanchang increased by 433.29 km^2, while the area of arable land decreased by 291.99 km^2; 2) The land surface temperature (LST) was divided into five classes according to the equal spacing method, and the areas with the highest and lowest temperature classes were the high temperature zone and the low temperature zone, respectively. Over the past 30 years, the LSTE in Nanchang has gradually deteriorated, with the area of the low temperature zone shrinking by 554.2 km^2 and the area of other classes appearing to increase significantly; 3) the contribution index and stepwise regression equation demonstrate that the primary reasons for the worsening of the LSTE are an increase in the scale of cultivated land and construction land. It was found that rationalization of urban LULC type, structure, and pattern can effectively reduce land surface temperature.

KEYWORDS

LUCC, landsat images, evolution in time and space, dynamic analysis, nanchang

1 Introduction

As industrialization and economic levels rise, the world is experiencing rapid urbanization (Souza et al., 2016). More than half of the world's population now lives in cities, and this figure is expected to rise further in the future (Wu et al., 2023). The key feature of present global urbanization is population mobility from rural to urban locations (Silva et al., 2018). However, as the urban population grows, the area of urban constructed land increases dramatically, having a

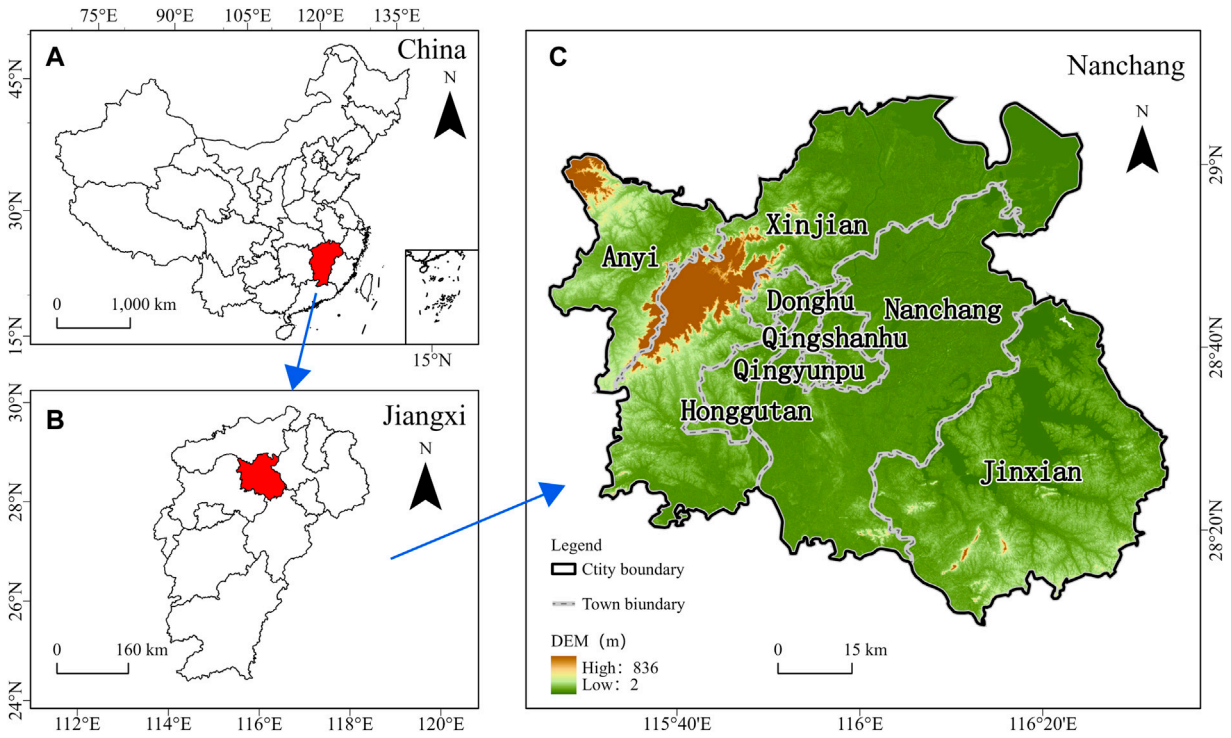

FIGURE 1
Location of the study area. **(A)** Location of Jiangxi province in China. **(B)** Location of the study area in Jiangxi province. **(C)** Location and elevation of the study area.

wide range of effects on regional ecosystems (Qiao et al., 2023). On the one hand, rapid urbanization has played a positive role in promoting urban-rural population mobility and the circulation of production factors. On the other hand, it has had a significant influence on urban LULC types, structures, and patterns, resulting in problems such as spatially disordered urban expansion, increased impervious surfaces, and the discharge of production and domestic waste from urban populations (Fu and Weng, 2016; Wong et al., 2016; Wang et al., 2018; Wang et al., 2022). Previous studies has shown that changing LULC disrupts land-atmosphere energy transfer, resulting in the urban heat island (UHI) phenomenon, which causes cities to have warmer weather than the surrounding countryside (Huang et al., 2015; Bokaie et al., 2016). At the same time, the UHI effect is strongly linked to global warming and local environmental changes in the region's climate (Guo et al., 2015), posing a serious threat to public health (Shiva et al., 2019), and is an important factor influencing the quality of life and safety of human settlements (Oke, 1982; Hang and Rahman, 2018; Pramanik and Punia, 2020).

The dynamics of LUCC and the LSTE are critical components of urban ecology research (Pelletier et al., 2015), and current research has reached a unified consensus that LUCC directly leads to changes in the LSTE (Chang et al., 2022; Chapman et al., 2017; Mushore et al., 2017; Souza et al., 2016; Tarawally et al., 2018; Yildiz et al., 2018; Zhao et al., 2020). Nevertheless, because of differences in research methodology and study locations, the effects of LUCC on the LSTE are not well defined (Sun and Chen, 2017). The findings demonstrate that the average temperature of trees changed in summer, as did their cooling effect on LST, and that treeless urban green spaces were less successful in lowering LST (Schwaab et al., 2021); similarly, different LULC patterns had different effects on LST. The intensity of the UHI effect has been found to be directly related to building density (Li et al., 2020); the effect of LULC change on LST also varies by season (Chen et al., 2017), with LUCC having a greater effect on LST in the winter than in the summer (Estalkhsari et al., 2022). And there are differences in the effects of LULC landscape patterns on LST (Schwaab et al., 2021). Existing studies have found that the size, shape complexity, and degree of aggregation of urban impervious surfaces and greenfield patches were significantly related to LST and that urban impervious surfaces had an average LST around 3°C higher than green fields (Estoque et al., 2017).

Existing studies, all have one flaw in common: they fail to recognize LUCC as a complex whole. Changes in LULC inevitably result in changes in LULC types, quantity, structure, function, and landscape pattern, and existing studies frequently develop from a single perspective of LULC types and quantity, lacking an integrated analysis between LULC types, structure, and pattern and the LSTE; second, most of the existing studies are mainly static, and the analysis of the dynamic changes between LULC and LST is more lacking; and third, in most existing studies, the impact of global climate change is ignored. According to the IPCC study (Intergovernmental Panel on Climate Change, 2023), the worldwide average LST has risen by around 1°C during 1850–1900, and the global temperature rise is predicted to approach or exceed 1.5°C over the next 20 years. Previous studies ignored this and did not take place in the same climatic context. In order to solve the above problems, this study investigated the dynamic

TABLE 1 Data sources.

Data name	Time	Data format	Data origin
China LULC Dataset	1990, 2000, 2010, 2020	Tiff	Resource and Environmental Science and Data Centre, Chinese Academy of Sciences (https://www.resdc.cn/)
Landsat 5 TM and Landsat 8 OLI images	1990, 2000, 2010, 2020 Summer	Tiff	Geospatial Data Cloud (https://www.gscloud.cn/)、USGS (https://www.usgs.gov/)
Data on administrative divisions	2020	Shpfile	National Centre for Basic Geographic Information (http://www.ngcc.cn/)

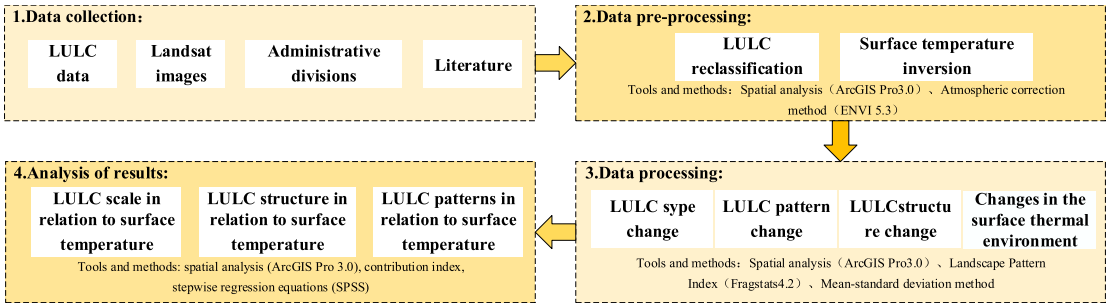

FIGURE 2
Methodological framework.

relationship between LULC type, structure, and pattern and LST by constructing a contribution index model and a stepwise regression equation based on eliminating the effect of climate change on LST.

China has been one of the world's fastest urbanizing countries in the last 30 years (Peng et al., 2018), with an urbanization rate of 60.31% as of 2019, exceeding the world average of 55.7%, and is expected to continue to grow at the fastest rate over the next 50 years. The urban heat island effect and heat waves will occur more frequently. At the same time, the need for solutions has become even more pressing (Yu et al., 2022). In 2017, the China Meteorological Administration's National Climate Centre (http://www.ncc-cma.net/) announced the ten hottest cities in China in summer, with Chongqing, Fuzhou, Hangzhou, and Nanchang dubbed the "Four Furnaces." Nanchang, the capital city of Jiangxi Province, has seen rapid population growth and increased building density over the last 30 years. The standard of living is constantly being challenged.

In summary, the study's objectives are threefold: 1) to analyze the changes in LULC and LSTE in Nanchang City during the summer (June-August) from 1990 to 2020; 2) to investigate the relationship between LULC type, structure, and pattern change and LSTE; and 3) to integrate the three dimensions of LULC type, structure, and pattern and systematically propose recommendations for improving LST reduction.

2 Material and methods

2.1 Study area

Nanchang is one of the most important central cities in East China, located in the north of central Jiangxi, downstream of the Gan and Fei rivers, and on the southwestern shore of Poyang Lake. One of the Yangtze River urban agglomeration's central cities (Wang et al., 2020). (Figure 1). Nanchang has a subtropical monsoon climate with plenty of heat, rain, and light, but it is prone to monsoon winds, uneven precipitation distribution, high temperatures and drought, and frequent meteorological disasters such as low temperatures and cold damage, along with torrential rainfall and flooding, and it is one of the hottest cities in China in summer. To mitigate the UHI effect and improve the living environment in similar cities, it is critical to investigate the relationship between LUCC and Nanchang's LSTE.

2.2 Data sources

LULC data, Landsat remote sensing image data, and administrative data were used in this paper. The 1990, 2000, 2010, and 2020 LULC data were obtained from the Chinese Academy of Sciences' Center for Resource and Environmental Science and Data (https://www.resdc.cn/), with a spatial resolution of 30 m, and included six primary types of cropland, forest land, grassland, watersheds, inhabited land, and unutilized land, as well as 25 secondary types. This dataset has been frequently utilized in LUCC research and related studies, and the data accuracy meets the requirements of the research. Landsat remote sensing images were chosen from Landsat 5 TM and Landsat 8 OLI remote sensing images collected during the summer of the corresponding year (June-August). The Landsat data used in this study were obtained from the Geographic Data Cloud (https://www.gscloud.cn/) and the United States Geological Survey (https://www.usgs.gov/), both in the summer of the year (June-August), and with a spatial

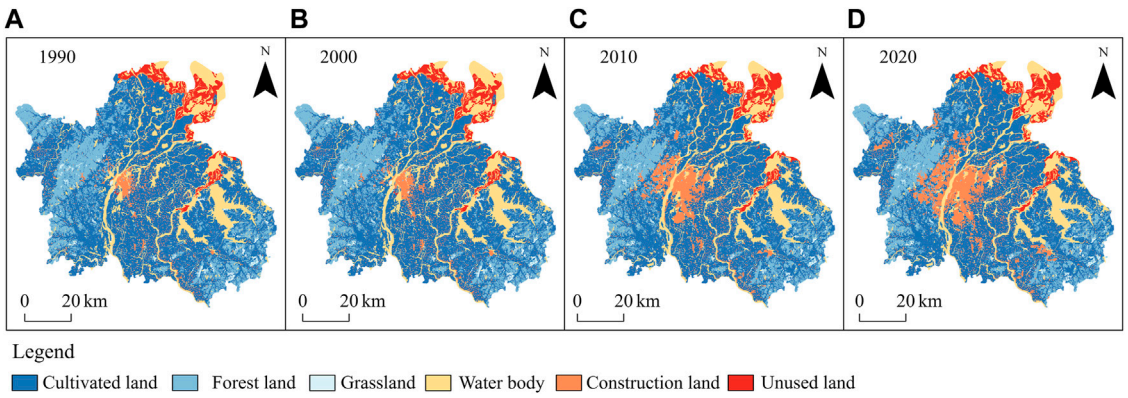

FIGURE 3
LULC of Nanchang City. **(A–D)** represent the years 1990, 2000, 2010 and 2020.

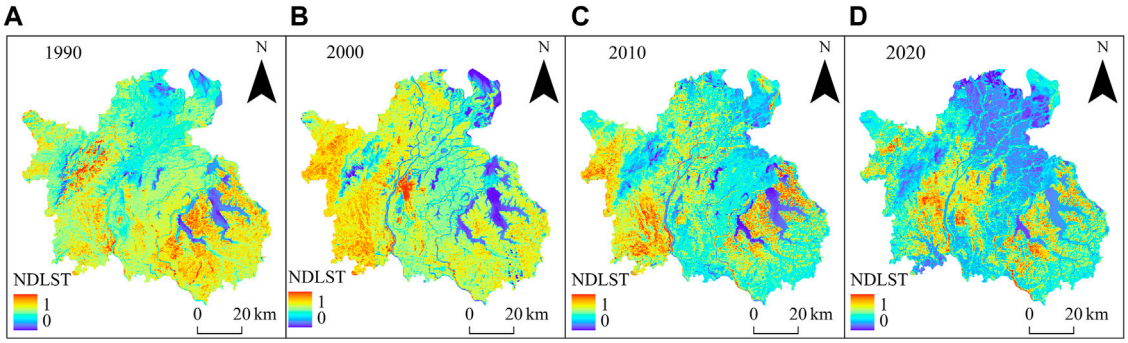

FIGURE 4
Normalised LST in Nanchang City. **(A–D)** represent the years 1990, 2000, 2010 and 2020.

TABLE 2 Percentage of LULC type in Nanchang.

	1990		2000		2010		2020	
LULC types	Area/km^2	%	Area/km^2	%	Area/km^2	%	Area/km^2	%
Cultivated land	4090.89	56.91	4066.56	56.57	3934.14	54.73	3798.90	52.85
Forest land	1214.07	16.89	1214.78	16.90	1188.54	16.53	1149.93	16.00
Grassland	98.09	1.36	96.67	1.34	76.18	1.06	75.40	1.05
Water body	1198.22	16.67	1196.50	16.64	1120.34	15.58	1133.39	15.77
Construction land	279.14	3.88	306.05	4.26	538.03	7.48	712.43	9.91
Unused land	308.31	4.29	308.16	4.29	331.48	4.61	318.66	4.43

resolution of 30 m. Landsat data are widely used for research on urban heat islands (Senf et al., 2015; Hang and Rahman, 2018). The National Basic Geographic Information Center (http://www.ngcc.cn/) provided the administrative zoning data. Despite administrative zoning changes during the study period, this study used the Nanchang City administrative zoning of 2020 uniformly. Table 1 lists the data sources in detail. To ensure a consistent coordinate system, all data in this paper were pre-processed.

2.3 Theory and methodology

Figure 2 depicts the detailed workflow of this study. Firstly, data collection was carried out to obtain LULC data and Landsat remote sensing images of the study area during the study period; Second, using ArcGIS Pro 3.0 software, LULC data were pre-processed and classified into six categories: cultivated land, forest land, grassland, water bodies, construction land, and unused land (Figure 3). Using

TABLE 3 LULC transfer matrix for Nanchang 1990–2020.

1990	2020/km²							Transfer out percentage (%)
	Cultivated land	Forest land	Grassland	Water body	Construction land	Unused land	Total	
Cultivated land	4048.04	3.77	0.02	16.73	22.33	0.01	4090.89	0.07
Forest land	2.59	1208.47	0.71	0.18	2.12	0	1214.07	0.06
Grassland	0.02	2.44	95.05	0.01	0.58	0	98.09	0.26
Water body	15.81	0.10	0.89	1178.97	1.98	0.47	1198.22	0.14
Construction land	0.09	0.01	0	0.01	279.03	0.00	279.14	0.10
Unused land	0.01	0	0	0.61	0.00	304.98	305.6	0.07
Total	4066.55	1214.78	96.67	1196.50	306.05	305.46	7185.99	

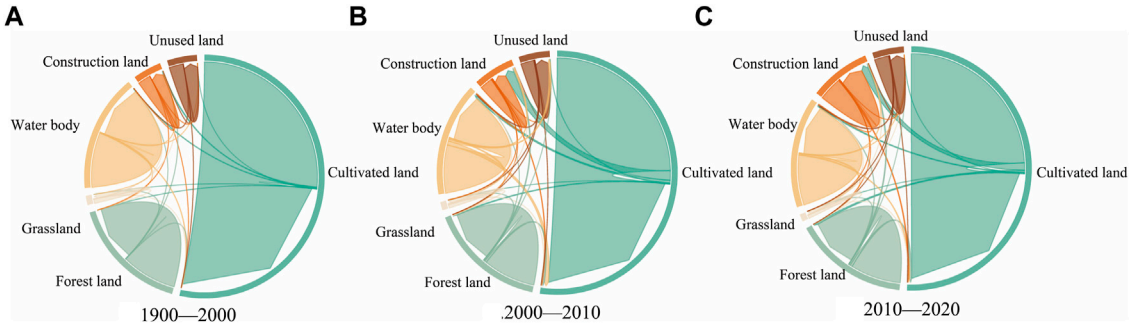

FIGURE 5
LULC transfer chord Map of Nanchang. **(A)** 1990–2020. **(B)** 1990–2020. **(C)** 1990–2020.

ENVI 5.3 software, Landsat remote sensing images were inverted to real LST, and the accuracy was verified, as well as the real LST was normalised for comparability (Figure 4). Finally, the contribution index approach and the stepwise regression method were used to study the relationship between LUCC and the LSTE.

2.3.1 LST inversion

2.3.1.1 Atmospheric correction Method

For LST inversion, the atmospheric correction method was used, with specific steps including thermal infrared radiation calibration, normalized vegetation index calculation, vegetation cover calculation, surface specific emissivity calculation, blackbody radiance brightness calculation, and true LST inversion (Zareie et al., 2016; Hang and Rahman, 2018).

2.3.1.2 LST accuracy verification

The data were processed using ArcGIS Pro 3.0 software to obtain the average LST data of Nanchang City in summer using the Chinese 1 km resolution daily LST data provided by the National Qinghai-Tibet Plateau Data Centre. Following that, the LST data from Landsat image inversion was resampled to make it consistent with the resolution of daily LST data at 1 km resolution in Nanchang, and finally 150 sample points were randomly selected to process the difference between the extracted sample point temperature data, and the results showed that the average difference between the sample points in the three periods of 2000, 2010, and 2020 was 3.37°C, 4.76°C, and 0.13°C, respectively. It demonstrates that the LST inversion results meet the research requirements.

2.3.2 Eliminating the effects of global climate change

According to the Blue Book on Climate Change in China 2022, global climate change caused the average LST in Asia in 2020 to be 1.06°C higher than the base period (1981–2010), with China's average LST showing a significant upward trend, with 2020 being the warmest year since the beginning of the 20th century. In order to eliminate the impact of global climate change on LST and truly reflect the relationship between LUCC and LST, this study takes 1990 as the base period, refers to the trend of annual LST change by climate impact in the region where Nanchang is located (East China) in the Blue Book on Climate Change in China 2022, and with the help of the raster calculator tool of the ArcGIS 3.0 Pro software, the value of climate change impacts was subtracted from the LST of the corresponding year to eliminate the impacts of global climate change to a certain extent.

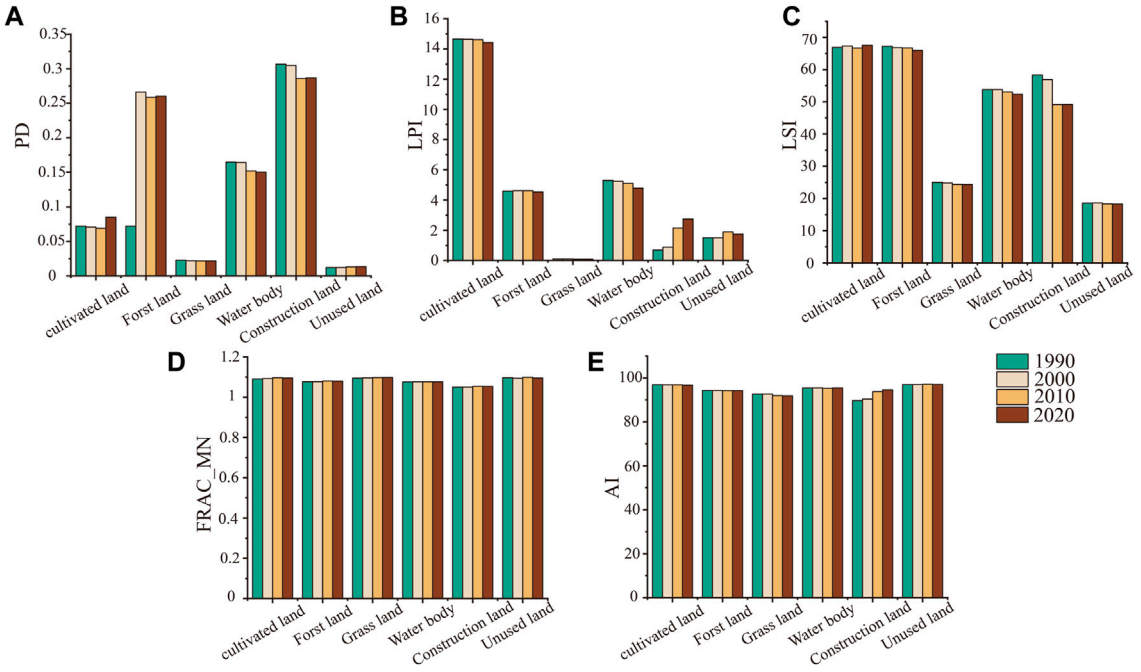

FIGURE 6
LULC class level changes in Nanchang. **(A)**PD, **(B)** LPI, **(C)** LSI, **(D)** FRAC_MN, **(E)** AI.

TABLE 4 Changes in LULC landscape levels in Nanchang.

Years	PD	LPI	LSI	FRAC_MN	CONTAG	SHDI	AI
1990	14.6638	60.3071	1.5771	229.0259	59.6765	1.2396	95.8831
2000	14.6424	60.4071	1.5798	228.5595	59.416	1.2485	95.8759
2010	14.6154	59.7776	1.6159	226.3275	57.9585	1.3013	95.9209
2020	14.4262	60.1775	1.6184	230.0326	56.902	1.3366	95.8933

2.3.3 Landscape pattern indices

The landscape pattern index is categorized into patch, class, and landscape levels and is a useful tool for quantifying landscape patterns within a region (Su et al., 2014; Saleh et al., 2022). Among them, class level and landscape level can reflect the landscape pattern indices of different LULCs within the study unit and the overall landscape pattern index, respectively. The following criteria have been set for the selection of landscape pattern indices in previous studies: 1) the chosen indicators can represent various aspects of landscape characteristics (size, shape, connectivity, and so on); 2) the chosen indicators should not be highly redundant; and 3) the chosen indicators should be widely accepted (Weng, 2007). In order to study the relationship between different LULC patterns and regional patterns with LST, following the above principles, five landscape pattern indices were chosen at the class level: patch density (PD), largest patch area index (LPI), landscape shape index (LSI), mean fractional dimension (FRAC MN), and aggregation index (AI), and at the landscape level: patch density (PD), largest patch area index (LPI), landscape shape index (LSI), mean fractional dimension (FRAC MN), aggregation index (AI), contagion index (CONTAG), and shannon diversity index (SHDI).

2.3.4 Contribution index

A contribution index (CI) was developed to investigate the contribution and spatial and temporal relationships between various land types and the LSTE during LUCC in Nanchang from 1990 to 2020 (Das Majumdar and Biswas, 2016; Sun and Chen, 2017; Huang et al., 2019). It was calculated as follows:

$$CI = \left(\overline{LST_d} - \overline{LST}\right) \times \left(\frac{S_d}{S}\right) \quad (1)$$

LST_d and LST denote the average land LST of Region d (6 LULC types) and the average LST of the entire area (Nanchang City), respectively; S_d and S denote the area of region d and the entire study area, respectively. If $CI > 0$, the region d contributes positively to the LST of the entire study area, indicating a warming effect, where as if $CI < 0$, the region das contributes negatively to the LST of the entire study area, indicating a cooling effect.

TABLE 5 Criteria for classification of LSTEs.

	Low temperature zone	Sub-moderate temperature zone	Medium temperature zone	Sub-high temperature zone	High temperature zone
Range	0–0.2	0.2–0.4	0.4–0.6	0.6–0.8	0.8–1

TABLE 6 Area and percentage of LSTE class.

	1990		2000		2010		2020	
Temperature class	Area/km^2	/%	Area/km^2	Area/%	Area/km^2	/%	Area/km^2	/%
Low temperature zone	554.3109	7.7171	4.7034	0.0655	0.3699	0.0051	0.1116	0.0016
Sub-moderate temperature zone	6454.2870	89.8563	2154.3102	29.9922	198.1206	2.7582	2255.8950	31.4065
Medium temperature zone	172.9647	2.4080	5011.8579	69.7749	4162.9788	57.9568	4361.3919	60.7191
Sub-high temperature zone	1.1412	0.0159	11.8134	0.1645	2722.8141	37.9069	564.5925	7.8602
High temperature zone	0.1926	0.0027	0.2115	0.0029	98.6130	1.3729	0.9054	0.0126

2.3.5 Stepwise regression

SPSS software was used to create stepwise regression equations to examine the association between LUCC and LST change, with LUCC serving as the independent variable and LST change serving as the response variable. To address the possibility of multicollinearity, factors with no significant regression connections were included and eliminated from the stepwise regression (Su et al., 2014).

3 Results

3.1 Land use and land cover changes

3.1.1 LULC type changes

Statistics on LULC types in Nanchang were picked up using the ArcGIS Pro software spatial analysis tool (Table 2). The findings show that the LULC area of Nanchang City changed significantly between 1990 and 2020, as evidenced by an increase in construction land and a decrease in cultivated land. After 30 years, Nanchang City's construction land area has grown from 279.14 km^2 to 712.43 km^2. In contrast, the area of cultivated land shrank from 4,090.89 km^2 to 3,798.90 km^2. The overall change in forest land, grassland, water, and unused land is small.

The reasons for this are that Nanchang has experienced rapid economic development and population growth since 1990, with total GDP increasing from 6.32 billion RMB in 1990 to 574.55 billion RMB in 2020 and the resident population increasing from 372.59 million to 625.55 million, resulting in an increasing scale of construction land. General Programme for the Reform of the Ecological Civilization System, which explicitly required the spatial use control of national land, limiting the disorderly expansion of construction land to the greatest extent possible, resulting in a moderating trend in the growth of construction land area in Nanchang during the period 2010–2020; on the other hand, to alleviate the deteriorating ecological environment, the Chinese government in the last few years has implemented a number of policies to address the issue. To address the deteriorating ecological environment, the Chinese government implemented a strategy of gradually returning farmland to forest and grass at the end of the last century, gradually returning farmland on slopes and mountains, as well as in critical ecological function areas, to forest and grass, resulting in a reduction in farmland area.

3.1.2 LULC structure changes

The spatial analysis tool of ArcGIS Pro 3.0 software was used to analyze the LULC structure change in Nanchang from 1990 to 2020, as well as the LULC shift matrix (Table 3) and the LULC shift chord diagram of Nanchang (Figure 5), to further investigate the relationship between LULC change and the LSTE.

The findings show that changes in LULC structure in Nanchang from 1990 to 2020 primarily take the form of arable land being transferred to other land and other land types being transferred to construction land. The area of arable land flowing into construction land is 383.01 km^2, with an upward and then downward trend, followed by arable land flowing into forest land and water bodies, which are 70.41 km^2 and 99.66 km^2, respectively, with other land types changing less.

The areas where the LULC structure of Nanchang City has changed significantly in terms of both temporal and spatial distribution are primarily located in Qingyunpu District, Xihu District, and Qingshan Lake District, specifically in the transformation of other land into construction land, owing primarily to the fact that the aforementioned areas are the central urban areas in Nanchang City General Urban Development Plan. The city's urban nature as a major economic, cultural, scientific and technological, and information center for the province, as well as the urban spatial pattern of development across the river, led to a gradual increase in the amount of construction land in Nanchang's central urban area.

3.1.3 LULC pattern change

LULC class level (Figure 6) and landscape level indices (Table 4) were calculated using Fragstats 4.2 software for 1990, 2000, 2010, and 2020.

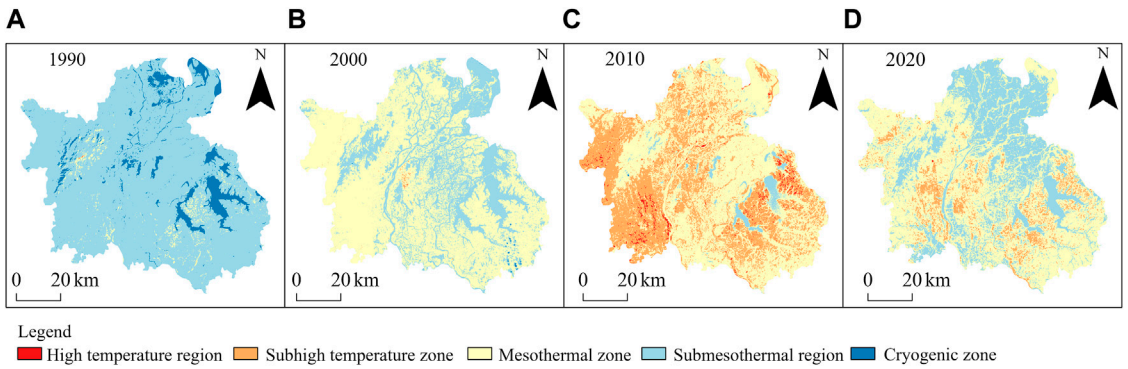

FIGURE 7
Distribution of LST classes. **(A–D)** represent the years 1990, 2000, 2010 and 2020.

TABLE 7 Changes in mean temperature and standard deviation of LULC types in Nanchang.

LULC types	1990		2000		2010		2020		Mean
	Mean	STD	Mean	STD	Mean	STD	Mean	STD	Mean
Cultivated land	13.5652	0.8798	27.8487	1.0000	26.1878	2.1157	29.6245	2.5523	24.3066
Forest land	11.6573	1.2279	27.7156	1.4247	25.1867	2.0213	29.7866	1.7856	23.5866
Grassland	13.7984	1.3213	27.9512	1.8060	25.7235	2.3658	30.2765	2.0593	24.4374
Water body	11.6573	1.2279	24.5491	2.1377	22.9426	2.6254	27.7939	2.0850	21.7357
Construction land	12.8589	0.8707	28.6314	1.8692	26.6068	1.4400	33.4805	1.9643	25.3944
Unused land	12.4325	0.7680	26.0963	1.1945	23.2915	1.3179	26.7905	1.0901	22.1527

3.1.3.1 The class level

The class level index calculation results show that the PD changed more clearly between 1990 and 2020, with cultivated land increasing to a greater extent, followed by unused land, while the PD of the other land types showed a decreasing trend or fluctuated less, indicating that cultivated land was more influenced by human activities, while the area of cultivated land transferred to other land types decreased. The most extensive LPI of construction land and unused land have increased significantly, while the rest of the land types have shown a decreasing trend, which also confirms the rapid economic development and population explosion at this stage, resulting in the continuous expansion of the area of construction land, leading to the rise of the landscape status of construction land; the LSI and PD change trends are similar, in which the FRAC_MN of each category and the AI have remained relatively stable over the last 30 years, indicating that the overall shape of each class category has remained relatively stable, with the AI of construction land showing a slight upward trend, indicating that the density of buildings in Nanchang has increased. Patches have become more aggregated as social and economic development has progressed.

3.1.3.2 The landscape level

The landscape level index calculation results show that between 1990 and 2020, the density of LULC patches, the LPI, and the CONTAG of Nanchang City all show a decreasing trend, while the AI, the FRAC_MN, and the LSI all show an increasing trend, indicating from both positive and negative perspectives that with socio-economic development, the patches among various LULC types in Nanchang will become more diverse. The SHDI that the complexity of LULC landscape composition has increased, confirming landscape type diversity while reflecting greater spatial heterogeneity of LULC landscape types within Nanchang and the diversification of LULC types.

3.2 Changes in the LSTE

To investigate the trend of LSTE change in Nanchang City, the normalized LST of Nanchang City was used in four periods and classified into five levels using the equidistant method, as shown in Table 5 (Siqi and Yuhong, 2020). The area and proportion of each temperature class in each of the four periods were counted separately (Table 6; Figure 7). The findings indicate that the relationship between LST and LULC types is very close; between 1990 and 2020, the high temperature and sub-high temperature zones of LST in Nanchang primarily belong to arable land and construction land, while the low temperature and sub-moderate temperature zones primarily belong to water bodies and forest land. The study found that

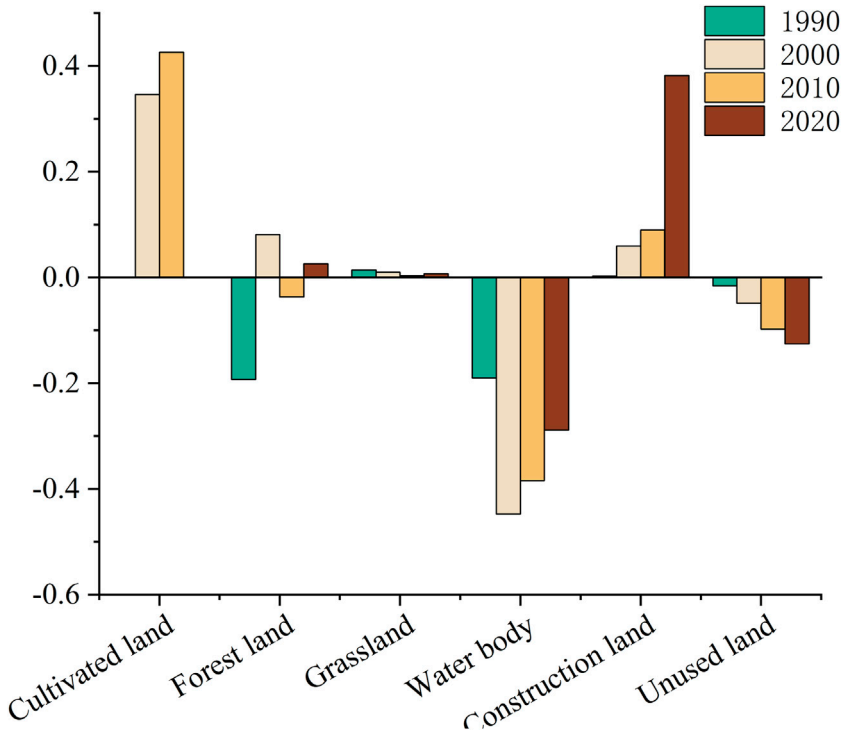

FIGURE 8
LULC types contribution.

TABLE 8 Relationship between changes in the LULC class level and LST.

	1990–2000		2000–2010		2010–2020	
LULC	Increasing	Decreasing	Increasing	Decreasing	Increasing	Decreasing
Cultivated land		LPI、PD	FRAC_MN	PD, LPI, LSI		LPI, LSI, PD
Forest land	LPI	AI	PD			LPI, LSI, AI
Grassland	PD	AI		LSI		PD
Water body	PD	LPI	PD, AI	LPI, FRAC_MN	PD	LPI,LSI
Construction land	PD, LPI,AI	FRAC_MN	LPI, LSI	PD	LPI、LSI	PD
Unused land	AI	LPI、FRAC_MN	LPI, LSI	PD, FRAC_MN		PD

water bodies and forest land can reduce LST to some extent, whereas construction land and arable land can increase LST. The LST in Nanchang has significant spatial heterogeneity. It gradually demonstrates the development trend of high- and secondary-temperature areas from the periphery to the center, owing to the concentration of construction land in Nanchang's central area. The construction land area is rapidly expanding, causing high-temperature areas to shift from the periphery to the center. In terms of temperature class expansion, the Sub-high -temperature zone has grown significantly in the last 30 years, covering 563.45 km^2, or about 7.84% of Nanchang's total area. The area of the low-temperature zone shrank by 554.1993 km^2 in 30 years, accounting for 7.72% of Nanchang's area, while the area of the sub-middle-temperature zone increased by 58.45% and the area of the middle-temperature zone decreased by 58.32%, indicating a significant change.

3.3 Impacts of LUCC changes on the LSTE

3.3.1 Impact of LULC type changes on LSTE

Since the LUCC in Nanchang City between 1990 and 2020 is mainly concentrated on cultivated land and construction land, this paper focuses on the relationship between cultivated land and construction land and LST. The four periods of LULC types and LST in Nanchang City from 1990, 2000, 2010, and 2020 were overlaid and analyzed using the ArcGIS Pro 3.0 software spatial overlay tool to obtain the LST of various LULC types in Nanchang

City from 1990 to 2020 (Table 7). The average LST of construction and cultivated land was found to be the highest, and the overall increase in LST over the past 30 years was very significant, indicating that urbanization had a significant effect on raising the LST. The contribution index was used to calculate the contribution of different LULC types to LST in Nanchang to further investigate the relationship between different LULC types and the LSTE (Figure 8). The results show that the contribution indices of arable land and construction land are all positive. The contribution index of cultivated land is significantly higher than that of construction land, indicating that the expansion of arable land and construction land contributes to the rise in LST.

In contrast, the year-on-year growth in the contribution index for constructed land is intrinsically related to Nanchang City's rapid economic development and the conversion of a substantial amount of cultivable land to construction land. At the same time, the studies suggest that bodies of water and undeveloped land have a considerable cooling effect.

3.3.2 Impact of LUCC structure on the LSTE

The LULC structure was characterized by the area share of different LULC types, and a 2 km × 2 km grid (1961 in total) was generated in the study area. The best regression equation was chosen (tolerance of each variable>1.0 and VIF<10, no covariance between variables), and the results are as follows:

$$\Delta NDLST_{1990-2000} = -520.246 - 13.012\Delta X_{Cultivated\ land} - 21.714\Delta X_{water\ body}$$

$$\Delta NDLST_{2000-2010} = -678.631 + 2.859\Delta X_{Cultivated\ land} + 9.233\Delta X_{Unused\ land} + 4.990\Delta X_{Construction\ land} + 2.373\Delta X_{Forest\ land}$$

$$\Delta NDLST_{2010-2020} = 514.702 + 7.066\Delta X_{Construction\ land}$$

The results show that at the scale of 2 km × 2 km grid, the increase in the area of construction land, cultivated land, and unused land all play a positive role in the rise of the LSTE, among which construction land has the most decisive influence on the LSTE. A 10% increase in the proportion of built-up land in the grid between 2010 and 2020 results in a 70.66 increase in the total normalized temperature of the grid, indicating that changes in the area of built-up land are highly correlated with changes in the area of the LSTE.

3.3.3 Impact of LUCC pattern on the LSTE

The class level index and landscape level index were calculated separately for each grid using Fragstats 4.2 software. The regression relationship between the difference in class level index, the landscape level index, and the difference in mean normalized LST was established using a stepwise regression method for the three time periods 1990–2000, 2000–2010, and 2010–2020. (The best regression equation was selected (tolerance of each variable >1.0, and VIF <10, no covariance between variables).

3.3.3.1 Class level index and normalized LST

According to a class level analysis, the degree of correlation between the difference in class indices and the difference in LST for different land types varied significantly over time, indicating that the landscape pattern indices had varying degrees of influence on LST over time. The regression analysis results were as follows (Table 8):

Cultivated land : $\Delta NDLST_{1990-2000} = -549.416 - 2.715\Delta X_{LPI} - 112.555\ \Delta X_{PD}$

$$\Delta NDLST_{2000-2010} = -706.954 - 1.061\Delta X_{LPI} - 6.445\Delta X_{PD} - 34.902\Delta X_{LSI} + 244.245\Delta X_{FRAC_{MN}}$$

$$\Delta NDLST_{2010-2020} = 533.419 - 8.143\Delta X_{LPI} - 59.573\Delta X_{LSI} - 1.772\Delta X_{PD}$$

Forest land : $\Delta NDLST_{1990-2000} = -541.315 + 3.087\Delta X_{LPI} - 2.874\ \Delta X_{AI}$

$$\Delta NDLST_{2000-2010} = -723.437 + 71.596\Delta X_{PD}$$

$$\Delta NDLST_{2010-2020} = 514.584 - 7.522\Delta X_{LPI} - 69.566\Delta X_{LSI} - 1.717\Delta X_{AI}$$

Grass land : $\Delta NDLST_{1990-2000} = -469.901 - 2.984\Delta X_{AI} + 361.622\Delta X_{PD}$

$$\Delta NDLST_{2000-2010} = -657.732 - 73.077\Delta X_{LSI}$$

$$\Delta NDLST_{2010-2020} = 474.683 - 211.446\Delta X_{PD}$$

Water body: $\Delta NDLST_{1990-2000} = -533.205 + 4.092\Delta X_{PD} - 6.072\ \Delta X_{LPI}$

$$\Delta NDLST_{2000-2010} = -709.562 - 5.912\Delta X_{LPI} + 1.220\Delta X_{PD} - 194.286\Delta X_{FRAC_{MN}} + 2.452\Delta X_{AI}$$

$$\Delta NDLST_{2010-2020} = 515.524 - 6.304\Delta X_{LPI} - 85.858\Delta X_{LSI} + 0.972\Delta X_{PD}$$

Construction land: $\Delta NDLST_{1990-2000} = -576.597 + 226.671\Delta X_{PD} + 9.223\Delta X_{LPI} - 2347.932\Delta X_{FRAC\_MN} + 27.457\Delta X_{AI}$

$$\Delta NDLST_{2000-2010} = -728.739 + 0.886\Delta X_{LPI} - 99.371\Delta X_{PD} + 47.012\Delta X_{LSI}$$

$$\Delta NDLST_{2010-2020} = 548.571 + 7.685\Delta X_{LPI} - 105.273\Delta X_{PD} + 59.345\Delta X_{LSI}$$

Unused land : $\Delta NDLST_{1990-2000} = -246.152 + 8.599\Delta X_{AI} - 1.676\Delta X_{\ LPI} - 555.41\Delta X_{FRAC\_MN}$

$$\Delta NDLST_{2000-2010} = -620.532 + 7.198\Delta X_{LPI} - 35.493\Delta X_{PD} + 189.888\Delta X_{LSI} - 205.674\Delta X_{FRAC_{MN}}$$

$$\Delta NDLST_{2010-2020} = 486.695 + 11.403\Delta X_{PD}$$

It was found that between 1990 and 2000, LPI and PD decreased LST for cultivated land; LPI increased LST and AI decreased LST for forested land; AI decreased LST and PD increased LST for grassland; PD increased LST and AI decreased LST for waterbodies; FRAC_MN decreased LST for constructed land; and LPI and FRAC_MN decreased LST for unused land.

Between 2000 and 2010, FRAC_MN for cultivated land increases LST while PD, LPI, and LSI decrease LST; PD for forest land increases LST; LSI for grassland decreases LST; PD and AI for water bodies increase LST while LPI and FRAC_MN decrease LST; LPI and LSI for construction land increase LST while PD decreases LST; and PD and FRAC_MN for unused land decrease LST while LPI and LSI increase LST.

From 2010 to 2020, LPI, LSI, and PD decrease LST for cultivated land and forest land; PD decreases LST for grassland; LPI and LSI decrease LST and PD increases LST for waterbodies; LPI and LSI increase LST and PD decreases LST for construction land; and PD decreases LST for unused land. In general, higher PD and LPI of construction land and cultivated

land can lead to increases in LST, while increases in landscape dominance and AI can lead to increases in the LST of cultivated land and cultivated land, while the opposite is true for forest land and water bodies, where higher aggregation, landscape dominance, and connectivity can improve the LST.

The results show that the class index of different LULCs has an unstable effect on LST and also indicate that the study of the relationship between the LULC landscape pattern index and LST in different periods is of great research significance for analyzing the changes in the LSTE.

3.3.3.2 Landscape level index and normalized LST

The following is the regression equation between the change in the landscape type index and the transformation of the thermal environment at the surface:

$$\Delta NDLST_{1990-2000} = -525.508 - 240.198\Delta X_{SHDI}$$

$$\Delta NDLST_{2000-2010} = -690.947 + 2054.006\Delta X_{FRAC_{MN}} - 1.397\Delta X_{PD} + 64.467\Delta X_{AI} + 153.802\Delta X_{LSI}$$

$$\Delta NDLST_{2010-2020} = 505.792 - 0.817\Delta X_{PD} - 1044.069\Delta X_{FRAC_{MN}} + 1.783\Delta X_{CONTAG} + 259.433\Delta X_{SHDI} + 14.277\Delta X_{AI}$$

The regression equation between the difference in landscape level indices and the difference in mean normalized LST demonstrates that the correlation between landscape level indices is also highly variable, implying that the influence of landscape level indices on the LSTE is also unstable.

From 1990 to 2000, the regression equation shows that only the difference in SHDI is associated with the difference in normalized LST while decreasing LST; from 2000 to 2010, FRAC_MN, AI, and LSI are all associated with the difference in normalized LST and will increase LST; from 2010 to 2020, PD, FRAC_MN, CONTAG, SHDI, and AI will all have an impact on LST.

3.3.3.3 Synthesized analysis

When the class level and landscape type level results are combined, it is discovered that the class level difference and landscape type level difference all influence the normalized LST difference. However, different landscape pattern indices correlate differently with the normalized LST difference over time. According to a thorough analysis, the lower the PD of woodlands and water bodies, the higher the LPI and LSI, and the more effective at lowering LST and mitigating the urban heat island effect. In contrast, the greater the aggregation and landscape dominance of construction and arable land, the more likely they are to produce the heat-gathering effect, increasing LST and deteriorating LSTE. At the same time, the spatial and temporal distribution of the LSTE in Nanchang shows that most of the areas with a higher LSTE are located in residential areas or arable land and gradually shift towards the city center, owing to the concentration of construction land and arable land patches in the area and the high degree of aggregation, proving that the landscape pattern has an influence on the LSTE. Finally, concentrated and large-scale arable and construction land will degrade the LSTE. Simultaneously, increasing the area of forests and water bodies in the region, as well as the complexity and diversity of the structure of the LULC, can effectively reduce the region's LST.

4 Discussion

4.1 Differences in the relationship between different LULC and LST

The analysis of the relationship between LUCC and the LST in Nanchang revealed that different LULC, structural, and landscape pattern changes all have a direct impact on the LST. In terms of static LULC, cultivated and constructed land has significantly higher average temperatures than other LULC. After conversion to cultivated or constructed land, the LST of various LULCs increased significantly. Some studies have found that changes in unused land areas have an impact on the LSTE (Huang et al., 2019), but this study found no significant warming effect of unused land. The classification of unused land in this study, where the majority of the unused land in the LULC is swamp and mudflat, could explain this. In contrast, the majority of unused land classification in existing studies is bare land, which has resulted in disparities in study results.

4.2 Scale of the research module

The dynamic role of LUCC on LST was discovered to vary at different scales (Kuang et al., 2017). To choose the best study scale, the study area was divided into 1 km × 1 km, 1.5 km × 1.5 km, and 2 km × 2 km fishing nets. It was discovered that the regression equations constructed for 1 km × 1 km and 1.5 km × 1.5 km fishing nets could not pass the significance test or there was no regression relationship, so the study scale was set to 2 km × 2 km, but in reality, LUCC have a strong influence on local climate (Tarawally et al., 2018), however, there may be differences in the effect and the range of influence, and the research on the effect of LULC on LST at different scales should be further deepened in the future.

4.3 Limitations of the study and future research directions

However, there are some flaws in this study. To begin, due to data constraints, the study's LST data were processed using Landsat data. The timing of Landsat image acquisition increased the study's uncertainty (Schwaab et al., 2020). Because the Landsat 5 TM and Landsat 8 OLI images used in the study were from cloud-free weather, it is impossible to conclude that the relationship between LUCC and LST on cloudy or rainy days. The second limitation is the research methodology. While this study concludes that increasing the area of built-up land and cultivated land increases LST, the article lacks research on the relationship between urban building height and LST in the case of built-up land, with urban building height and area also being an influencing factor on urban heat islands (Morabito et al., 2016; Chen et al., 2022; Han et al., 2023). The study confirms that changes in LULC type, structure, and pattern all affect LST; however, LUCC contains many elements, such as arable land quality, water quality, changes in different types of trees in forest land, and changes in vegetation cover, all of which may affect LST, and the above studies should be strengthened in the future.

Notwithstanding its limitations, the study methodology reflects the relationship between type, structure, pattern, and LSTE of LUCC. It has no direct effect on the study's findings.

5 Conclusion

Nanchang, a "furnace city," was chosen for the study because of the complexity of LUCC and the close relationship between LUCC and LSTE change. The contribution index and regression analysis were used to study the relationship between scale, structure, morphology, and LSTE in LULC change separately. The study found that LUCCs in Nanchang primarily show a decrease in the area of cultivated land, a continuous expansion of construction land, a rapid increase in the proportion of construction land within the urban area, a gradual fragmentation of the overall patches, and a tendency to diversify the LULC structure. Also confirmed The thermal environment of Nanchang's land surface is deteriorating, with high-temperature areas gradually expanding, primarily in densely built-up areas in the city center, while low-temperature areas are primarily located in the area of Poyang Lake in the north of Nanchang, with obvious spatial heterogeneity. According to the contribution index, construction land and arable land are the main contributors to the deterioration of the urban LSTE, whereas water bodies can effectively improve the LSTE. The regression equation also confirms that increasing the proportion of arable land and construction land area will significantly worsen the LSTE, while increasing the proportion of water body area will improve the LSTE. At the same time Different land type patterns have different effects on surface thermal conductivity. Different land-use patterns have different effects on the LSTE. For example, higher LPI and LSI for woodlands and water bodies can be effective in reducing LST and improving thermal trends in the LSTE. Therefore, in order to avoid the generation of urban heat island effect, the layout arrangement of land use type, quantity and landscape structure should be considered comprehensively in urban planning and design, and the deterioration of LSTE should be mitigated and the UHI effect should be avoided by appropriately increasing urban green areas and water bodies and enriching landscape structure types.

Data availability statement

The original contributions presented in the study are included in the article/Supplementary material, further inquiries can be directed to the corresponding author.

Author contributions

YZ and HC: methodology, YZ: software, YZ and TZ: validation, YZ, HC and TZ: formal analysis, YZ: investigation, XG: resources, JZ: data curation, JZ and LH: writing—original draft preparation, YZ: writing—review and editing, YZ and HC: visualization, YZ and TZ: supervision, HC: project administration, TZ and HC: funding acquisition. All authors contributed to the article and approved the submitted version.

Funding

This research was funded by National Natural Science Foundation of China, grant No. 31660140 and 42001232; Natural Science Foundation of Jiangxi province, grant No. 20171BAA218021; Key Re-search Bases of Humanities and Social Sciences for Universities in Jiangxi province, grant no. 2018-32; and Special Funding Program for Graduate Student Innovation in Jiangxi Province, grant No. YC2022-s414.

Conflict of interest

The authors declare that the research was conducted in the absence of any commercial or financial relationships that could be construed as a potential conflict of interest.

Publisher's note

All claims expressed in this article are solely those of the authors and do not necessarily represent those of their affiliated organizations, or those of the publisher, the editors and the reviewers. Any product that may be evaluated in this article, or claim that may be made by its manufacturer, is not guaranteed or endorsed by the publisher.

References

Bokaie, M., Zarkesh, M. K., Arasteh, P. D., and Hosseini, A. (2016). Assessment of urban heat island based on the relationship between land surface temperature and land use/land cover in tehran. *Sustain. Cities Soc.* 23, 94–104. doi:10.1016/j.scs.2016.03.009

Chang, Y., Xiao, J. F., Li, X. X., Zhou, D. C., and Wu, Y. P. (2022). Combining GOES-R and ECOSTRESS land surface temperature data to investigate diurnal variations of surface urban heat island. *Sci. Total Environ.* 823 (15), 153652. doi:10.1016/j.scitotenv.2022.153652

Chapman, S., Watson, J. E. M., Salazar, A., Thatcher, M., and McAlpine, C. A. (2017). The impact of urbanization and climate change on urban temperatures: a systematic review. *Landsc. Ecol.* 32 (10), 1921–1935. doi:10.1007/s10980-017-0561-4

Chen, J. K., Zhan, W. F., Du, P. J., Li, L., Li, J. F., Liu, Z. H., et al. (2022). Seasonally disparate responses of surface thermal environment to 2D/3D urban morphology. *Build. Environ.* 214 (15), 108928. doi:10.1016/j.buildenv.2022.108928

Chen, Y. C., Chiu, H. W., Su, Y. F., Wu, Y. C., and Cheng, K. S. (2017). Does urbanization increase diurnal land surface temperature variation? Evidence and implications. *Landsc. Urban Plan.* 157, 247–258. doi:10.1016/j.landurbplan.2016.06.014

Das Majumdar, D., and Biswas, A. (2016). Quantifying land surface temperature change from LISA clusters: an alternative approach to identifying urban land use transformation. *Landsc. Urban Plan.* 153, 51–65. doi:10.1016/j.landurbplan.2016.05.001

Estalkhsari, B. M., Mohammad, P., and Razavi, N. (2022). Change detection in a rural landscape: a case study of processes and main driving factors along with its response to thermal environment in Farim, Iran [Article; Early Access]. *Environ. Sci. Pollut. Res.* 17. doi:10.1007/s11356-022-24504-5

Estoque, R. C., Murayama, Y., and Myint, S. W. (2017). Effects of landscape composition and pattern on land surface temperature: an urban heat island study in the megacities of Southeast Asia. *Sci. Total Environ.* 577, 349–359. doi:10.1016/j.scitotenv.2016.10.195

Fu, P., and Weng, Q. H. (2016). A time series analysis of urbanization induced land. use and land cover change and its impact on land surface temperature with Landsat imagery. *Remote Sens. Environ.* 175, 205–214. doi:10.1016/j.rse.2015.12.040

Guo, G. H., Wu, Z. F., Xiao, R. B., Chen, Y. B., Liu, X. N., and Zhang, X. S. (2015). Impacts of urban biophysical composition on land surface temperature in urban heat island clusters. *Landsc. Urban Plan.* 135, 1–10. doi:10.1016/j.landurbplan.2014.11.007

Han, D., An, H., Cai, H., Wang, F., Xu, X., Qiao, Z., et al. (2023). How do 2D/3D urban landscapes impact diurnal land surface temperature: insights from block scale and machine learning algorithms. *Sustain. Cities Soc.* 99, 104933. doi:10.1016/j.scs.2023.104933

Hang, H. T., and Rahman, A. (2018). Characterization of thermal environment over heterogeneous surface of National Capital Region (NCR), India using LANDSAT-8 sensor for regional planning studies. *Urban Clim.* 24, 1–18. doi:10.1016/j.uclim.2018.01.001

Huang, C. C., Zhang, M. L., Zou, J., Zhu, A. X., Chen, X., Mi, Y., et al. (2015). Changes in land use, climate and the environment during a period of rapid economic development in Jiangsu Province, China. *Sci. Total Environ.* 536, 173–181. doi:10.1016/j.scitotenv.2015.07.014

Huang, Q. P., Huang, J. J., Yang, X. N., Fang, C. L., and Liang, Y. J. (2019). Quantifying the seasonal contribution of coupling urban land use types on Urban Heat Island using Land Contribution Index: a case study in Wuhan, China. *Sustain. Cities Soc.* 44, 666–675. doi:10.1016/j.scs.2018.10.016

Intergovernmental Panel on Climate Change (2023). *Climate change 2022 – impacts, adaptation and vulnerability*. doi:10.1017/9781009325844

Kuang, W. H., Yang, T. R., Liu, A. L., Zhang, C., Lu, D. S., and Chi, W. F. (2017). An EcoCity model for regulating urban land cover structure and thermal environment: taking Beijing as an example. *Sci. China-Earth Sci.* 60 (6), 1098–1109. doi:10.1007/s11430-016-9032-9

Li, Y., Schubert, S., Kropp, J. P., and Rybski, D. (2020). On the influence of density and morphology on the Urban Heat Island intensity. *Nat. Commun.* 11 (1), 2647. doi:10.1038/s41467-020-16461-9

Morabito, M., Crisci, A., Messeri, A., Orlandini, S., Raschi, A., Maracchi, G., et al. (2016). The impact of built-up surfaces on land surface temperatures in Italian urban areas. *Sci. Total Environ.* 551-552, 317–326. doi:10.1016/j.scitotenv.2016.02.029

Mushore, T. D., Mutanga, O., Odindi, J., and Dube, T. (2017). Linking major shifts in land surface temperatures to long term land use and land cover changes: a case of Harare, Zimbabwe. *Urban Clim.* 20, 120–134. doi:10.1016/j.uclim.2017.04.005

Oke, T. R. (1982). The energetic basis of the urban heat island. *Q. J. R. Meteorological Soc.* 108 (455), 1–24. doi:10.1002/qj.49710845502

Pelletier, J. D., Murray, A. B., Pierce, J. L., Bierman, P. R., Breshears, D. D., Crosby, B. T., et al. (2015). Forecasting the response of Earth's surface to future climatic and land use changes: a review of methods and research needs. *Earths Future* 3 (7), 220–251. doi:10.1002/2014ef000290

Peng, J., Ma, J., Liu, Q. Y., Liu, Y. X., Hu, Y. N., Li, Y. R., et al. (2018). Spatial-temporal change of land surface temperature across 285 cities in China: an urban-rural contrast perspective. *Sci. Total Environ.* 635, 487–497. doi:10.1016/j.scitotenv.2018.04.105

Pramanik, S., and Punia, M. (2020). Land use/land cover change and surface urban heat island intensity: source-sink landscape-based study in Delhi, India. *Environ. Dev. Sustain.* 22 (8), 7331–7356. doi:10.1007/s10668-019-00515-0

Qiao, Z., Lu, Y., He, T., Wu, F., Xu, X., Liu, L., et al. (2023). Spatial expansion paths of urban heat islands in Chinese cities: analysis from a dynamic topological perspective for the improvement of climate resilience. *Resour. Conservation Recycl.* 188, 106680. doi:10.1016/j.resconrec.2022.106680

Saleh, S. K., Sanaei, A., Amoushahi, S., and Ranjbar, S. (2022). Effect of landscape pattern changes and environmental indices on land surface temperature in a fragile ecosystem in southeastern Iran [Article; Early Access]. *Environ. Sci. Pollut. Res.* 17. doi:10.1007/s11356-022-24602-4

Schwaab, J., Davin, E. L., Bebi, P., Duguay-Tetzlaff, A., Waser, L. T., Haeni, M., et al. (2020). Increasing the broad-leaved tree fraction in European forests mitigates hot temperature extremes. *Sci. Rep.* 10 (1), 14153. doi:10.1038/s41598-020-71055-1

Schwaab, J., Meier, R., Mussetti, G., Seneviratne, S., Burgi, C., and Davin, E. L. (2021). The role of urban trees in reducing land surface temperatures in European cities. *Nat. Commun.* 12 (1), 6763. doi:10.1038/s41467-021-26768-w

Senf, C., Leitão, P. J., Pflugmacher, D., van der Linden, S., and Hostert, P. (2015). Mapping land cover in complex Mediterranean landscapes using Landsat: improved classification accuracies from integrating multi-seasonal and synthetic imagery. *Remote Sens. Environ.* 156, 527–536. doi:10.1016/j.rse.2014.10.018

Shiva, J. S., Chandler, D. G., and Kunkel, K. E. (2019). Localized changes in heat wave properties across the United States. *Earths Future* 7 (3), 300–319. doi:10.1029/2018ef001085

Silva, J. S., da Silva, R. M., and Santos, C. A. G. (2018). Spatiotemporal impact of land use/land cover changes on urban heat islands: a case study of Paco do Lumiar, Brazil. *Build. Environ.* 136, 279–292. doi:10.1016/j.buildenv.2018.03.041

Siqi, J., and Yuhong, W. (2020). Effects of land use and land cover pattern on urban temperature variations: a case study in Hong Kong. *Urban Clim.* 34, 100693. doi:10.1016/j.uclim.2020.100693

Souza, D. O. d., Alvalá, R. C. d. S., and Nascimento, M. G. d. (2016). Urbanization effects on the microclimate of Manaus: a modeling study. *Atmos. Res.* 167, 237–248. doi:10.1016/j.atmosres.2015.08.016

Su, S., Wang, Y., Luo, F., Mai, G., and Pu, J. (2014). Peri-urban vegetated landscape pattern changes in relation to socioeconomic development. *Ecol. Indic.* 46, 477–486. doi:10.1016/j.ecolind.2014.06.044

Sun, R., and Chen, L. (2017). Effects of green space dynamics on urban heat islands: mitigation and diversification. *Ecosyst. Serv.* 23, 38–46. doi:10.1016/j.ecoser.2016.11.011

Tarawally, M., Xu, W. B., Hou, W. M., and Mushore, T. D. (2018). Comparative analysis of responses of land surface temperature to long-term land use/cover changes between a coastal and inland city: a case of freetown and bo town in Sierra Leone. *Remote Sens.* 10 (1), 112. doi:10.3390/rs10010112

Wang, C., Yu, C., Chen, T., Feng, Z., Hu, Y., and Wu, K. (2020). Can the establishment of ecological security patterns improve ecological protection? An example of Nanchang, China. *Sci. Total Environ.* 740, 140051. doi:10.1016/j.scitotenv.2020.140051

Wang, S. M., Ma, Q. F., Ding, H. Y., and Liang, H. W. (2018). Detection of urban expansion and land surface temperature change using multi-temporal landsat images. *Resour. Conservation Recycl.* 128, 526–534. doi:10.1016/j.resconrec.2016.05.011

Wang, Y. X., Li, X. S., Zhang, C., and He, W. K. (2022). Influence of spatiotemporal changes of impervious surface on the urban thermal environment: a case of Huai'an central urban area. *Sustain. Cities Soc.* 79 (11), 103710. doi:10.1016/j.scs.2022.103710

Weng, Y.-C. (2007). Spatiotemporal changes of landscape pattern in response to urbanization. *Landsc. Urban Plan.* 81 (4), 341–353. doi:10.1016/j.landurbplan.2007.01.009

Wong, P. P. Y., Lai, P. C., Low, C. T., Chen, S., and Hart, M. (2016). The impact of environmental and human factors on urban heat and microclimate variability. *Build. Environ.* 95, 199–208. doi:10.1016/j.buildenv.2015.09.024

Wu, S., Chen, B., Webster, C., Xu, B., and Gong, P. (2023). Improved human greenspace exposure equality during 21(st) century urbanization. *Nat. Commun.* 14 (1), 6460. doi:10.1038/s41467-023-41620-z

Yildiz, N. D., Avdan, U., Yilmaz, S., and Matzarakis, A. (2018). Thermal map assessment under climate and land use changes; a case study for Uzundere Basin. *Environ. Sci. Pollut. Res.* 25 (1), 940–951. doi:10.1007/s11356-017-0424-1

Yu, W. P., Shi, J. A., Fang, Y. L., Xiang, A. M., Li, X., Hu, C. H., et al. (2022). Exploration of urbanization characteristics and their effect on the urban thermal environment in Chengdu, China. *Build. Environ.* 219 (13), 109150. doi:10.1016/j.buildenv.2022.109150

Zareie, S., Khosravi, H., Nasiri, A., and Dastorani, M. (2016). Using Landsat Thematic Mapper (TM) sensor to detect change in land surface temperature in relation to land use change in Yazd, Iran. *Solid earth.* 7 (6), 1551–1564. doi:10.5194/se-7-1551-2016

Zhao, J. C., Zhao, X., Liang, S. L., Zhou, T., Du, X. Z., Xu, P. P., et al. (2020). Assessing the thermal contributions of urban land cover types. *Landsc. Urban Plan.* 204 (11), 103927. doi:10.1016/j.landurbplan.2020.103927

frontiers | Frontiers in Environmental Science

TYPE Original Research
PUBLISHED 05 February 2024
DOI 10.3389/fenvs.2023.1288933

OPEN ACCESS

EDITED BY
Hualin Xie,
Jiangxi University of Finance and Economics, China

REVIEWED BY
Bo Wen,
Nanjing Forestry University, China
Piling Sun,
Qufu Normal University, China

*CORRESPONDENCE
Wei Zheng,
zw597404460@xauat.edu.cn

RECEIVED 05 September 2023
ACCEPTED 19 December 2023
PUBLISHED 05 February 2024

CITATION
Zheng W, Guo B, Su H and Liu Z (2024), Study on multi-scenarios regulating strategy of land use conflict in urban agglomerations under the perspective of "three-zone space": a case study of Harbin-Changchun urban agglomerations, China.
Front. Environ. Sci. 11:1288933.
doi: 10.3389/fenvs.2023.1288933

Study on multi-scenarios regulating strategy of land use conflict in urban agglomerations under the perspective of "three-zone space": a case study of Harbin-Changchun urban agglomerations, China

Wei Zheng [1]*, Bin Guo[1], Hao Su[2] and Zijun Liu[1]

[1]School of Public Administration, Xi'an University of Architecture and Technology, Xi'an, China, [2]School of Public Policy and Administration, Xi'an Jiaotong University, Xi'an, China

Introduction: Against the background of rapid global urbanization, the urban space expansion has led to increasingly acute land-use conflicts. Accurately understanding the spatial and temporal evolution characteristics of land-use conflict patterns and measuring the level of spatial conflicts are crucial for intensifying sustainable use and management of land resources. Existing research focuses on analyzing the current status of land-use conflicts, while there is limited discussion on tracking spatial-temporal dynamic patterns and simulating future conflict trends.

Method: In this paper, the level of spatial conflict was measured by constructing a spatial comprehensive conflict index (SCCI) model, and the spatio-temporal evolution characteristics of land use conflict in Harbin-Changchun urban agglomeration from 2000 to 2020 are discussed. In addition, the PLUS model is used to simulate and predict the pattern of land use conflict in 2030, finally put forward the control strategy.

Results: Result shows that: (1) Over the past 20 years, urban space has expanded rapidly with two provincial capitals as growth poles. Land-use conflicts generally exhibit a distribution pattern of "high in the west and low in the east, high in the core and low in the periphery." (2) During the past 20 years, conflicts have intensified initially and then eased. Severe uncontrolled conflicts are concentrated in the transition zone between urban and rural areas of urban agglomerations. (3) Agricultural space is the core resource and key area contested by different interest subjects in the process of land development and utilization.

Discussion: The agricultural space priority scenario proves to be the most effective in controlling spatial conflicts. However, a single space priority scenario cannot adequately address multiple spatial rights and interests. Therefore, different spatial management modes should be implemented in

different areas. The purpose of this paper is to provide scientific strategies and suggestions for controlling land-use conflicts in urban agglomerations and achieving sustainable development of regional land use.

KEYWORDS

three-zone space, urban spatial expansion, land-use conflict, spatial-temporal dynamic patterns, multi-scenario simulation, Harbin-Changchun urban agglomeration

1 Introduction

Land, as a comprehensive resource that carries human production and life, social and economic development, and ecological civilization protection, plays a crucial role in realizing the interests of various stakeholders (Von Der Dunk et al., 2011). With the rapid advancement of global urbanization, original urban land is unable to meet the growing needs of human survival and development, leading to the disorderly outward expansion of cities (Liu et al., 2023). The increasing intensity of use of space resources has led to frequent land use conflicts, which not only pose a serious threat to food and ecological security, but also pose a major challenge to sustainable land planning and management.

The issue of land use conflicts gained early attention from foreign scholars, with the British Countryside Association highlighting it as one of the key themes in a 1977 conference (Yu and, 2006). They identified the disharmony between land use allocation and the regional needs of social, economic, and ecological development as the essence of these conflicts (Wehrmann, 2008). However, foreign scholars have never formed a unified definition of the concept of land use conflict. Compared with foreign countries, domestic research on land use conflicts is relatively late. Relevant research only began in 2000. Yu Bohua, Lu Changhe introduced the concept of stakeholders and defining land use conflicts as "The various stakeholders have inconsistencies and uncoordinated views on land use methods and quantities, as well as the contradictory status between various land use methods and the environment" (Yu and, 2006; Chen et al., 2012).

The so-called three-area space (hereinafter referred to as "three-area space") refers to the urban space, agricultural space, and ecological space that directly to the geographical function division and development strategy requirements of urban development, food security, and ecological environmental protection in the provincial main function zones (Wang et al., 2023; Wang et al., 2019), they serve as important technology approach for undertaking macro-scale (main function zones) and micro-scale (land use). Moreover, it aligns with the 11th goal of United Nations' Sustainable Development Goals (SDGs) "Build inclusive, safe, risk-resistant and sustainable cities and human settlements" released in 2015 (Allen et al., 2020).

From the perspective of research, the studies on urban-rural land use conflicts, ecological resources-land use conflicts are more extensive (WuBie et al., 2021), Some scholars have measured land use conflicts from the perspective of the Production-Life-Ecological Space which is called "three-life space" (Yang et al., 2020), while the "three-life space" focuses on the assessment of a single function and lacks a comprehensive consideration of the functions of the region (Chen H et al., 2021). The "three-zone space" is a further deepening of the "three-life space," which is not only integrating the functional aspects of land use, but also evolving the objective spatial pattern of land into a basic consensus linking the evaluation of the carrying capacity of resources and the environment and the evaluation of the appropriateness of spatial development of the national territory. Therefore, this paper selects the three-zone space as a research perspective to carry out the research on the management and control strategy for the land use conflicts. Which not only aligns with the national land spatial control system, but also take into account the production, ecological and social benefits, making the research content more comprehensive and persuasive.

Regarding research content, with the continuous aggravation of land use conflicts, the research on this issue at home and abroad has become more extensive. At the theoretical level, the existing research on land use conflict mainly focuses on the internal mechanism of conflict occurrence (Andrew, 2003), the causes of generation (Dong et al., 2021), the type identification and diagnosis of conflict (De Groot, 2006; De Groot, 2006; Chen W et al., 2021), etc. Empirical studies have explored spatial spillover effect of land use conflict and the conflict relationship between different elemental objects from a multi-factor perspective, mainly focusing on urban-rural land use conflict, the conflict between economic development and food protection, and land use conflict related to water resources and green resources (Wang et al., 2022), There are also scholars from the perspective of ecology and geography, using landscape ecology and ecosystem services and other related theories to explore the relationship between spatial development and utilization and regional ecological environmental protection (Ma et al., 2020), based on the landscape pattern to analyze the spatial distribution heterogeneity characteristics of the land use conflict (Jiang et al., 2021; Xie et al., 2023), in order to identify and coordinate land use conflicts. (Ran et al., 2018).

In terms of research scale, regional urban agglomerations and city and county levels have been studied more extensively, characterization of spatial conflicts in urban agglomerations and simulation of future expansion of land use are the hot spots of land use conflict research in recent years, Bao chose the Beijing-Tianjin-Hebei urban agglomeration as the research area to identify and evaluate land use conflicts by constructing the Spatial Comprehensive Conflict Index (SCCI), and simulated land use conflicts under the 2030 adaptation scenario. The results prove that in 2030, land use conflicts in Beijing will show an overall mitigating trend under the ecological security (ES) scenario, while showing an intensifying trend under the normal business (BAU) scenario and cultivated land protection (CP) scenario (Bao et al., 2021); Wang used the Spatial Comprehensive Conflict Index (SCCI) and the Pythagorean Fuzzy Conflict Information System (PFCI) to measure the absolute and relative conflicts of land use in the Lanzhou-Xining urban agglomeration under different scenarios (Meimei et al., 2023); Jiang drew on the conceptual framework of ecological risk assessment and the theories in landscape ecology, and developed a methodology to derive the spatio-temporal patterns of land use conflict in China urban agglomeration from 2001 to 2017, used multilevel regression model to identify the driving factors of land

use conflict at different levels (Jiang et al., 2021). Zhou taking the Hangzhou Bay Ring urban agglomeration as an example to explore the spatial conflicts and complexity of land use. The Yangtze River Delta urban agglomeration (Qiao et al., 2023) and so on also have been taken as research areas for quantitative measurement of conflicts; some scholars have also selected economic development zones to carry out the identification and evaluation of land use conflict zones.

Compared with the urban agglomeration regions selected in these studies, the Harbin-Changchun urban agglomeration is a national key regional city cluster approved by China's central government in 2016, an important gateway for opening up to Northeast Asia, and an important growth pole leading the revitalization of the Northeast's economic development. In terms of agricultural space, the Harbin-Changchun urban agglomeration has the most important agricultural production base and the largest commercial grain base in the country, with the Sanjiang Plain and Songnen Plain providing sufficient and fertile land resources for agricultural production and grain cultivation. In terms of ecological space, the Harbin-Changchun urban agglomeration has a number of national forest parks, national nature reserves and key ecological function areas within the urban agglomeration. However, the northeast region urban agglomeration expansion is rapid, the phenomenon of disorderly spread is serious, land use conflicts occur frequently, and the ecological environment is poor in nature, and the control and optimization of land space is imminent. Based on this, we focuses on the Harbin-Changchun urban agglomeration, the only national-level urban agglomeration in Northeast China, from the perspective of the "three-zone space."

Regarding research methods, both qualitative and quantitative approaches have been employed. 1) Qualitative methods such as public participation and game theory have been effective in exploring the evolution process and driving mechanisms of land use conflicts (Alston et al., 2000; Brown and Raymond, 2014; Adam et al., 2015), but which cannot effectively quantify conflict levels. 2) Quantitative measurement methods include multi-criteria evaluation (MCE) methods (Rahman et al., 2014; Kim and Arnhold, 2018), pressure-state-response (PSR) models (Nyangena, 2000) and land system complexity-Vulnerability-dynamic landscape ecological risk assessment method (Peterseil et al., 2004; Wang et al., 2023). Among them, the landscape ecological risk assessment method of land system complexity-vulnerability-dynamics can be updated and implemented in detail at the grid level, and is more suitable for flexible integration with land use simulation models.

In summary, from a research perspective, the three-zone space not only focuses on the spatial leading function of land use, but also emphasizes the macro-main functional zoning layout and micro-land use, which aligns with the framework of the current domestic and foreign land spatial regulation systems. In terms of content, there are relatively abundant studies on land use conflicts at home and abroad, and have provided rich insights into the definition, causes, classification types, driving mechanisms and control strategies of land use conflicts. Due to the mediation process of land use conflicts has obvious the regional differences and stages, it not only needs to pay attention to the impact of the conflict, but also needs to track its evolution. Otherwise, it will be impossible to comprehensively analyze and resolve potential land use conflicts in the future. However, existing quantitative research focuses more on static research at a certain point in time. There is a lack of describing the dynamic evolution of land use conflicts from a long time series, as well as simulating and predicting future development trends. It is difficult to accurately understand future land use evolution trends only in this way.

Therefore, the objectives of this study are as follows: 1) Portray the spatial-temporal evolution characteristics of the land-use conflict pattern in terms of both deformation and quantitative changes in the period of 2000-2020, and analyze the change rules. 2) Construct a spatial comprehensive conflict index (SCCI), using the grid as the evaluation unit to assess the level of land-use conflicts, and identify areas with uncontrolled conflicts. 3) Conduct multi-scenario simulations to predict land-use conflict trends in 2030 by employing the PLUS model, and propose conflict control strategies under different scenarios based on the prediction results. This study can not only provide data reference for the scientific delineation of the "three zones and three lines," but also provide new ideas for the optimization of the land space layout of urban agglomerations and the control of land use conflicts in China and even in the world (Figure 1).

2 Study area and data sources

2.1 Overview of the study area

The Harbin-Changchun urban agglomeration is a geographical -level urban agglomeration approved by the State Council in the context of promoting the construction of the Belt and Road and the revitalization strategy of the new round of old industrial bases in the northeastern region, as well as the in-depth development of new urbanization. It consists of 11 prefecture-level cities (states) and 63 counties (county-level cities) in Harbin, Daqing, Qiqihar, Suihua, and Mudanjiang in Heilongjiang Province, and Changchun, Jilin, Siping, Liaoyuan, Songyuan, and Yanbian Korean Autonomous Prefecture in Jilin Province (Figure 2). The land area is 336,100 square kilometers, with a core area of about 51,100 square kilometers, a resident population of about 42.6 million, and a combined gross regional product of about RMB 2.09 trillion.

2.2 Data sources and spatial classification systems

2.2.1 Data sources and processing

The data used in this study mainly include the surface cover dataset, physical geographic factor dataset, socio-economic factor dataset, and policy factor dataset. The surface cover raster data used to extract the three phases of the "three-zone space" (2000, 2010, and 2020) are mainly obtained from the Geoscience and Resources Data Centre of the Chinese Academy of Sciences (https://www.resdc.cn/), which is based on Landsat series satellite remote sensing images. The data is based on Landsat satellite remote sensing images, processed by ENVI 5.1 and interpreted by manual interactive visual interpretation, with a spatial resolution of 30 × 30 m and a resolution of 93% or more for the first level of land class interpretation, which is highly reliable.

The Harbin-Changchun urban agglomeration has a temperate continental monsoon climate, with a high topography in the east and a low topography in the west. Topographic relief, precipitation, temperature, and other basic natural geographical factors have a

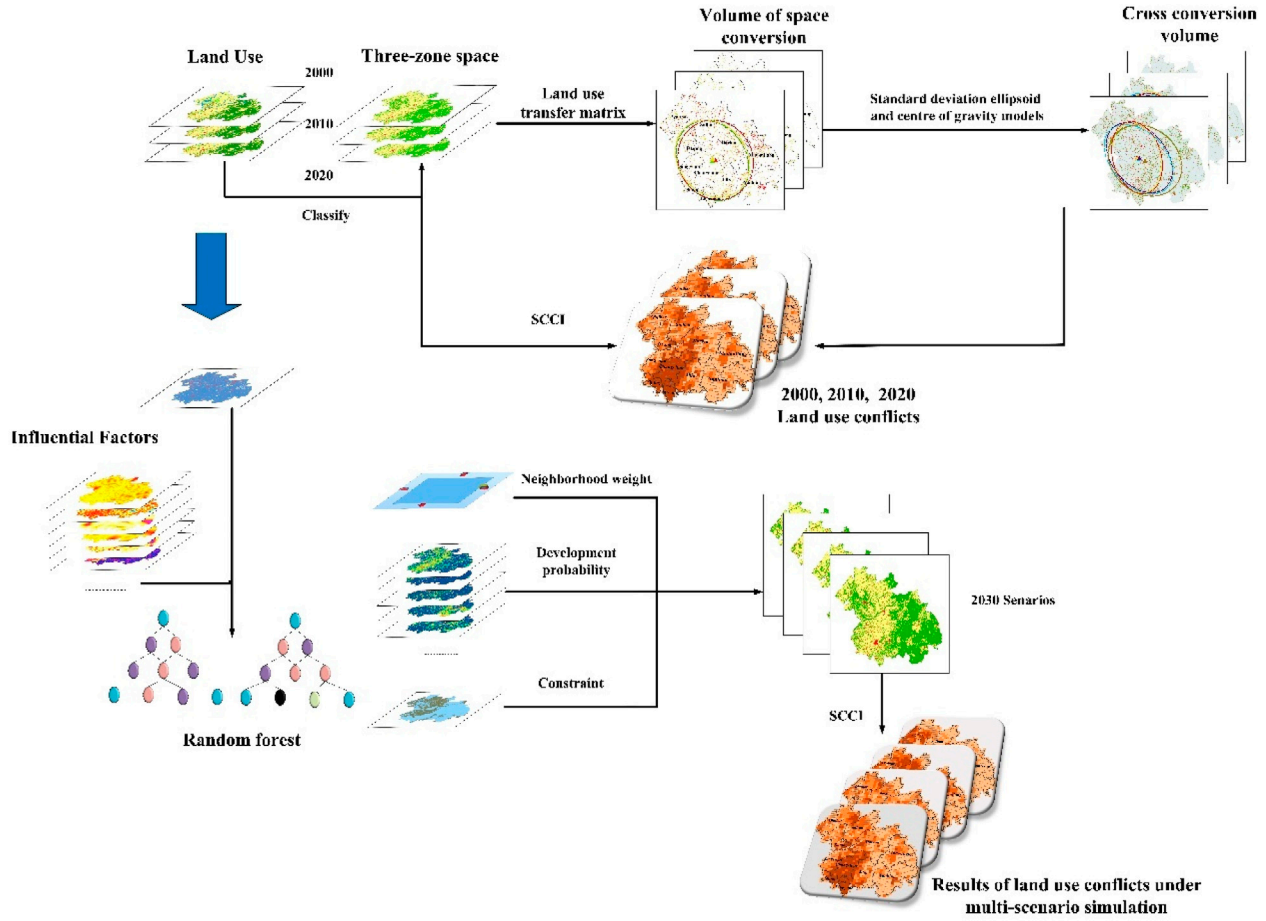

FIGURE 1
Flowchart of the proposed method.

significant impact on the ecological and spatial environment of the study area. At the same time, as an important growth pole for the revitalization and development of the old industrial bases in Northeast China and an important gateway for the construction of the "China-Mongolia-Russia Economic Corridor" land and sea Silk Road Economic Belt, the regional spatial changes of the Harbin-Changchun urban agglomeration are closely linked to multiple factors such as the level of socio-economic development, population density, distance from roads and enterprises. In particular, land development policies play a crucial role in driving the evolution of the pattern of the "three-zone space" (Wei and Yin, 2023). Therefore, in this study, the 30 drivers that have a strong correlation with the changes in the "three zones" were selected, and the sources of the data set are shown in Table 1. Considering that some of the data are updated and iterated rapidly, some of the socio-economic and physical-geographical drivers were selected from 2005 to 2015 respectively to ensure the timeliness of the drivers. The various data sets were resampled to 100 m × 100 m resolution before being imported into the PLUS model.

2.2.2 Classification system of "three-zone space"

By the "Guidelines for the Evaluation of the Carrying Capacity of Resources and Environment and the Suitability of Land Spatial Development (for Trial Implementation)" (hereinafter referred to as the dual evaluation guidelines) and the CNLUCC data classification system standards issued by the State Council, and taking into account the current situation of land use in the urban agglomeration, the land use types of the "three-zone space" of the Harbin-Changchun urban agglomeration are classified. To effectively connect the dominant land functions with the technical path of land spatial planning and management, the spatial pattern of the three zones and three lines in the outline of land spatial planning is taken as the basis for classification, and the classification system of the "three zones and spaces" of the land of the Harbin-Changchun urban agglomeration is established concerning the relevant literature (Wei et al., 2022) as shown in Table 2.

3 Methodology

3.1 Land use transfer matrix

The land use transfer matrix was used to analyze the quantity, structure, and transformation of various land use types in the

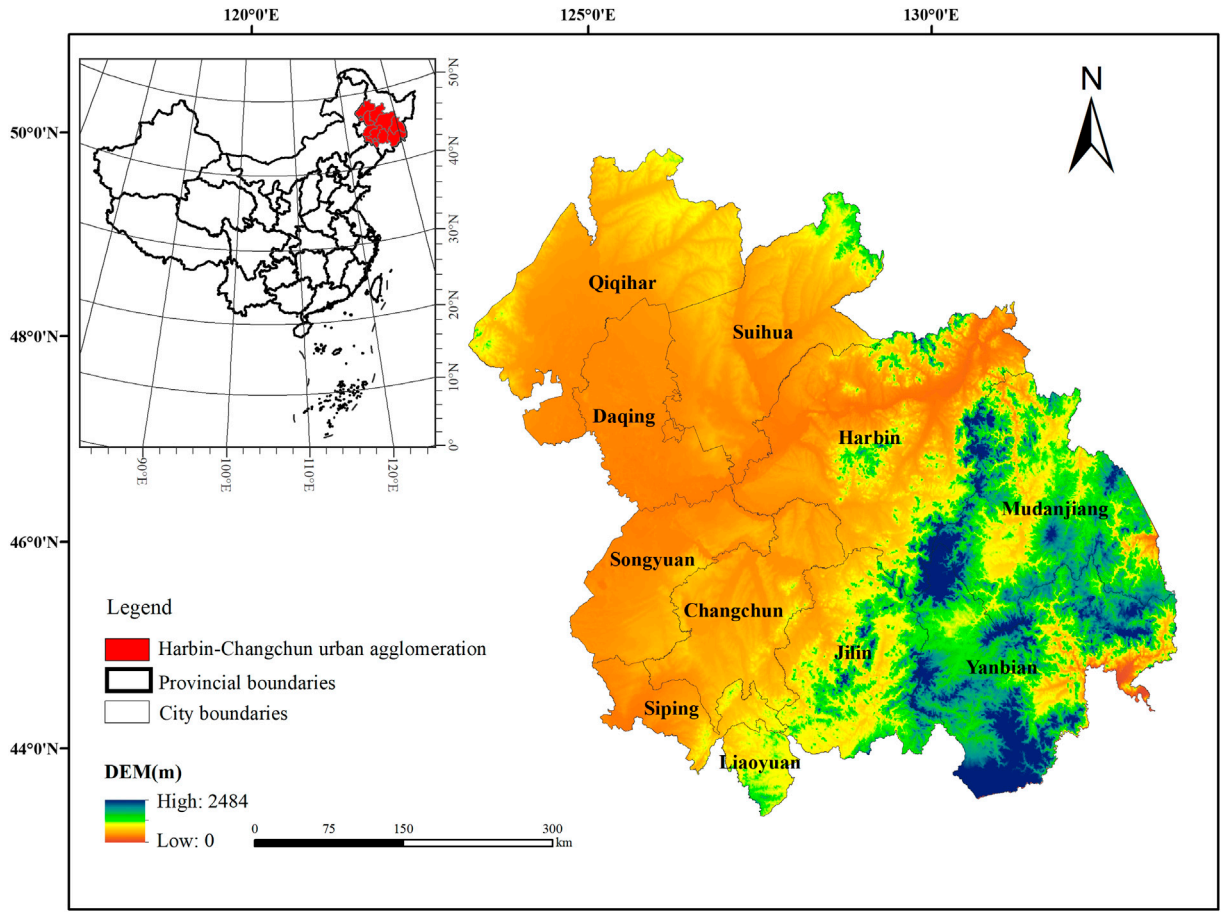

FIGURE 2
Geographical location of the Harbin-Changchun urban agglomeration.

Harbin-Changchun urban agglomeration based on the "three spatial zones" land use classification system. With the help of ArcGIS10.8 software, the three phases of land use data were spatially overlaid to obtain cross-transformation data tables for the periods 2000–2010, 2010–2020, and 2000–2020, based on which a land use cross-transformation matrix was constructed. Its mathematical form is shown as follows (Eq. 1):

$$S_{ij} = \begin{bmatrix} S_{11} & S_{12} & \cdots & S_{1n} \\ S_{21} & S_{22} & \cdots & S_{2n} \\ S_{31} & S_{32} & \cdots & S_{3n} \\ S_{41} & S_{33} & \cdots & S_{4n} \end{bmatrix} \quad (1)$$

In this equation, where S is the area; I, and j are the land use types at the beginning and end of the study period respectively; n is the number of land use types.

3.2 Standard deviation ellipsoid and centre of gravity models

Standard Distance Elipse (SDE) (Also known as a directional distribution tool) It is mainly used to identify the distribution characteristics of the spatial elements of the country, where SDE represents the spatial distribution characteristics of economic factors, the long-axis direction and short-axis direction represent the primary and secondary trend directions of the spatial distribution of the factors respectively, and the long- and short-axis distances represent the extent to which the factors deviate from the centre of gravity in the primary and secondary trend directions (Zhang et al., 2022). The elliptical standard deviation equation is as follows Eqs 2–3:

$$\left(\frac{X}{\sigma_X}\right)^2 + \left(\frac{Y}{\sigma_Y}\right)^2 = S \quad (2)$$

$$\tan\theta = \frac{\left(\sum_{k=1}^{n} w_k^2 x'^2_k - \sum_{k=1}^{n} w_k^2 y'^2_k\right) + \sqrt{\left(\sum_{k=1}^{n} w_k^2 x'^2_k - \sum_{k=1}^{n} w_k^2 y'^2_k\right)^2 + 4\left(\sum_{k=1}^{n} w_k^2 x'^2_k y'^2_k\right)^2}}{2\sum_{k=1}^{n} w_k^2 x'_k y'_k}$$

$$\sigma_x = \sqrt{\frac{\sum_{k=1}^{n} \left(w_k x'_k \cos\theta - w_k y'_k \sin\theta\right)^2}{\sum_{k=1}^{n} w_k^2}}$$

$$\sigma_y = \sqrt{\frac{\sum_{k=1}^{n} \left(w_k x'_k \sin\theta - w_k y'_k \cos\theta^2\right)}{\sum_{k=1}^{n} w_k^2}} \quad (3)$$

TABLE 1 Source of data.

Data type		Data name	Time	Time data source
Basic data; Drivers	Study area vector boundaries	Administrative division boundaries	2022	https://www.resdc.cn/
	Land use data	Surface cover data	2000,2010,2020	https://www.resdc.cn/
	Natural geographic factor data	DEM/m	2015	http://www.gscloud.cn/
		Average annual temperature/°C		https://www.resdc.cn/
		Average annual precipitation/mm	2015	WorldClim version 2.1 (http://www.worldclim.org/)
		Annual sunshine hours		(https://www.resdc.cn/)
		NDVI	2005,2015	
		Soil types	2015	http://www.rserforum.com
		Soil organic matter composition		
		CO2 annual emissions/tonnes		http://www.cityghg.com/toCauses?id=4
		Slope		
		Aspect		
	Socio-economic data	Population density	2005,2015	WorldPop (www.worldpop.org)
		Population	2005,2015	
		Urbanization rate		
		GDP	2005,2015	
		Night light index		(https://www.resdc.cn/)
		Trunk roads	2005,2015	OpenStreetMap (https://www.openstreetmap.org/)
		Sub-trunk roads		
		Highway		
		Railway		
		Major rivers		
		lakes		
		Suburban country road		
		Urban and rural settlements		
		Major enterprises		
		Administrative centers at the city and county level		
		Industrial added value		Statistical yearbooks of provinces and cities
	Policy factor data	Main functional area planning		http://jldrc.jl.gov.cn/fzgz/201311/t20131106_5212662.html; https://www.hlj.gov.cn/hlj/c108410/202110/c00_31180927.shtml
		Ecological function area planning		https://www.mee.gov.cn/gkml/hbb/bgg/201511/t20151126_317777.htm

In these equations P (xj, yj) are the coordinates of the centre of gravity of region j; the angle of rotation of the ellipse characterising the standard deviation is obtained from tanθ, i.e., the angle formed by a clockwise rotation in the due north direction to the long axis of the ellipse; $x_k^{'}$ $y_k^{'}$ are the relative coordinates of subregion i from the centre of gravity of region j, respectively; σ_x σ_y denote the standard deviation along the x-axis and y-axis, respectively.

3.3 Construction of a comprehensive conflict index model for the "three-zone space"

In the process of rapid urbanization, the spatial changes of urban agglomerations are mainly characterized by two forms neighborhood advancement and urban area expansion (Yang et al., 2023). The land use conflict and the resulting landscape

TABLE 2 Classification of land use types in the "three-zone space" of the Harbin-Changchun urban agglomeration.

"Three-zone space" land use classify	Land use classification system		Classification basis
	First order land class	Secondary land classes	
Agricultural space	Cultivated land	Land used for growing crops, including paddy fields, irrigated drylands, rain-fed drylands, vegetable fields, agricultural greenhouses, pasture fields, land mainly used for growing crops, intermixed with fruit trees and other economic trees	Carry the functions of agricultural production and food security
Town space	Artificial surface	The surface formed by artificial construction activities includes urban and rural residential land, industrial and mining land, and transportation facilities such as airports, excluding large-scale and contiguous green land and water bodies within the construction land	Carry the function of urban development
Ecological space	Forest	Refers to natural forests and plantations with a closure of >30%. Including deciduous broadleaved forests, evergreen broadleaved forests, deciduous coniferous forests, evergreen coniferous forests, mixed forests and sparse forest lands	Carry the function of ecological security
	Grassland	Refers to all kinds of grassland mainly growing herbs and covering more than 5%, including grassland, forest meadow, savanna, desert grassland and urban artificial grassland	
	Shrub land	Refers to the shade >40%, height of less than 2 m in the dwarf woodland and scrub woodland.It includes mountain shrubland, deciduous and evergreen shrubland, and desert shrubland with more than 10% coverage in desert areas	
	Wetland	Inland lake marshes, river flooding wetlands, forest/shrub wetlands, peat bogs, salt marshes	
	Water	Areas covered by liquid water in the land range, including canals, lakes, reservoirs, pits, offshore, etc.	
	Bare ground	Desert, sandy land, gravel land, bare rock, saline-alkali land, etc.	

fragmentation are the spatial epitome of the conflict of interests and the transformation of the spatial carrying function of the country. Land use conflict systems are complex, fragile, and dynamic in nature (Jiang et al., 2021). Based on the existing research results, this paper constructs a comprehensive conflict index model based on the landscape pattern index of land use patches and measures the land use conflict degree (SCCI) from the complexity, vulnerability, and stability of the land use system with the help of Fragstats 4.2 software moving window method. The spatial conflict composite index is abstractly expressed as "complexity + vulnerability—stability" of the land use system, and all the indicators are normalized (Wang et al., 2022).

1) Spatial complexity index (CI): The intensification of land use conflict makes the spatial pattern of the natural landscape and the shape of various types of land patches tend to be complex, and a fractal is an effective tool and an important language to describe the spatial complexity of the spatial pattern of nature and the development of urban geographic phenomena (Zhou et al., 2015a), so the area-weighted average patch fractal dimension index (AWMPFD) is usually used as a measure of land use complexity. This is used to characterize the degree of disturbance to the measured patches by the process of land use change in neighboring patches, with the index ranging from [1,2], with larger values indicating more complex landscape patterns and more intense land use conflicts (Table 3).
2) Spatial vulnerability index (FI): The vulnerability of land use types reflects the degree of response and resistance of patches when they are subjected to internal and external pressures such as the degree and frequency of type conversion, and is usually measured by the landscape vulnerability index (Xu et al., 2021); the higher the vulnerability, the stronger the land use conflict. Existing studies have shown that ecosystems with simple food chain structures and low biodiversity indices are relatively vulnerable (Peng et al., 2020). From the perspective of landscape ecology and concerning existing results (Zhou et al., 2015a), the landscape vulnerability of the "three-zone spaces" is ranked from strong to weak as urban space, agricultural space, and ecological space (Wang et al., 2023); (Table 3).
3) Spatial stability index (SI): In general, the higher the degree of fragmentation of the spatial pattern of the landscape, the less stable and the stronger the spatial conflict (Jiang S et al., 2021), while the fragmentation of land use type patches is reflected in the clustering and increasing density of point-like space or the diffusion of linear space and the fragmentation of face-like patch space (Wang et al., 2023). Therefore, patch density (PD) is usually chosen to measure the land use stability index, with higher patch density leading to higher spatial fragmentation and therefore lower spatial stability (Table 3).
4) Analysis scale selection: The landscape pattern index is dependent on the scale of the patch cells, to avoid the loss of spatial information due to the large scale and the inaccuracy of the landscape index due to the small scale due to subjective

TABLE 3 Calculation of the composite land use spatial conflict index.

Index name	Calculation formula	Description
Land Use Complexity Index	$CI = \sum_{i=1}^{m}\sum_{j=1}^{n}[\frac{2ln(0.25P_{ij})}{ln(a_{ij})}(\frac{a_{ij}}{A})]$	P_{ij} is the plaque perimeter, a_{ij} is the jth patch area of the Category I land type; A is the total area of the space type; m is the total number of spatial evaluation units in the study area; n is the total number of spatial types
Land Use Vulnerability Index	$FI = \sum_{i=1}^{n}(F_i * \frac{a_i}{S})$	F_i is the fragility index of class i space type; n is the spatial landscape area ; S is the total area of the space unit
Land Use Stability Index	SI = 1-PD, $PD = \frac{n_i}{A}$	n_i is the fragility index of class i space type; n is the total number of space types; a_i is the area of each type of landscape within the unit; S is the total area of the space unit
Land use space Conflict Composite Index	SCCI = CI + FI-SI	SCCI is a composite index of spatial conflict; CI, FI and SI are spatial complexity, spatial vulnerability and spatial stability indices respectively

selection, this paper takes into account the scale of the study area, the number of spatial patches and the information characteristics of the raster data, and selects 10,000, 15,000, 20,000, 25,000 In this paper, we select 10,000, 15,000, 20,000, 25,000, 30,000 and 30,000 m window cells and construct a fishing net, measure the landscape pattern index at each spatial scale and substitute it into the semi-variance function model (Bao et al., 2021), calculate the ratio of Nugget (C0) to Sill (C + C0) (C0/(C + C0)), refer to the conclusion of previous studies (Li et al., 2014), keep narrowing the interval for calculation, and finally select 18,000m, which is the first to reach a stable point, as the window cell. As a window unit, the study area was divided into 1224 fishnet units for the analysis and calculation of the spatial land use conflict index.

3.4 PLUS model

3.4.1 PLUS model core algorithm

The PLUS model is a CA model that integrates Land Expansion Strategy Analysis (LEAS) and multi-type random patch seeding (CARS) (Yang et al., 2023). The model is based on raster data and obtains the development probability of each type of land use within a unit image element and the contribution of drivers to land use expansion by mining land expansion transition principles and drivers, and predicts land use over time with the help of the Markov chain module. The Markov chain module is used to forecast the land use change matrix over time, and the spatiotemporal dynamic slab is automatically generated under the mechanism of seed generation and decreasing threshold. Compared with the traditional linear prediction and typical spatial causal models, the PLUS model with multiple types of patches effectively compensates for the difficulty of obtaining land use rules at specific time intervals and the lack of spatiotemporal dynamics and can simulate the simultaneous evolution of land use patches over time in a more realistic way (Liang et al., 2021).

3.4.2 Scenario setting

To effectively connect the dual evaluation technical paths, accelerate the optimal zoning of the geographical functions of urban, agricultural, and ecological spatial land use under the spatial pattern of the country, and then guide the descending scale of the main functional areas to conduct the task of promoting the delineation of the three zones and three lines (Fan, 2019), and achieve many of the visionary goals put forward in the "UN 2030 Agenda for Sustainable Development" (Guo et al., 2022). In this study, four scenarios of natural development: the priority of agricultural space, the priority of urban space, and the priority of ecological space are set up to simulate the spatial pattern of land use and changes in the Harbin-Changchun urban agglomeration in 2030, to realize the analysis of the diversity of scenarios of spatial conflicts in land use, and the scenarios are described as follows:

① Scenario A: Land use change under the natural development scenario does not take into account any human plans and public planning policies that limit and interfere with land use change, and by default evolves according to the characteristics of land use conversion under the historical scenario, with the transfer probability of each land use type remaining unchanged, without adjusting the parameters, and without setting any constraints in the simulation experiment, and using Markov chains to predict the demand for each type of land use in 2030, extending the original land weighting coefficients of the n weights from 2010 to 2020.

②Scenario B:Under the scenario of prioritizing agricultural space, starting from two parts of space, agricultural production and agricultural life, and in accordance with the "Double Evaluation Guidelines" (https://www.gov.cn/zhengce/zhengceku/2020-01/22/content_5471523.htm) and the "Harbin-Changchun urban agglomeration Development Plan" (https://www.ndrc.gov.cn/xxgk/zcfb/ghwb/201603/t20160311_962177.html), "All high-quality black soil arable land will be designated as permanent basic agricultural land, and special protection and spatial layout adjustment and optimisation will be carried out for it" "To establish a modern agricultural industry system, promote the integrated development of grain, warp and feed, agriculture, forestry, animal husbandry and fishery, and the integration of breeding, raising and processing, and optimize the agricultural industry structure and regional layout", the permanent basic farmland and the main production areas of

agricultural and forestry products shown in the documents of the Main Functional Area Planning of Heilongjiang Province and the Main Functional Area Planning of Jilin Province were vectorisation process to make them consistent with the scope of the study area, and merge them as prohibited development areas into the model; take the amount of high-standard arable land area in 2020 as the lower limit of land use demand, and the predicted value as the upper limit; in the setting of land use transfer rules, significantly increase the probability of transferring grassland, shrubland and wetland into arable land, appropriately increase the probability of transferring forest, bare land and artificial land surface, and restrict the transfer of arable land to other. In order to realise the principle of giving priority to agricultural space.

③Scenario C: Under the town space priority scenario, the national and provincial key development town clusters are vectorized in accordance with the scope of town spatial development suitability delineated in the "Dual Evaluation Guidelines", so that they are consistent with the scope of the study area, and data on land use types closely related to human development activities, such as man-made surfaces and reservoir pits within the scope, are extracted as the functional areas of urban clusters, which are combined with national nature reserves and jointly set as Prohibited development zones are entered into the model. In the "Development Plan for the Harbin-Changchun Urban Agglomeration," the spatial strategy of "developing in the same direction, upgrading the twin cores, extending north and south, expanding one axis, expanding openness and growing two belts" is followed. In the setting of land use rules, the probability of transferring arable land, shrub land, and forest land to man-made land is significantly increased, and the probability of transferring grassland and bare land is appropriately increased. Reduce or restrict the transfer of man-made surfaces to other land types, while increasing the value of man-made surface neighborhood weights. Realize the principle of prioritizing urban space for development.

④ Scenario D: Under the priority ecological space scenario, the first thing to ensure is that ecological space is not occupied. The Harbin-Changchun Urban Cluster Development Plan clearly emphasizes "the protection of arable ecological sub-regions, soil erosion control, wind and sand control, urban ecological landscape pattern, accelerated ecological restoration of old industrial areas and land reclamation." In accordance with the classification of ecological service functional areas by the ecological protection importance assessment in the Dual Evaluation Guide, this study relies on the National Ecological Function Zoning (https://www.mee.gov.cn/gkml/hbb/bgg/201511/t20151126_317777.htm) to vectorize the national nature reserves and key ecological In this study, the land in national nature reserves and key ecological function zones was vectorized according to the National Ecological Function Zone Zoning (https://www.mee.gov.cn/xxgk2018/xxgk/xxgk06/202112/t20211215_964234.html), and the three types of land in provincial key ecological function zones, namely, forests, shrublands and water bodies, were extracted according to the Technical Guidelines for the Protection and Restoration of Ecological Buffer Zones of Rivers and Lakes (https://www.mee.gov.cn/xxgk2018/xxgk/xxgk06/202112/t20211215_964234.html). The three types of primary land within the provincial key ecological function areas were extracted, and a 60-m range around the site area was set as the ecological buffer zone (Su et al., 2022). The final scope is consistent with the scope of the study area, and the ecological function areas, nature reserves, and ecological buffer zones are finally combined into the input model of the prohibited development zone; the forest coverage rate is set to be no less than the 2020 standard (greater than 43.8%), and the area of grassland and bare land is constrained to account for no less than 2.5% of the total land area from the perspective of biodiversity. In the rule-setting, the probability of transferring arable land into ecological space is increased significantly, the probability of transferring man-made land into ecological space is increased appropriately, and the conversion between land types within ecological space follows the principle of transferring land types with low economic benefits to land types with high economic benefits. Strictly control the transfer of ecological space land to other land categories to realize the principle of prioritizing the development of ecological space.

3.4.3 Neighbourhood weight parameter setting

The neighborhood weight parameter represents the ability of the land type to expand itself as driven by external factors, with a threshold range of [0,1]. It is believed that the historical expansion pattern of each land type is the best representation of their respective expansion capacity. This paper draws on the historical scenario approach (Wang et al., 2019) from existing studies to set the neighborhood weights, calculated as follows (Eq. 4):

$$W = \frac{\Delta TA\mathrm{i} - \Delta TA\,\mathrm{min}}{\Delta TA\,\mathrm{max} - \Delta TA\,\mathrm{min}} \tag{4}$$

In this equation Where ΔTA_i is the amount of TA change for the land type; ΔTA_{min} indicates the land type with the smallest change; and ΔTA_{max} indicates the land type with the largest change.

4 Results

4.1 Analysis of the characteristics of the evolution of the spatial-temporal pattern of the three regions from 2000 to 2020

4.1.1 Changes in the structure and scale of the spatio-temporal pattern of the "three-zones space"

From the land use distribution map for 2000–2020 (Figure 3), it can be seen that the distribution of the "three-zone space" in the Harbin-Changzhou urban agglomeration has significant geographical and functional structural characteristics: 1) urban space formed along the Harbin-Daqing-Qiqihaer-Mudanjiang development belt and the Changchun-Jilin-Tumen development belt, with the cities of Harbin and Changchun as the main development axis. 2) The agricultural space formed by the Songnen Plain and the Sanjiang Plain, which provide agricultural and forestry products; 3)The ecological space formed around the Great and Small Xing'an Mountains, the Changbai Mountains and the Zhang Guangcai Ridge, with the wind and sand control, water conservation and soil conservation as the main functions, There is also some ecological space located at the confluence of the

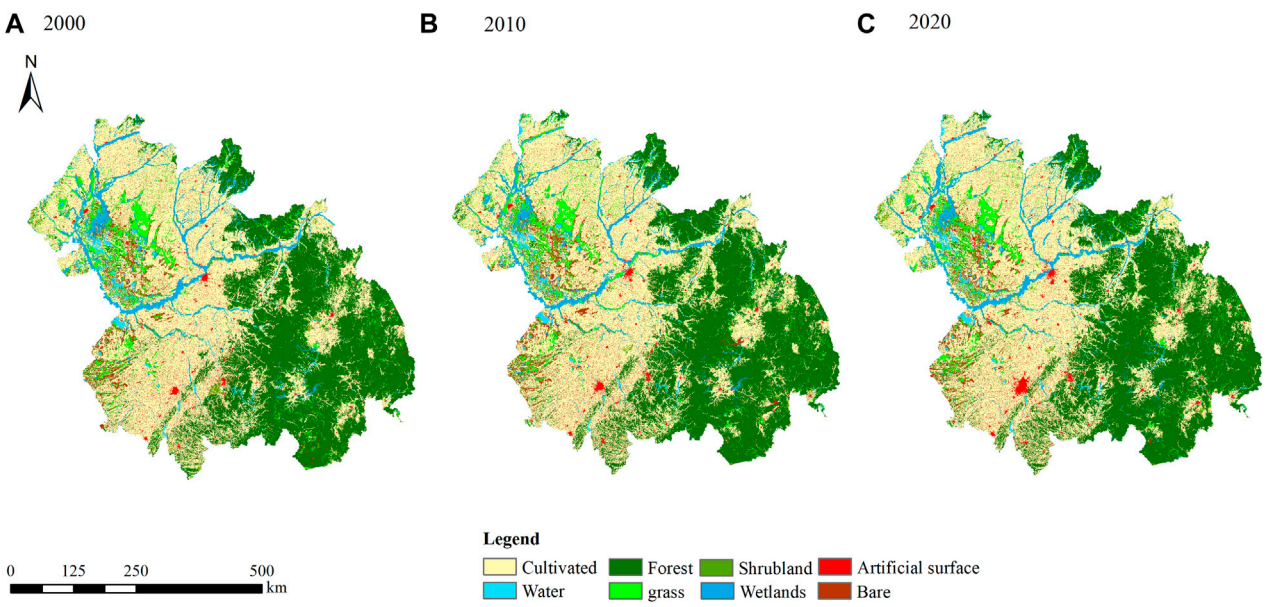

FIGURE 3
Land use classification maps for 2000 **(A)**, 2010 **(B)** and 2020 **(C)**.

Nengjiang, Songhua, and Ussuri Rivers, with biodiversity conservation and flood storage as the main functions.

In general, ecological space and agricultural space occupy the main part of the space, and the proportion of the two types of space in the total area is about 86%, while urban space accounts for a relatively small proportion, except for the urban space around the main axis of development of Harbin and Changchun city, which is distributed in agglomeration, the rest of the area as a whole shows a scattered dotted layout.

It can be seen from Figure 4 that the overall distribution structure of the "three-zone space" of the Harbin-Changchun urban agglomeration did not change significantly during the period 2000–2020, while the spatial evolution of various types of space is more characteristic.

1) Unlike other regions in Northeast China where agricultural space has decreased significantly, the scale of agricultural space in the Harbin-Changchun urban agglomeration decreased first and then increased, with a decrease of 2.29% in the first 10a and an increase of 6.48% in the second 10a. The spatial scale of agriculture has increased by 627.14 km^2 compared to 2000, and the centre of gravity has moved 23,433 m to the southwest (Table 4).
2) The scale area of ecological space continues to decrease, with a cumulative reduction of 2137.42 km^2 in 20a, with the spatial centre of gravity moving southwards by 12638 m. The first 10a of spatial change is relatively small, with a 0.30% decrease, and the scale of ecological space reduction is more concentrated around the Changbai Mountain Range in the southeastern part of the urban agglomeration in the Yanbian Korean Autonomous Prefecture and the Daxinganling area in the northwestern part, which is associated with the high ecological vulnerability of the region, while the decrease in the second 10a is 1.32%. The scale of reduction is more obvious in the national key ecological function areas in the north of the study area and the Songyuan and Siping areas in the southwest, with the difference between the long and short axes of the 20a standard deviation ellipse first decreasing and then increasing, the area of the ellipse gradually increasing, and the space becoming increasingly dispersed.
3) The expansion of urban space is the largest. In the past 20 years, the space has continued to expand in the southeast direction along the development axis of Harbin-Daqing-Qiqihaer-Mudanjiang, which is consistent with the spatial pattern planning guidance of "dual core, one axis, and two belts" for urban clusters in recent years: With Harbin and Changchun as the core pole, and with the Harbin, Daqing and Qiqihaer Railway as the link, it gradually radiates along the northwest and southeast direction to drive the development belt of the two major cities of "Harbin-Daqing-Qiqihaer-and Mudanjiang" and "Changchun-Jilin-Tumen," creating a network pattern of axial and belt connectivity. From 2000 to 2010, the urban space increased by 7.31%, and the spatial center of gravity moved to the northeast by 3,852 m. The expansion scope of the two provincial capitals of Harbin and Changchun and some surrounding areas were relatively concentrated, with a large scale, but the expansion volume of other areas was relatively low, especially the urban space coverage in the northeast of Mudanjiang City and the southeast of Yanbian Korean Autonomous Prefecture was small. In addition to the continuous concentrated expansion of provincial capital cities, a large number of urban Spaces have been generated in Qiqihar, Daqing, and Mudanjiang in the northwest. In 20a, the urban space in the urban agglomeration increased by 13.13%, with a total increase of 1,488.85 km^2. The spatial center of gravity moves

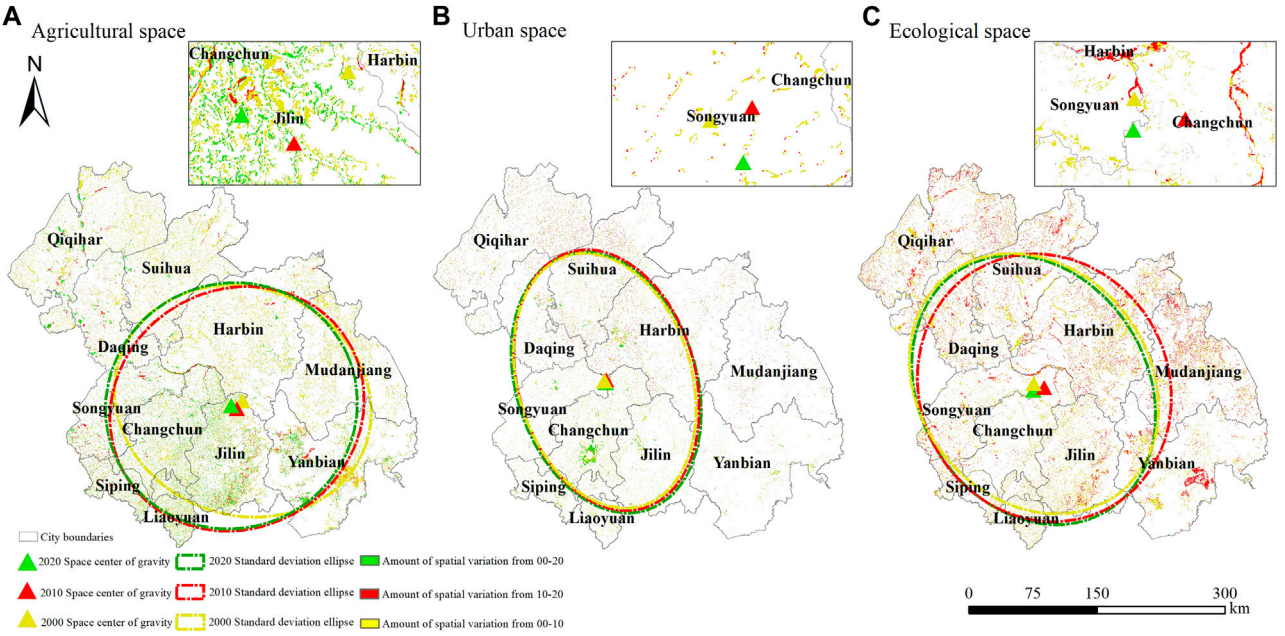

FIGURE 4
Spatio-temporal dynamics of the "three-zone space". **(A)** Agricultural space **(B)** Urban space **(C)** Ecological space.

TABLE 4 Land use area and share from 2000 to 2020.

Space type	2000		2010		2020		Area variation in 2000-2010	Area variation in 2010-2020	Area variation in 2000-2020
	Land area (km^2)	Share of total area (%)	Land area (km^2)	Share of total area (%)	Land area (km^2)	Share of total area (%)			
Agriculture Spaces	150122.83	0.4656	149779.12	0.4645	150749.97	0.4676	−0.00229	0.006482	0.004178
Ecology Spaces	160987.25	0.4993	160501.72	0.4978	158849.83	0.4927	−0.00302	−0.01029	−0.01328
Towns Spaces	11332.91	0.0351	12162.40	0.0377	12820.48	0.0398	0.073193	0.054108	0.131,261

eastward and southward, and the difference between the ellipse and the axis of urban space is the largest, and the dynamic migration direction is the most obvious. However, the ellipse area does not change much, the coverage of space expansion is limited and the dispersion is low.

4.1.2 Cross-conversion features of "three-zone space"

The Arcgis10.8 software was used to calculate and analyze the scale and direction of the spatio-temporal dynamic cross-transformation of the "three-zone space" of the Harbin-Changchun urban agglomeration from 2000 to 2020 (Figure 5), and statistical data of various spatial cross-transformation in 20a (Table 5) were collected. According to the main functional zoning planning of the two provinces and the national ecological function zoning documents, the characteristics of various spatial transformations were analyzed respectively from the conversion direction, conversion scale, and conversion position:

1) The conversion scale of agricultural space and ecological space is the most significant 9,508.89 km^2 of ecological space was transformed into agricultural space, and the agricultural space had a net inflow of 1,927.54 km^2 from ecological space. From the perspective of longitudinal time series, 13,309.98 and 13,776.63 km^2 of these two types of spatial land participated in the transformation in the first 10a, respectively, while the conversion scale in the second 10a was relatively small. The conversion areas of the two types of space mainly occurred in the main agricultural production areas such as the western Songnen Plain, the main forest product production areas such as the central part of Jilin and the northwest part of Heilongjiang Province, and the national nature reserves. In the context of the rapid expansion of urban space in the past 20 years, the urban space of Harbin-Changchun urban agglomeration has still carried out a large-scale transfer to agricultural space, accounting for 88.7% of the total urban space transfer scale, which is a rare cross-conversion feature in

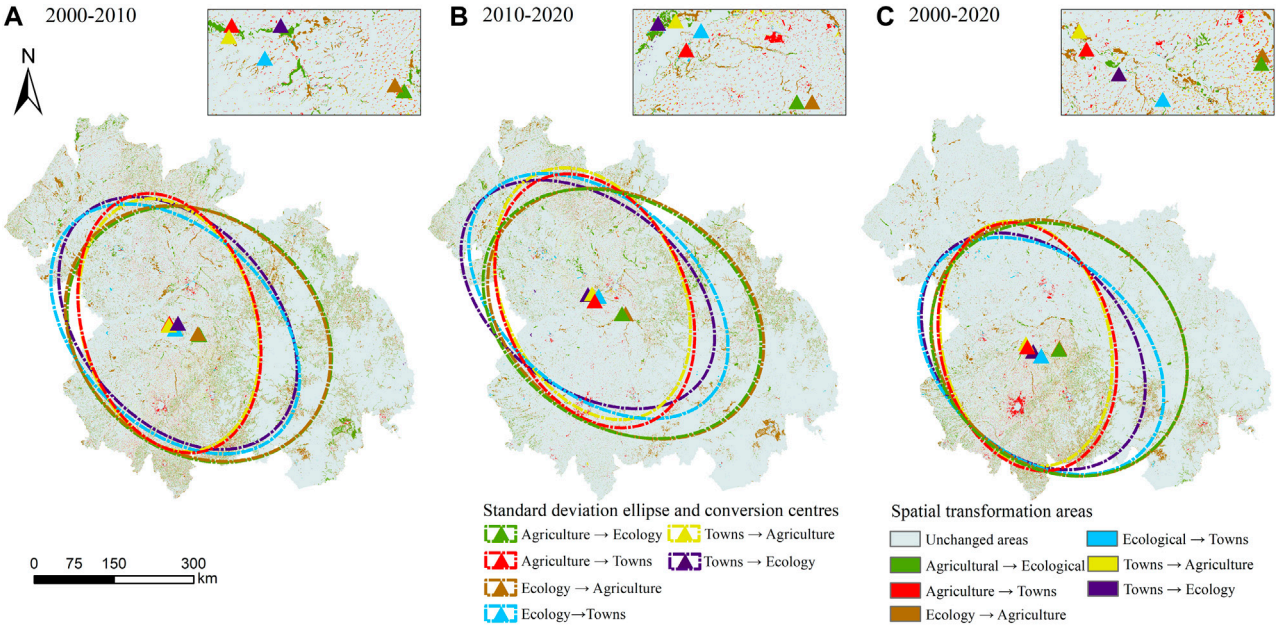

FIGURE 5
Spatio-temporal dynamics of the "three-zone space" crossover. **(A)** 2000–2010 **(B)** 2010–2020 **(C)** 2000–2020.

northeast China compared with other regions of China. Urban space transfer areas are mainly concentrated in the outlying rural areas far away from the built-up areas and high-quality farmland, while the key development areas near the main urban areas are less distributed.

2) The expansion of urban space mainly comes from agricultural space, and the outflow of ecological space is relatively low. In the past 20a, agricultural space conversion land accounted for more than 85% of the new urban space, especially in Changchun and Jilin. In the first 10a, the agricultural space conversion scale reached 4,271.37 km^2, accounting for nearly 90% of the new urban space. The latter 10a saw a slight decline in the scale of conversion under the policy constraint of the State's proposal to protect the construction of basic farmland and the vigorous development of functional areas for agroforestry products. In general, the transformation of agricultural space and ecological space to urban space is along the direction of northwest to southeast, but the direction of ecological space transformation is more obvious. The agricultural spatial conversion center moved 16,024 m to the southeast, while the ecological spatial conversion center moved eastward and northward. The spatial conversion area gradually approached the main producing areas of agricultural and forestry products and ecological protection function areas from the surrounding areas of the key and core development zones of the urban agglomeration, and the derivative of urban space and the encroachment on other spaces became gradually obvious.
3) The conversion of ecological space mainly depends on agricultural space. In the past 20 years, 7,581.35 km^2 of agricultural space has been converted into ecological space, with a relatively discrete distribution; The scale of urban spatial transformation is small, mainly concentrated in the Greater and Lesser Hing'an Mountains, the southern part of the Sanjiang Plain and near key ecological functional areas, and the transformation center gradually shifts to the east.

4.2 The spatial and temporal evolution of the conflict in the "three-zone space"

Taking into account the definition of the core area in the Development Plan of Harbin and Changchun Urban Agglomerations and the division of the core-periphery structure of Harbin and Changchun Urban Agglomerations by existing studies, dividing Daoli district, Nangang district, Daowai district, Xiangfang district, Pingfang district, Songbei district, Acheng district and Shuangcheng district in Harbin City; Saltu district, Longfeng district Ranghulu district, Honggang district of Daqing City; Chaoyang district Nanguan district, Kuancheng district, Erdao district, Lvyuan district, Jiutai district of Changchun City, and Changyi district, Longtan district, Chuanying district and Fengman district of Jilin City, a total of 22 regional units into core areas, while the rest are peripheral districts (Zhang and Qi, 2018). The spatial comprehensive conflict index of land use represents the conflict degree of three types of Spaces. According to the distribution characteristics of the cumulative frequency curve of spatial conflict index and the evolution law of the inverted "U" shaped curve model of spatial conflict (Zhou et al., 2022), this study adopts the equal spacing method to divide the comprehensive index of land use spatial conflict into: There are four grades: stable and controllable [0,0.25), basically controllable [0.25,0.5), basically out-of-control [0.5,0.75) and seriously out-of-control [0.75,1.0]. Then,

TABLE 5 Dynamic cross-transformation data of the "three district space" from 2000 to 2020.

Conversion phase	Cross-conversion scale					
	Agriculture →Ecology	Agriculture →Towns	Ecology →Agriculture	Ecological →Towns	Towns →Agriculture	Towns →Ecological
2000–2010	13309.98	4271.37	13776.63	512.22	3461.84	492.19
2010–2020	8763.76	2869.28	10222.44	483.74	2385.74	309.13
2000–2020	7581.35	3456.96	9508.89	467.34	2161.88	274.95

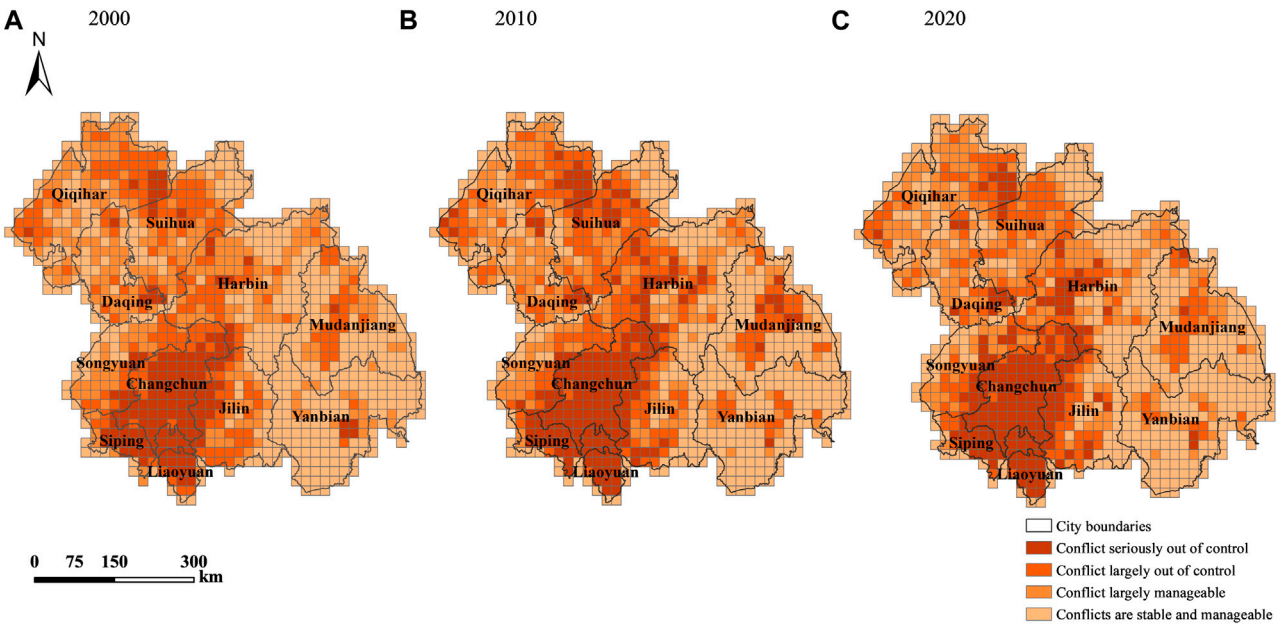

FIGURE 6
Conflict pattern distribution characteristics of the "three-zone space" in 2000 **(A)** 2010 **(B)**, and 2020 **(C)**.

Arcgis10.8 is used to conduct a fishnet unit analysis of land use spatial conflicts (Figure 6).

1) From the perspective of spatial distribution structure, the seriously out-of-control areas are mainly distributed around the core areas of the central part of the urban agglomeration, such as the main axis line of Harbin and Changchun and the development belt of Harbin-Daqing-Qiqihar-Mudanjiang. Among them, the spatial conflicts in the main urban areas of Changchun and Harbin are the most serious and concentrated, and the conflicts in Changchun are the most extensive. Except for the major out-of-control areas in the main urban areas, the basic out-of-control areas spread to the surrounding counties and towns along the administrative division. And with the main urban area as the core, it spreads to the surrounding areas until it connects with the out-of-control area of Harbin City in the north to form an "out-of-control belt." Compared with the core area, there are fewer serious out-of-control areas in the peripheral areas, and the basic out-of-control areas are presented in the shape of a dot, set in it: the spatial conflicts are strongest in the central and northern parts of Siping City and Liaoyuan City, and the southeastern part of Songyuan City; the spatial conflict at the junction of municipalities is more significant, Mudanjiang City and Yanbian Korean Autonomous Prefecture which are located in the southeastern part of the urban agglomeration only have a large distribution of runaway areas in the center of the City By summarizing the spatial characteristics of conflict zones, it can be found that out-of-control zones, especially serious out-of-control zones, are concentrated in urban spatial areas and spread to peripheral areas with administrative centers as the core. The spatial conflicts near the major river systems are also intensified, the ecological and agricultural spaces near the Songhua River and Nenjiang River basins are frequently transformed, and the regions with weak conflicts are mainly distributed in the key ecological functional areas and national nature reserves in the northwest and east, among which the spatial conflicts in the forest ecological functional areas of Changbai Mountain in the east are the weakest, and the controllable area units account for 72.3% of the total units. The remaining controllable areas are mainly in the outer contour areas of urban agglomerations and are relatively discrete.
2) From the perspective of dynamic change of spatial conflict pattern (Table 6 and Figure 7), the intensity of conflict in 20a "three-zone space" showed a trend of first increasing and then decreasing, in

TABLE 6 Conflict index data for the "three-zone space" from 2000 to 2020.

The type of spatial conflict	2000		2010		2020	
	Quantity (pcs)	Percentage (%)	Quantity (pcs)	Percentage (%)	Quantity (pcs)	Percentage (%)
Stable and controllable	470	42.30	461	41.94	449	40.45
Basically controllable	306	27.54	221	19.89	281	25.29
Basically out of control	188	16.92	224	20.16	193	7.34
Severely out of control	147	13.23	205	18.45	188	16.92

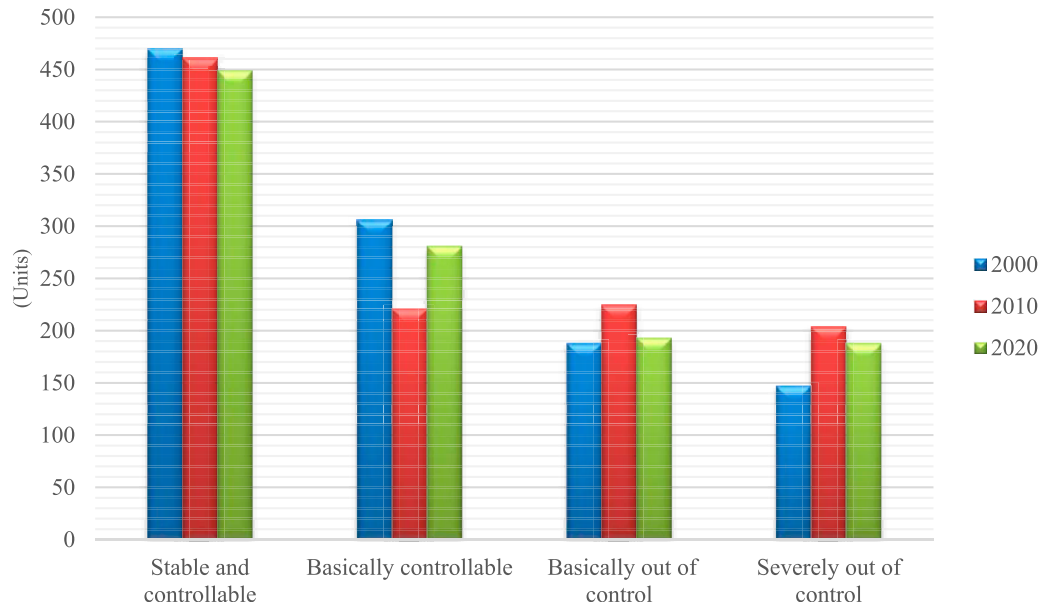

FIGURE 7
Conflict index table.

which the basic controllable area decreased first and then increased, the number of stable controllable area units decreased year by year, and the scale of reduction increased from 1.9% to 2.7%. The controllable area reduction area was mainly located in the agricultural and ecological space around the municipal administrative center. The proportion of out-of-control areas has changed from 30.09% in 2000 to 38.65% in 2010, and 34.26% in 2020. The number of out-of-control areas in the first 10a has increased dramatically, and the number of seriously out-of-control areas alone has increased by 58 pcs. From the distribution map, the additional units are mainly distributed in the core area of urban agglomeration and its surrounding agricultural space. After 10a, the number of runaway zones declined, but the scale of the reduction was smaller, The reduction area is mainly concentrated in the main production areas of agricultural and forestry products, key ecological function areas and nature conservation areas of the Sanjiang Plain outside the urban agglomeration, conflicts in some agricultural spaces and most ecological spaces far from the core areas were alleviated, while in the central and southern part of the Songnen Plain, the concentration of basically out-of-control and seriously out-of-control units along the main axis of the development of Harbin-Changchun continued to increase.

The dynamic change of spatial conflict pattern is closely related to the interference of human activities during urban development and construction. In the past 20 years, due to the rapid development of urbanization, and industrialization, the core area of urban agglomerations has a dense population, relatively concentrated industrial distribution, high urbanization level, and relatively developed economy, while the peripheral area is mainly distributed with rural settlements and lacks industrial types. Cultivated land has become the core production factor in rural areas, so a large amount of reclaimed agricultural land is spread around. With the continuous spillover of population and industry, a large number of "satellite cities" have been derived from the periphery of the core area. With the continuous outward expansion of urban built-up areas, agricultural space is invaded by urban space on a large scale, the transformation scale of ecological space and urban space is gradually significant, and the

fragmentation and complexity of spatial patches are increasing, thus leading to the increasingly intensified conflict of "three-zone space" in this region. In 2018, the central government required provincial and municipal people's governments to demarcate the main functional areas. The protection of basic farmland and agricultural and forestry product areas should be strengthened, and the development restriction of ecological protection areas should be enhanced. The spatial conflicts in the study area are generally alleviated as a result, but the conflicts in the core area and its surrounding areas are still serious.

4.3 Multi-scenario simulation results of "three-zone space"

4.3.1 Accuracy verification

After the Extract Land Expansion module built-in PLUS model was used to extract the raster data of land expansion from 2000 to 2010, the selected driver data set was added to the LEAS module, the random forest decision tree was set as the default value 20, the sampling rate was 0.01, and the number of trained RF features was 30. The random forest algorithm was used to mine each type of land use expansion and driving factors one by one, and the contribution data of driving factors and the suitability atlas of eight land use types were obtained. The land use type suitability atlas and 2010 land use distribution grid data were input into the CARS module to simulate the spatial distribution of land use in 2020, and the results were compared with the real data. The Kappa coefficient of the image was 0.88, the overall accuracy was 0.95, and the model prediction accuracy was excellent. On this basis, the spatial distribution of land use in 2030 was simulated concerning the set rules of multi-scenario simulation and the distribution pattern of "three-region space" was obtained after reclassification (Figure 8) (Table 7). Cross-conversion data of various types of land use from 2020 to 2030 were calculated and a string diagram was drawn (Figure 9).

4.3.2 Distribution pattern of "three-zone space" under multi-scenario simulation

Combined with Figures 8, 9 it can be seen that: compared with 2020, there is no significant structural change in the spatial pattern of the three regions under the natural development scenario, with agriculture and ecological space as the main body, but there are significant differences in spatial distribution characteristics in the priority scenarios of agriculture, urban and ecological space. Among the four scenarios, the conversion scale of grassland, cultivated land, forest land, wetland, and artificial land surface is more obvious, while other land types have little change, as shown in

1) under the natural development scenario, the agricultural, ecological and urban spatial area of the Harbin-Changchun urban agglomeration in 2030 will increase by 788.01 km^2, decrease by 1,295.84 km^2, and increase by 507.84 km^2 compared with 2020. Ecological space as the main turn-out space in which the grassland area changed the most, decreasing by 1,039.88 km^2, and the main outflow direction was wetland and artificial surface. The proportion of agricultural space is almost the same as that in 2020; With the continuous development of urban agglomeration, the urban space continues to increase, with the proportion of space rising from 3.97% to 4.13%. However, with an average growth rate of 0.04% over the last 10a, the rate of expansion has become slower than in the past, the expansion area occurs mainly in the south-eastern part of Daqing City linking the main axis of Harbin-Changchun urban agglomeration.
2) Under the agricultural space priority scenario, the agricultural space 10a increased by 10,943.32 km^2, which was 13.71 times of that under the natural development scenario, and the expansion effect was significant. The proportion of ecology and urban space decreased by 2.58% and 0.8% respectively, and the urban space scale stopped expanding. In terms of spatial cross-conversion, the expansion of agricultural space mainly comes from ecological space. A total of 6,722.31 km^2 of ecological space is transformed into agricultural space, among which the conversion of grassland into cultivated land accounts for the largest proportion, but the conversion area of artificial surface single land type accounts for 61.40% of the total land conversion area of the six types of ecological space. From the perspective of transformation position, the agricultural spatial expansion effect of provincial key urban group development zones and forest ecological function zones is remarkable.
3) Under the urban space priority scenario, the urban space 10a increased by 9,782.30 km^2, and the space proportion increased from 3.97% to 7.01%. The increase in area was 12.41 times that under the natural development scenario, and the average annual growth rate increased to 0.7%, indicating a strong expansion of urban space. At this time, the agricultural space and ecological space were reduced by 4,249.35 and 5,532.94 km2 respectively. In terms of spatial cross-conversion, the conversion area of agricultural space to urban space is the largest, accounting for 67.02% of its total growth area. For the ecological space, the scale of grassland conversion is the largest. From the perspective of conversion position, urban spatial growth regions are concentrated in the central and western parts of urban agglomerations: The large-scale transformation of agricultural space along the railway formed a "strip urban space belt." Nearly 82% of agricultural space in Nongan County, Dehui City, and Yushu City in the north of Jilin City was transformed into urban space, forming an "urban space network" with Changchun City and Jilin City as the core and spreading to the surrounding areas, while the urban space expansion in Qiqihar City and Suihua City was relatively uniform. In the eastern region, the expansion is mainly scattered, and the agricultural space around the core built-up areas of districts and counties in Mudanjiang City and Yanbian Korean Autonomous Prefecture and the ecological space close to the residential areas are transformed on a large scale.
4) Under the ecological space priority scenario, the ecological space 10a increased by 16,432.89 km^2, and the space proportion increased from 49.26% to 54.3.6%. The growth area is 12.6 times of that under the natural development scenario. Unlike other scenarios, while the ecological space increases rapidly, the urban space also expands significantly, increasing by 1,869.31 km^2. In terms of spatial cross-conversion, agricultural space is the main source of

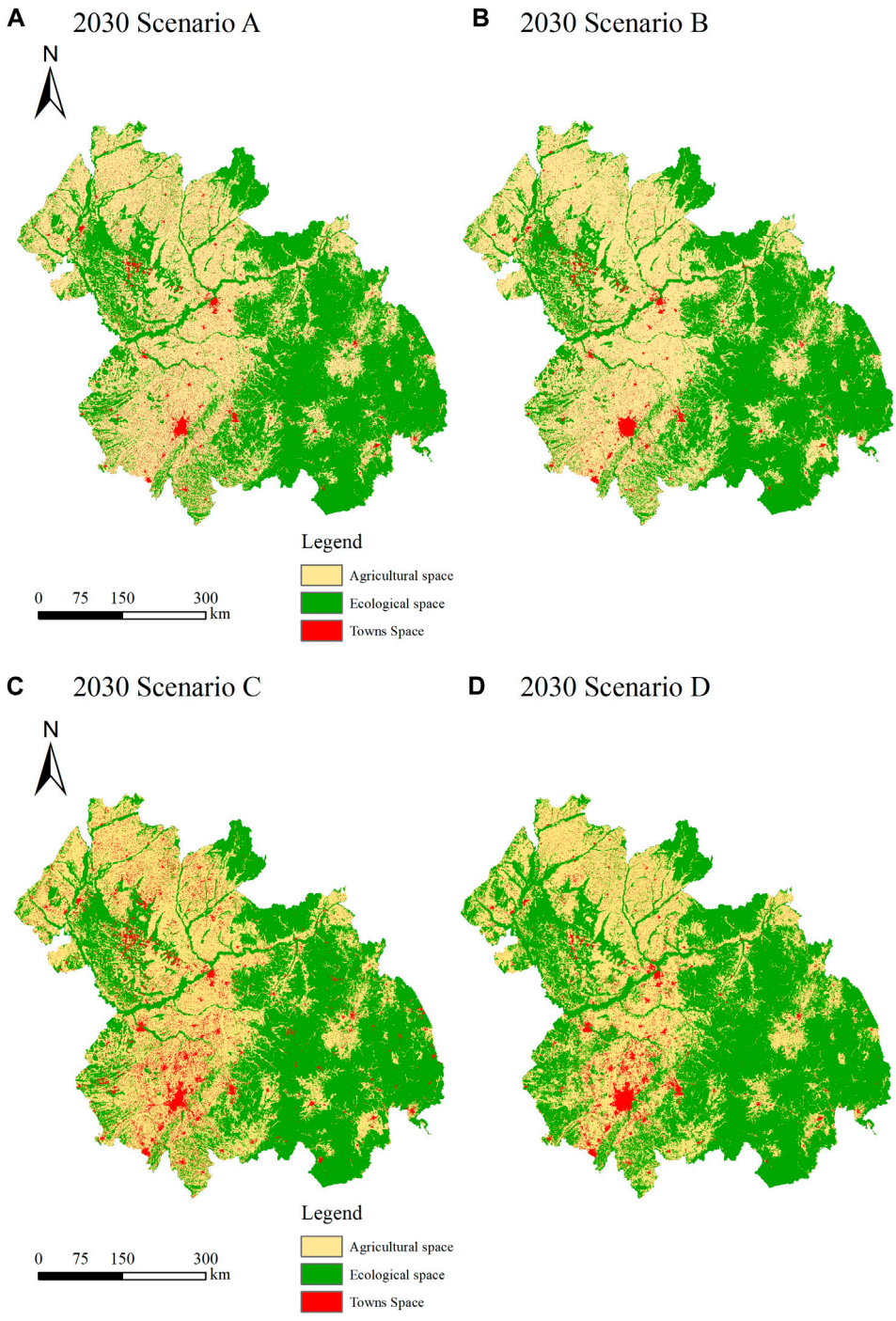

FIGURE 8
Distribution of the "three-zone spatial" pattern of the Harbin-Changchun urban agglomeration under multiple scenarios in 2030. **(A)** 2030 Scenario A **(B)** 2030 Scenario B **(C)** 2030 Scenario C **(D)** 2030 Scenario D.

ecological space, in which the area of arable land to the forest is the largest and most extensive, and the scale of conversion between different land types in ecological space is small. Of these, the largest scale of conversion is between bare ground and grassland. In terms of the conversion position, the expansion of ecological space mainly occurred in the flat Songnen plain in the central and western part of the urban agglomeration, and the water content was relatively sufficient in the Nenjiang and Songhua River basins, while the expansion scale in the eastern part was relatively small.

4.3.3 Multi-scenario simulation of land use conflict distribution characteristics in the "three-zone space"

The multi-scenario simulation "three-zone space" data in 2030 was imported into the Arcgis10.8 software to create a

TABLE 7 Distribution data of "three-zone space" pattern under multi-scenario simulation.

Type of space	Scenario type							
	Natural scenario		Agricultural spatial priority scenario		Urban spatial priority scenario		Ecological space priority scenario	
	Area (km2)	Area share (%)	Area (km2)	Area share (%)	Area (Km^2)	Area share (%)	Area (km2)	Area share (%)
Agricultural space	151537.98	47	161693.29	50.15	146500.62	45.44	132447.78	41.08
Ecological space	157553.98	48.87	150495.52	46.68	153316.88	47.55	175282.71	54.36
Urban space	13328.32	4.13	10231.47	3.17	22602.78	7.01	14689.79	4.56

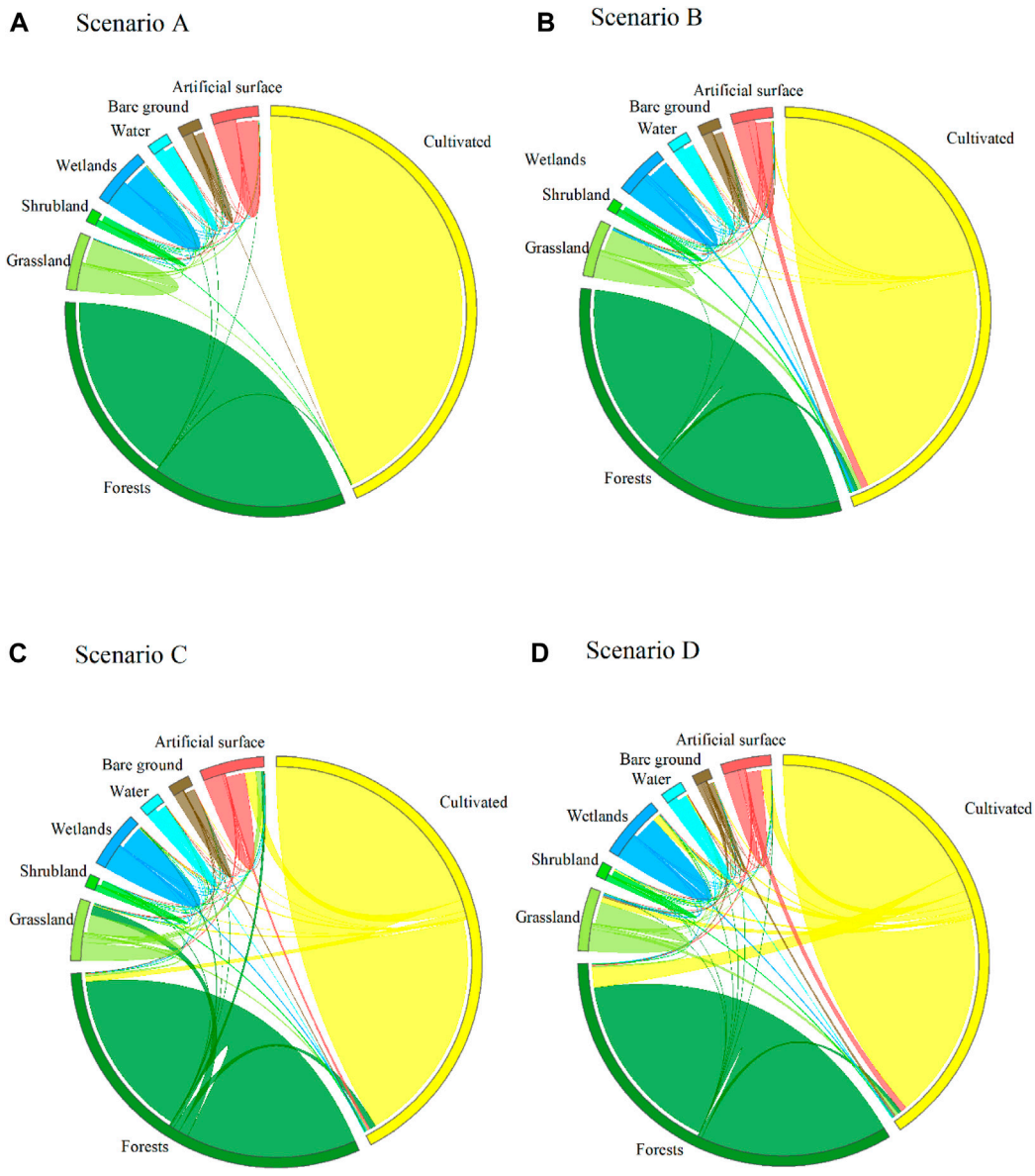

FIGURE 9
Land use transfer chord diagram for the Harbin-Changchun urban agglomeration under the multi-case simulation for 2020–2030. **(A)** Scenario A **(B)** Scenario B **(C)** Scenario C **(D)** Scenario D.

fishing net, and the comprehensive conflict index of "three-zone space" in 2030 was measured with the Fragstats4.2 software moving window method, to obtain the spatial conflict pattern of the Harbin-Changchun urban agglomeration under four types of scenarios (Figure 10). The results show that (Table 8):

1) Under the natural development scenario, there is no significant change in the distribution structure of the "three-zone space" conflict pattern compared to 2020, and the number of units in the out-of-control zone continues to decline, while the stable and controllable zone remains the largest in terms of scale but also experiences the largest reduction among the four conflict zones. In addition to the mutual transformation between the seriously out-of-control area and the basic out-of-control area, there are also some seriously out-of-control areas located at the edge of the peripheral area and the core area that are directly developed into the basic out-of-control area. However, under this scenario, the number of units in the seriously out-of-control area exceeds the basic out-of-control area for the first time, significant growth at administrative district boundaries. It is evident that the spatial conflicts in the core area and surrounding area are constantly intensified with the improvement of urbanization level and urban expansion. Resolving conflicts and reducing the seriously uncontrolled areas will require a considerable amount of time.
2) Agricultural spatial priority scenario was the most ideal simulation result for spatial conflict control among the four types of scenarios. The number of units in the severely out-of-control area decreased by 62 compared with the natural development scenario, and the total number of units in the out-of-control area decreased by 52 compared with the natural development scenario, accounting for only 26.37% of the total number of the areas. The highly concentrated and seriously out-of-control areas in the main axis of the development of Harbin and Changchun have been significantly reduced, and the spread of conflict to the surrounding areas has also been curbed. Most of the areas in the core area have been transformed from the seriously out-of-control areas to basic out-of-control area or controllable areas, especially the controllable area of the conflict area in the development zone of Harbin, Daqing, and Qing has been significantly expanded. In the peripheral areas, only Siping City and Liaoyuan City still have a certain scale of serious out-of-control areas.

The priority scenario of agricultural space aims to protect basic farmland and ensure agricultural and forestry product supply, from the perspective of ensuring national food security and improving comprehensive agricultural productivity. As the insufficient supply of mainland sources for urban spatial expansion. After the development of agricultural space is limited, the urban expansion process slows down with it, thus alleviating the aggravation of the contradiction between man and land. However, while fully protecting agricultural space, this scenario also delays the development process of urbanization.

3) In the urban spatial priority scenario, the "three-zone space" conflict is the most intense, and the total number of out-of-control district units is 491, an increase of 112 space units compared with 2020. The proportion of space area increased by 9.36% compared with the natural development scenario. The spatial conflicts in the main built-up areas and the surrounding counties and towns are intensified, and the spatial conflict layout structure has obvious attributes of urbanization core expansion. The conflict in the core area is the most serious, and the out-of-control area expands dramatically. Harbin and Changchun are the two growth centers, and significant diffusion effects are generated in both radial and axial directions. The basic out-of-control area distributed in key development areas and urban groups has undergone a large-scale transformation to the severely out-of-control area. The original conflict-controllable "buffer zone" between the two poles is connected with each other to form a "seriously out-of-control gathering area" of spatial conflicts. In the outer areas, the conflicts between Qiqihar City and Suihua City developed strongly along the direction of the development belt of Ha-Da-Qi-Mu.

Urban spatial priority is crucial for adapting to the future economic development situation, strengthening the spatial connection between medium satellite cities and key small towns, and ensuring the steady progress of urbanization level. National key development urban groups are given priority development rights, which makes urban space large-scale encroachment on surrounding ecological and agricultural land, and the complexity and fragmentation of land patch landscape pattern significantly increase the conflicting index. Such a scenario is an extreme pursuit of economic benefits at the expense of agricultural and ecological rights.

4) Under the ecological space priority scenario, the structure of the "three-zone space" conflict pattern was significantly different from other scenarios, and the areas of the stable and controllable conflict zones and the seriously out-of-control conflict zones increased significantly. There are 322 units in the serious conflict zone and 525 units in the stable controllable conflict zone, accounting for the largest proportion among the four scenarios. The layout of spatial conflicts is seriously extreme: the out-of-control conflict zones are distributed in the core areas of urban agglomerations and the industrial corridor of Harbin-Daqing-Qiqihar, of which 75.8% are seriously out-of-control areas. In the outer regions, Mudanjiang City, Suihua City, the whole of Yanbian Korean Autonomous Prefecture, and the northern region of Qiqihar are in the range of controllable conflict zones, of which 77.9% are stable controllable areas. The basic controllable area and the basic out-of-control area are mainly distributed in the middle transition zone of the two types of conflict Spaces and near the urban agglomeration contour area.

The ecological space priority scenario is an important scenario to promote the transformation of urban agglomeration from extension and expansion to connotation and promote the harmonious and sustainable development of man and nature. National nature reserves and key ecological function areas have been fully protected, while another ecological land has been given priority for development. Under ecological protection measures such as returning farmland to

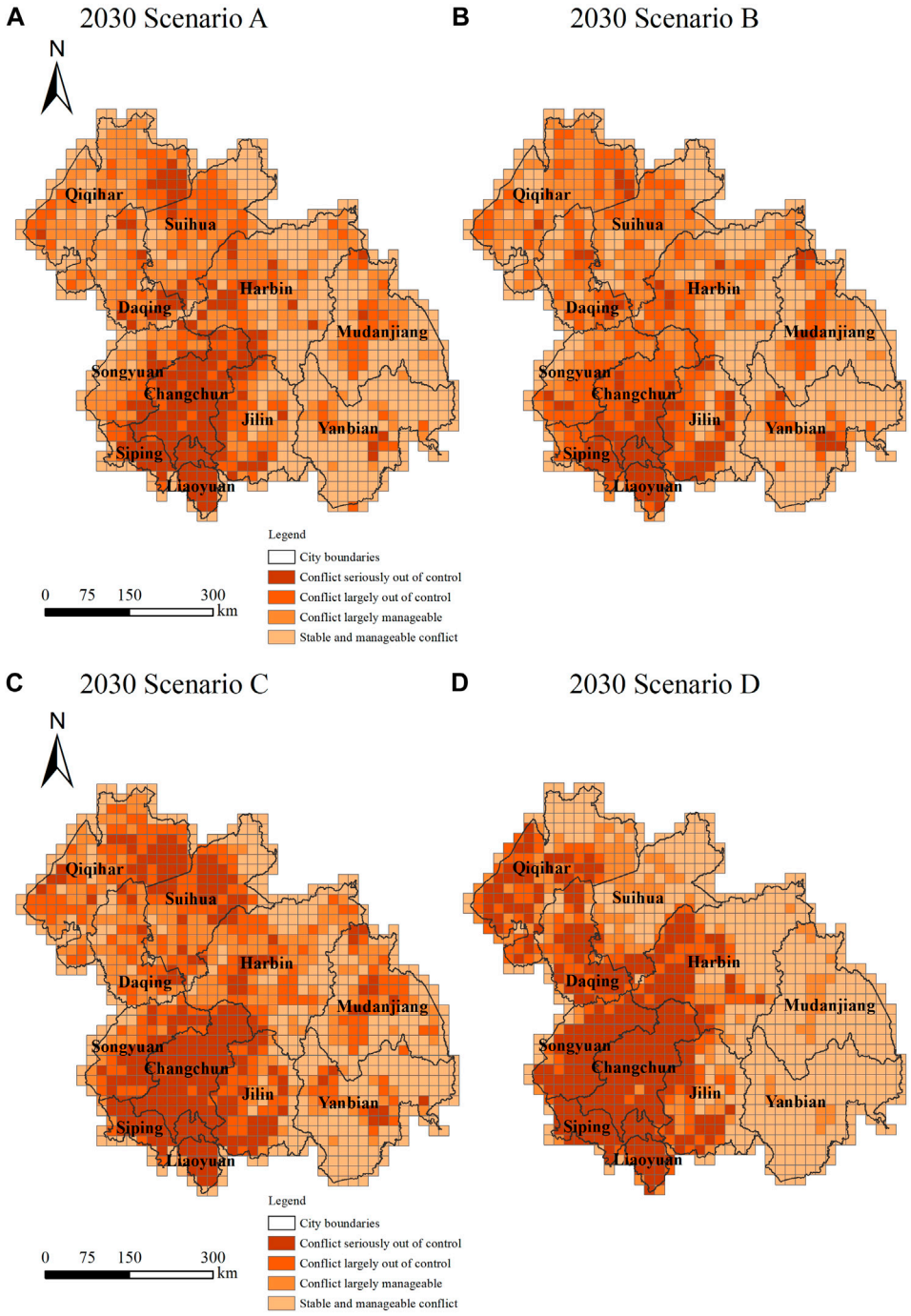

FIGURE 10
Spatial conflict pattern of the "three-zone space" in the Harbin-Changchun urban agglomeration under multiple scenarios in 2030. **(A)** 2030 Scenario A **(B)** 2030 Scenario B **(C)** 2030 Scenario C **(D)** 2030 Scenario D.

forests and grasslands, the ecological space of forests and grasslands has expanded significantly, with the highest level of forest and grass area. In space competition, the artificial land surface is at the priority level (Chen, W et al., 2023), resulting in an increase in urban space area. As the mainland supply area, agricultural space is invaded by both urban and ecological space, resulting in a severe impact on landscape pattern, which results in a high coincidence between spatial conflict pattern and agricultural spatial distribution.

5 Discussion and conclusion

5.1 Discussion

The fundamental purpose of land use conflict research is to prevent and eliminate potential conflicts in the future. Compared with the static characterization of the land use conflict pattern and the exploration of the driving factors in the existing studies

TABLE 8 Comprehensive conflict index of "three-zone space" in Harbin-Changchun urban agglomeration under multi-scenario simulation.

Spatial conflict type	Natural scene		Agricultural spatial priority scenario		Urban spatial priority scenario		Ecological space priority scenario	
	Number (pcs)	Percentage (%)	Number (pcs)	Percentage (%)	Number (pcs)	Percentage (%)	Number (pcs)	Percentage (%)
Stable and controllable	479	43.07	513	46.17	408	36.69	525	47.21
Basically controllable	288	25.89	305	27.45	213	19.15	149	13.40
Basically out of control	171	15.37	181	16.29	230	20.68	116	10.43
Seriously out of control	174	15.64	112	10.08	261	23.47	322	28.96

(Liu et al., 2022; Ma et al., 2022) the evolutionary patterns of the three types of spaces are firstly accurately portrayed and discussed in detail from two dynamic dimensions, namely, time and space, in terms of physical and quantitative changes in this paper. And discovers the potential rules of spatial evolution that have been neglected in the previous studies, These are the factors that cannot be ignored in land use conflict management. However, few studies have paid attention to this basic work.

In terms of simulation research on urban land expansion, existing studies mostly focus on the improvement of model precision and accuracy verification (Qiao et al., 2023) while there is a lack of discussion on how the simulation results can effectively support the determination of urban planning and management policies. In this paper, in accordance with the requirements of the content of the "Harbin-Changchun Urban Agglomeration Development Plan," four scenarios of urban space priority, agricultural space priority, and ecological space priority and natural development are set up, rationalize the setting of restricted development zone, and the four simulation scenarios ensure the upper limit of the occurrence of conflict, the *status quo*, and the lower limit, identify the potential conflict areas and form a contrasting effect among each other, so that the decision makers can obtain the results under different scenarios, and formulate reasonable conflict control policies according to the differentiated characteristics of different regions.

1) The research results demonstrate that agricultural space represented by cultivated land is the core resource and key area contested by different interest subjects in the process of land development and utilization, and it is also a high-incidence area where spatial conflicts arise and escalate (Haregeweyn et al., 2012). In the process of urban expansion, urban space has a large amount of encroachment upon agricultural space. Under ecological protection measures such as returning farmland to forest and grassland, cultivated land also should provide the place for the sustainable and healthy development of ecological environment. Agricultural spatial pattern directly determines the pattern of spatial conflicts to some extent.
2) The spatial conflicts in the Harbin-Changchun urban agglomeration have slightly eased in 2010 and 2020, but the regions with reduced conflict levels were mainly distributed in the peripheral areas. The spatial conflicts caused by urban spatial expansion in the core and surrounding areas were difficult to produce significant reverse resolution effects through policy-oriented means in a short period of time, reflecting obvious distance effects. The scenario setting of single space priority can satisfy the control of conflict scale in the study area, but cannot balance the distribution of multiple spatial rights and conflict locations.

Based on the above analysis of the prediction results of different simulation scenarios, optimization strategies are proposed in the following aspects:

① Overall planning of the "three-zone space" layout and implementing the urban optimization model for the core area of urban agglomerations. It is an inevitable trend that the spatial conflict in the core area of urban agglomerations will intensify. Therefore, the efficient and intensive use of space within the core area, the rational planning and configuration of industrial and infrastructure space layout, and the promotion of industrial structure upgrading while limiting the unbridled expansion of the built-up area. Strictly control the amount of construction land to reduce the space conflict caused by the outward diffusion of the core area.
② Implementation of a comprehensive development model for satellite towns and villages outside the core area. The satellite towns mainly undertake the overflow industries and population of the main urban area, but they are in the transition zone between urban space and agricultural space. The dual benefits of economic development and agricultural protection should be realized comprehensively, so the production and construction of land and agricultural land should be integrated to achieve intensive utilization. In addition, a regional buffer zone is set up between rural settlements, high-quality cultivated land, and basic farmland to delay the high-intensity conflict between urban space and agricultural space.
③ Strict cultivated land protection mode shall be implemented in the range of high-quality cultivated land, permanent basic farmland and main producing areas of agricultural products to avoid the loss of high-quality cultivated land and ensure food security and stability.
④ Implement ecological protection models within key ecological functional areas and nature reserves, strictly implement

ecological protection red lines, and formulate hierarchical management and control policies to strengthen the protection of ecologically fragile areas.

⑤ Implement the urban development model in peripheral areas such as Mudanjiang City and Yanbian Korean Autonomous Prefecture, Appropriate expansion of urban spatial scale in areas with the relatively concentrated distribution of conflict controllable areas, strengthen economic and industrial development in built-up areas, and make up for the limited economic increment in the core area, so as to achieve the balance of social and economic benefits of the entire urban agglomeration.

5.2 Conclusion

This paper takes the perspective of "three-zone space" as the pointcut, and selects 2000, 2010, and 2020 as observation nodes, portrays the Harbin-Changchun urban agglomeration from the dimensions of "transformation scale" and "landscape pattern," quantitatively describes the spatio-temporal dynamic changes of land use distribution and spatial conflict pattern of the urban agglomerations in the past 20 years, and combines the PLUS model with multiple scenarios to simulate the conflict evolution trend, draws the following conclusions:

1) The land use spatial pattern of the Harbin-Changchun urban agglomeration is highly consistent with the main functional areas. Agricultural and ecological spaces are mainly distributed in the central and eastern regions, while urban space is distributed along the Harbin-Daqing-Changji-corridor development zone with Harbin-Changchun as the development axis. In the past 20 years, urban space has continued to expand outwards, and agricultural space has become the main source, resulting in a large loss of high-quality farmland. At the same time, the scale of cross-conversion between agricultural space and ecological space is the largest, mainly in the main producing areas of agricultural and forestry products and national nature reserves, with the cross-conversion center shifting to the southeast. Relatedly, the spatial conflict pattern of the Harbin-Changchun urban agglomeration is closely related to the trajectory of human development activities. Areas with out-of-control conflicts are concentrated in core areas with high levels of economic development and dense population, while key ecological functional areas and nature reserves in the northwest and east are areas with the weakest conflicts. In the past 20 years, the intensity of conflicts in the "Three-zone space" has shown a trend of first increasing and then decreasing. However, in ecological functional areas far away from the city, conflicts are increasingly becoming more extreme. Although the promotion of national policies and measures has alleviated spatial conflicts, the problem of agricultural and ecological spatial deprivation in the core area is still an inevitable contradiction.
2) Simulation and prediction results indicate distinct distribution differences in the "three-zone space" under various scenario planning. Under the natural development scenario, ecological and agricultural space still dominate, and spatial transformation remains relatively balanced. Although urban space continues to expand, the growth rate has slowed down. However, under the scenario of giving priority to the development of urban and ecological space, the "three-zone space" pattern has changed significantly. Agricultural space has been greatly encroached, and the proportion has dropped sharply. Only under the scenario of giving priority to agricultural space, the agricultural area will increase. And urban space is reduced. Agricultural space and urban space show opposite trends in spatial transformation, and the competition between them is particularly fierce. Under the four scenarios, the overall conflict pattern of the "three-zone space" showed a spatio-temporal distribution pattern of "high in the south, low in the north, high in the west, low in the east, and with high in the core, low in the periphery, high in the plains, and low in the mountains." The conflicts in the urban space priority scenario are the most intense. The proportion of out-of-control areas is the highest in 30 years, and it spreads disorderly to the surrounding areas. The contradiction between man and land is acute. The agricultural spatial priority scenario has the best control effect on spatial conflicts. Although serious conflict areas still exist in Siping City and Liaoyuan City, the spatial conflicts in the core area are significantly reduced. Under the ecological space priority scenario, conflict areas, stable controllable areas, and severely out-of-control areas show a highly concentrated and polarized distribution in the east and west, while the basically out-of-control areas and basically controllable areas are located in the intermediate transition zone.

Research results show that the continued deterioration of land use conflicts in core areas is an inevitable development trend. Agricultural space represented by cultivated land is the core resource and key area that different stakeholders compete for in the process of land development and utilization. As urban space is expanding on a large scale, it is also constantly transforming outwards, it has always shown an opposite development trend to the agricultural space. There is no optimal solution to the land use model that can achieve balanced and coordinated development of urbanization, food production and ecological protection. Therefore, in the next 10 years, the government should formulate differentiated land use policies for core and peripheral areas, giving priority to ecological environment improvement and Reasonable layout of regional space and optimization of spatial configuration for regional economic transformation. Promoting governments at all levels to further carry out land use optimization research and policy innovation is of great significance to promoting the coordinated and sustainable development of the Harbin-Changchun urban agglomeration.

Data availability statement

The original contributions presented in the study are included in the article/supplementary material, further inquiries can be directed to the corresponding author.

Author contributions

WZ: Conceptualization, Data Curation, Methodology, Software, Investigation, Formal Analysis, Writing–Original Draft, Visualization. BG: Conceptualization, Supervision, Project administration, Writing–review and editing. HS: Visualization, Investigation, Software, Validation, Writing–review and editing. ZL: Resources, Supervision, Validation

Funding

The author(s) declare this research was supported by the National Natural Science Foundation of China (42201272)

Conflict of interest

The authors declare that the research was conducted in the absence of any commercial or financial relationships that could be construed as a potential conflict of interest.

Publisher's note

References

Adam, Y., Pretzsch, J., and Darr, D. (2015). Land use conflicts in Central Sudan: perception and local coping mechanisms. *Land Use Policy* 42, 1–6. doi:10.1016/j.landusepol.2014.06.006

Allen, C., Reid, M., Thwaites, J., Glover, R., and Kestin, T. (2020). Assessing national progress and priorities for the Sustainable Development Goals (SDGs): experience from Australia. *Sustain Sci.* 15, 521–538. doi:10.1007/s11625-019-00711-x

Alston, L. J., Libecap, G. D., and Mueller, B. (2000). Land reform policies, the sources of violent conflict, and implications for deforestation in the Brazilian Amazon. *Econ. Manag.* 39 (2), 162–188. doi:10.1006/jeem.1999.1103

Andrew, J. S. (2003). Potential application of mediation to land use conflicts in small-scale mining. *Clean. Prod.* 11 (2), 117–130. doi:10.1016/s0959-6526(02)00032-x

Bao, W., Yang, Y., and Zou, L. (2021). How to reconcile land use conflicts in mega urban agglomeration? A scenario-based study in the Beijing-Tianjin-Hebei region, China. *J. Environ. Manag.* 296, 113168. doi:10.1016/j.jenvman.2021.113168

Brown, G., and Raymond, C. M. (2014). Methods for identifying land use conflict potential using participatory mapping. *Landsc. Urban Plann.* 122, 196–208. doi:10.1016/j.landurbplan.2013.11.007

Chen, Z., Lu, C., and Fan, L. (2012). Farmland changes and the driving forces in yucheng, north China plain. *J. Geogr. Sci.* 22, 563–573. doi:10.1007/s11442-012-0947-9

Chen H, H., Yang, Q., Su, K., Zhang, H., Lu, D., Xiang, H., et al. (2021). Identification and optimization of production-living-ecological space in an ecological foundation area in the upper reaches of the Yangtze River: a case study of Jiangjin District of Chongqing, China. *Land* 10 (8), 863. doi:10.3390/land10080863

Chen W, W., Zhang, Q., Kong, X., Duan, X., Zuo, X., Tan, M., et al. (2021). Optimization rules of provincial permanent basic farmland layout based on "Three-line" overall planning and empirical research. *Trans. Chin. Soc. Agric. Eng.* 37 (15). (in chinese). doi:10.11975/j.issn.1002-6819.2021.15.030

Chen, W., Wang, G., Gu, T., Fang, C., Pan, S., Zeng, J., et al. (2023). Simulating the impact of urban expansion on ecosystem services in Chinese urban agglomerations: a multi-scenario perspective. *Environmental Impact Assessment Review* 103, 107275. doi:10.1016/j.eiar.2023.107275

De Groot, R. (2006). Function-analysis and valuation as a tool to assess land use conflicts in planning for sustainable, multi-functional landscapes. *Landsc. Urban Plann.* 75 (3–4), 175–186. doi:10.1016/j.landurbplan.2005.02.016

De Jong, L., De Bruin, S., Knoop, J., and van Vliet, J. (2021). Understanding land-use change conflict: a systematic review of case studies. *J. Land Use Sci.* 16 (3), 223–239. doi:10.1080/1747423x.2021.1933226

Dong, G., Ge, Y., Jia, H., Sun, C., and Pan, S. (2021). Land use multi-suitability, land resource scarcity and diversity of human needs: a new framework for land use conflict identification. *Land* 10 (10), 1003. doi:10.3390/land10101003

Fan, J. (2019). Spatial organization approach of regional function-structure: discussion on the implementation of the functional zoning strategy in territorial spatial planning. *Geogr. Res.* 38 (10), 2373–2387. (in chinese). doi:10.11821/dlyj020190865

Guo, R., Wu, T., Wu, X., Luigi, S., and Wang, Y. (2022). Simulation of urban land expansion under ecological constraints in harbin-changchun urban agglomeration, China. *Chin. Geogr. Sci.* 32, 438–455. doi:10.1007/s11769-022-1277-1

Haregeweyn, N., Fikadu, G., Tsunekawa, A., Tsubo, M., and Derege, T. M. (2012). The dynamics of urban expansion and its impacts on land use/land cover change and small-scale farmers living near the urban fringe: a case study of Bahir Dar, Ethiopia. *Landsc. Urban Plan.* 106 (2), 149–157. doi:10.1016/j.landurbplan.2012.02.016

Jiang, S., Meng, J., Zhu, L., and Cheng, H. (2021). Spatial-temporal pattern of land use conflict in China and its multilevel driving mechanisms. *Sci. Total Environ.* 801, 149697. doi:10.1016/j.scitotenv.2021.149697

Kim, I., and Arnhold, S. (2018). Mapping environmental land use conflict potentials and ecosystem services in agricultural watersheds. *Sci. Total Environ.* 630, 827–838. doi:10.1016/j.scitotenv.2018.02.176

Li, D., Ding, S., Liang, G., Zhao, Q., Tang, Q., and Kong, L. (2014). Landscape heterogeneity of mountainous and hilly areas in the western Henan Province based on the moving window method. *Acta Ecol. Sin.* 34 (12), 3414–3424. (in chinese). doi:10.1109/Geoinformatics.2013.6626190

Liang, X., Guan, Q., Clarke, K., Liu, S., Wang, B., and Yao, Y. (2021). Understanding the drivers of sustainable land expansion using a patch-generating land use simulation (PLUS) model: a case study in Wuhan, China. *Comput. Environ. Urban Syst.* 85, 101569. doi:10.1016/j.compenvurbsys.2020.101569

Liu, H., Soares-Filho, B. S., Leite-Filho, A. T., Zhang, S., Du, J., and Yi, Y. (2023). How to balance land demand conflicts to guarantee sustainable land development. *Iscience*, 26 (5), 106641. doi:10.1016/j.isci.2023.106641

Liu, X., Zhang, Z., Li, M., Fu, Y., and Hui, Y. (2022). Spatial conflict simulation of land-use based on human-land-landscape elements intercoordination: a case study in Tianjin, China. *Environ. Monit. Assess.* 194 (5), 317. doi:10.1007/s10661-022-09947-0

Ma, G., Li, Q., Yang, S., Zhang, R., Zhang, L., Xiao, J., et al. (2022). Analysis of landscape pattern evolution and driving forces based on land-use changes: a case study of Yilong Lake watershed on Yunnan-Guizhou Plateau. *Land* 11 (8), 1276. doi:10.3390/land11081276

Ma, W., Jiang, G., Chen, Y., Qu, Y., Zhou, T., and Li, W. (2020). How feasible is regional integration for reconciling land use conflicts across the urban–rural interface? Evidence from Beijing–Tianjin–Hebei metropolitan region in China. *Land Use Policy* 92, 104433. doi:10.1016/j.landusepol.2019.104433

Meimei, W., Zizhen, J., Tengbiao, L., Yongchun, Y., and Zhuo, J. (2023). Analysis on absolute conflict and relative conflict of land use in Xining metropolitan area under different scenarios in 2030 by PLUS and PFCI. *Cities*, 137, 104314. doi:10.1016/j.cities.2023.104314

Nyangena, W. (2000). *Land tenure, land use, environmental degradation and conflict resolution. A PASIR analysis for the narok district, Kenya*.

Peng, K., Jiang, W., Deng, Y., Liu, Y., Wu, Z., and Chen, Z. (2020). Simulating wetland changes under different scenarios based on integrating the random forest and CLUE- S models: a case study of Wuhan urban agglomeration. *Ecol. Indic.* 117, 106671. doi:10.1016/j.ecolind.2020.106671

Peterseil, J., Wrbka, T., Plutzar, C., Schmitzberger, I., Kiss, A., Szerencsits, E., et al. (2004). Evaluating the ecological sustainability of Austrian agricultural landscapes—the SINUS approach. *Land Use Pol.* 21 (3), 307–320. doi:10.1016/j.landusepol.2003.10.011

Qiao, W., Hu, B., Guo, Z., and Huang, X. (2023). Evaluating the sustainability of land use integrating SDGs and its driving factors: A case study of the Yangtze River Delta urban agglomeration, China. *Cities* 143, 104569. doi:10.1016/j.cities.2023.104569

Rahman, M. R., Shi, Z. H., and Chongfa, C. (2014). Assessing regional environmental quality by integrated use of remote sensing, GIS, and spatial multi-criteria evaluation for prioritization of environmental restoration. *Environmental monitoring and assessment* 186, 6993–7009. doi:10.1007/s10661-014-3905-4

Ran, N., Jin, X., Fan, Y., Xiang, X., Liu, J., Zhou, Y., et al. (2018). Research on "three-line" demarcation method based on land use conflict identification and coordination: a

case study of Jintan District, Changzhou City. *Resour. Sci.* 40 (02), 284–298. doi:10.18402/resci.2018.02.06

Von Der Dunk, A., Grêt-Regamey, A., Dalang, T., and Hersperger, A. M. (2011). Defining a typology of peri-urban land-use conflicts–A case study from Switzerland. *Landsc. urban Plan.* 101 (2), 149–156. doi:10.1016/j.landurbplan.2011.02.007

Wang, B., Tian, J., and Wang, S. (2022). Process and mechanism of transition in regional land use function guided by policy: a case study from Northeast China. *Ecol. Indic.* 144, 109527. doi:10.1016/j.ecolind.2022.109527

Wang, X., Wang, D., Gao, W., Lu, J., and Jin, X. (2023). Investigation of spatial coupling coordination development: identifying land system states from the adaptation–conflict perspective. *Int. J. Environ. Res. Public Health* 20 (1), 373. doi:10.3390/ijerph20010373

Wang, Y., Fan, J., and Zhou, K. (2019). Optimized zoning of territorial functions based on the integration of "double evaluation. *Geogr. Res.* 38 (10), 2415–2429. (in chinese). doi:10.11821/dlyj020190327

Wehrmann, B. (2008). *Land conflicts: a practical guide to dealing with land disputes*. Eschborn: GTZ.

Wei, W., Yin, L., Xie, B., and Bo, L. (2023). Evolution characteristics and mechanism of "three-zone space" in the Yellow River Basin under the background of territorial spatial planning. *Econ. Geogr.* 42 (03), 44–55+86. doi:10.13249/j.cnki.sgs.2023.02.014

Wei, W., Yin, L., Xie, B., and Bo Liming, (2022). Evolution characteristics and mechanism of "three-zone space" in the Yellow River Basin under the background of territorial spatial planning. *Econ. Geogr.* 42 (03), 44–55+86. doi:10.15957/j.cnki.jjdl.2022.03.005

Wubie, A. M., de Vries, W. T., and Alemie, B. K. (2021). Synthesizing the dilemmas and prospects for a peri-urban land use management framework: evidence from Ethiopia. *Land Use Policy* 100, 105122. doi:10.1016/j.landusepol.2020.105122

Xie, H., et al. (2023). Study on the extent and spatial pattern differentiation of terraced land in China. *Acta Geogr. Sin.* 78 (01), 3–15. doi:10.11821/dlxb202301001

Xu, W., Wang, J., Zhang, M., and Li, S. (2021). Construction of landscape ecological network based on landscape ecological risk assessment in a large-scale opencast coal mine area. *J. Cleaner Production* 286, 125523. doi:10.1016/j.jclepro.2020.125523

Yang, J., Yang, S., Li, J., Gong, J., Yuan, M., Li, J., et al. (2023). A distance-driven urban simulation model (DISUSIM): accounting for urban morphology at multiple landscape levels. *Cities* 134, 104156. doi:10.1016/j.cities.2022.104156

Yang, S., and Su, H. (2022). Multi-scenario simulation of ecosystem service values in the guanzhong plain urban agglomeration, China. *Sustainability* 14, 8812. doi:10.3390/su14148812

Yang, Y., Bao, W., Li, Y., Wang, Y., and Chen, Z. (2020). Land use transition and its eco-environmental effects in the beijing–tianjin–hebei urban agglomeration: a production–living–ecological perspective. *Land* 9, 285. doi:10.3390/land9090285

Yu, B., and Lu, C. (2006), Land use conflict analysis: concepts and methods. *Adv. Geogr. Sci.* (03), 106–115. (in chinese). doi:10.3969/j.issn.1007-6301.2006.03.013

Zhang, S., and Qi, Y. (2018). Study on core-periphery structure and development stage judgment of Harbin and Yangtze River Agglomerations. *Sci. Geogr. Sin.* 38(10):1699–1706. (in chinese). doi:10.11821/dlyj020210375

Zhang, Y., Jiang, P., Cui, L., Yang, Y., Ma, Z., Wang, Y., et al. (2022). Study on the spatial variation of China's territorial ecological space based on the standard deviation ellipse. *Frontiers in Environmental Science* 10, 982734. doi:10.3389/fenvs.2022.982734

Zhou, D., Xu, J. C., and Wang, L. (2015a). Progress and prospects of land use conflict research in China in the past 15 years. *China Land Sci.* 29 (02), 21–29. doi:10.13708/j.cnki.cn11-2640.2015.02.003

Zhou, M., Ma, Y., Tu, J., and Wang, M. (2022). SDG-oriented multi-scenario sustainable land-use simulation under the background of urban expansion. *Environ. Sci. Pollut. Res. Int.* 29 (48), 72797–72818. doi:10.1007/s11356-022-20904-9

Frontiers in Environmental Science

Explores the anthropogenic impact on our natural world

An innovative journal that advances knowledge of the natural world and its intersections with human society. It supports the formulation of policies that lead to a more inhabitable and sustainable world.

Discover the latest Research Topics

See more →

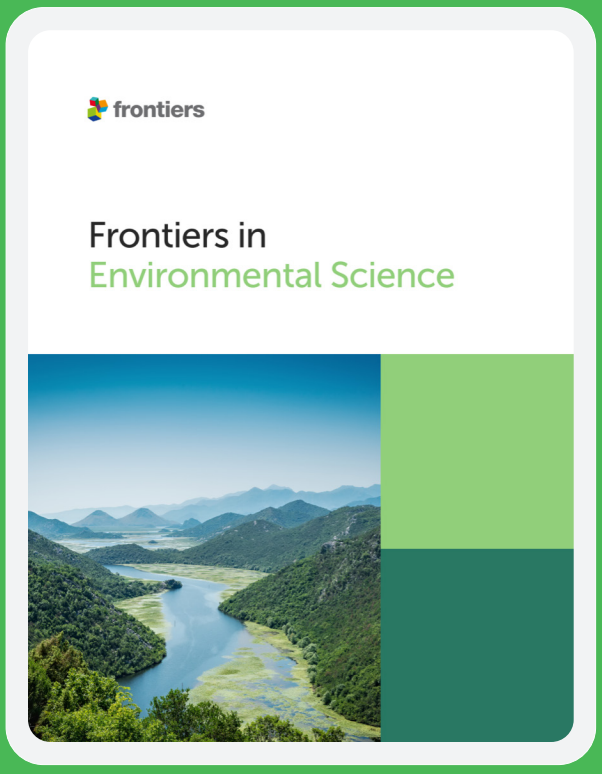

Frontiers

Avenue du Tribunal-Fédéral 34
1005 Lausanne, Switzerland
frontiersin.org

Contact us

+41 (0)21 510 17 00
frontiersin.org/about/contact